University of Nottingham

Improved Cement Bound Base Design for Flexible Composite Pavements

by

Muhammad Aslam Shahid

Thesis submitted to the University of Nottingham
for the degree of Doctor of Philosophy

October, 1997

Department of Civil Engineering

Improved Cement Bound Base Design for Flexible Composite Pavements

By

Muhammad Aslam Shahid

Thesis submitted to the University of Nottingham
for the degree of Doctor of Philosophy

October, 1997

To Najmi

Acknowledgements

The research work presented in this thesis was sponsored by the Commonwealth Scholarship Commission in the UK, the British In-situ Concrete Paving Association (BRITPAVE) together with a contribution from the British Cement Association. I would like to acknowledge my sincere thanks for all this support.

I would like to express my gratitude to my supervisor Dr N.H. Thom for his friendly, encouraging and expert guidance throughout my research work. Without his enthusiastic help this thesis would have never been completed. Thanks are also due to my co-supervisor Mr A.R. Dawson for his constructive criticism and technical advice, and to Dr. C.H. Peaston with whom I had useful technical discussions. Special thanks are due to Professor S.F. Brown, the leader of the Pavements and Geotechnics group, for his encouragement.

A particular debt of gratitude is due to Mr. David York of Sitebatch (Contracting) Ltd. for his remarkable assistance in organising the site visits and trials. Without his help the field investigation would have been impossible. Many thanks are also due to the UK Department of Transport, for their willingness to perform site trials, the various County Councils and the many site contractors for their invaluable assistance in agreeing to site visits and trials, and to SWK Pavement Engineering Ltd. for providing their Falling Weight Deflectometer and other equipment.

Thanks are also due to all those technicians who helped me in experimental work, in particular, the names of Darren Belcher, Andy Leyko, Balbir Loyla, Shane Malkin, and Ehsan Sharegh should be mentioned. My thanks also go to Barry Brodrick (experimental officer) for his help, and to all my colleagues and friends who have assisted in this research in one way or another.

Finally, I would like to thank my wife for her unending patience and support throughout the period of my studies at the University of Nottingham.

Declaration

The research described in this thesis was carried out at the University of Nottingham, Civil Engineering Department, between October 1993 and February 1997.

This dissertation is the result of my own original work, except where specific reference has been made to the work of others. No part of the work has been, or is currently being submitted for any degree, diploma or other qualification.

M A Shahid
University of Nottingham
October 1997

Abstract

Cement bound bases exhibit several advantages over conventional bituminous bases for pavements in terms of cost and mechanical efficiency. An equivalent thickness of cement bound material (CBM) would, as well as being much cheaper, form a stiffer layer than a bituminous material, increasing protection to the subgrade. Besides these advantages, CBMs are environment-friendly from the view point of construction.

The perceived problems with cement bound base roads have generally stemmed from the tendency for discrete cracks within the base to propagate through bituminous surfacing layers, termed reflective cracking, giving rise to maintenance concerns. The use of a thick bituminous layer (current UK practice) to combat reflective cracking makes these roads less cost effective. The phenomenon of cracking, transverse and longitudinal, is in fact the chief cause of significant reduction in the performance of a cement bound base and hence, eventually, pavement distress.

This thesis attempts to provide an improved understanding of important aspects, such as the sensitivity of the CBM mix design and strength parameters to variations in the mix water content, together with the investigation of performance characteristics of CBMs with different aggregates. Tensile properties have been determined through a direct tensile test, developed in this project, both under static and repeated loading. The strength properties and elastic stiffness results have been inter-related.

The thesis presents two techniques, that is controlled cracking and steel fibre reinforcement, to combat reflective cracking resulting from the crack activity in a CBM base. The results of field investigation, from two site trials, and a laboratory study confirm the occurrence of frequent narrow cracks, induced due to shrinkage and thermal stresses, with superior aggregate interlock as a result of the controlled cracking system. Laboratory test data both from element tests and scale pavements demonstrates that fracture of CBM in a steel fibre reinforced base, due to traffic and thermal loading, would lead to cracks of negligibly small width with almost no loss of

load transfer. The load transfer characteristics, in terms of relative vertical and horizontal movements, of cracks in the CBM bases subjected to traffic, have been studied through model pavement tests in the laboratory. Relationships have been established between aggregate interlock, crack width and CBM strength. The influence of these parameters upon reflective cracking has been studied through analytical modelling, based on a simplified approach and a finite element program. The results suggest that both the steel fibre reinforcement and controlled cracking in a CBM base have a great potential to cause a significant reduction in the thickness of bituminous surfacing for a flexible composite pavement.

Table of Contents

List of Figures

Chapter 3: Development of a Direct Tensile Test

Chapter 4: Mechanical Properties of Cement Bound Materials

Chapter 5: Controlled Cracking of Cement Bound Bases

Chapter 6: Steel Fibre Reinforced Cement Bound Bases

Chapter 7: Load Transfer Investigation of Cracks in CBM Bases

Chapter 8: Analytical Modelling and Design Implication

List of Tables

Introduction

1.1 BACKGROUND

The use of cement bound, or cement treated or stabilized base roads dates from Roman times. In some of the Roman roads built in Europe, a layer of small aggregates bound with a natural cement laid over a compacted soil foundation, was used as a support for flat quarried stone surfacing [Margery, 1987]. In 1865, low strength concrete bases, compacted by a heavy roller, were used in Scotland underneath a surfacing comprising stone setts, wood blocks or asphalt [Croney and Croney, 1991].

The actual concept of cement stabilized base roads in the UK was pioneered by Brooke-Bradley with trials on Salisbury Plain in 1917 [Andrews, 1955]. In the USA, cement stabilization in roads was started with projects in Iowa and South Dakota in 1922 [PCA, 1942]. These were followed by trials in Ohio, California and Texas in 1924 [PCA, 1956]. South Carolina State Highway Department deserve the credit for first developing soil-cement as a highway material, and for constructing and reporting successful soil-cement bases [Hveem and Zube, 1963]. The state of Washington started the use of cement treated materials by constructing nearly 24 km of two lane road between 1938 and 1947 [Leclerc, 1966]. In contrast, almost 160 km of plant-mixed cement treated base was completed in California by the end of 1943 [Hveem and Zube, 1963]. Similarly, the use of cement stabilization began in Australia in 1935 with the construction of a soil-cement road in Sydney [Lilley, 1970].

Significant progress was made by Germany in the use of soil-cement bases during the Second World War (1939-1945), when at least 140 airfields were constructed for the German air force [Lilley, 1972]. Apart from all this development, cement treated roadbases were not seen in France until the end of 1950 [Bonnot and Paute, 1976]. Likewise, cement stabilization in Sweden was firstly used on airfields during the mid 1950s [Örbom, 1965]. Almost at the same period, cement stabilized bases and

sub-bases were extensively used in the Netherlands over a variety of paving facilities [Lilley, 1972]. In South Africa, cement stabilized gravels were first used in the Transvaal during early 1940s [Marais, 1973]. Also in the Cape Province, cement stabilization was used on runways for military airfields during 1942 to 1944 [Biesenbach, 1973]. According to PIARC [1983], materials of this type are the most widespread for use in roadbases and sub-bases designed for medium and heavy traffic throughout the world.

Concentrating on developments in the UK, the urgent need for airfields during the Second World War and the increasing demands for highway construction during post war years led to tremendous progress in the use of cement bound base roads. During this era, a particular type of cement bound material, termed lean concrete, was extensively used for roadbase construction in many parts of the country, and over the full range from motorways to minor housing state roads [Williams, 1986]. This material involved high quality washed aggregates, a low cement content and a low water content to produce a uniform mix of a very low workability which was compacted by rolling. In the following years (during 1960's and 70's), lean concrete had been the most common roadbase material [Brooks, 1972].

Although lean concrete is often used as a sub-base under concrete pavements, it is essentially a roadbase material which is laid directly underneath a bituminous layer [Williams, 1986]. Its use has always been accompanied by impressive cost savings. Based on an early 1970s cost analysis of the lowest three tender prices on eight motorway contracts in the Midlands, Brooks [1972] concluded that the alternatives of concrete paving, dense bitumen macadams and rolled asphalt roadbases were 2 to 4%, 5% and 8% more expensive, respectively, than a cement bound base. In the following years, the prices of bituminous mixes have gradually increased, thus leading to an even larger difference between the costs. According to current prices, for example, the average cost for a conventional bituminous roadbase mix, i.e. a dense bitumen macadam (DBM) or a heavy duty macadam (HDM), is approximately 1.8 to 2.6 times of that for a typical cement bound (roadbase) material.

Until 1986, cement stabilized materials were classified as soil cement, cement bound granular material and lean concrete [Department of Transport (DoT) Specification, 1976] for use in sub-base and roadbase. Later on these were referred to more logically as cement bound material (CBM) categories of CBM1, CBM2 and CBM3 respectively [DoT Specification, 1986]. In addition, a new stronger category CBM4 was also introduced. However, the UK developments did not stop here, as an even stronger category, CBM5 has been recently included in the current design specifications [DoT, HD 26/94, 1994]. As a further step, this classification has been extended up to CBM6 in the present research. A detailed description of the different CBM categories is given in Chapter 2.

1.2 ADVANTAGES AND DISADVANTAGES OF CEMENT BOUND BASES

Cement bound base roads exhibit several advantages over conventional bituminous base pavements in terms of cost and mechanical efficiency. A brief description of these is given below:

1. Cement bound (CBM) bases have a much higher stiffness (i.e. elastic stiffness or elastic modulus) and strength than a conventional bituminous base. On one hand, they provide a relatively rigid and sufficiently strong support to the upper pavement structure. On the other hand, they furnish a good protection for the underlying layers [Brown et al, 1993] by significantly reducing the traffic induced stresses.
2. CBM bases, being resistant to permanent deformation (unless they are badly cracked), help in minimizing the problems of rutting and traffic induced fatigue cracking in the overlying bituminous surfacing [Brown, 1979].
3. The use of cement bound materials (CBMs) can accelerate the progress of construction work [Markwick and Keep, 1943]. The convenience of producing these materials on sites through readily available batching plants makes them "contractor-friendly".
4. A CBM sub-base is best suited for rigid pavements [DoT, HA 35/87, 1987] for two main reasons. First they enable to obtain a uniform thickness of the concrete slab

by providing a smooth and even platform, and second they minimize the risk of foundation damage caused by water penetrating into the slab joints. This water can help to cause a granular sub-base to weaken and then eventually the subgrade.

5. The use of CBM bases is environment friendly. Even in the past (towards the end of the Second World War), the use of lean concrete as a roadbase material was encouraged by the Ministry of Health [Blake, 1958].
6. CBM bases provide an excellent all-weather working platform for construction traffic. In particular, a CBM base is the best option if the construction has to be carried out during wet weather [Powell et al, 1984]. An interesting example is the construction of Heathrow airport which was carried out under the wet working conditions during late 1944 and early 1945. The use of a well compacted (unbound) gravel sub-base was only possible under favourable weather conditions [Graham and Martin, 1946]. The best alternative, therefore, was a lean concrete (with an aggregate cement ratio of 14.5 to 1), and was used on a massive scale in 225 mm thick layers [Williams, 1986].
7. The most attractive advantage of a CBM base is its significant cost effectiveness compared to a conventional bituminous base. Depending on the location of the construction site and availability of local aggregates, cement contents of up to 15% by mass of the dry aggregates have been reported to be economically viable [Kennedy, 1980].

The main disadvantage of a CBM base is its susceptibility to cracking due to shrinkage caused by cement hydration, water evaporation and thermal effects. These cracks can propagate through the bituminous layers and reflect on surface, thus allowing ingress of water into the pavement structure and foundation. This can lead to such a significant damage that the pavement might demand a major maintenance.

Experience demonstrates that wider cracks, at greater spacing, occur in a CBM base if the cement content is increased, suggesting that the mechanism of shrinkage and the resulting cracking, is related to the chemical properties of the cement binder.

1.3 CEMENT

Cement can be defined as a material with adhesive and cohesive characteristics which make it capable of bonding mineral aggregates into a compact whole mass. Cement has a particular property of setting and hardening through chemical reaction with water. The word 'cement' has been in use, for many years in the past, to represent a binder that attains strength by adding water.

The history of the use of cement shows that first the ancient Egyptians had used calcined impure gypsum. Subsequently the Greeks and the Romans used calcined limestone, then added water, sand and crushed stone or bricks and broken tiles, to create the first ever concrete in history [Neville, 1995]. Since lime mortar does not harden under water, the Romans found another way for the underwater construction. They ground together lime and a volcanic ash or finely ground burnt clay tiles. The active silica and alumina present in the ash and the tiles combined with lime. The resulting product was termed as "pozzolanic cement" from the name of the village of Pozzuoli, Vesuvius, where the volcanic ash was first found. The term pozzolanic cement is used to this day and describes the cements which are produced simply by grinding natural materials at normal temperature [Neville, 1995].

In 1824, Joseph Aspdin a Leeds bricklayer, stonemason and builder prepared a cement by heating a mixture of finely ground clay and limestone in a furnace until carbon dioxide (CO_2) escaped. The temperature was much lower than that necessary for clinkering. This cement was patented as Portland cement [Neville, 1995]. Thereafter, in 1845, Issac Johnson burnt a mixture of clay and chalk until clinkering to produce what resembles the modern cement. The name "Portland cement" was given because the colour and quality of the hardened cement resembles Portland stone, a limestone quarried in Dorset [Neville, 1995].

1.3.1 Chemical Composition of Cement

The term Portland cement currently describes a cement which is obtained by: (i) mixing together materials containing oxides of silica, alumina, and iron, (ii) burning

them at a clinkering temperature, and (iii) cooling down and grinding the resulting clinkers. During burning in the kiln, more complex compounds are formed through chemical reactions. The major constituents of cement are the four compounds given in Table 1.1, where C, S, A and F stand for CaO, SiO_2, Al_2O_3 and Fe_2O_3. Similarly, H_2O is denoted by H and SO_3 by S^* in the hydrated cement.

Table 1.1. Major constituents of Portland cement.

Name of Compound	Oxide Composition	Notation
Tricalcium silicate	$3CaO.SiO_2$	C_3S
Dicalcium silicate	$2CaO.SiO_2$	C_2S
Tricalcium aluminate	$3CaO.Al_2O_3$	C_3A
Tetracalcium aluminoferrite	$4CaO.Al_2O_3.Fe_2O_3$	C_4AF

In addition, some minor compounds such as MgO, TiO_2, Mn_2O_3, K_2O and Na_2O also exist in cement. Of these, K_2O and Na_2O, known as alkalis, are particularly important, because they react with some aggregates, thereby causing disintegration of concrete [Czernin, 1962], and have also been observed affecting the rate of gain of strength of cement [Neville, 1959].

The composition ranges of different oxides in the present day Portland cement are as given in Table 1.2 and, the composition of a typical Portland cement of the 1960s is shown in Table 1.3. The insoluble residue results mainly from impurities and is determined by treating with hydrochloric acid [Czernin, 1962]. The loss on ignition shows the extent of carbonation and hydration of free lime and free magnesia due to the exposure of the cement to the atmosphere [Neville, 1995]. Its maximum value, permitted by BS 12: 1991 and ASTM C 150-94, is 3%, and could be up to 4% for cements in the tropics [BS 12: 1991]. Any change in the composition of various oxides influences the chemical properties of cement. Table 1.4 shows five major types of the Portland cement resulting from the variation in composition of the same constituent compounds.

Table 1.2. Composition limits of oxides in Portland cement [Neville, 1995].

Oxide Name	Range (%)
CaO	60 – 67
SiO_2	17 – 25
Al_2O_3	3.0 – 8.0
Fe_2O_3	0.5 – 0.6
MgO	0.5 – 4.0
Alkalis (as Na_2O, K_2O)	0.3 – 1.2
SO_3	2.0 – 3.5

Table 1.3. Composition of oxides in a typical Portland cement of 1960s [Czernin, 1962].

Oxide Name	Content (%)
CaO	63
SiO_2	20
Al_2O_3	6
Fe_2O_3	3
MgO	1.5
SO_3	2
Na_2O and K_2O	1
Others	1
Loss on ignition	2
Insoluble residue	0.5

Table 1.4. Typical compound compositions for different types of Portland cement [US Bureau of Reclamation, 1949].

Type[1] of Portland Cement	Mean Values of Compound Composition (%)							
	C_3S	C_2S	C_3A	C_4AF	$CaSO_4$	Free CaO	MgO	Ignition loss
Ordinary cement	49	25	12	8	2.9	0.8	2.4	1.2
Modified cement	46	29	6	12	2.8	0.6	3.0	1.0
Rapid hardening	56	15	12	8	3.9	1.3	2.6	1.9
Low heat cement	30	46	5	13	2.9	0.3	2.7	1.0
Sulphate resisting	43	36	4	12	2.7	0.4	1.6	1.0

[1] According to ASTM description, the cement types given in Table 1.4, i.e. ordinary cement to sulphate resisting cement, are termed Type I to Type V cements, respectively.

1.3.2 Hydration of Cement

The constituent compounds of cement (silicates and aluminates) chemically react with water producing certain products which develop strength with time and become a hard mass. This process is known as hydration of cement. It has been reported that the products obtained from the hydration of cement are chemically the same as those from the hydration of the individual compounds under similar conditions [Steinour, 1952; Bogue and Lerch, 1934]. Tricalcium and dicalcium silicates are the two main constituents in cement with cementitious properties, and the behaviour of these two compounds (alone) is very similar to that of the cement during the process of hydration [Flint and Wells, 1934].

The rate of hydration keeps decreasing continuously, so that there remains an appreciable amount of unhydrated cement even after a long time. It has been reported that the grains of cement are hydrated only up to 4 microns depth after 28 days in contact with water, and the hydration depth reaches up to 8 microns after one year [Giertz, 1938]. Under normal conditions, complete hydration can be possible only for cement particles smaller than 50 microns, and demands grinding of cement in water continuously for five days [Powers, 1949].

The process of hydration proceeds by a progressive reduction in the size of the cement particles. The percentage composition of the residue of a cement grain, after a certain period of hydration, remains the same as that of the original grain [Copeland, 1956], but the composition of the residue does change throughout the period of the hydration of cement [Copeland et al, 1960].

Hydration of Calcium Silicates

Both the tricalcium and dicalcium silicates (C_3S and C_2S) react with water to form the same product according to the following chemical equations [Neville, 1995]:

$$C_3S + 6H \rightarrow C_3S_2H_3 + 3Ca(OH)_2 \quad (1.1)$$

$$2C_2S + 4H \rightarrow C_3S_2H_3 + Ca(OH)_2 \quad (1.2)$$

The proportions of masses by parts by weight of reactants and products in Eqs. 1.1 and 1.2 are as follows:

For Eq. 1.1, $100 + 24 \rightarrow 75 + 49$ (1.3)

For Eq. 1.2, $100 + 21 \rightarrow 99 + 22$ (1.4)

Eqs. 1.3 and 1.4 show that although there is less difference between the water demands for C_3S and C_2S, the C_3S produces twice as much $Ca(OH)_2$ as is formed by the hydration of the C_2S. The rates of hydration for both the silicates are also considerably different as shown in Figure 1.1 [Copeland and Bragg, 1953].

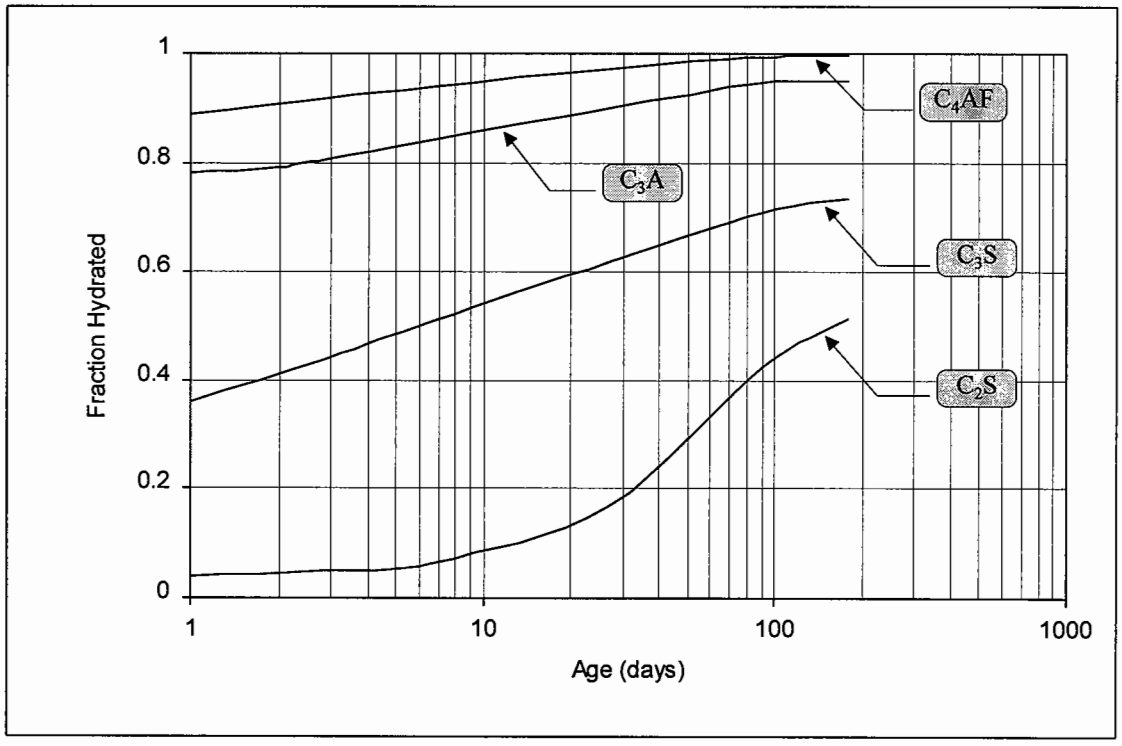

Figure 1.1. The rate of hydration of pure calcium silicates and aluminates [Copeland and Bragg, 1953].

Hydration of C_3A and C_4AF

The C_3A is extremely reactive to water. This reaction causes immediate stiffening of the cement paste, termed flash set, which is prevented by adding gypsum to cement clinkers [Neville, 1995] at the time of grinding. Gypsum and C_3A react to form insoluble calcium sulphoaluminate ($3CaO.Al_2O_3.3CaSO_4.31H_2O$), which changes into a product $3CaO.Al_2O_3.CaSO_4.12H_2O$, and eventually leads to the formation of tricalcium aluminate hydrate C_3AH_6, which is a stable product [Steinour, 1952].

C_3A does not contribute to the strength of cement paste except at early ages [Neville, 1995]. Its presence in cement is rather harmful as it leads to the formation of calcium sulphoaluminate when the hardened cement paste is attacked by sulphates. This calcium sulphoaluminate expands in volume and causes damage to the hardened cement paste. The only advantage of C_3A is during the manufacture of cement, because it acts as a flux and reduces the temperature of burning of clinkers and supports the combination of lime and silica. C_4AF also acts as a flux. Both the C_3A and C_4AF accelerate the progress of reactions in the kiln. Moreover, gypsum reacts with C_3A and C_4AF to produce some calcium sulphoaluminate and calcium sulphoferrite which may accelerate the hydration of silicates [Neville, 1995]. The chemical reactions of C_3A and C_4AF are given by Eqs. 1.5 and 1.6:

$$C_3A + 6H \rightarrow C_3AH_6 \tag{1.5}$$

$$C_4AF + 2Ca(OH)_2 + 10H \rightarrow C_3AH_6 + C_3FH_6 \tag{1.6}$$

The amounts of water which react chemically with C_3A and C_4AF are approximately 40% and 37% by mass, respectively [Neville, 1995]. These are much higher than those required by C_3S and C_2S (24% and 21% respectively).

1.3.3 Influence of Cement Hydration

The hydration of cement is an exothermic chemical reaction. The rate of hydration is related to the rate of heat evolved during the course of hydration [Bye, 1983]. Figure 1.2 provides an understanding of the rate of hydration in terms of the rate of heat evolution.

It seems that the first very high peak (Figure 1.2) is caused by the initial hydration of C_3A (refer Figure 1.1), and occurs during the first two hours after the addition of water into dry cement [Neville, 1995]. Figure 1.2 shows that the maximum rate of heat evolution occurs during the first 24 hours, indicating the maximum rate of cement hydration. The rate of hydration remains relatively high during the first three days, and thereafter, it slows down over an extended period [Brunauer et al, 1973].

At any stage of the hydration process, the hardened cement paste comprises crystallized hydrates of various compounds, termed gel, of crystals of $Ca(OH)_2$, some minor components, unhydrated cement, and the residue of the water-filled spaces in the fresh paste which are called capillary pores. In addition, there are some interstitial voids within the gel, known as gel pores with a size of 3 nm nominal diameter [Neville, 1995]. On the other hand, the size of the capillary pores is nearly 2 to 3 times that of the gel pores [Neville, 1995].

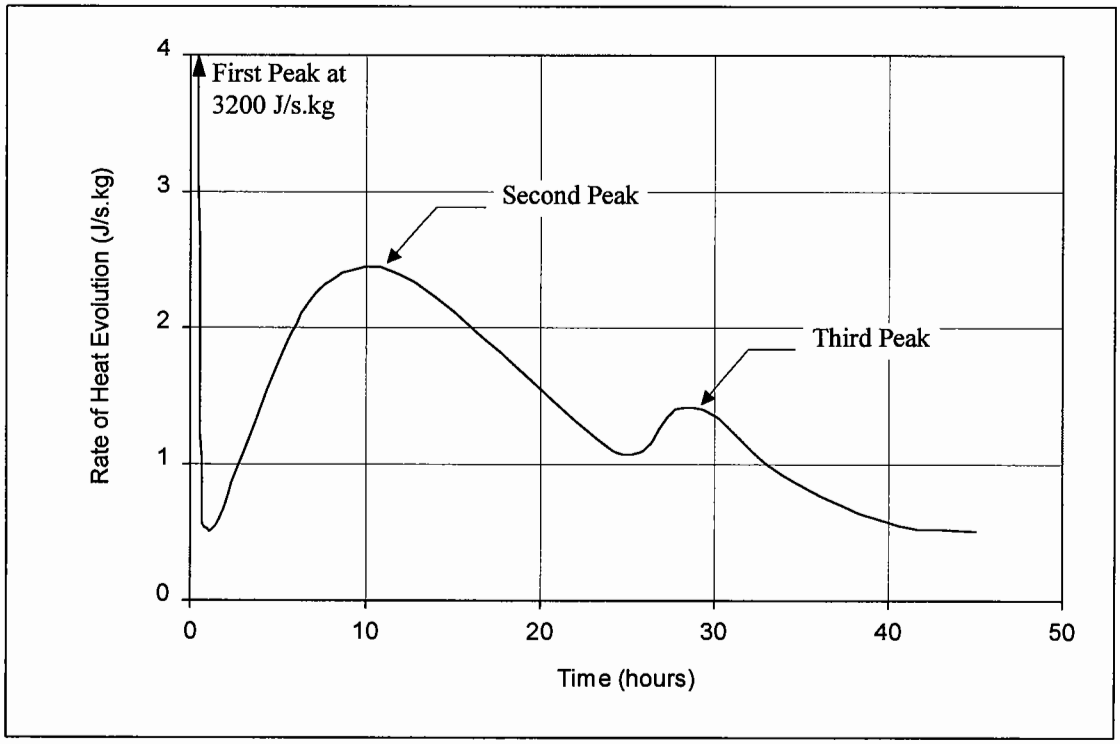

Figure 1.2. Relationship between the rate of heat evolution and time for Portland cement [Bye, 1983].

The process of hydration has been reported [Neville, 1995] to cause a considerable increase in the surface area of the solid phase that absorbs a large amount of free water. In the absence of any movement of water to and from the cement paste (by curing), the reaction of hydration keeps using up the water until too little is left to saturate the solid surface. The relative humidity within the paste decreases, thus leading to the phenomenon of self-desiccation [Neville, 1995]. This self-desiccation is one main reason for shrinkage in cement bound materials [George, 1973].

1.4 SHRINKAGE IN CEMENT BOUND BASES

Cement bound bases are susceptible to shrinkage from an early stage after their construction. The two main reasons are hydration of cement and thermal effects. Accordingly, the overall shrinkage of the CBM bases can be sub-divided into primary and thermal shrinkage depending on the two different factors responsible for this phenomenon.

1.4.1 Primary Shrinkage

Primary shrinkage, also called drying shrinkage, is strictly associated with moisture movement in a CBM mix [Han and Lytton, 1995]. As described above (Section 1.3.3), the loss of moisture from capillary pores, caused by self-desiccation due to the hydration of cement and drying of a CBM, is actually responsible for this type of shrinkage.

The loss of water by evaporation, from the surface of a CBM, can be expected even at the very early stage, while the mix is still in the plastic form [Neville, 1995]. A similar loss can also occur through suction by the underlying dry sub-base or subgrade [Hermite, 1960]. These factors cause a slight contraction of the CBM mix in its plastic form, termed plastic shrinkage [Neville, 1995]. The amount of the water lost from the surface is influenced by the surrounding temperature, ambient relative humidity, and wind velocity (Table 1.5). Therefore, construction during hot weather demands special attention to keep the rate of evaporation to a minimum.

Table 1.5. Plastic shrinkage of cement paste in air at 50% relative humidity and 20°C temperature [Hermite, 1960]

Wind Velocity (mph)	Plastic Shrinkage (10^{-6}) (8 hours after placing)
0	1700
1.35	6000
2.25	7300
16 to 18	14000

According to George [1973], cement can absorb up to 38% of water by its own weight during complete hydration. He observed the shrinkage resulting from the hydration process on soil-cement beams coated with wax, and found that these beams shrank by 17% of their maximum shrinkage without any loss of moisture due to evaporation.

There are three major shrinkage mechanisms: surface tension, disjoining pressure, and hydrostatic tension in the capillary pores [Young, 1982; Vos, 1971; Nilson, 1980]. Disjoining pressure is developed in capillary zones where adsorption is hindered [Young, 1982; Vos, 1971]. Hydrostatic tension is developed in a capillary pores, when menisci are formed due to the lost water. Both the disjoining pressure and hydrostatic tension are active when relative humidity is over 50%, whereas surface tension is active for a relative humidity below 50% [Han and Lytton, 1995]. The removal of adsorbed water takes place once the capillary water is lost [Neville, 1995]. All these mechanisms lead to shrinkage. A part of the primary shrinkage may be related to the removal of intercrystalline water, thereby leading to a change in the lattice structure, because calcium silicate hydrate has been seen to undergo a change in the lattice spacing from 1.4 to 0.9 nm on drying [Bernal, 1952]. Hydrated C_4AF and calcium sulphoaluminate also show a similar response [Lea, 1960].

The magnitude of primary shrinkage tends to increase at higher cement contents, higher temperatures, and possibly with finer cements [Houk et al, 1969], and with cements containing a higher content of C_3A and C_4AF [Neville, 1995]. The use of a higher cement, in a CBM, leads to a larger volume of the hydrated cement paste

which is susceptible to shrinkage. The average aggregate size and water cement ratio also influence the primary shrinkage [Marais et al, 1973]. Mix water content appears to have the most significant effect, such that compaction of a CBM at a moisture content wet of the optimum results in an appreciably higher shrinkage [Marais et al, 1973]. The amount of shrinkage, however, can be reduced by adding some amount of fly-ash into a constant content of blended cement [Houk et al, 1969], and by improving compaction [George, 1968].

The phenomenon of shrinkage is not only attributable to cement, but also to other hydraulic binders such as fly-ash, slag and lime [Judycki, 1991]. Table 1.6 shows that lean concrete has the lowest primary shrinkage in comparison with other stabilized materials. This may be because of the relatively less amounts of cement and water required by the washed and graded aggregates [Marais et al, 1973]. The soils stabilized with cement, lime and fly ash (0.5:0.5:8), show a reduced shrinkage compared to those stabilized with cement [Natt and Joshi, 1984]. Shrinkage is usually expressed as a linear strain [Neville, 1995], as given in Table 1.6, although it is a three-dimensional parameter.

Table 1.6. Primary shrinkage of different types of stabilized materials.

Stabilized Material	Characteristics	Shrinkage (microstrain)	Researcher
Lean concrete	Washed aggregate	150-700	Marais et al, 1973
Soil cement	Clay[1] content < 5 % 5-10 % 10-15 % 15-20 %	500-1400 900-2400 1400-3700 3000-5500	George, 1968
Cement stabilized gravel-sand mixture	50% passing 2mm 18% passing 74 μm (cement content 5.5%)	400-1100	Pretorious and Monismith, 1971
Lime stabilized soils	PI of soil < 10 % 10-20 % 20-28 %	1700-2300 2300-6300 6300-11000	TRB, 1978
Stabilized sand or gravel-sand mixture	Cement, lime and fly-ash[2] (0.5 : 0.5 : 8)	400-800	Natt and Joshi, 1984

Note [1] : Montmorillonite clay particles cause more shrinkage than those of kaolinite.
[2] : Total binder content is 20%, another combination may be cement or lime with fly-ash (1:8).

Estimation of Primary Shrinkage

The most recent model for calculating primary shrinkage has been given by Gardner and Zhao [1993]. This involves correction factors for: (i) age of CBM (or concrete), (ii) strength of CBM, (iii) type of cement, (iv) size of a CBM base, and (v) relative humidity. According to this model, the shrinkage of a CBM base, at any time t with a relative humidity H_r can be calculated from its ultimate shrinkage at 40% relative humidity by using the following relations:

$$\varepsilon_s = \varepsilon_{su} \times \beta(H_r) \times \beta(t) \tag{1.7}$$

$$\varepsilon_{su} = 900 \times K \times [f_c'/f_{cmt}]^{\frac{1}{2}} \times [25/f_c']^{\frac{1}{2}} \times 10^{-6} \tag{1.8}$$

$$\beta(t) = \left[\frac{7.27+\ln(t-t_c)}{17.18}\right] \times \left[\frac{t-t_c}{(t-t_c)+0.0125\times(V/S)^2}\right] \tag{1.9}$$

$$\beta(H_r) = [1-(H_r)^4]$$

where:

ε_s : shrinkage

ε_{su} : ultimate shrinkage at 40% relative humidity

H_r : relative humidity expressed as decimal ($H_r < 0.99$)

t : age of CBM (days)

t_c : age of CBM when drying commenced (days)

K : constant with values: 1, 0.7 and 1.33 for ordinary cement (Type I), modified cement (Type II) and rapid hardening cement (Type III), respectively.

f_c' : mean compressive strength of CBM at 28 days (N/mm^2)

f_{cmt} : mean compressive strength of CBM when drying commenced (N/mm^2)

V/S : volume to surface ratio of a CBM base (mm)

Eq. 1.7 is applicable to CBMs (or concrete) comprising non-shrinking aggregates, such as granite, quartzite and limestone [Gardner and Zhao, 1993]. In contrast, CBMs

made with shrinking aggregates, such as (some) dolerites, basalts, and some sedimentary rocks (e.g. greywacke) and mudstone, have been reported [Neville, 1995] to cause excessive deflection or warping, leading to serviceability problems.

The magnitude of shrinkage is greatly influenced by the relative humidity of the surrounding medium. Figure 1.3 shows two relationships, between the relative humidity and the corresponding relative shrinkage value, given by ACI 209R-92 [1994], and Hansen and Almudaiheem [1987]. These relationships can be used for estimating shrinkage at a given relative humidity on the basis of a known value of shrinkage at some other relative humidity (40%). The mathematical expression of the ACI 209R-92 [1994] relationship is given by Eq. 1.10:

$$\varepsilon_s = \frac{t}{35+t}\varepsilon_{su} \tag{1.10}$$

where:

ε_s : shrinkage after t days, since the end of moist curing

ε_{su} : ultimate shrinkage

t : time in days, since the end of moist curing

Differential Shrinkage

In the field, moisture loss normally takes place from the surface of a CBM base due to evaporation, so that a moisture gradient is established with depth, which leads to the situation of differential shrinkage. This induces internal stresses, tensile near the surface and compressive near the bottom [Neville, 1995], thus resulting in warping (or curling) of the CBM base. The progress of shrinkage from the drying surface downwards is gradual, but very slow. Ross [1944] found the difference between shrinkage in a mortar slab at the surface and at a depth of 150 mm to be 470×10^{-6} after 200 days. With such a value of differential shrinkage, and considering an average value of 21 GPa for the elastic modulus of mortar, the magnitude of tensile stress is almost 10 MPa, which is sufficient to induce surface cracking [Neville, 1995].

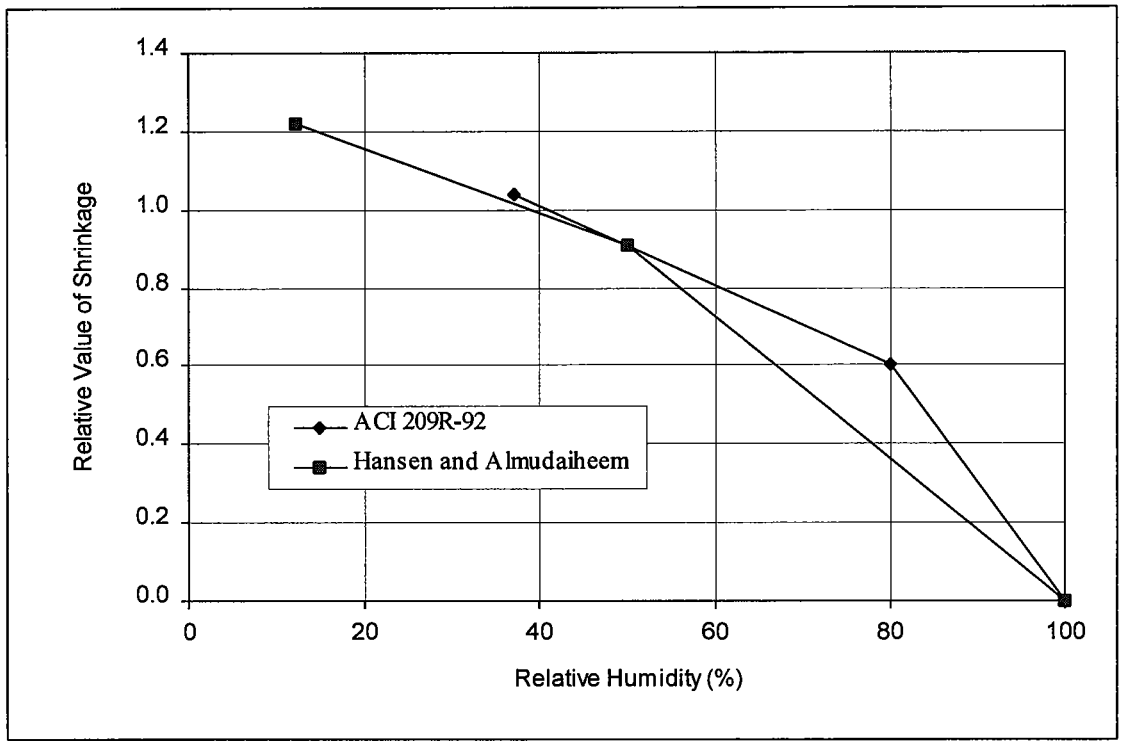

Figure 1.3. Relative value of shrinkage as a function of the ambient relative humidity [ACI 209R-92, 1994; Hansen and Almudaiheem, 1987].

Tensile Stresses Induced by Primary Shrinkage

According to Pretorius and Monismith [1971], free shrinkage in a CBM base is restrained by the friction of adjoining (top and bottom) layers, differential shrinkage, and continuity of the layer. By using a finite element method, they found that the shrinkage induced stresses could be in the range 0.07 to 0.17 MPa under uniform shrinkage. The conditions of uniform shrinkage refer to the same level of relative humidity at the top and bottom of a cement bound base. In practice, it is almost impossible to achieve the uniform humidity conditions. Non-uniform humidity, leading to a differential shrinkage, induces relatively high tensile shrinkage stresses (Figure 1.4). These stresses increase with time and may attain values of the order of 2.0 MPa at an early stage after construction (Figure 1.5), which are sufficiently higher than the tensile strength of a relatively fresh CBM layer [Pretorius and Monismith, 1971]. The result is therefore the occurrence of transverse cracks. After cracking, the shrinkage stresses are greatly reduced, near the cracks, due to elastic recovery of the material. The occurrence of a crack relieves the tensile stresses in a zone of approximately 100 cm on either side [George, 1973, 1974].

George [1971] found that the tensile shrinkage stresses attain their maximum value during an early stage of 40 to 100 hours depending on the restraint conditions and thereafter gradually decrease. Therefore, a CBM base needs special attention for its curing during the first 2 to 4 days after construction. During this period, the maximum shrinkage stress on the exposed surface of the CBM base can be estimated as follows [George, 1971]:

With no restraint, $$\sigma_{su} = 0.208 E \varepsilon_{su} \quad (1.11)$$

With complete restraint, $$\sigma_{su} = 0.273 E \varepsilon_{su} \quad (1.12)$$

where:

σ_{su} : maximum tensile stress due to primary shrinkage (N/mm^2)

ε_{su} : maximum strain due to primary shrinkage

E : modulus of elasticity of the CBM (N/mm^2)

George [1973] concluded that, regardless of the restraint conditions, the shrinkage stresses are highly localized on the exposed surface and decrease sharply with depth.

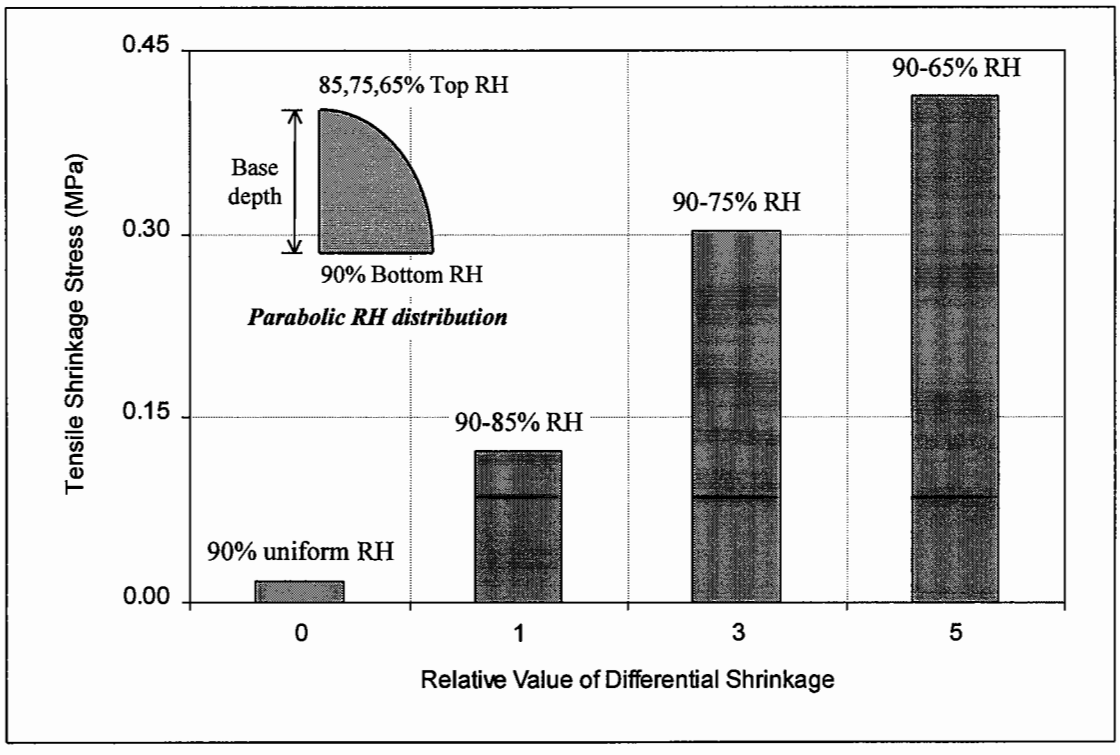

Figure 1.4. Effect of relative humidity (RH) on the tensile shrinkage stresses in a soil-cement base [Pretorius and Monismith, 1971].

Figure 1.5. Effect of age on the tensile shrinkage stresses [Pretorius and Monismith, 1971].

1.4.2 Thermal Shrinkage

After construction, a CBM base is subjected to variations in temperature, which causes thermal shrinkage. This type of shrinkage is mainly attributable to the thermal properties of aggregates. Its magnitude is dependent on the amount of temperature drop and the values of thermal coefficient for different aggregates (Table 1.7). By assuming a cement bound layer as a linear elastic material, the thermal shrinkage corresponding to a temperature drop ΔT in a free CBM base (with no restraints or friction), can be defined as follows:

$$\varepsilon_t = \alpha \Delta T \tag{1.13}$$

If the shrinkage is restricted in a CBM base due to restrained conditions, i.e. continuity of the CBM base and friction of the adjoining layers, tensile stresses would be developed in accordance with the following relation:

$$\sigma_t = E \alpha \Delta T \tag{1.14}$$

Table 1.7. Mean thermal coefficient of concrete made with different aggregates [Bonnell and Harper, 1951; Shacklock, 1974; Taylor and Williams, 1981]

Description of Aggregate	Thermal Coefficient, α ($\times 10^{-6}$ per ^{o}C)
Quartzite	13.1
Flint	12.8
Chert	11.8
Sandstone	11.7
Gravel	11.4
Quartz	11.3
Blastfurnace slag	10.6
Dolerite	9.5
Granite	9.5
Basalt	9.2
Silicious Limestone	9.0
Portland stone	7.4
Limestone	7.3
Gritstone	6.0
Marble	5.8

When these stresses approach the tensile strength, they fracture the CBM base by inducing transverse cracks. The temperature drop which causes this fracture, can be calculated as follows:

$$\Delta T_f = \frac{f_t}{E\alpha} \tag{1.15}$$

where:

ε_t : thermal shrinkage strain

σ_t : tensile stress due to thermal shrinkage (N/mm^2)

f_t : tensile strength of the CBM base (N/mm^2)

E : elastic modulus of the CBM base (N/mm^2)

α : coefficient of thermal expansion

ΔT : temperature drop inducing tensile stress σ_t (^{o}C)

ΔT_f : temperature drop causing fracture of the CBM base (^{o}C)

From an experimental study, Colombier et al [1988] found the following values of the fracture temperature drop for two types of stabilized materials:

$\Delta T_f = 6\ ^{o}C$ for gravel-sand mixture

$\Delta T_f = 10$ to $15\ ^{o}C$ for sand-slag mixture

Considering such low values of ΔT_f, it can be seen that cracking due to thermal changes is inevitable in cement bound layers. Through a laboratory investigation, Colombier et al [1988] found that the value of thermal shrinkage is lower for fine graded aggregates (stabilized sands) with no clay content, than for coarse graded aggregates (stabilized gravels).

1.5 CRACKING IN CEMENT BOUND BASES

Cracking in a CBM base is mainly the result of its failure in tension. It is well established that a pavement layer, whether cement bound, concrete or asphalt, will crack when the induced stresses, either externally applied or internally developed, exceed the tensile strength of the material [George, 1973; Wang, 1973; Haas and Topper, 1969; Hajek and Haas, 1972]. Externally applied stresses may be due to traffic and drag resulting from the cracking of an adjacent layer (sub-base or subgrade), whereas internally induced stresses are associated with primary and thermal shrinkage. In brief, the two important factors contributing to cracking are, therefore [George, 1973]:

- Primary shrinkage, thermal shrinkage due to diurnal and seasonal temperature variations, and traffic induced stresses.
- Stresses developing from shrinkage cracking of the sub-base or subgrade.

Whether or not cracking is present depends not only on the potential shrinkage, but also on the extensibility of a CBM base, its strength, and its degree of restraint to deformation [Kelly, 1964]. Cracking can be avoided only if the induced stresses are, at all times, smaller than the tensile strength. The effect of time on shrinkage cracking is two-fold: the strength increases, thereby reducing the risk of cracking, but the elastic modulus also increases so that the stress induced for a given amount of shrinkage becomes larger [Neville, 1995].

Depending on mechanism, cracking in the CBM bases is categorized into primary and secondary cracking. Each type of cracking is associated with a different mode of influence on the performance of a pavement.

1.5.1 Primary Cracking

Primary cracking is caused by the tensile stresses developed in the longitudinal direction of a cement bound base due to primary and thermal shrinkage [Mayhew & Potter, 1986: George, 1971]. It appears in the form of transverse cracks.

There is a difference in opinion, from various researchers, about the basic mechanism of primary cracking. According to Pretorius and Monismith [1971], Wang [1973], and George [1971, 1973, 1974], it is mainly caused by primary shrinkage. George [1971] has reported that self-desiccation due to cement hydration causes about 15 to 20 percent of primary cracking. On the other hand, Colombier et al [1988] believe that thermal shrinkage is the main cause of this type of cracking in CBM bases, and is purely related with temperature changes.

Transverse cracks may be initiated by primary shrinkage and developed by thermal shrinkage [Otte, 1978; Wang, 1973]. Nonetheless, shrinkage and cracking do not go hand-in-hand with each other. Factors such as geometric and restraint characteristics of the CBM layer, tensile properties, and environmental factors such as mix proportions, curing and temperature also control the development of the shrinkage stresses and cracking behaviour [Wang, 1973]. The warping and subgrade restraint stresses also contribute to primary cracking [Williams, 1986]. Such stresses are developed when temperature variations tend to warp and shorten a continuous CBM base, thus acting against its self weight and the friction of the foundation [DoT, HA 38/88, 1988]. Cracking starts at the weakest locations on the surface of a stabilized layer, such as microcracks formed by rolling, and penetrates downwards in a direction perpendicular to that of the maximum shrinkage stresses. In fact, under shrinkage stresses, small flaws in a CBM base start growing and coalescing to form firstly microcracks and thereafter macrocracks [George, 1973].

Water content is one of the most important factors which influence primary cracking. An increase in the water/cement ratio tends to increase shrinkage and, at the same time, decrease the CBM strength, thus enhancing the cracking susceptibility. An increase in the cement content also increases shrinkage and, therefore, the cracking tendency, but its effect on the CBM strength is positive. In the field, there is a further complication where surface cracking affects the amount of actual shrinkage and causes a redistribution of the internal stresses [Neville, 1995]. This is because the cracking possibly increases the rate of loss of water. Such a surface cracking is, however, minimal in the case of small sized laboratory specimens.

The performance of a pavement can be adequate with good load transfer as long as the cracks are of less than 0.5 mm width and resistant to deterioration (details are given in Chapter 5). These cracks increase in number when the shrinkage and temperature stresses are increased by traffic. As an example, Figure 1.6 shows the occurrence of primary cracking visualized 14 days after the construction of a 150 mm thick CBM sub-base at Stumpcross, near Cambridge. This pavement involved a flint gravel plus sand aggregate, and was constructed in July 1994.

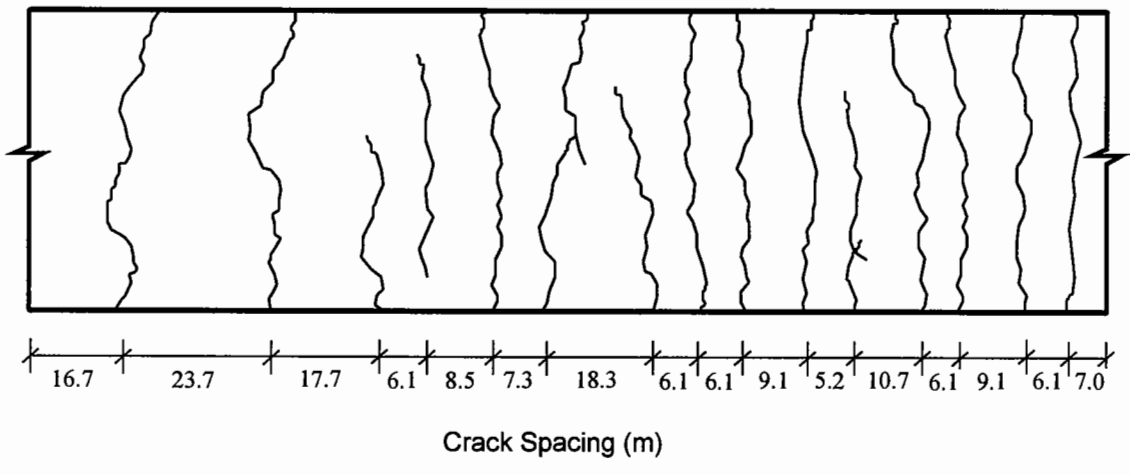

Figure 1.6. Primary cracking in a flint gravel sand cement bound sub-base at Stumpcross, near Cambridge.

Crack Spacing and Width

The spacing and width of primary cracking in a CBM base are closely related to its tensile strength. The use of a relatively stronger CBM leads to relatively wider transverse cracks at larger spacing, in comparison with a weak soil-cement base which develops many frequently spaced narrow cracks. Norling [1973] studied the crack width distribution 77 days after the construction of soil-cement bases for different airfield sites in Australia. The results of his study (Figure 1.7) indicate that the width of most of the cracks is less than 1.0 mm. These cracks occur at fairly regular intervals over a range of spacing, from 3 to 50 m [Shahid, 1996], depending on the type of aggregate involved and strength of the CBM base. According to George [1973, 1974], the crack spacing is a function of the following factors:

- Shrinkage stresses.
- Variations of CBM strength along the base length (due to distribution of flaws).
- Width of the stress relief zone surrounding individual cracks.

Among the factors governing crack spacing and width, the influence of cement content is quite important. The use of a lower cement content reduces the amount of shrinkage, but increases the tendency of closely spaced cracks due to a lower tensile strength of the resulting CBM base. On the other hand, with increased cement content, the tensile strength increases, leading to the occurrence of widely spaced cracks of greater width. Thermal properties of aggregates are equally important. Limestone CBM, having a relatively lower thermal coefficient, is less affected by temperature variations and develops transverse cracks at larger spacing [DoT, HA 38/88, 1988], than a flint gravel sand CBM, provided that both the CBMs belong to the same category.

According to George [1968] and Colombier et al [1988], crack spacing can be defined by the following relation:

$$l_c = \frac{2 f_t}{\mu \gamma} \tag{1.16}$$

Similarly, crack width, as defined by George [1968, 1971], can be expressed through the following relation:

$$\delta = \varepsilon_c l_c - \frac{\mu\gamma l_c^{\,2}}{4E_t} \tag{1.17}$$

The above relation (Eq. 1.17) was modified by Colombier et al [1988] as follows:

$$\delta \cong \frac{2\varepsilon_c f_t}{\mu\gamma} \tag{1.18}$$

where:

l_c : maximum crack spacing (m)
δ : crack width (m)
f_t : ultimate tensile strength of material (N/m^2)
μ : coefficient of sliding friction
γ : unit weight of material (N/m^3)
ε_c : shrinkage strain at cracking stage
E_t : elastic modulus of CBM in tension (N/m^2)

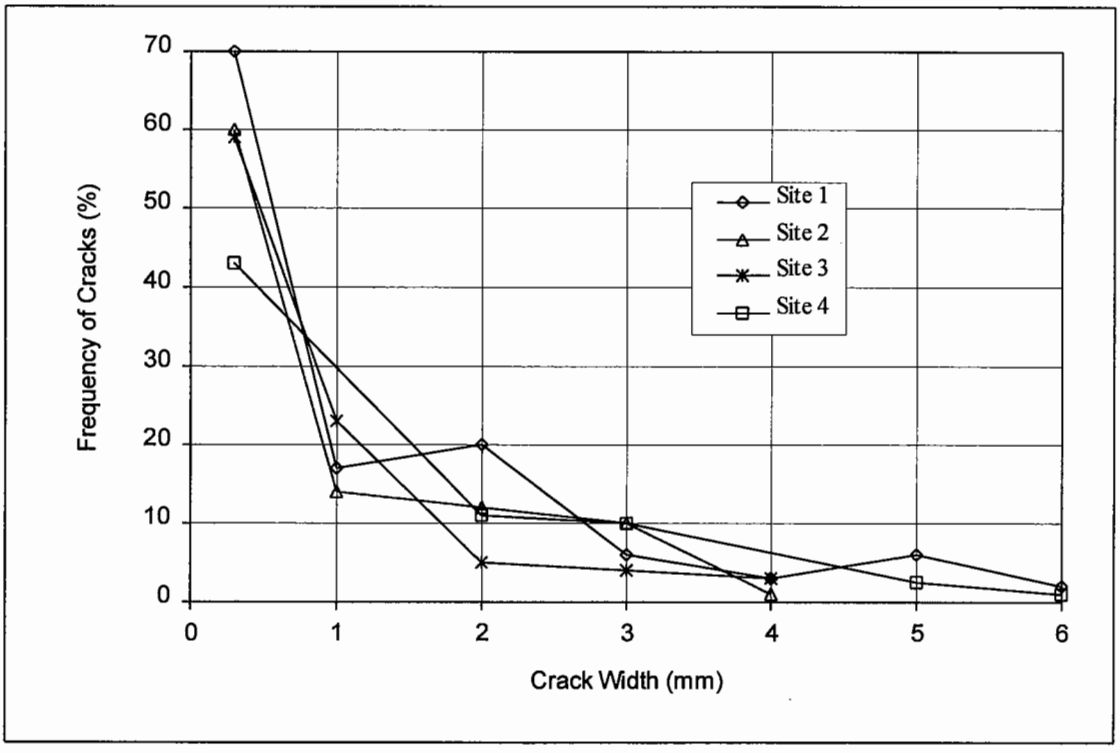

Figure 1.7. Crack width distribution from different soil-cement base airfields in Australia [Norling, 1973]

1.5.2 Secondary Cracking

Once a CBM base has developed transverse primary cracks, there is a tendency for differential vertical movement across the crack faces under trafficking. If the CBM is not strong enough, the material will deteriorate further due to repeated traffic loading, and will provide a limited load transfer in the long term. With the progress of deterioration of the material adjacent to the cracks, the differential vertical movement increases, and heavy traffic loading starts inducing relatively higher flexural stresses due to excessive deformation of the CBM base segments (bounded by the transverse cracks). This ultimately leads to the occurrence of longitudinal wheel-path cracks. This phenomenon is termed as secondary cracking (Figure 1.8). Construction joints and differential settlement of the road foundation also contribute to secondary cracking.

Unlike primary cracking, secondary cracking is generally responsible for more serious damage to the structural integrity of a pavement. Experience from the evaluation of actual pavements indicates that an initial elastic stiffness modulus for a typical intact cement bound base is almost in the range 20,000 to 30,000 MPa, but the effective stiffness modulus is generally reduced to a value as low as 1000 to 3000 MPa after the occurrence of secondary cracking. This explains why a (down-rated) value of 500 MPa was assumed, after the occurrence of secondary cracking, by Pell and Brown [1972] in their two stage design. This cracking, accompanied by a reduced stiffness of the CBM base, starts deterioration of the whole of the pavement structure at a fairly rapid rate, and causes a drastic reduction in the load spreading capability of the structural layers [DoT, HA 38/88, 1988].

Further progressive damage can convert a (relatively weak) cement bound pavement into blocks due to the formation of severe polygonal cracking. The crack intersections may lead to the formation of local depressions, causing full depth failure of the pavement [Blight, 1973].

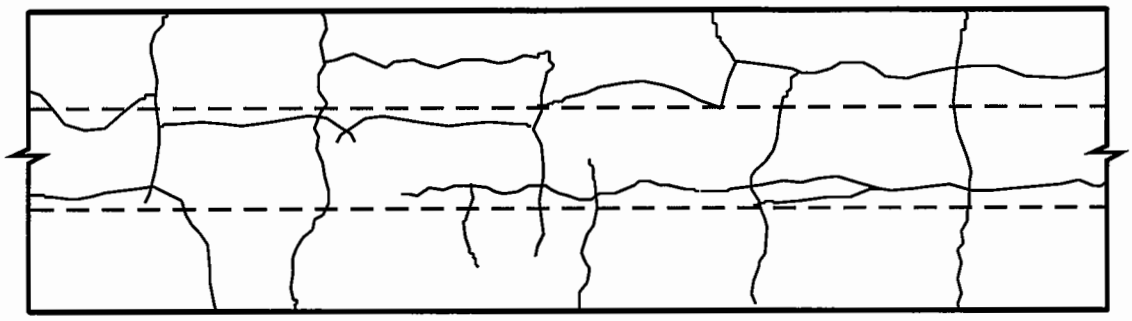

Figure 1.8. Secondary cracking pattern on a motorway in Scotland [scale 500 : 1, Brown et al, 1993].

1.5.3 Factors Affecting the Cracking of CBM Bases

There are several factors which influence the extent of cracking in cement bound bases, as discussed above (in various sections). A brief summary of these is given in the following paragraphs.

CBM Strength

Stronger CBM bases develop less transverse cracks, and are more resistant to traffic induced cracking. A weaker CBM base is subjected to more extensive cracking. The strength of the CBM base also determines the crack width and spacing [Bonnot, 1972].

Cement Content

The use of a higher cement content, in a CBM, leads to larger volume of the hydrated cement paste which is liable to shrinkage [Houk et al, 1969] and therefore increases the potential for cracking [Neville, 1995]. On the other hand, a lower cement content reduces the amount of shrinkage, but increases the cracking tendency because of a lower tensile strength of the resulting CBM base.

Water Content

An increase in the mix water content tends to an increased shrinkage [Marais et al, 1973], and decreases the CBM strength, thus enhancing the cracking susceptibility

[Neville, 1995]. A laboratory study [Colombier et al, 1988] also showed that shrinkage decreases at relatively low water contents.

Thermal Properties of Aggregates

CBMs comprising aggregates having lower thermal coefficients, are less sensitive to thermal shrinkage, and develop fewer transverse cracks [DoT, HA 38/88, 1988] at greater spacing.

Grading of Aggregates

Larger aggregates enhance crack intensity by virtue of their ability to intensify stresses in the shrinking matrix, thus increasing the cracking tendency [George, 1973, 1974]. Fine graded aggregates, for example stabilized sands, are more resistant to thermal shrinkage cracking [Colombier et al, 1988].

Clayey Admixtures in Aggregates

The presence of clayey admixtures increases the shrinkage of a CBM base, and hence cracking susceptibility [Colombier et al, 1988].

Degree of Compaction

Better compaction increases the strength of a CBM base, therefore making it more resistant to cracking. Poor compaction leads to weak zones (flaws) in the CBM base which can support crack initiation [George, 1973]. The amount of shrinkage can also be reduced to some extent by improved compaction [George, 1968].

Thickness of Bituminous Surfacing

The use of a thick bituminous surfacing may provide a better thermal insulation for a CBM base, thereby possibly reducing the risk of thermal shrinkage and resulting cracking in extreme climates.

Friction of the Sub-base or Subgrade

The shrinkage stresses induced in a CBM base also depend on the frictional restraint conditions [Wang, 1973; Kelly, 1964], provided by the underlying sub-base or subgrade.

Stiffness of the Sub-base or Subgrade

A CBM base laid over a relatively stiff sub-base or subgrade is less likely to undergo excessive deflection under traffic loading. The primary cracks would be subjected to a smaller amount of differential vertical movement. As a result, the CBM base will have a greater resistance against secondary cracking. A stiffer foundation is also useful in attaining a better compaction of the CBM base.

Traffic

CBM bases are particularly susceptible to the effects of heavy wheel loads unless they are appropriately designed. For example, only a few passes of a medium sized truck can crack a 100 to 120 mm thick cement (or lime) stabilized base [Bulman, 1972]. Brengarth and Roche [1979] further confirmed that cement stabilized bases of inadequate thickness may perform well only under light traffic, but a very few passes of the heavy vehicles can cause rapid deterioration of the pavement.

Construction Temperature

The dimensions of a CBM layer, at the time when the fresh mix ceases to deform plastically, are related to temperature during construction [Neville, 1995]. A subsequent drop in temperature will produce potential contraction. Steep temperature or moisture gradients produce severe internal restraints and are associated with a high cracking tendency. Therefore, construction of a CBM base during hot weather will have a high tendency to crack. However, if a CBM base is constructed in cold weather, it is subjected to less thermal shrinkage, and consequently it develops relatively fewer narrow cracks [DoT, HA 38/88, 1988]. Similarly, small variations between the day and night temperatures are also desirable during the construction of a CBM layer.

1.6 REFLECTIVE CRACKING

The occurrence of primary and secondary cracking in a CBM base is undesirable mainly because it leads to the phenomenon of 'reflective cracking' in flexible composite pavements (comprising CBM bases and a bituminous surfacing*). This can be defined as a process of the propagation of cracks, in a cement bound base, through the overlying bituminous layers to the surface [Foulkes and Kennedy, 1986]. The governing mechanism for reflective cracking is the excessive relative horizontal and vertical movements, resulting from both traffic loads and thermal stresses [Coetzee and Monismith, 1980], at the tip of the cracks in a CBM base. These movements develop high tensile strains in the bituminous surfacing, therefore causing the initiation and propagation of cracks. These cracks may propagate from the underside of a bituminous layer to the surface or from its top to the bottom to join the existing cracks in a CBM base [Nunn, 1989; DoT, HA 38/88, 1988], but the mechanism is not yet very well-defined.

Secondary cracking, once developed, dominates in the phenomenon of reflective cracking [George, 1973]. Depending on the cracking susceptibility, the extent of reflective cracking is influenced by the type of a stabilized base comprising different aggregates and binders. A greater number of reflected cracks have been reported on pavements involving stabilized gravel bases than those with stabilized sands [Colombier et al, 1988]. Figure 1.9 shows the results of a study over a period of 10 years. The horizontal lines, inside the bars, represent the data collected from different roads involving the same type of stabilized base.

The most harmful aspect of reflective cracking is that it makes the whole pavement structure susceptible to water infiltration, which: accelerates the deterioration of cracks in (weaker) CBM and bituminous layers, decreases the subgrade strength by softening it [DoT, HA 38/88, 1988], and thus leads to a premature failure of the pavement.

---

*The term *surfacing* is used throughout this thesis to mean the combined bituminous thickness, that is a wearing course, basecourse, and upper roadbase.

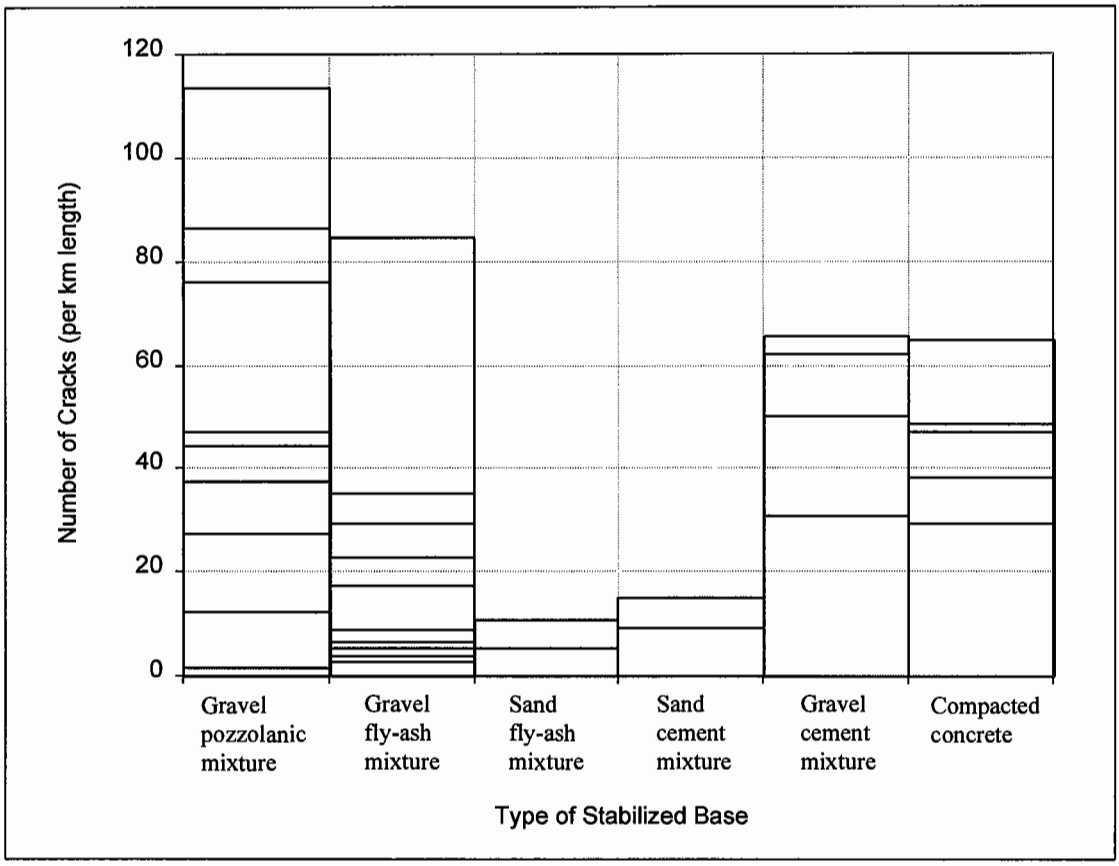

Figure 1.9. Effect of type of stabilized base on transverse cracking (per km length) [Colombier et al, 1988].

1.6.1 Measures to Control Reflective Cracking

The problem of reflective cracking is not only associated with new flexible composite pavements, but is also a major concern for the maintenance of existing roads. There are several measures, currently in use, to prevent or delay reflective cracking.

Use of Thick Bituminous Surfacing

The current UK design specification [DoT, HD 26/94, 1994] permits a minimum of 200 mm thick bituminous surfacing over a CBM base for indeterminate design (over 20 million standard axles). This increases the time elapsed for the crack propagation by decreasing the stress per unit area directly above the crack [Jacob, 1993] in a CBM base, but does not prevent the phenomenon. This technique increases the cost of the pavement.

Open Graded Bituminous Surfacing

The use of an open graded bituminous mix (100 mm thick) over a cracked CBM base (or an old cracked pavement), covered with a 20mm gap-graded bituminous base course and a normal wearing course, can be used as a crack relief layer [Hensley, 1980] in order to delay reflective cracking. The strain concentrations, at the crack tips, are dissipated into the interconnecting voids of this crack relief layer.

Stress Absorbing Membrane Interlayer (SAMI)

An interlayer of a modified type of asphalt (≅ 10 mm thick), placed between an existing cracked pavement and the new overlay, may perform like a slip plane to isolates the thermal effects of the old pavement from the new overlay [Jacob, 1993]. A SAMI is not intended to increase the tensile strength of the overlay, but it may absorb, to some extent the vertical and horizontal strains because of its unique characteristics of flexibility, elasticity and improved temperature susceptibility [Jacob, 1993].

Stress Absorbing Membrane (SAM)

The fibre-reinforced microsurfacing technique, termed SAM, is another thin layer of a modified type of asphalt (≅ 10 to 13 mm thick), which is used as surface dressing. According to Alberola and Gordillo [1993], it may help in delaying reflection cracking through two-fold action. Firstly, it seals the existing cracks to inhibit the ingress of water into the road foundation. Secondly, it may add somehow to the tensile strength of the bituminous overlay [Alberola and Gordillo, 1993].

Geotextiles and Geogrids

Geotextiles (or fabrics) and geogrids are made from different synthetic polymers, such as polypropylene, polyethylene, polyester, polyamide (Nylon) and vinyls (PVC). Various researchers [Murray, 1982; Smith, 1982; Majidzadeh et al, 1982] have reported that these fabrics and geogrids help in extending the useful life of an overlay and in reducing the severity of reflective cracking, unless it is caused by severe differential vertical movements [Hughes, 1986]. The fabrics and geogrids from polyethylene, polypropylene and polyester, have been reported to exhibit a reinforcing

or strengthening function [Vanelstraete and Francken, 1993]. According to Haas and Ponniah [1989], a geotextile or geogrid may perform like a tensile reinforcement in the bituminous overlay in a way similar to that of steel in concrete.

Polymer grid reinforcement is a combination of the techniques of wire mesh and fabric reinforcement in pavements. It has an elastic stiffness similar to that of a wire mesh, but is not susceptible to corrosion [Hughes, 1986]. The use of a wire mesh reinforcement has already been reported to be effective in delaying reflective cracking caused by relative vertical movement [Haywood, 1955; Croney, 1962]. According to Hughes [1986], reflective cracking can be retarded by using a polymer grid at the base of a bituminous overlay, which helps in reducing the strain concentration at the crack tips through the phenomenon of debonding from the underlying layer.

Polymer Modified Bituminous Mix

A layer of a polymer modified bituminous mix, having improved properties of flexibility, elastic modulus and temperature susceptibility, seems to help in delaying reflection cracks, but there is limited evidence about their improved performance. However, these mixes have shown less benefit compared to the use of geotextiles and grids (Caltabiano, 1990).

1.7 PROBLEM STATEMENT

Strength and elastic stiffness are two important, but different, parameters relating to the performance a pavement. The strength of the pavement is a function of the strength of its component layers, and is related to the maximum load carrying capacity of a structure. Stiffness is associated with the displacements at working loads. The stresses transmitted to a road foundation heavily depend on the elastic stiffness of different pavement layers [Croney and Croney, 1991].

The roadbase plays a key role in the structure of a pavement. Its strength and stiffness greatly influence the performance of the whole of the pavement structure. The roadbase should provide a strong support to the upper layers, and an adequate protection for the underlying layers [Brown et al, 1993] (particularly for low strength subgrades), by reducing the traffic induced stresses. The advantages of CBM bases (refer Section 1.2), demonstrate that they can meet both the strength and stiffness criteria, and can sometimes provide a superior performance, at a much lower cost, than conventional bituminous bases.

Unfortunately, the occurrence of primary and secondary cracking, leading to reflective cracking, has been a serious obstacle to the use of cement bound base roads. Reflective cracking is a major concern for engineers facing the problem of road maintenance and rehabilitation. Several years of research and practice have provided evidence that new materials and procedures (discussed in Section 1.6.1) have the potential to improve the situation, but, in spite of the extensive investigation, there is no unique standard solution for the problem of reflective cracking (Degeimbre and Rigo, 1989; Francken, 1993). The current UK practice [DoT, HD 26/94, 1994 (revised in February 1996)] of using a relatively thick bituminous surfacing (200 mm minimum for indeterminate design) in order to delay the reflective cracking in flexible composite pavements, indicates that this problem still needs a more refined solution. The use of a thick bituminous surfacing to combat reflective cracking makes the flexible composite pavement less cost effective.

1.8 SCOPE OF THIS PROJECT

The research presented in this thesis is focused on the improved design of a cement bound base. This is aimed at controlling the occurrence of primary and secondary cracking, thereby providing a high quality support for bituminous surfacing, but without incurring the penalty of early reflective cracking and associated maintenance problems. In this connection, two techniques, controlled cracking and steel fibre reinforcement in the CBM bases, have been presented.

Controlled Cracking of CBM Bases

The concept of a controlled cracking, also termed precracking, system is to deliberately induce frequent cracks in a CBM base. This minimizes crack width and maximizes load transfer capability, through a superior aggregate interlock, by maintaining differential vertical movement to a minimum. In consequence, it can prevent or at least delay reflective cracking, without necessitating the large thickness of bituminous surfacing which would, otherwise, be essential to withstand the strains developed in the bituminous layer as a result of crack activity. This technique has become quite well established [Shahid et al, 1995; Shahid, 1996, Shahid and Thom, 1996a and 1996b] and is presented in Chapter 5. Following this system, some other precracking techniques, for example the use of plastic film, have also been recently tried [Jofre et al, 1996; Verhée, 1996].

Steel Fibre Reinforcement in CBM Bases

Steel fibre reinforcement in cement bound bases is another innovative technique [Shahid et al, 1996] to help prevent reflective cracking, and is described in Chapter 6. In a steel fibre reinforced CBM base, CBM cracks at a stress level much lower than the ultimate strength of the composite material. These cracks have a negligibly small width, and a high shear resistance, and are accompanied by a significantly reduced differential vertical movement. With an increased tensile strength, the cracks are also less likely to deteriorate under traffic, and the CBM base is more resistant to secondary cracking.

A detailed description of various CBM categories and mix design is given in Chapter 2. The tensile characteristics of CBMs are of significant importance in the design of a CBM base. Such properties have been investigated, through a new direct tensile test (described in Chapter 3), for a wide range of the CBMs produced in the laboratory and on different construction sites. The results are presented in Chapter 4. The load transfer across different widths of cracks in the CBM bases with different categories, was investigated through a new laboratory test system, developed in this research. This system, accompanied by the load transfer investigation results, is described in Chapter 7.

Chapter 8 presents two approaches for analytical modelling of the flexible composite pavement structures in which any of the two techniques (controlled cracking and steel fibre reinforcement) for a CBM base has been involved. The results from analytical examples, given in this chapter, indicate a significant potential for using an appreciably reduced thickness of bituminous surfacing. Finally, Chapter 9 contains important conclusions and recommendations for future research.

1.9 SUMMARY

Cement bound bases have much higher stiffness (i.e. elastic modulus) and strength than conventional bituminous bases. They perform like a relatively rigid slab and help in significantly reducing the tensile strain at the bottom of bituminous surfacing. The most attractive advantage is their significant cost effectiveness compared to their competitive bituminous bases.

CBM bases are susceptible to shrinkage, which includes primary shrinkage due to hydration of cement and drying of a CBM, and thermal shrinkage which is mainly attributable to thermal properties of aggregates. The amount of primary shrinkage is influenced by the average aggregate size, surrounding temperature, ambient relative humidity, and wind velocity. It tends to increase at higher contents of cement and water in the CBM mix. Maximum shrinkage stresses are developed in the CBM base during an early age of 40 to 100 hours depending on the restraint conditions. These

stresses are highly localized on the exposed surface, decrease sharply with depth, and are relieved by the occurrence of surface cracking. The amount of thermal shrinkage, however, is mainly dependent on the magnitude of temperature drop and the values of the thermal coefficients of various aggregates.

Cracking occurs when the stresses, induced by shrinkage and traffic, exceed the tensile strength of a CBM base. It can be divided into two types depending on two different mechanisms. Primary cracking comprising transverse cracks is due to primary and thermal shrinkage, and initiates at the weakest locations in a CBM layer, such as small flaws and microcracks formed by rolling, which coalesce to form macrocracks. Crack spacing ranges from 3 to 50 m depending on the CBM type and strength. Stronger CBM bases develop relatively wider transverse cracks at larger spacing. Frequently spaced narrow cracks in a weak CBM base are more likely to rapidly deteriorate under traffic. Secondary cracking includes the deterioration of primary cracks due to differential vertical movement, and the occurrence of longitudinal wheel-path cracks. It is responsible for a significant reduction in the stiffness of a CBM base, and substantial damage to the structural integrity of a pavement.

Under excessive relative horizontal and vertical movements, the cracks in a CBM base propagate through bituminous surfacing, termed reflective cracking. This allows the ingress of water, which softens supporting layers, thus leading to an early failure of a pavement structure. Although reflective cracking can be delayed using relatively expensive methods, it can be economically avoided in new pavements by using the new techniques presented in this thesis.

Cement Bound Materials

2.1 INTRODUCTION

Cement bound materials (CBMs) constitute a distinctive group of pavement materials. They involve a wide spectrum of aggregates ranging from a locally available, as-dug or by-product material to a concrete quality borrow aggregate [Kennedy, 1990; DoT, MCHW, Volume 1, 1993]. In CBMs, cement is used as a binder, the amount of which corresponds to a desired strength level, and a water content is added which is compatible with compaction by rolling. CBMs are normally produced on sites through readily available batching plants, and are laid by a slip-form paver or by a grader.

CBMs are extensively used in the construction of sub-bases and roadbases in flexible composite pavements. They are also widely used as sub-bases for concrete pavements. In comparison with concrete, CBMs involve a fairly flexible and wide range of aggregates, which are sometimes unsuitable for concrete. They demand much smaller amounts of cement and water, thus resulting in a mix of low workability which is compacted by rolling.

In the UK, the terminology 'cement bound materials' is used, and in other countries, these materials are described by different names. In France, for example they are mainly termed as cement treated sands, and cement treated aggregates. In the USA, they are known as [Norling, 1973]:

- Soil cement
- Cement treated base
- Cement stabilized soil
- Cement stabilized soil aggregate
- Cement stabilized crushed aggregate
- Roller compacted concrete

2.2 CLASSIFICATION OF CBMS

According to the Highways Agency's Specification for Highway Works [DoT, MCHW-1, 1993], CBMs have been classified into four categories based on their 7 day cube compressive strength (Table 2.1). The compaction of cubes is carried out in accordance with the procedure described in Clause 4.2 of BS 1924: Part 2: 1990. CBM1 and CBM2 are mainly sub-base materials, whereas CBM3 and higher categories are used in roadbases, although CBM3 is also used in the sub-bases for concrete pavements. CBM1 and CBM2 may also perform satisfactorily in the bases of lightly trafficked roads.

The current UK design [DoT, HD 26/94, 1994] recommends a minimum thickness of 150 mm for CBM3 and higher categories. When the design thickness of a CBM3 roadbase exceeds 200 mm, the design guide allows the use of stronger CBMs with a reduced thickness. Present research (Chapter 4) has shown that there is a significant difference in the magnitudes of tensile strength of CBMs comprising different types of aggregate. For instance a CBM4 involving a crushed limestone tends to be much stronger in tension than a gravel sand CBM4. This consideration has been recently included in the revised design for flexible composite pavements [DoT, HD 26/94, 1994, revised February 1996]. In a recent laboratory investigation (discussed in Chapter 7), a gravel sand CBM has been found to be more susceptible to deterioration at cracks than a limestone CBM, under similar traffic conditions. Therefore, some relatively stronger CBM categories, termed high strength CBMs, have been included in this study (Table 2.2). These CBMs have performed more satisfactorily [Shahid et al, 1996]. The specification given for CBM5 and CBM6 have been used during this research but have not been issued by the Highways Agency.

The term 'lean concrete' was used in the UK in the past and corresponds to the current CBM3 category with a minimum 7 day cube compressive strength of 10 N/mm^2. This term is, however, still being used in some countries with rather different specification. For example, in Germany, the strength requirement for a lean concrete is 7 N/mm^2 to 12 N/mm^2 [Schmidt, 1989]. In Poland, lean concrete is produced from a mixture of

unwashed crushed stone, and gravel sand mixture acquiring a 7 day cube compressive strength of 6 to 9 N/mm^2 [Judycki, 1991].

Table 2.1. Specification for CBMs in the UK [DoT, MCHW, Volume 1, 1993]

CBM category	Method of mixing	Method of batching	Minimum compaction	Minimum 7 day cube compressive strength (N/mm^2)	
				Ave. of 5	Individual
CBM1	Mix-in-place or Plant	Volume or Mass	95% of the cube density	4.5	2.5
CBM2	"	"	"	7.0	4.5
CBM3	Plant	Mass	"	10.0	6.5
CBM4	"	"	"	15.0	10.0

Table 2.2. Specification for high strength CBMs [Shahid et al, 1996]

CBM category	Method of mixing	Method of batching	Minimum compaction	Minimum 7 day cube compressive strength (N/mm^2)	
				Ave. of 5	Individual
CBM5	Plant	Mass	95% of the cube density	20.0	13.5
CBM6	"	"	"	25.0	17.0

2.3 SELECTION OF AGGREGATE FOR CBMS

CBMs include a fairly wide range of materials. Selection of any of these materials depends on the CBM category and site conditions. A description of the materials suitable for different CBM categories is given by the Specification for Highway Works [DoT, MCHW-1, 1991], and is shown in Table 2.3. It has been reported [Kennedy, 1990] that granular materials ranging from clean sand or gravel sand to variable mixtures of gravel, sand, silt and clay can be used for CBMs. Some silty clays and silts such as brickearths are also suitable. In addition, uniformly graded materials, silty sandy clays, and materials slightly contaminated with acidic or organic matter may also be stabilized after some pretreatment [Kennedy, 1990].

Table 2.3. Description of UK materials for cement treatment [DoT, MCHW-1, 1991]

CBM Category	Range of Materials
CBM1	Washed or processed granular material, crushed rock or slag, naturally occurring soil, pulverized fuel ash, chalk, well burnt or spent oil shale or any combination of these.
CBM2	Washed or processed granular material, naturally occurring gravel sand mixture, crushed rock or slag or any combination of these, recycled materials such as crushed concrete.
CBM3 and CBM4 (also applicable to CBM5 and CBM6)	Either separate coarse and fine aggregate or an all-in aggregate, the quality and cleanliness complying with the requirements of aggregates for conventional concrete, artificial or recycled aggregates conforming to the requirements of BS 882:1983.

2.3.1 Grading Requirements for CBMs

The grading requirements of materials for different categories of CBM are given in Tables 2.4 to 2.6 [DoT, MCHW-1, 1993]. The determination of particle size distribution is carried out using the procedure given in Section 9 of BS 1377: Part 2: 1990. For CBM1, in addition to the specified grading zone, the following two requirements should also be met [Croney and Croney, 1991]:

- The material should be well graded with a coefficient of uniformity ≥ 5, which is obtained from the grading curve, and is defined as the ratio of the particle sizes corresponding to 60 percent and 10 percent passing.
- The material should be free from heavy clays. The plastic material passing through 0.425 mm sieve should have a liquid limit and plastic limit not more than 45% and 20%, respectively. This requirement permits the use of sandy and silty clays.

Figures 2.1 to 2.3 are probably more useful to gain a quick understanding of the grading limits of aggregate for different CBM categories. The grading zone in Figure 2.3 (for CBM3 to 6) is fairly narrow, and demands relatively cleaner and coarser material than for CBM1 and CBM2. To comply with this grading envelope, the aggregates of different sizes generally need to be reconstituted, thus adding to the overall construction cost. But present research has demonstrated that, although most

of the as-dug gravel sand mixtures and as-available crushed rock aggregates in the UK do not conform to the specified grading criterion in its entirety, they can still meet the strength and density requirements for a specified CBM. However, small variations of the aggregate grading (towards the finer side), from the given envelope, may cause a slight increase in the cement requirement.

Table 2.4. Material requirements for CBM1: Grading limit [DoT, MCHW-1, 1993]

BS Sieve Size (mm)	Percentage Passing (by mass)
50.0	100
37.5	≥ 95
20.0	≥ 45
10.0	≥ 35
5.0	≥ 25
0.6	≥ 8
0.3	≥ 5

Table 2.5. Material requirements for CBM2: Grading limits [DoT, MCHW-1, 1993]

BS Sieve Size (mm)	Percentage Passing (by mass)
50.0	100
37.5	95–100
20.0	45–100
10.0	35–100
5.0	25–100
2.36	15–90
0.6	8–65
0.3	5–40
0.075	0–10

Table 2.6. Material requirements for CBM3 to CBM6: Range of grading [DoT, MCHW-1, 1993]

BS Sieve Size (mm)	Percentage Passing (by mass)	
	20 mm maximum size	40 mm maximum size
50.0	—	100
37.5	100	95–100
20.0	95–100	45–80
5.0	35–55	25–50
0.6	10–35	8–30
0.15	0–8*	0–8*
0.075	0–5	0–5

Note * 0–10 for crushed rock fines

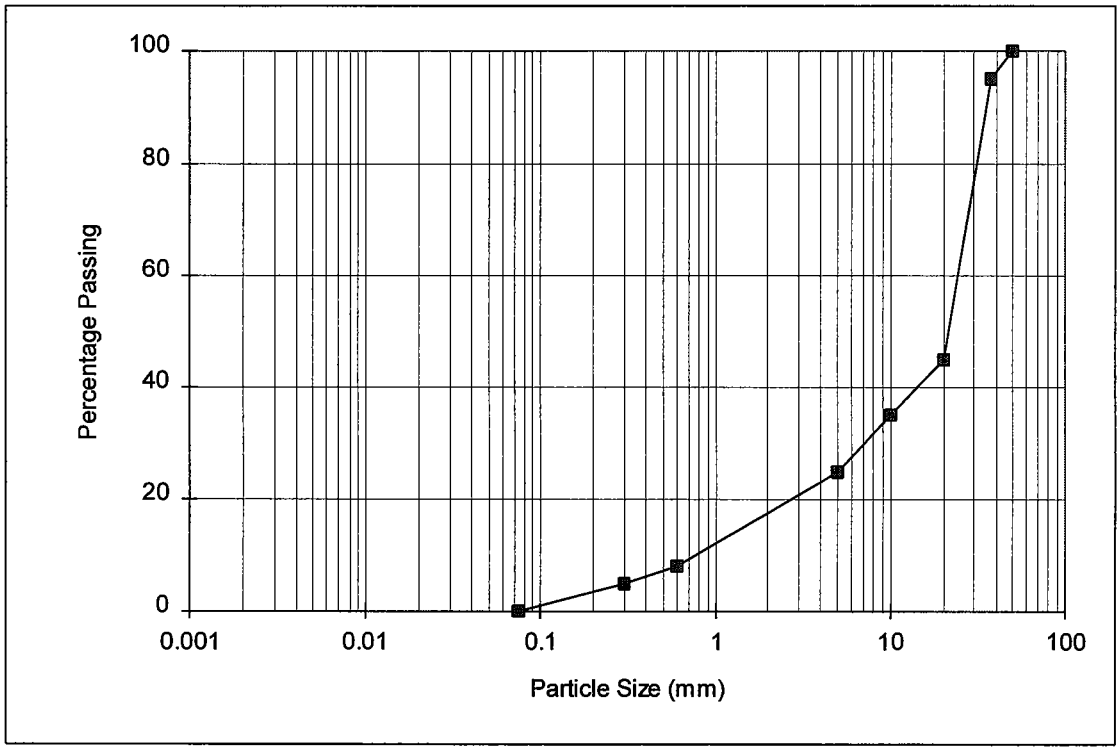

Figure 2.1. Coarse grading limit for CBM1

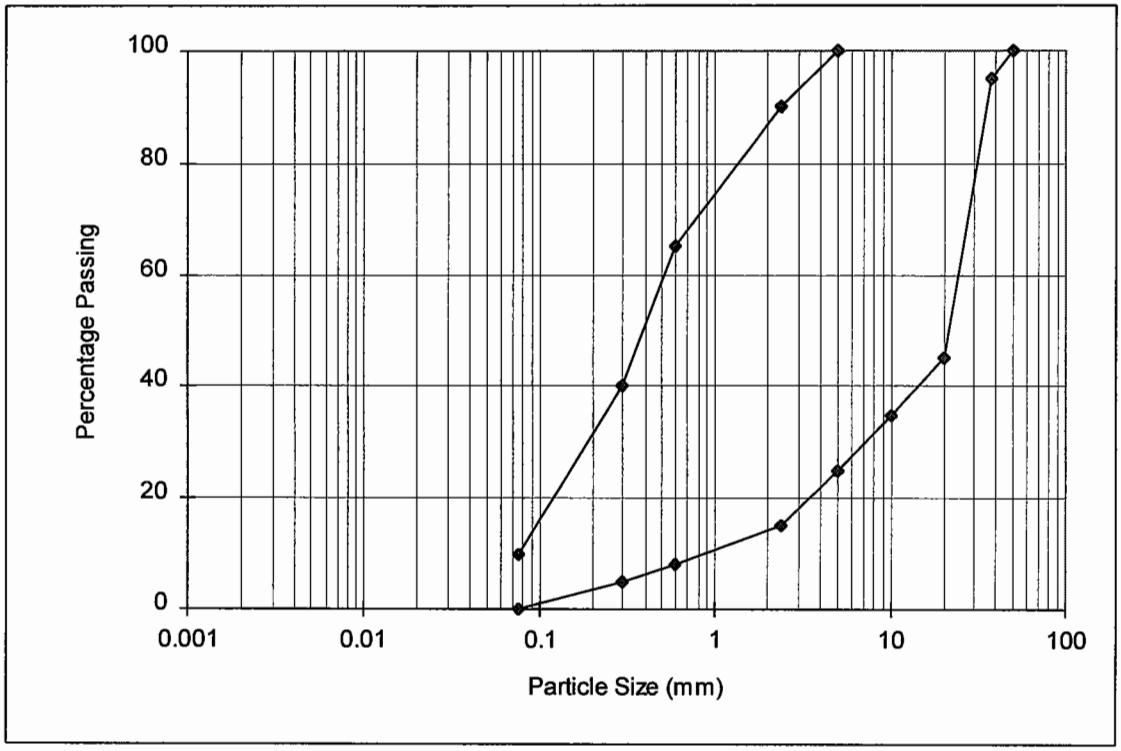

Figure 2.2. Coarse and fine grading limits for CBM2

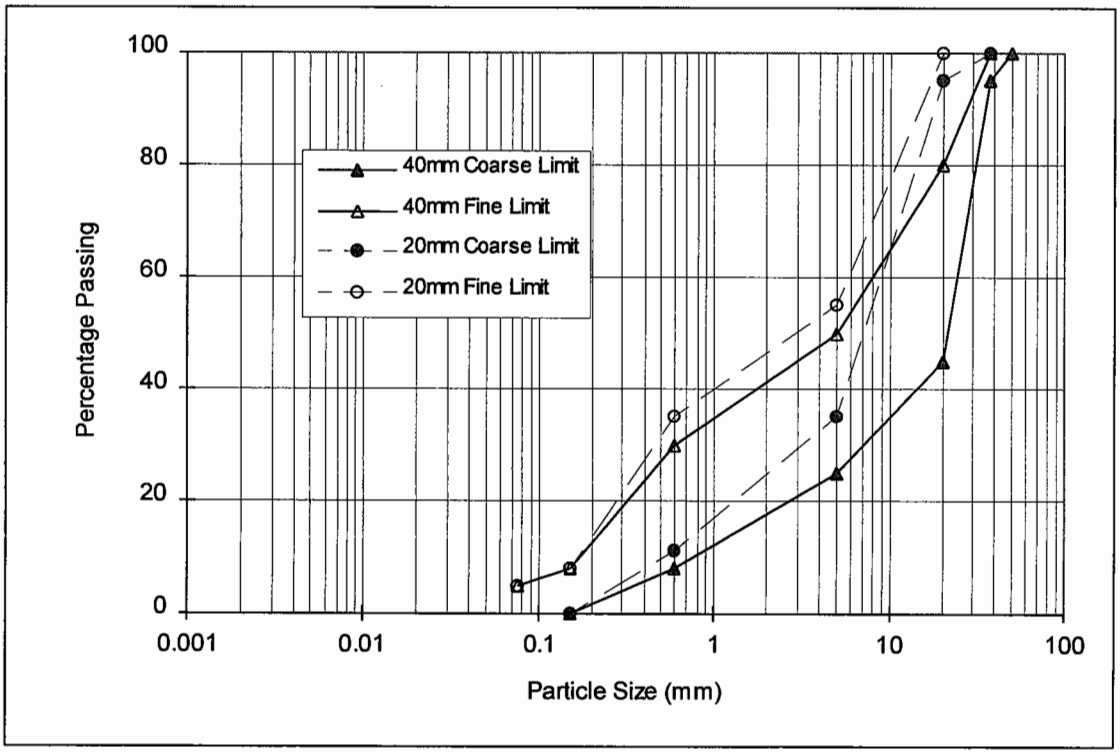

Figure 2.3. Coarse and fine grading limits for CBM3 to CBM6, with 40mm and 20mm maximum aggregate size.

2.3.2 Maximum Size of Aggregate

If the aggregate grading is extended to a larger size, it lowers the water requirement of the mix, so that, for a given workability and cement content, the water cement ratio can be lowered with a consequent increase in strength [Neville, 1995]. This behaviour has been verified for aggregates with up to 38.1 mm maximum size, and is usually assumed to be applicable to larger sizes as well [Bloem, 1959]. For concrete with aggregates above the 38.1 mm maximum size, however, the gain in strength due to a reduced water content is offset by the detrimental effects of a lower bond surface area and discontinuities introduced by the very large aggregate particles. This makes the concrete a heterogeneous mix [Neville, 1995]. Therefore, the effect of an increase in the largest size aggregate particles on the decrease in water requirement is dominant, but only up to 38.1 mm. For larger sizes, the balance of the two effects governs and is dependent on the richness of the mix [Bloem and Gaynor, 1963; Higginson et al, 1963], as shown in Figure 2.4. It has also been confirmed [Nichols, 1982] that, for any given strength of concrete, that is, for a given water/cement ratio, there is an optimum maximum size of the aggregate.

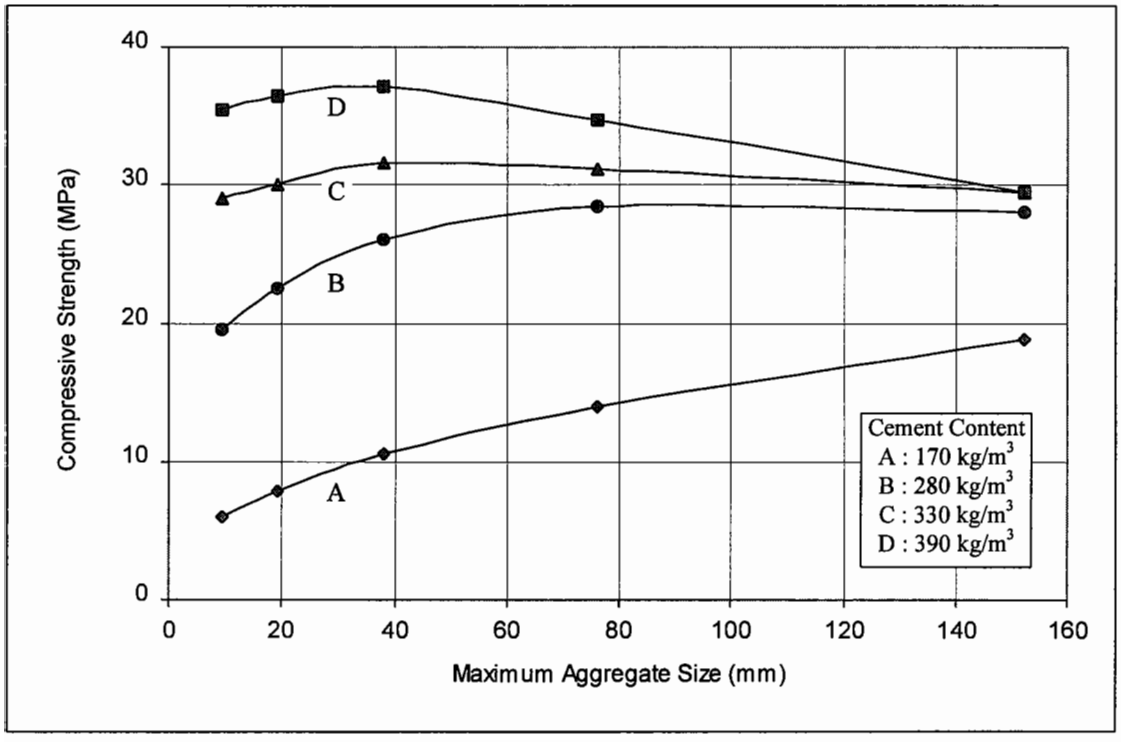

Figure 2.4. Influence of maximum aggregate size on the 28 day compressive strength of different grades of concrete [Higginson et al, 1963]

In the case of a lean concrete, with cement content of the order of 165 kg/m^3, the use of aggregates with size, larger than 38.1 mm, even up to 150 mm seems advantageous (Figure 2.4). However, in structural concrete, from the strength point of view, there is no advantage in using aggregate with a maximum size greater than 40 mm. The use of larger aggregate would also require the handling of a separate stockpile and may increase the risk of segregation in the mix. In no case, should the maximum size of aggregate be more than 1/5 to 1/4 of the minimum dimension of the concrete section [Neville, 1995].

2.4 MIX DESIGN

The mix design of a CBM is concerned with determining a cement content to attain a specified cube compressive strength from a given material, and an optimum water content corresponding to maximum density of a CBM mix obtainable through roller compaction.

The mix design of a CBM is fundamentally different from that of concrete. The concept of water/cement ratio is invalid because most of the CBMs have a water/cement ratio of almost unity (due to lower cement content involved), yet their workability is too low to allow their compaction by vibration alone [Williams, 1986]. Field compaction of CBMs by rolling has revealed that they exhibit a relationship between the mix water content and dry density, which is similar to that found by Proctor for soils [Kennedy, 1990]. It has been noticed that the strength of a CBM mix depends on the cement content and dry density, such that [Kennedy, 1990]:

- A CBM mix is associated with a unique optimum water content, above and below which the dry density decreases.
- The strength increases with an increase in dry density for a CBM mix with constant cement content and water content.
- The strength increases with an increase in the cement content, for a CBM mix with constant dry density and water content.

In comparison with concrete and bituminous mixes, the mix design of CBMs presents an entirely different situation. The designer has to be very careful about variations in the natural moisture and grading of aggregates, especially in the case of as-dug materials. The natural moisture content of the aggregate is influenced by weather conditions, and may vary even within one stockpile. Additional amount of water required to attain the correct moisture content needs to be carefully controlled during plant mixing by a regular inspection and testing procedure.

2.4.1 Laboratory Investigation

Since the mix design parameters are highly sensitive to variations in aggregate type and grading [Williams, 1986; Kennedy, 1990; Croney and Croney, 1991], a laboratory investigation was performed into the mix design of CBMs involving two types of aggregate, that is:

- A river gravel (uncrushed) blended with sand, with grading shown in Figure 2.5.
- An crushed limestone (from Dene quarry, Derbyshire), with grading shown in Figure 2.6.

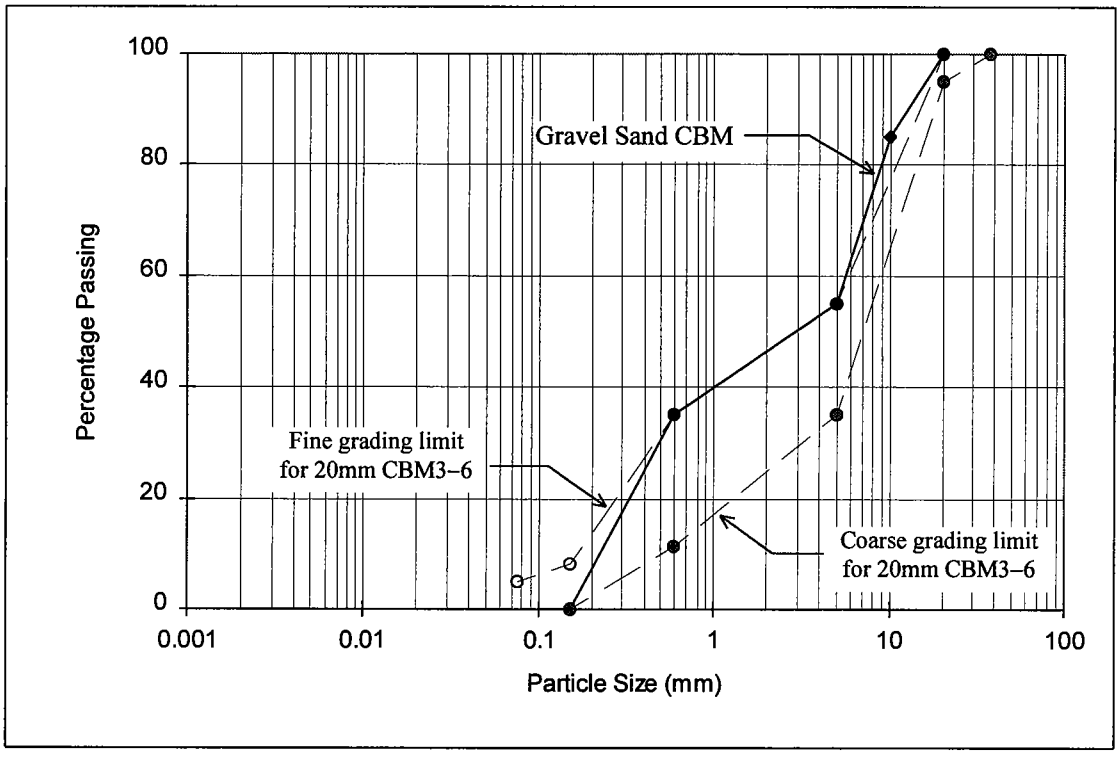

Figure 2.5. Grading of gravel sand CBM, and the grading limits for 20mm CBM3 to CBM6

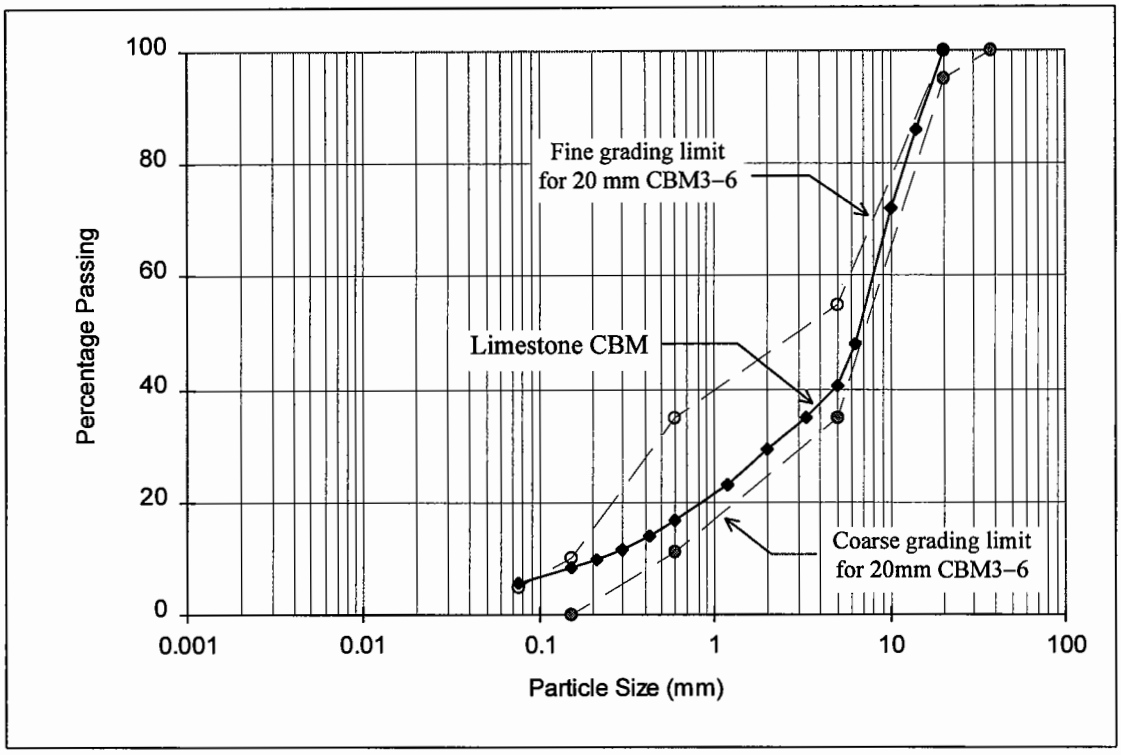

Figure 2.6. Grading of crushed limestone CBM, and the grading limits for 20mm CBM3 to CBM6

The maximum particle size for both the aggregates was 20mm. Batching of the ingredients was performed by mass using unwashed material (in both cases). Following a detailed mix design, the investigation of the resulting CBMs was extended to include the measurement of mechanical characteristics (in Chapter 4).

2.4.2 Water Content

The mix design of CBMs is very sensitive to variations in water content. An excess of water leads to a reduced CBM strength. Depending on the type and grading of material, any particular CBM is associated with a unique optimum water content, that corresponds to a maximum density of the mix.

To determine the optimum water content (omc), the aggregates should be (preferably) oven dried. Alternatively, air dried aggregates can be used with their known natural moisture content, and allowance is then made during mixing for the existing (natural) amount of water. The sampling and preparation of test portions is carried out

according to the procedures given in Sections 5 and 6 of BS 1924: Part 1: 1990. A relationship between dry density and water content is obtained through compactibility tests in accordance with Section 2.1.5 of BS 1924: Part 2: 1990. For these tests, the method of vibratory compaction is recommended for highly permeable stabilized granular (non-cohesive) materials, such as clean gravels, uniformly graded and coarse clean sand [Section 2, BS 1924: Part 2: 1990]. In addition, this method partially simulates field compaction by vibratory rollers.

For compactibility tests, as a starting point, a general idea of the approximate range of optimum water content for various materials can be obtained from Table 2.7. Using two values above and below this range, the tests are carried out over a series of water contents with 1 to 2% equal intervals. The resulting values of dry density and residual water content are plotted. The curve thus obtained indicates an approximate location of the optimum water content over a relatively small zone. Further tests are then performed, within this zone, at water content intervals of 0.5% to determine the precise location of the optimum water content.

Table 2.7. Approximate range of optimum water content for different materials [Kennedy, 1990; Present research]

Description of Material	Range of Optimum Water Content (% by mass of dry aggregate)
Clean gravel sand mixtures	4 to 6
As-dug gravel sand mixtures	5 to 7
Crushed rock aggregate	3.5 to 5.5
Sands	8 to 10
Silts and clays	Plastic limit

OMC at Different Cement Contents

Since the added cement constitutes a part of the CBM mix, any variation of the cement content will alter the corresponding optimum water content. It was, therefore, decided to study the relationships between dry density and water content at three different cement contents. The selected amounts of cement were 6%, 5% and 4% (by

mass) for the gravel sand CBM, and 5%, 4% and 3% (by mass) for the limestone CBM. These percentages were taken by mass of the oven dried aggregate.

For each CBM, three series of compactibility tests were performed corresponding to the three cement contents. For the first series, with a cement content of 6% and 5% for gravel sand and limestone CBM respectively, a comparatively greater number of compactibility tests were carried out for purposes of repeatability of the results. Looking at the pattern of the first series results, the number of tests was reduced for the second and third series. The resulting dry density versus water content curves, for both the CBMs, are shown in Figures 2.7 and 2.8.

Figure 2.7 shows a distinct peak for a gravel sand CBM at 6% cement content (by mass). This peak gradually diminishes with a reduction of the cement content. At 4% cement, the curve does not show a clear peak. This is because the material (gravel sand) used does not contain particles finer than 0.15 mm except the cement (refer Figure 2.5). The lack of fines in clean gravel sand materials is responsible for the absence of a clear peak in the water content versus dry density curve [DoT, MCHW-2, 1991], and sometimes, makes it difficult to determine the exact value of optimum water content. A higher cement content increases the amount of fines, leading to an increased probability of the occurrence of a clear peak. In contrast, the water content versus dry density relationship is less affected by the amount of cement in a limestone CBM, shown in Figure 2.8, because the crushed limestone aggregate contains a relatively greater amount of fines (see Figure 2.6). There is, indeed, a variation in the location of the optimum water content in the three curves (Figure 2.8), caused by the changed cement content. The optimum water content for a gravel sand CBM with 6% cement is found to be 5.1%, whereas for a limestone CBM containing 5% cement it is 4.35%. These values are in close agreement with those reported by Manser [1969], that is, 5.5% and 4.5% respectively for the two types of CBMs. The lower optimum water content, in the case of the limestone CBM, may be due to the dust generated by abrasion during mixing and vibratory compaction, leading to an increase in the paste content, which is reported acting as a pore filler and lubricant without necessitating extra water [Manser, 1969].

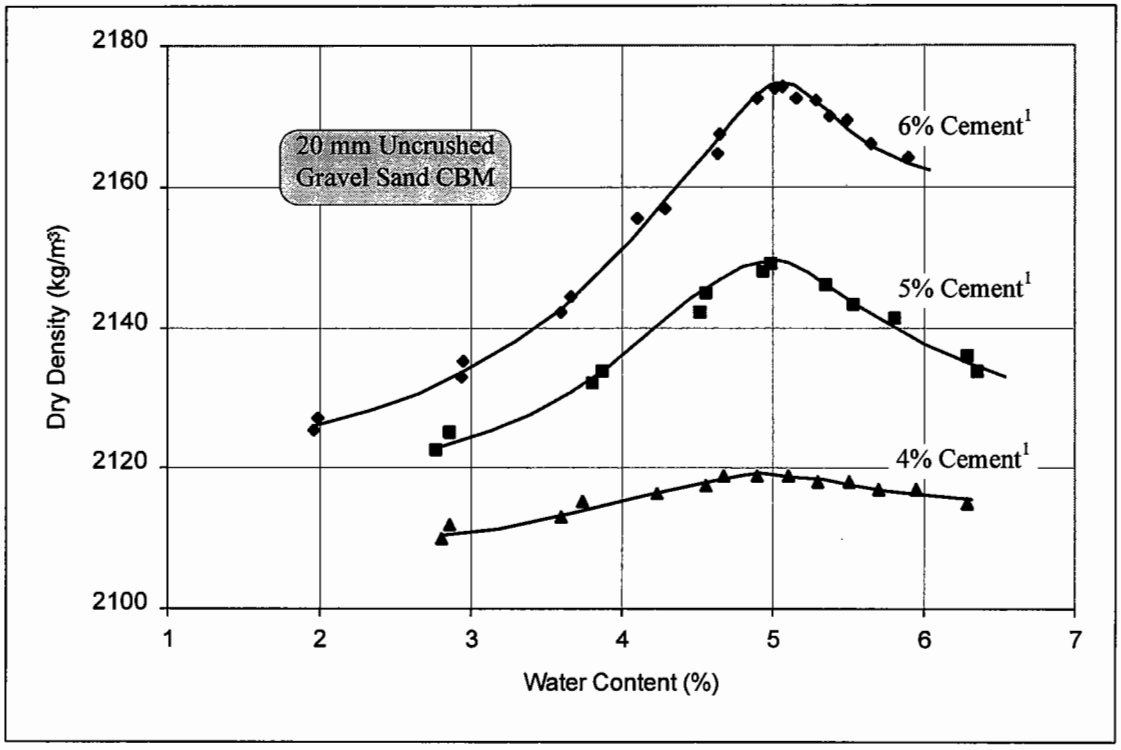

Figure 2.7. Water content[2] versus dry density relationships for gravel sand CBMs

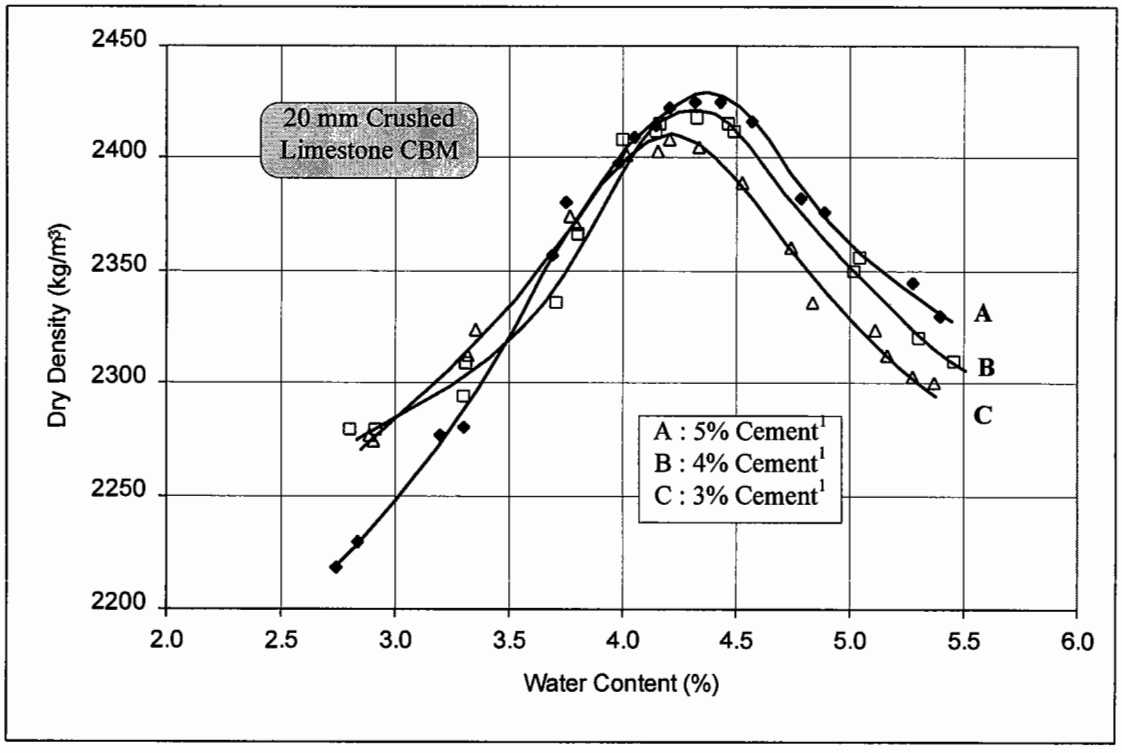

Figure 2.8. Water content[2] versus dry density relationships for limestone CBMs

[1] Cement content is in terms of a percentage by mass of the dry aggregate.
[2] Water content is in terms of a percentage by mass of the dry aggregate plus cement.

2.4.3 Cement Content

Cement Content is the most important factor affecting strength of a CBM mix, as well as shrinkage cracking [Felt, 1955; George and Davidson, 1963; Nakayama and Handy, 1965; Pendola et al, 1970]. The amount of cement in a CBM is directly related to its resulting strength, provided that water content and compactive effort are constant, and varies from less than 4% for a clean aggregate to 10% for a fine grained soil [Williams, 1986]. However, cement contents of up to 15% (by mass) can be economically used in stabilised soils [Kennedy, 1980], but it depends on the location of a construction site and availability of local aggregates. For general guidance, Table 2.8 shows the approximate range of the cement requirements for some materials.

Determination of Cement Content

The determination of an exact cement content to attain a particular CBM strength, requires establishing a relationship between the cement content and cube compressive strength for a given material grading. This involves compacting cube specimens over a range of cement contents at their respective optimum water contents. The procedures for preparing, curing and testing of the specimens are given in Section 4.2 of BS 1924: Part 2: 1990. The results of the compressive strength are plotted against the corresponding cement contents.

In this research, such relationships were produced for both the gravel sand and limestone CBMs. Cement content was changed in successive mix batches by 0.5%. From each batch, ten specimens (100 mm cube) were prepared, to enable testing of the two groups of five specimens at 7 and 28 days. The specimens were cured inside the moulds, covered with polyethylene, for 24 hours, and thereafter, under water at temperature 20 ± 2°C until required for testing. The relationships between cement content and cube compressive strength are shown in Figures 2.9 and 2.10 for the two types of CBM. A summary of the average results is given in Tables 2.9 and 2.10, where each value of the cube compressive strength represents the mean of five specimens.

Table 2.8. Approximate cement demand of different materials for CBMs [Kennedy, 1990]

Description of Material	Approximate Cement Content
Well graded hard granular materials	80 to 120 kg/m^3
Pulverized fuel ash	80 to 240 kg/m^3
Poorly graded/uniform hard granular materials, and well graded weak rocks such as shale	130 to 190 kg/m^3
Brickearths	170 to 200 kg/m^3
Soft chalk	180 to 225 kg/m^3

Table 2.9. Average cube compressive strength and density of gravel sand CBM comprising different cement contents used at the optimum water content.

Cement content	Opt. water content	7 day				28 day			
		Cube Strength, f_c (N/mm^2)		Sat. Density, γ_{sat} (kg/m^3)		Cube Strength, f_c (N/mm^2)		Sat. Density, γ_{sat} (kg/m^3)	
(%)	(%)	f_c	St. dev.	γ_{sat}	St. dev.	f_c	St. dev.	γ_{sat}	St. dev.
4.0	4.9	6.2	0.46	2313	11.2	8.9	0.20	2324	10.5
4.5	5.0	9.8	0.45	2350	6.6	13.0	0.35	2347	3.5
5.0	5.0	14.0	0.42	2357	9.5	17.4	0.41	2359	7.9
5.5	5.1	17.3	0.39	2357	2.6	21.7	0.49	2368	11.3
6.0	5.1	21.3	0.42	2372	12.7	25.8	0.48	2378	6.6

Table 2.10. Average cube compressive strength and density of limestone CBM comprising different cement contents used at the optimum water content.

Cement content	Opt. water content	7 days				28 days			
		Cube Strength, f_c (N/mm^2)		Sat. Density, γ_{sat} (kg/m^3)		Cube Strength, f_c (N/mm^2)		Sat. Density, γ_{sat} (kg/m^3)	
(%)	(%)	f_c	St. dev.	γ_{sat}	St. dev.	f_c	St. dev.	γ_{sat}	St. dev.
3.0	4.20	8.5	0.35	2520	5.7	13.8	0.45	2518	2.7
3.5	4.30	12.2	0.44	2522	3.3	17.9	0.50	2520	2.9
4.0	4.30	16.3	0.38	2519	6.6	22.2	0.52	2523	5.6
4.5	4.35	20.5	0.38	2519	4.2	26.8	0.42	2525	4.3
5.0	4.35	24.2	0.41	2521	9.9	31.0	0.47	2523	5.5

Note: Cement content (c.c.) is in terms of a percentage by mass of the dry aggregate,
Water content (w.c.) is in terms of a percentage by mass of the dry aggregate plus cement.

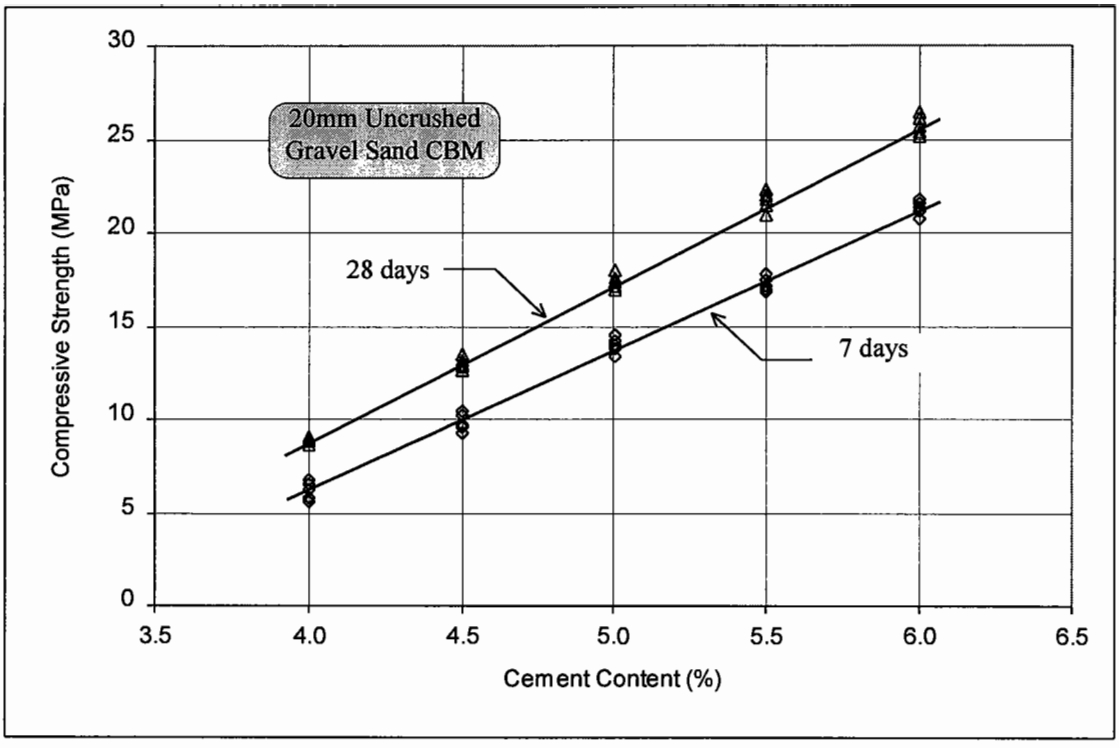

Figure 2.9. Relationship between cube compressive strength and cement content (by mass) for gravel sand CBM at optimum water content.

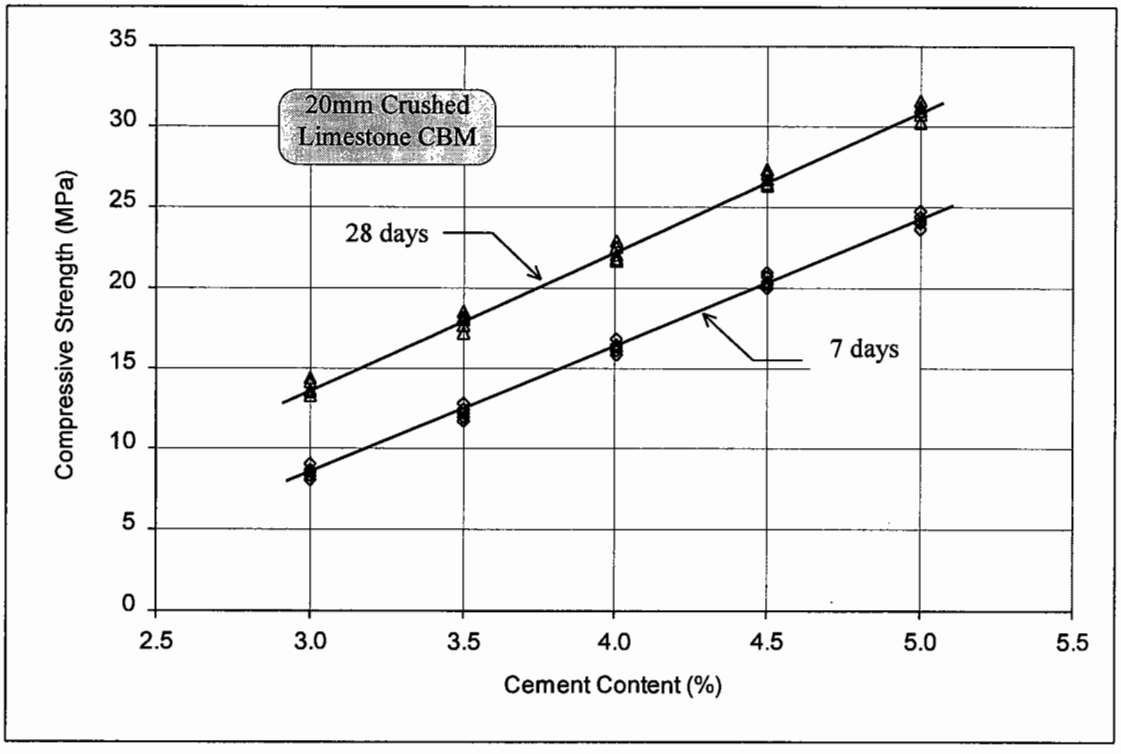

Figure 2.10. Relationship between cube compressive strength and cement content (by mass) for limestone CBM at optimum water content.

The relationships in Figures 2.9 and 2.10 can be used to determine the exact cement demand corresponding to a particular strength for the (given grading of) gravel sand and limestone CBMs. Tables 2.9 and 2.10 indicate that the effect of a change in cement content is less significant upon the mix density than strength. Moreover, the density of the gravel sand CBM is lower than that of the limestone CBM at their optimum water contents, which is mainly attributable to the different shapes of the two types of aggregates involved. The consistency of the cube compressive strength results can be seen from the low values of standard deviation (Tables 2.9 and 2.10).

2.5 DISCUSSION OF RESULTS

The (total) water content plays an important role in the mix design of CBMs. Its effects on the amount of shrinkage (discussed in Chapter 1) and strength properties of a CBM are very significant. In particular, the influence of a variation in water content on the amount of cement, for a particular CBM category, is dominant. For instance, an increased water content leads to a reduced density with a consequent decrease in strength. In order to offset this reduction of strength, an extra amount of cement is then required [Marais et al, 1973].

For explanation purposes, Figures 2.11 and 2.12 show the effect of an increased water content, by 0.5% above the omc, upon the 7 day cube compressive strength of a gravel sand and limestone CBM respectively. The magnitude and rate of reduction in strength is greater for the gravel sand CBM than for the limestone CBM, which seems to be due to the relatively cleaner aggregate in the former case. In fact, depending on the degree of cleanliness, the coarse graded aggregate can not hold water beyond a certain limit. After attaining the optimum water content, not only the excess water is pumped out of the wetter mixes [Manser, 1969], but also the water-cement paste escapes under vibration [DoT, MCHW-2, 1991]. The probability of the loss of the water-cement paste is greater in the case of round shaped gravel CBM mixes than for a CBM with angular aggregate. This is applicable even for a small increase of water content over the omc such as 0.5%. Since the total cement used in a CBM is already small, the loss of even a very small amount of the water-cement paste causes a

significant reduction in strength, but its effect on the CBM density is almost negligible. By comparing Table 2.11 with Tables 2.9 and 2.10, it can be seen that the loss of the cement paste, due to a water content 0.5% higher than the optimum, has an insignificant effect on the density of both types of CBMs. Each value in Table 2.11 represents the average from a group of five specimens. Any increase of the mix water content above the omc, therefore, demands an increased amount of cement to maintain the same level of CBM strength. For CBMs involving coarse grained materials, it is rather more advantageous that the compaction be carried out at a water content slightly on the dry side of the optimum, because it can help in achieving a maximum density, maximum strength, and at the same time minimum shrinkage cracking [Cauley and Kennedy, 1973].

For a given aggregate grading, there is a linear relationship between the cement content and optimum water content required for different CBM categories. Such relationships, for the gravel sand and limestone CBMs under discussion, are shown in Figure 2.13, which indicates that the cement requirement for a limestone CBM is much less than for a gravel sand CBM. This may be due to the self binding property and comparatively coarser grading of the limestone aggregate (see Figures 2.5 and 2.6). The lower surface area of the coarser particles, compared to fine graded aggregate, not only requires less cement, but also leads to a higher CBM strength [Catton, 1940]. This feature has been discussed in Section 2.3.2. The increased strength of the limestone CBM, even with a smaller cement content, is also due to its surface texture and angularity, which are more important than the inherent strength of the aggregate [Cauley and Kennedy, 1973]. Although the limestone aggregate is weaker than a gravel, its rough surface texture and angularity provide a stronger bond with the cement matrix, and better packing of the CBM mix, thus leading to a denser material [Cauley and Kennedy, 1973]. The mode of failure may also be a factor influencing the CBM strength. It has been reported [Pendola et al, 1970] that, in limestone CBM specimens, the aggregate failed before the cement matrix did, whereas with gravel sand, the initial failure was at the aggregate-cement interface.

Table 2.11. Average cube compressive strength and density results from gravel sand and limestone CBMs at a water content = omc + 0.5%.

	Gravel Sand CBM at 7 days					Limestone CBM at 7 days				
c.c.	w.c.	Cube Strength, f_c (N/mm^2)		Sat. Density, γ_{sat} (kg/m^3)		Water cont.	Cube Strength, f_c (N/mm^2)		Sat. Density, γ_{sat} (kg/m^3)	
(%)	(%)	f_c	St. dev.	γ_{sat}	St. dev	(%)	f_c	St. dev.	γ_{sat}	St. dev
3.0	–	–	–	–	–	4.7	6.5	0.40	2474	10.4
3.5	–	–	–	–	–	4.8	10.1	0.38	2483	10.6
4.0	5.4	4.6	0.22	2328	3.7	4.8	14.0	0.39	2497	5.7
4.5	5.5	7.2	0.32	2351	5.1	4.85	17.8	0.48	2499	2.3
5.0	5.5	9.6	0.39	2351	9.0	4.85	21.5	0.41	2507	1.6
5.5	5.6	12.4	0.37	2355	7.9					
6.0	5.6	15.2	0.42	2361	5.6					

Note: c.c. : cement content as a percentage by mass of the dry aggregate
w.c. : water content as a percentage by mass of the dry aggregate plus cement

During the research, it was noted that the limestone CBM required a longer compaction, at its optimum water content, than the gravel sand CBM to achieve the target density of the specimens. On average, the compaction duration for the former was 1.5 times that of the latter. It appears that the extra amount of compactive effort is needed for CBMs involving crushed aggregates to overcome the lack of workability caused by the angular particles. In the absence of this added compactive effort, the strength properties of the resulting CBM will be affected, due to a reduction in the mix density. It has been reported that a 5% shortfall in density reduces the cube compressive strength of a CBM by as much as 40 to 50% [Williams, 1986]. This ratio varies with the richness of the mix, so that a value of 30% is associated with conventional concrete [Glanville et al, 1947]. A mathematical expression of the effect of density on the cube compressive strength is given by the following relationship [Williams, 1986]:

$$\frac{f_1}{f_2} = \frac{D_1^{10}}{D_2^{10}} \tag{2.1}$$

Where:

f_1 : cube compressive strength (MPa) at a reduced density D_1 (kg/m^3)

f_2 : cube compressive strength (MPa) at a refusal density D_2 (kg/m^3)

Equation 2.1 can be used to estimate the reduction in the cube compressive strength as a result of the reduced density of a CBM caused by an inappropriate or reduced compaction.

The construction of a CBM base requires careful attention and regular testing to ensure good quality of work. This is because of the possible variations in natural moisture content and grading of the aggregates, within any stock-pile. Since there is a unique value of the optimum moisture content corresponding to a particular grading and aggregate type at a specified cement content, a variation in the natural moisture content, grading and/or type of aggregate will change the omc of a CBM mix. Moreover, for the given values of cement content and moisture content, any change in the aggregate grading influences the strength properties of a CBM.

It is recommended that CBM pavements should not be constructed in hot weather or under conditions of high wind and low humidity [George[1], 1968; George[2] 1968]. At higher temperatures, although the rate of gain in CBM strength increases at early stages because of accelerated curing, the ultimate strength is generally reduced [Anagnos et al, 1970; Pendola et al, 1970]. High temperatures are also accompanied by a higher rate of loss of water which promotes shrinkage cracking. On the other hand, at temperatures below about 4°C, the hydration of cement stops [PCA, 1965], showing that the CBM bases need to be protected from freezing for a minimum period of 7 days after they are laid.

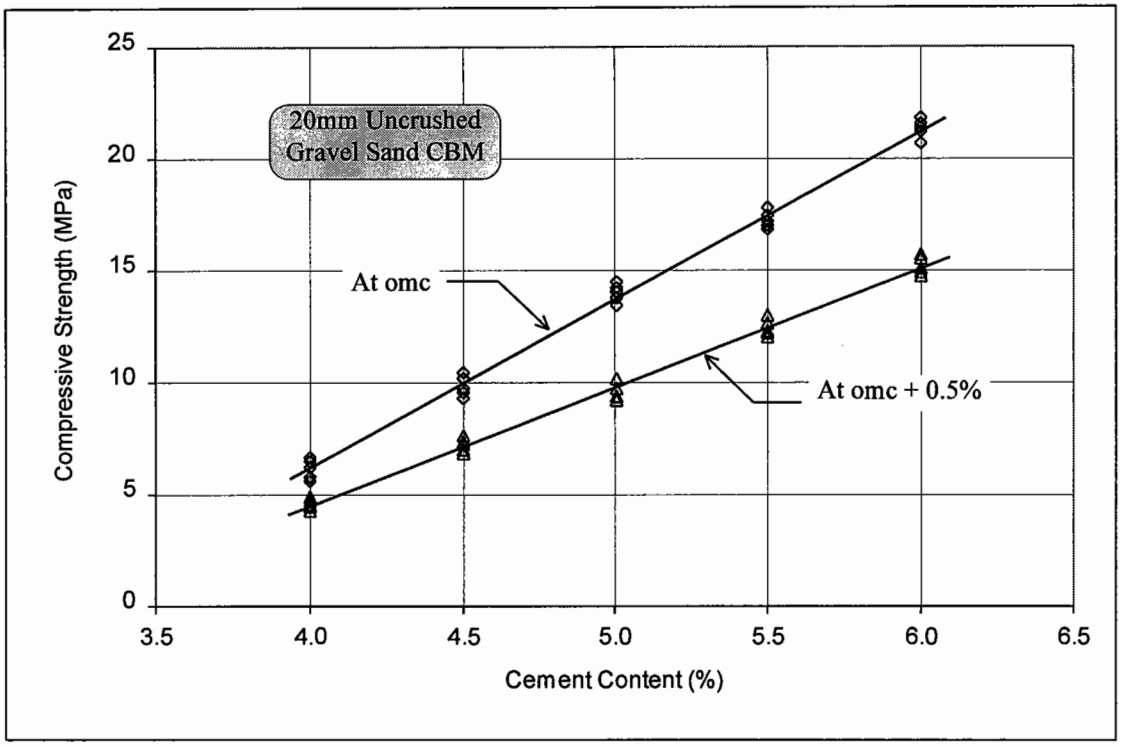

Figure 2.11. Cube compressive strength (7 day) versus cement content relationships for a gravel sand CBM at omc, and a water content = omc + 0.5%.

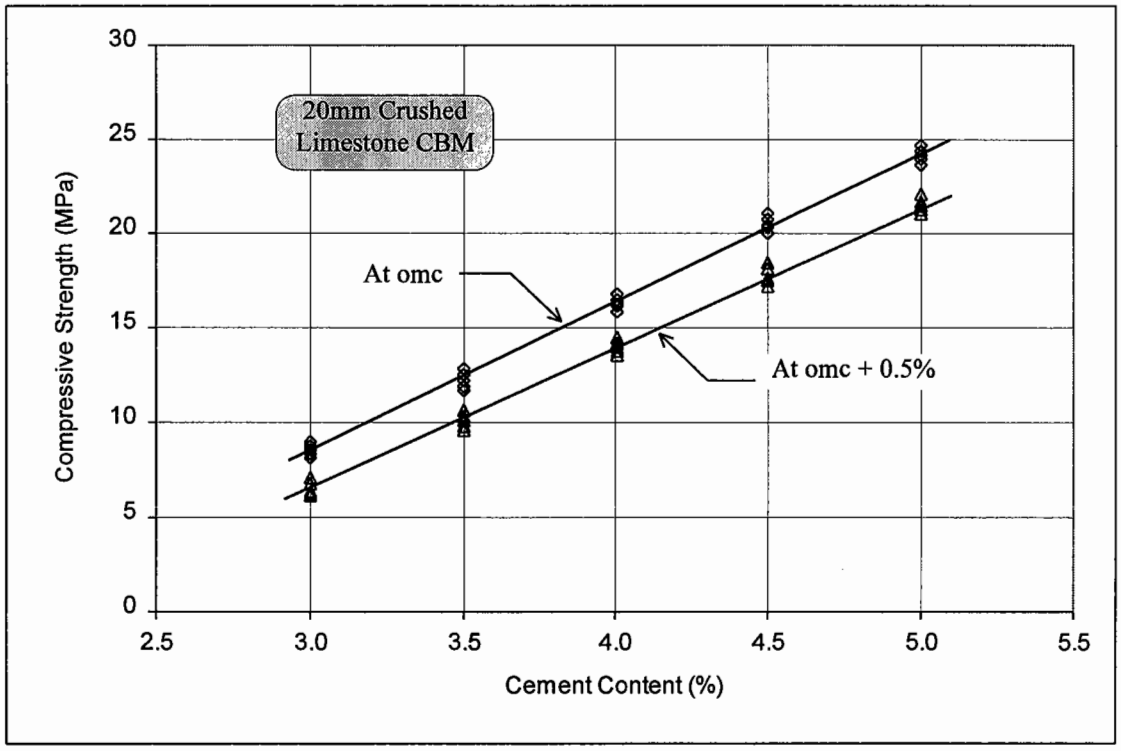

Figure 2.12. Cube compressive strength (7 day) versus cement content relationships for a limestone CBM at omc, and a water content = omc + 0.5%.

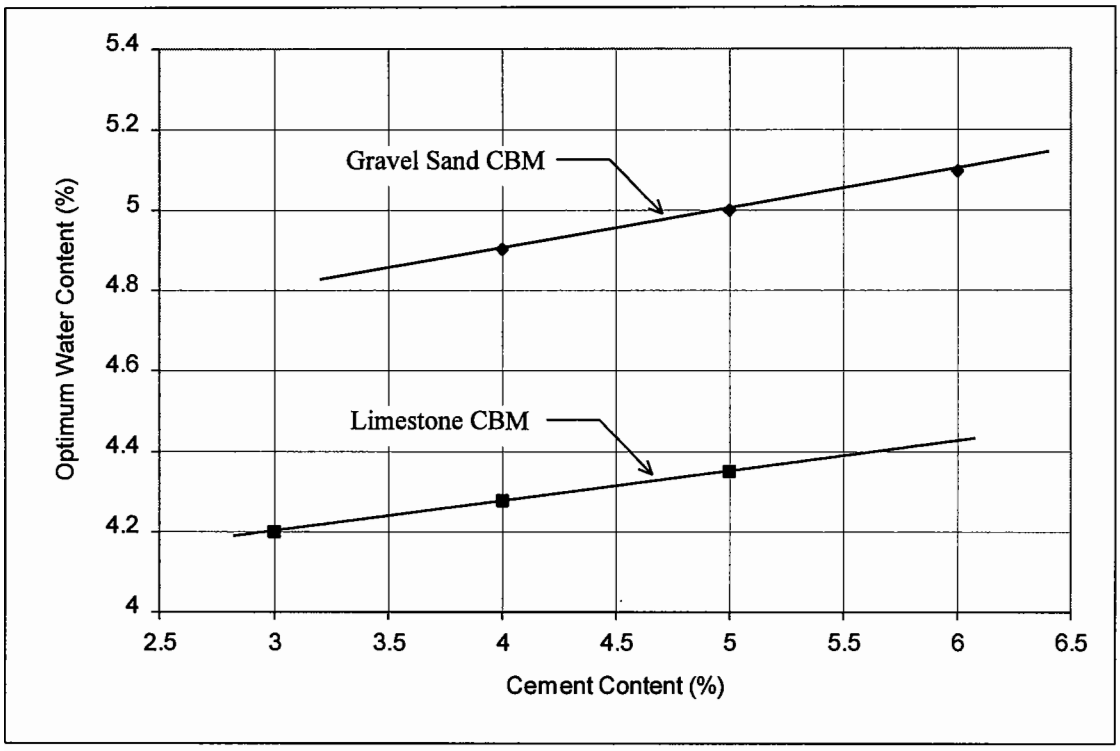

Figure 2.13. Relationship between cement content and optimum water content for 20mm gravel sand and limestone CBMs.

2.6 SUMMARY

Cement bound materials (CBMs) involve a large variety of materials ranging from a poor quality by-product or as-dug material to high quality washed gravels and crushed rock aggregate. In CBMs, cement is used as a binder and a water content compatible with roller compaction is added. The mix design of a CBM includes determining a cement content and an optimum water content for a specified cube compressive strength. The shape of the water content versus dry density curve for a CBM is heavily dependent on the grading of aggregate.

The mix design of a CBM is highly sensitive to variations in mix water content. An increased water content, above the omc, requires additional cement to attain a specified CBM strength. Even a small increase in water content, such as 0.5% above the omc, is enough to cause a significant reduction in the CBM strength. The magnitude and rate of the strength reduction is greater for gravel sand CBM (with

relatively cleaner aggregate) than for limestone CBM, and is mainly due to the loss of the water-cement paste, which is pumped out of the wetter mixes under vibrations. However, the effect on the CBM density is negligible.

A change in the cement content directly affects the CBM strength, whereas its effect on density is less significant. Limestone CBM requires less cement and water, but acquires a higher density than an uncrushed gravel sand CBM. For a given aggregate grading, there is a linear relationship between the cement content and optimum water content required for different CBM categories. The compactive effort for a limestone CBM, at optimum water content, is almost 1.5 times of that for a gravel sand CBM to achieve their respective target densities.

Development of a Direct Tensile Test

3.1 INTRODUCTION

The immense significance of tensile characteristics, for designing a cement bound base, is well established. Properties, such as tensile strength, are useful in predicting the conditions of crack appearance and crack width in the base layers comprising different thicknesses and types of CBMs. The ratio of tensile stress, due to traffic loading, to the tensile strength of a CBM base is used to represent its fatigue life [Brown, 1979].

The current UK design criteria [DoT, HD 26/94, 1994] for flexible composite pavements are based on the cube compressive strength, which, in fact, is not a reliable representative of any of the properties of CBMs relating to a pavement's performance [Brown et al, 1993]. In comparison, the tensile strength and elastic stiffness are the real performance related parameters for characterizing cement bound base pavements [Bonnot, 1972]. These parameters can not be correctly derived from the cube compressive strength.

The accurate assessment of the tensile strength is best carried out through a direct tensile test [Dempsey, 1984; Bonnot, 1972], because it obviates the need for making any assumption in the calculation of tensile strength. In contrast, the indirect tensile tests (flexural and cylinder splitting) involve the use of unrealistic assumptions, due to their complex stress distribution, which lead to an overestimate in the magnitude of the tensile strength. Similarly, the stress strain relationship of a CBM specimen under direct tension is used for determining the elastic stiffness, because the relatively uniform stress conditions attained in direct tension are thought to give the most accurate measurement of the elastic stiffness [Brown et al, 1993; Bonnot, 1972].

This chapter describes the development and validation of a new direct tensile test, along with a brief review of the previous direct and indirect tensile strength measuring techniques. This test has been used, in this research, for investigating the stress strain properties (Chapter 4) of different CBMs.

3.2 METHODS OF MEASURING TENSILE STRENGTH

Different types of direct and indirect tensile tests have been used in the past to determine the tensile properties of CBMs. A brief description of these techniques is given in the following paragraphs.

3.2.1 Flexural Strength Test

Most of the researchers [Brown et al, 1993; Galloway et al, 1979; Kolias and Williams, 1978; Bofinger, 1970; Otte, 1978; Williams and Patankar, 1968] have used a four point bending test (Figure 3.1). This test is described in BS 1881: Part 118: 1983. Although this test seems to at least partially simulate the response of a pavement layer under wheel loading, this is not actually the case because the pavement layer is subjected to two dimensional bending. In the flexural test, the calculation of tensile strength is based on the assumptions that the material is homogeneous and behaves elastically up to failure, which are also not realistic, particularly in the case of CBMs. The flexural strength is given by the following equation:

$$f_b = \frac{Pl}{bd^2} \tag{3.1}$$

where:

f_b : flexural strength (N/mm^2)

P : maximum applied load (N)

l : span length between supporting rollers (mm)

b : width of beam (mm)

d : depth of beam (mm)

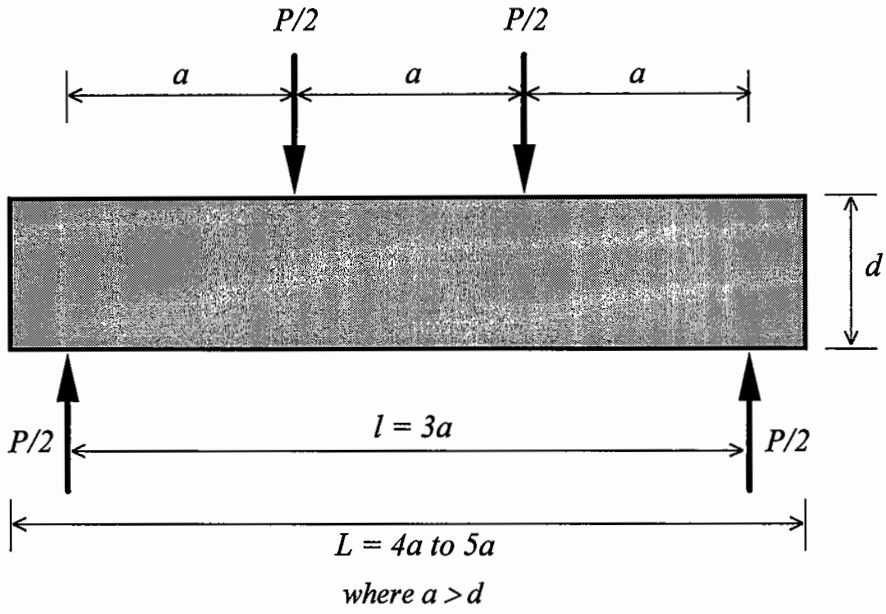

Figure 3.1. Four point bending test

According to Brown et al [1993], the flexural test is not useful for measuring either tensile strength or elastic stiffness of CBMs. In fact, the direct tensile strength is approximately 60% of the flexural strength and can be estimated from the following equation [Kolias and Williams, 1978]:

$$f_t = 0.53 f_b + 0.15 \tag{3.2}$$

More specifically, Dempsey et al [1984] recommended the following relation for use in design:

$$f_t = 0.5 f_b \tag{3.3}$$

Where:

f_t : direct tensile strength (N/mm^2)

f_b : flexural strength (N/mm^2)

3.2.2 Cylinder Splitting Test

This test, described in BS 1881: Part 117: 1983, is shown in Figure 3.2. As in the case of the flexural test, the tensile strength is computed by involving the use of the theory of elasticity [Timoshenko, 1934; Sokolnikoff, 1956; Muskhelishivili, 1953]. This theory is based on the following assumptions, which are unrealistic for CBMs.

- The material is homogeneous
- The specimen is subjected to plane stress conditions
- The material behaves in a linear elastic manner up to failure

By considering these assumptions, the tensile strength (horizontal stress along the vertical diameter) is approximated through the following equation:

$$f_{sp} = \frac{2P}{\pi dl} \tag{3.4}$$

where:

f_{sp} : splitting strength (N/mm^2)

P : maximum applied load (N)

d : diameter of cylinder (mm)

l : length of cylinder (mm)

In the cylinder splitting test, packing strips are used to attain a uniform load distribution. Without packing strips, the measured strength is lower, typically by 8% [Neville, 1995]. ASTM C 496-90 prescribes plywood strips, 3.0 mm thick and 25 mm wide. British Standard BS 1881: Part 117: 1983 specifies hardboard strips, 4.0 mm thick and 15 mm wide. These packing strips cause the formation of wedges, at top and bottom, under the applied load. In consequence, the resistance to crack propagation around these wedges controls the maximum load sustained by the specimen, thus leading to a severe overestimation [Williams, 1986]. The distribution of the horizontal stress on a section containing the vertical diameter is shown in Figure 3.3. Relative stress distributions along x-axis and y-axis are illustrated in detail elsewhere [Read, 1996].

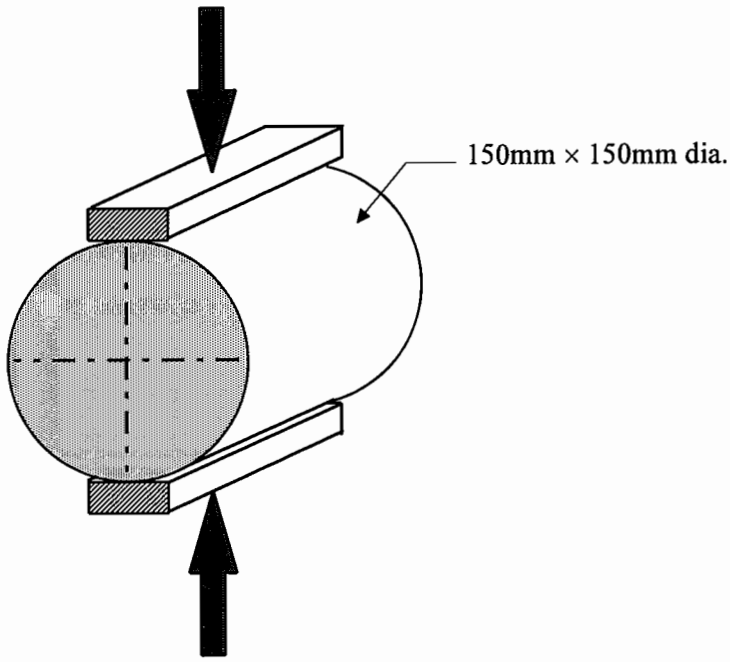

Figure 3.2. Cylinder splitting test

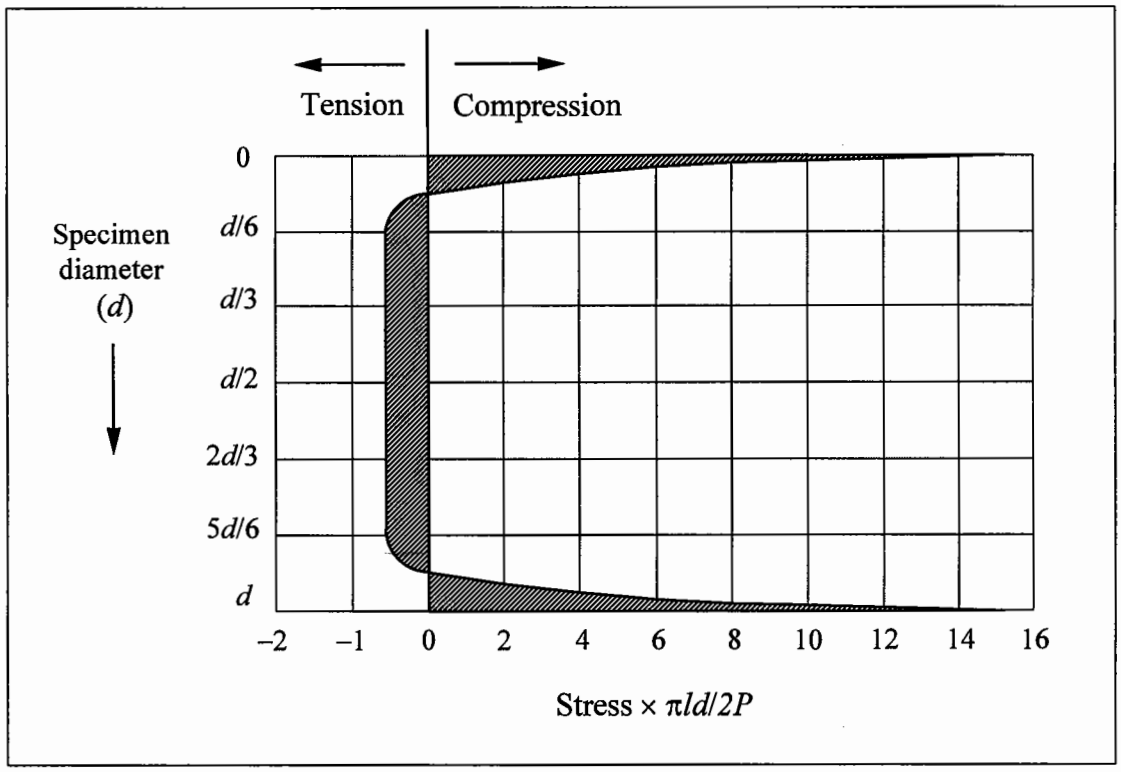

Figure 3.3. Horizontal stress distribution along the vertical diameter of a cylindrical specimen loaded over a width of 1/12 of the diameter [Wright, 1955].

3.2.3 Necked Specimen

Bofinger and Sullivan [1971] used very small sized necked specimens to measure the direct tensile strength of soil cement (CBM1). The specimens were 76 mm long, 25.4 mm square at their neck, and with enlarged ends as shown in Figure 3.4. These specimens were gripped through a special kind of jaws for applying a tensile force.

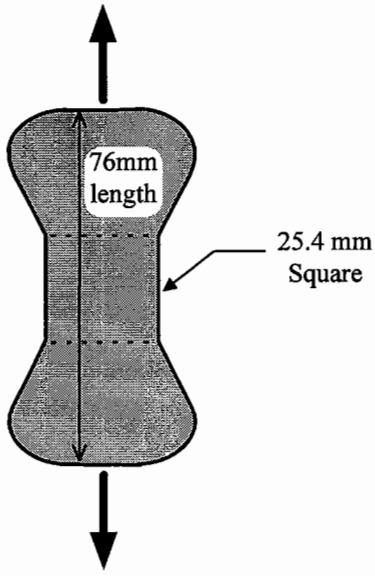

Figure 3.4. Necked specimen

3.2.4 Cemented Plates

Bofinger [1970] tried metal plates cemented to the ends and sides of rectangular soil cement (CBM1) specimens in order to apply a direct tensile force. For this purpose, a polyester resin adhesive was used. This technique, shown in Figure 3.5, did not work on stronger CBMs.

3.2.5 Friction Grip System

A friction grip loading system was developed by Johnston and Sidwell [1968] for use on concrete. Kolias and Williams [1978] tried this loading system to perform uniaxial tension tests on standard beam (102×102×508 mm) CBM specimens. Linear variable differential transformers (LVDTs) were used, on the four faces of the specimen, to measure very small deformations. It was found that the tensile strength, determined through this test, was an underestimate of the true value for the following reasons [Williams, 1986]:

- The final failure was induced by local stress concentrations.
- The application of a true axial load, avoiding bending stresses, was found to be difficult.

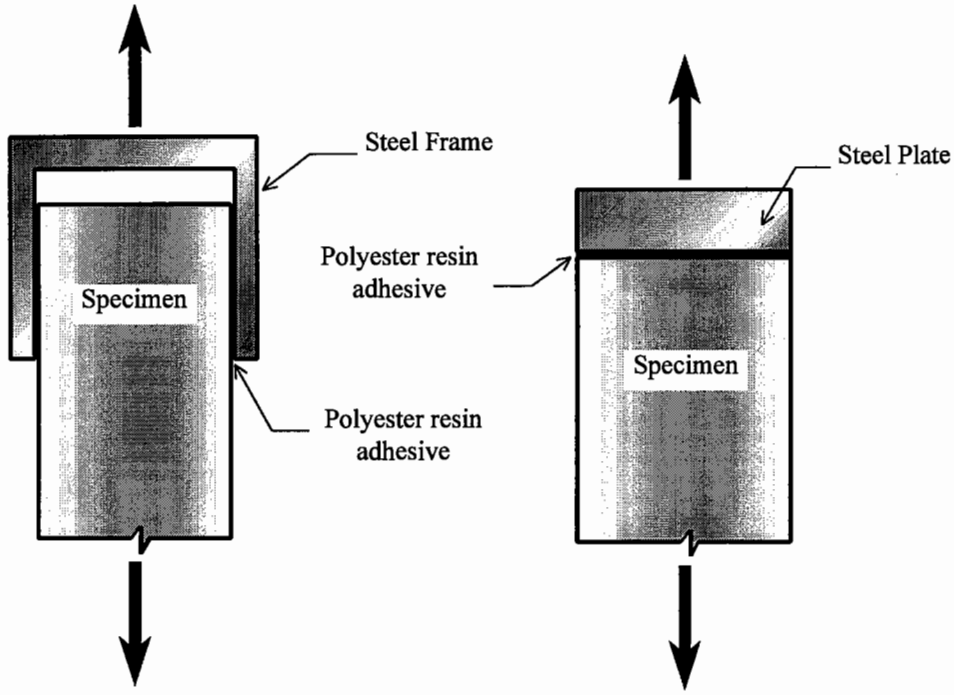

Figure 3.5. Specimens with cemented plates

3.2.6 French Direct Tensile Test

French Standard [NF P98-232-2, 1992] describes a test to determine the strength and elastic stiffness of materials treated with hydraulic binders under direct tension. Specimen shape is cylindrical with enlarged ends, illustrated in Figure 3.6. Fixing of the specimen in a testing machine requires two steel caps, with a minimum thickness of 20 mm, and two joints to avoid any bending. The two caps are stuck to the flat surfaces of the enlarged ends, and are kept in line with each other. Longitudinal deformation is measured over a distance of 120 to 140 mm within the central part of the specimen by using three measuring devices, which are equally spaced from each other. A relationship between tensile stress and strain is obtained. The elastic stiffness is calculated as the slope of a line, passing through the origin, corresponding to a stress level of 30% of the ultimate tensile strength.

The specimens are prepared using a vibrocompression equipment. This consists of applying vibrations in the horizontal plane, and a vertical force (maximum 10 kN) by

means of a piston over the entire cross section of the specimen [NF P98-230-1, 1992]. This is a laboratory technique and inhibits the compaction of specimens from CBMs mixed in a batching plant on construction sites. However, for materials treated with other hydraulic binders, that is slag, lime and fly-ash, this is not as critical as for CBMs, and the bulk mixes can be transported to the laboratory.

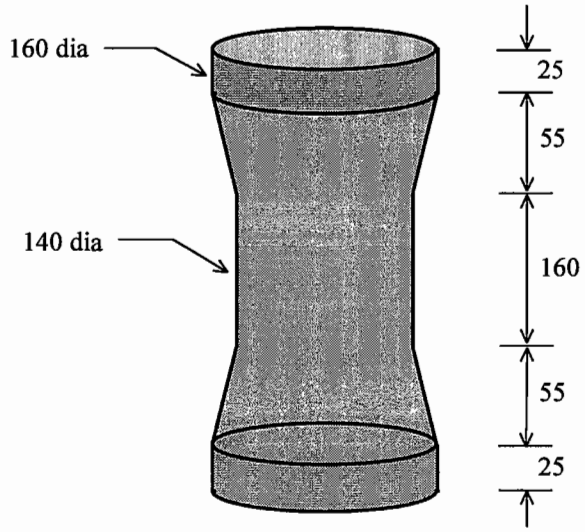

Figure 3.6. French direct tensile test specimen shape

3.3 DIRECT TENSILE TEST

This Section describes the development and validation of a new direct tensile test. This test has been used for investigating the mechanical characteristics of a wide range of CBMs, presented in Chapter 4 of this thesis. In particular, the main objective of this test was to measure the following functional parameters which are of primary importance in the analytical design of flexible composite pavements [Brown, 1979].

- Stiffness in direct tension
- Stiffness in compression (for comparison purposes)
- Tensile strength of CBMs
- Fatigue strength of CBMs

The shape and dimensions of the direct tensile specimen are illustrated in Figure 3.7. Because of the dimensions of the middle part of the specimen, the application of this test is limited to CBMs comprising a 20 mm maximum aggregate size. So far, this test has been successfully used over a large number of specimens prepared from CBM2 to CBM6. These specimens were prepared in the laboratory, as well as on construction sites. The possibility of preparing specimens on site is an added advantage, and has been of significant help in comparing the tensile properties of the CBMs mixed in plant to those produced in the laboratory.

3.3.1 Preparation of Specimen

The cement content and optimum water content are obtained from the mix design against a target CBM cube compressive strength. For specimens prepared in the laboratory, the combined mass of dry aggregates plus cement, for a target dry density, is calculated through the following relation [NF P98-230-1, 1992]:

$$M_a = \frac{\gamma_d (w + 100)}{100} \times V_s \qquad (3.5)$$

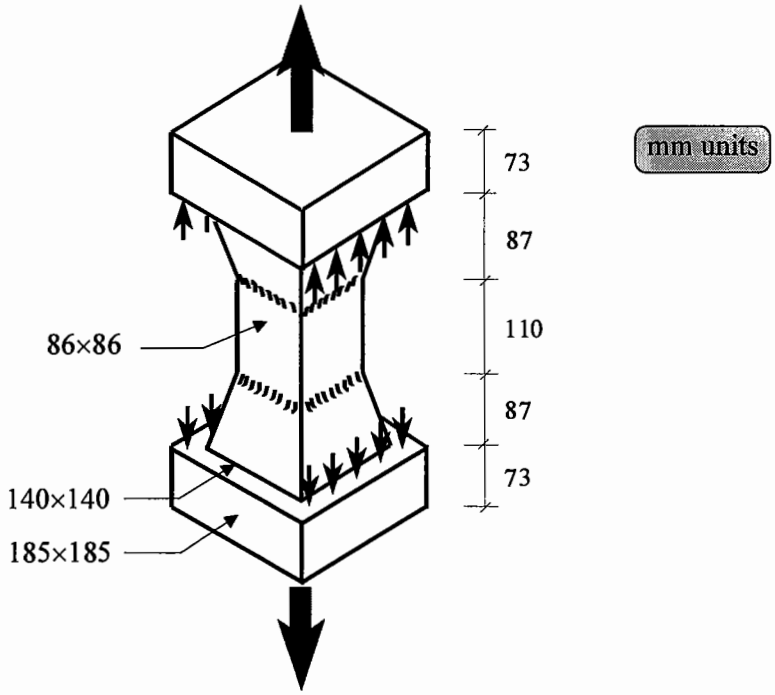

Figure 3.7. Direct tensile test specimen

In Eq. 3.5, M_a is mass of aggregates and cement (kg), γ_d is dry density of the CBM mix (kg/m^3), w is the optimum water content (by percentage of M_a), and V_s is volume of the specimen (m^3).

The specimen is prepared in a steel mould, coated from inside with a mould release oil. The mould is positioned upright on a steel plate, which is then clamped to the mould. The specimen preparation involves the use of a vibrating hammer and three tamping feet of different sizes corresponding to the dimensions of the mould at its different levels.

The mould is filled, approximately up to one third of its height, with fresh CBM mix. Compaction is started using the smallest sized tamping foot (of rectangular shape). During compaction, a constant downward axial force is applied manually. The position of the tamping foot is changed at regular intervals, over the surface of material, to attain a kneading action. The surface of the compacted layer is scarified,

using a long sharp edge, before the next layer is placed. The entire compaction of the specimen is completed in five layers. The top layer is compacted using an extension and is finished level to the mould brim using a smooth wooden plate. Next the mould is turned upside down, and the other end of the specimen is further compacted. Finally, steel plates are clamped at both ends of the mould.

3.3.2 Curing of Specimen

The specimen is cured for 48 hours inside the mould, which is wrapped with damp matting and further covered with polyethylene. Afterwards, the mould is stripped off and the specimen is stored under water at a temperature of 20 ± 2°C [BS 1881: Part 111: 1983].

3.3.3 Instrumentation of Specimen

The specimen is taken out of water and dried in air. On each of the four faces of the middle part (110×86×86 mm) of specimen, a line is marked along its longitudinal axis. Two brass pips are fixed on this line, using a quick setting adhesive. The gauge distance between the centres of the pips is set at 100 mm. The adhesive is allowed to set for a minimum of 24 hours. After it has attained adequate strength, one LVDT is fixed on each face, using screws, as shown is Figures 3.8 and 3.9.

3.3.4 Specimen Lifting System

For testing, a special arrangement (Figure 3.8) has been developed to hold and load the specimen. This lifting system is used in a universal testing machine capable of applying a tensile and compressive force of up to 50 kN.

The square ends of the specimen are supported on two pairs of steel angles (28×30×6 mm) via 2mm thick rubber seats as shown in Figure 3.8. The angles are connected to steel plates (12 mm thick), on top and bottom of the specimen, by means of 150 mm long M10 vertical bolts. Both the plates have elongated holes, which allow adjustment of these bolts in a horizontal plane. The angles are kept in position by 230 mm long M10 horizontal bolts.

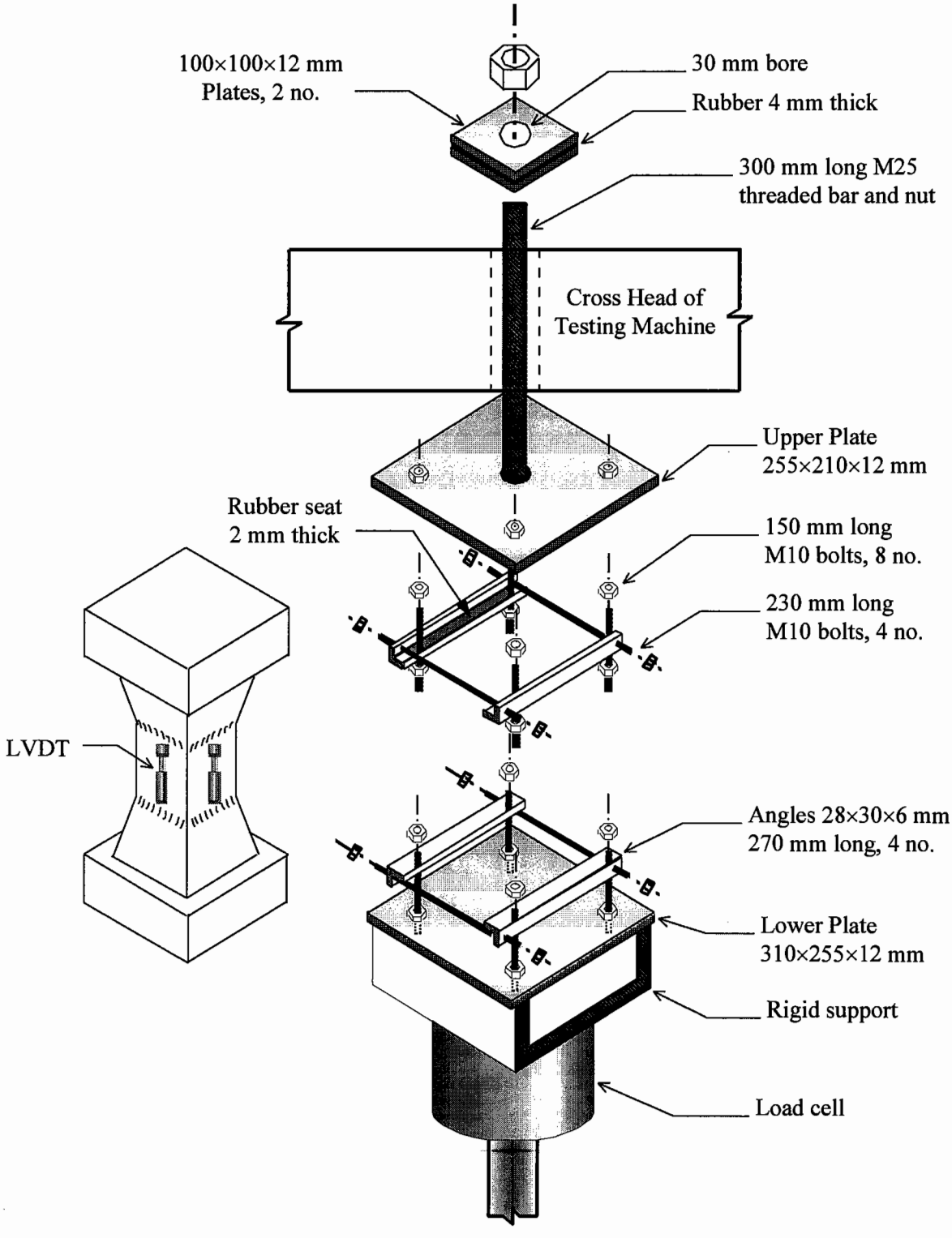

Figure 3.8. System for holding and loading of the tensile specimen

The lower plate (310×255×12 mm) is fixed on a rigid support which is connected to the load cell of the testing machine. The upper plate (255×210×12 mm) is connected, from its centre, to a 300 mm long M25 bolt which passes through a 55 mm bore in the machine's cross head. This bolt then passes through two steel plates (100×100×12 mm) containing a 4 mm thick rubber cushion in between. The bolt is then provided with washers and a nut at the end. The two (100×100×12 mm) plates act as a constraint against the cross head when the specimen is loaded. The rubber cushion, in between the constraining plates, and the rubber seats on the angles, provide flexibility which is of significant importance during adjustment of the lifting system.

3.3.5 Testing of Specimen under Tension

An important consideration during a direct tensile test is that the specimen must be in true alignment in order to prevent the occurrence of any bending stresses. This suggests that the deformations measured from LVDTs on all faces of the specimen must be consistent. For this purpose, a few preloading cycles of up to 3 or 4 kN are applied and the corresponding deformations, from different faces of the specimen, are compared. If they are not in agreement with each other, the lifting system is adjusted accordingly. This procedure is repeated until the deformations are found to be consistent.

After the specimen is properly aligned, the actual test is started. The tensile force is applied in increments of 1 to 2 kN (or continuously using an automatic control system) and the corresponding LVDT readings are recorded. The test is continued until the specimen is failed (Figure 3.9). The values of tensile stress are calculated and a stress strain relationship is then obtained. A typical stress strain relationship for a CBM specimen (Figure 3.10) is linear up to a substantial proportion of the ultimate strength, the slope of which gives a measure of the elastic stiffness. The calculation of elastic stiffness in tension E_t is based on the magnitude of strain corresponding to a stress level of 50% of the tensile strength [Kolias and Williams, 1978].

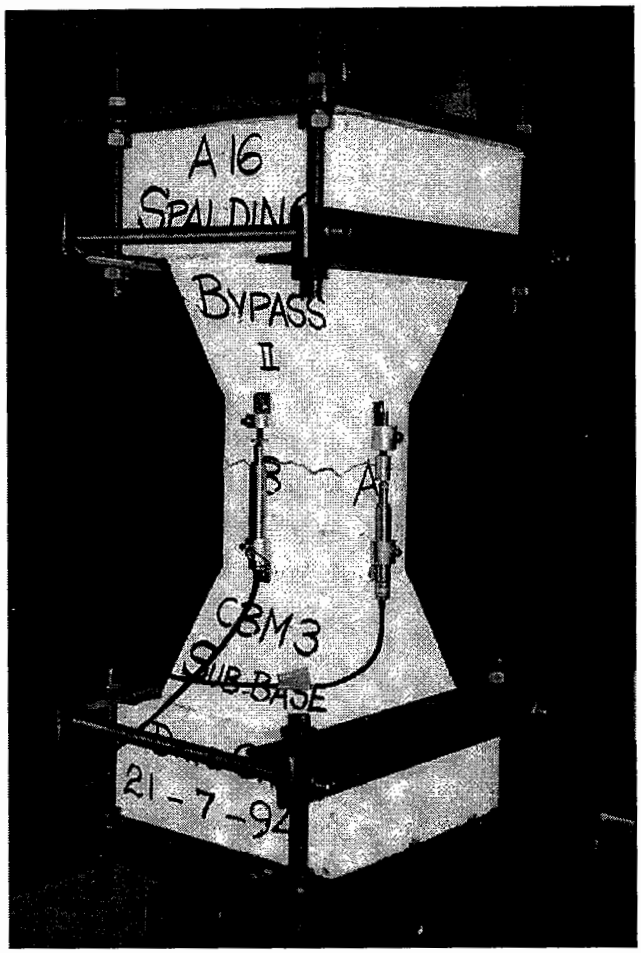

Figure 3.9. Direct Tension Test

3.3.6 Testing of Specimen under Compression

The tensile specimens have also been tested in compression, mainly to compare the magnitudes of elastic stiffness under tension and compression. Testing in compression can either be performed on the same specimen prior to a direct tensile test, or on another specimen from the same CBM mix.

The compression test on a tensile specimen is relatively simpler. The same arrangement (Figure 3.8) is used, with small changes, though provision of the angles is no longer necessary. A steel block is inserted underneath the lower plate (310×255×12 mm) to increase its rigidity. Rubber seats, 2 mm thick, are provided on the top and bottom of the specimen. To attain the conditions of point loading, a circular aluminium block (230 mm diameter × 55 mm height) is centrally placed on

top end of the specimen. A steel ball (30 mm diameter) is positioned at the centre of the aluminium block. This ball comes in contact with the upper plate (255×210×12 mm) of the arrangement during testing.

After two preloading cycles of up to 10 kN, the compressive force is applied in increments of 2 to 3 kN (or continuously using an automatic control system) and the respective deformations are recorded from the LVDTs. This test is intended to be a non-destructive one, and is continued up to almost one third of the failure load. A representative stress strain curve under compression, for a CBM specimen, is shown in Figure 3.10, where it can be seen that the curve is linear within the stress range tested. The slope of this line gives the elastic stiffness in compression E_c. This is in accordance with the prior practice of calculating the elastic stiffness, based on a magnitude of strain corresponding to a stress level of 30% of the ultimate compressive strength [Kolias and Williams, 1978].

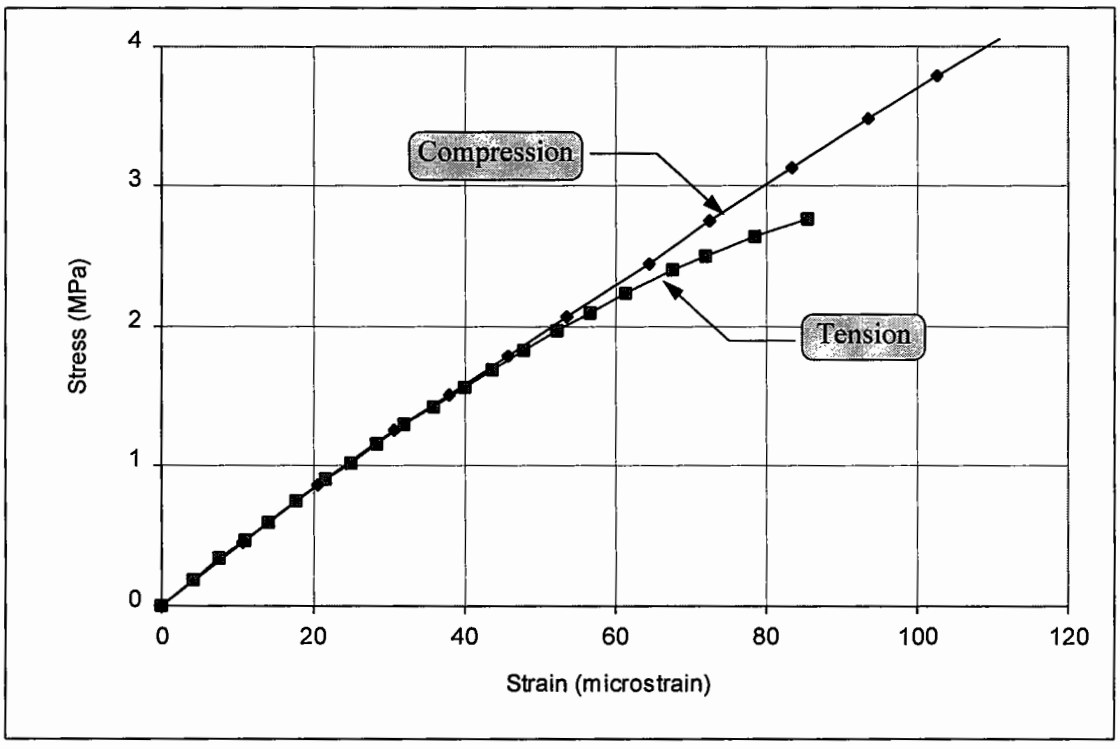

Figure 3.10. Stress strain relationships for a CBM specimen under direct tension and compression

3.4 ASSESSMENT OF STRAIN DISTRIBUTION

An investigation has been carried out to determine the strain distribution at different levels of the specimen under direct tension. For this purpose, specimens were prepared from a cement sand (1:4) mortar comprising a 4 mm maximum aggregate size. One of the specimens was instrumented with 28 strain gauges (Figure 3.11). For strain measurement, the strain gauge size was selected as 10 mm (length), which was 2.5 times the maximum aggregate size involved. The reading indicated by each strain gauge was an average magnitude of the strain developing over a length of 10 mm. The strain gauges were fixed on the four faces A, B, C and D of the middle part of the specimen using a high strength epoxy adhesive. The arrangement of the strain gauges on different faces of the specimen is shown in Figure 3.12. It is to be noted here that face A is opposite face C, and face B is opposite face D. The adhesive was allowed to harden properly for 4 days, while the strain gauges were provided with a plastic cover and were kept under a constant dead load for proper adhesion to the specimen surface. Afterwards the strain gauges were connected to separate channels of a data logger system which was further connected to a computer. A signal from the load cell of the testing machine was also connected to the data logger system, so that the relationships between applied load and resulting strains could be directly monitored on the screen during the test.

Before starting the actual testing, a small amount of load, up to 4 kN, was applied and the readings from strain gauges on the four faces of the specimen were compared. Looking at the load versus strain relationships, the lifting system was adjusted. This procedure was repeated four times until the readings from the strain gauges, at the same levels of the four faces, were found to be consistent. Then the actual test was started. The load was applied in increments and the corresponding readings were recorded. Meanwhile the load versus strain plots were continuously monitored. The test was continued until failure of the specimen.

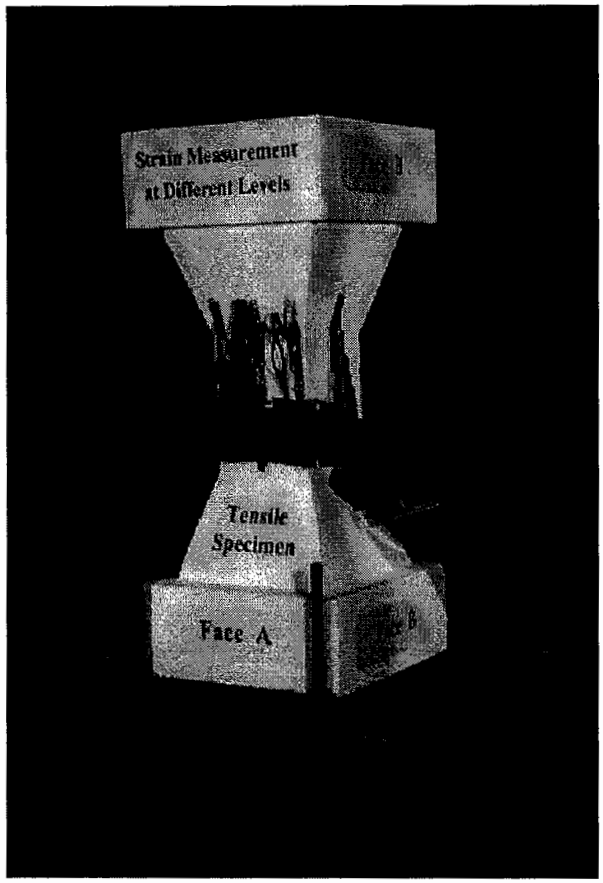

Figure 3.11. Tensile specimen fitted with strain gauges

3.5 DISCUSSION OF RESULTS

From Figure 3.12, it is clear that the strain gauges were attached to each face of the specimen at four different levels. Level 1 and 2 are on either side of the intersection of the slanting part and the central rectangular part of the specimen. Level 4 mirrors level 2, and level 3 is at the mid height.

By comparing the magnitudes of the level 1 strains from faces A and C (Figure 3.13), it can be seen that the strains near corners of the slanting surfaces (gauges 1, 11, 3 and 13) are almost 16% higher than those in the middle (gauges 2 and 12). This could be due to the geometrical configuration of the slanting part of specimen. However, it is obvious from Figure 3.13 that the strains at respective positions on faces A and C are almost identical. A re-assuring finding is that, even with this 16% strain difference, the level 1 strains are less than those of levels 2 to 4 (in Figures 3.14 and 3.15), which

indicates that the strain concentrations within the slanting part are of no practical significance.

The strains at levels 2 and 4, from specimen faces A and C, are shown in Figure 3.14, where the above pattern of strain concentration is substantially diminished. Although level 2 strain gauges 5 and 15 (in line with gauges 2 and 12 of level 1), have recorded slightly lower values, they are in close agreement with the corresponding level 4 strain gauges 10 and 20. The level 3 strains from the two faces A and C are even more consistent (in Figure 3.15) than all those at other levels. The magnitudes of level 3 strains are actually slightly higher than those of levels 2 and 4. This may be because levels 2 and 4 are very close to the intersection of two surfaces, and this intersection is slightly curved rather than having sharp corners. This demonstrates that the most critical area is the middle portion of the central rectangular part of the specimen, the area which is subjected to the most uniform strains. Indeed, the truth of this finding is evidenced by the failure, within this length, of a majority of the CBM specimens tested under direct tension. For example Figure 3.19 shows the failure of two specimens from the same CBM mix.

The performance of the lifting system can be verified from a comparison of the respective strains at the same level from the four faces of the specimen. The corresponding strains at different levels are shown in Figures 3.16 to 3.18. These figures indicate that the level 1 strains from the four faces are in good agreement with each other, but smaller in magnitude than those at the other levels. The consistent pattern of the respective strains at different levels, in Figures 3.16 to 3.18, proves that the specimen was truly aligned and the lifting system had applied an axial tensile force with negligible (if induced) flexural stresses. Another important finding is that the performance of the strain gauges has been found to be almost unaffected by the aggregate particles. This may be because the strain gauge size used was 2.5 times that of the maximum size of the aggregate.

The tensile specimens were also investigated for the possibility of any variation in the density of different parts, from top to bottom, of the specimen. This study, carried out

on several specimens, comprised slicing of a tensile specimen at different levels and dividing it into five parts. Each part was then weighed in water and in air to calculate its density. The results indicated that the densities from various portions of the specimen were consistent.

The direct tensile test (discussed above) has been used to investigate the mechanical characteristics, over a wide range of CBMs. These included tensile strength, stiffness in tension and in compression, and fatigue strength. The results of these properties, measured through this test and from other methods, are described in Chapter 4.

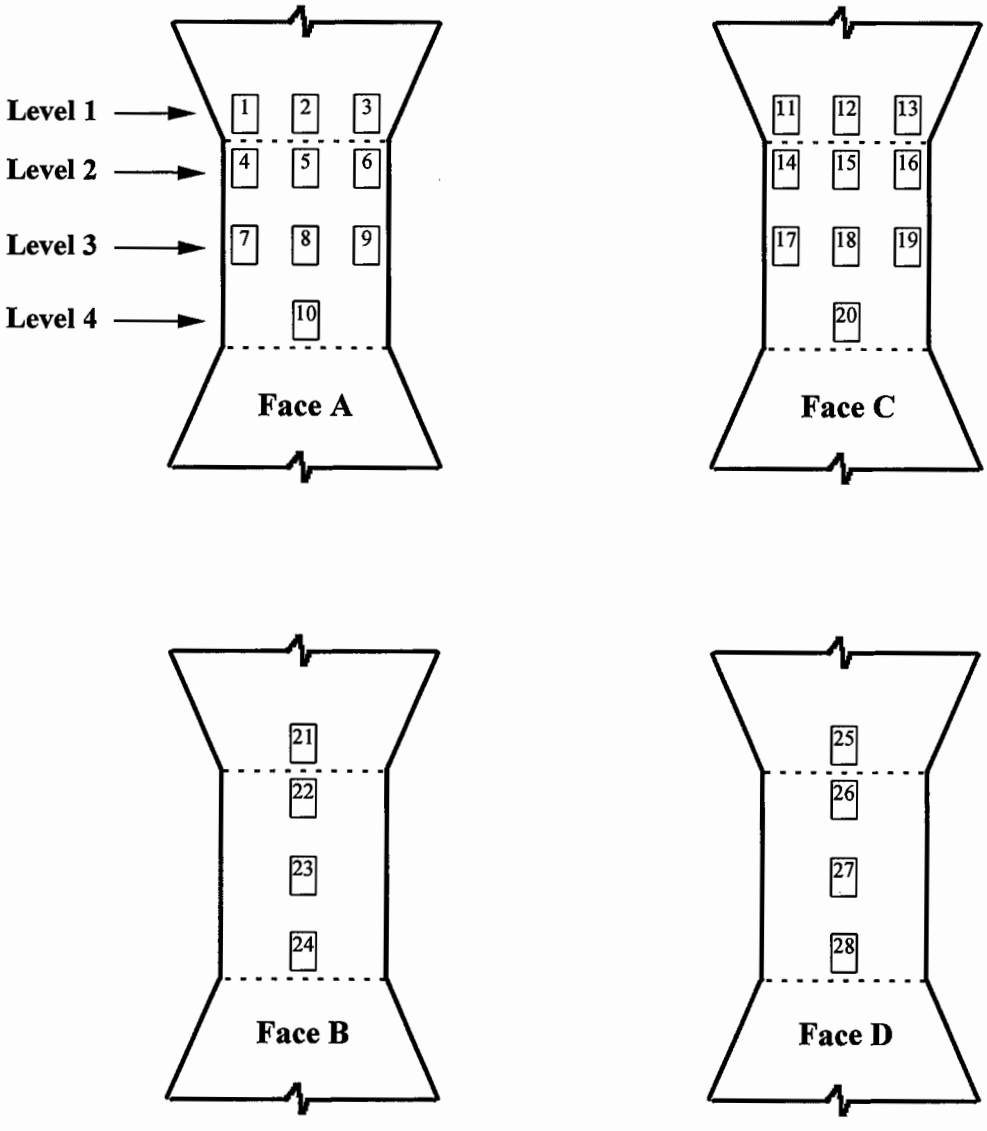

Figure 3.12. Arrangement of strain gauges on different faces of the specimen

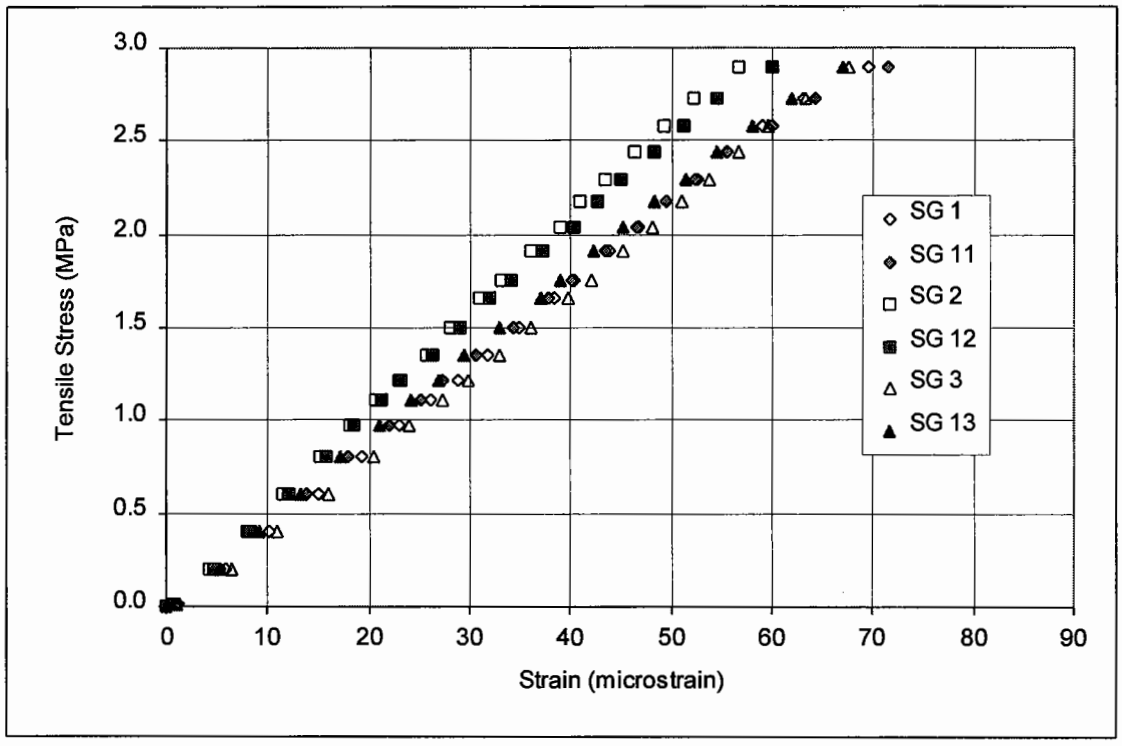

Figure 3.13. Comparison of strains at level 1 of faces A and C

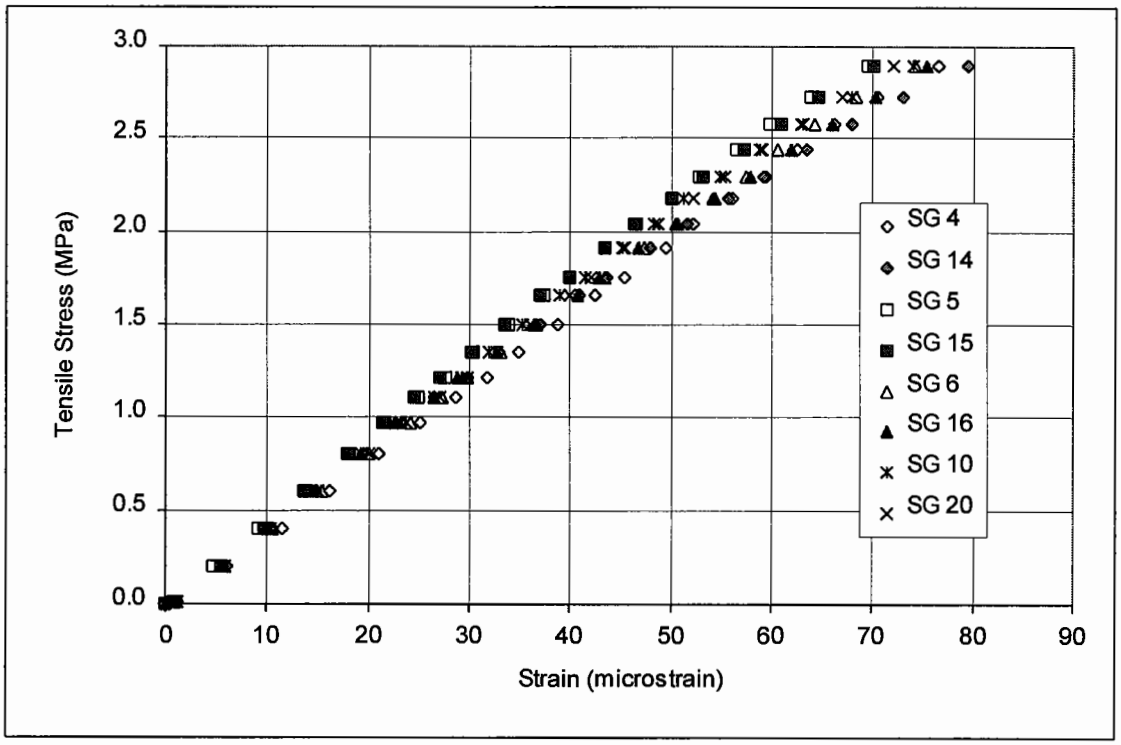

Figure 3.14. Comparison of strains at levels 2 and 4 of faces A and C

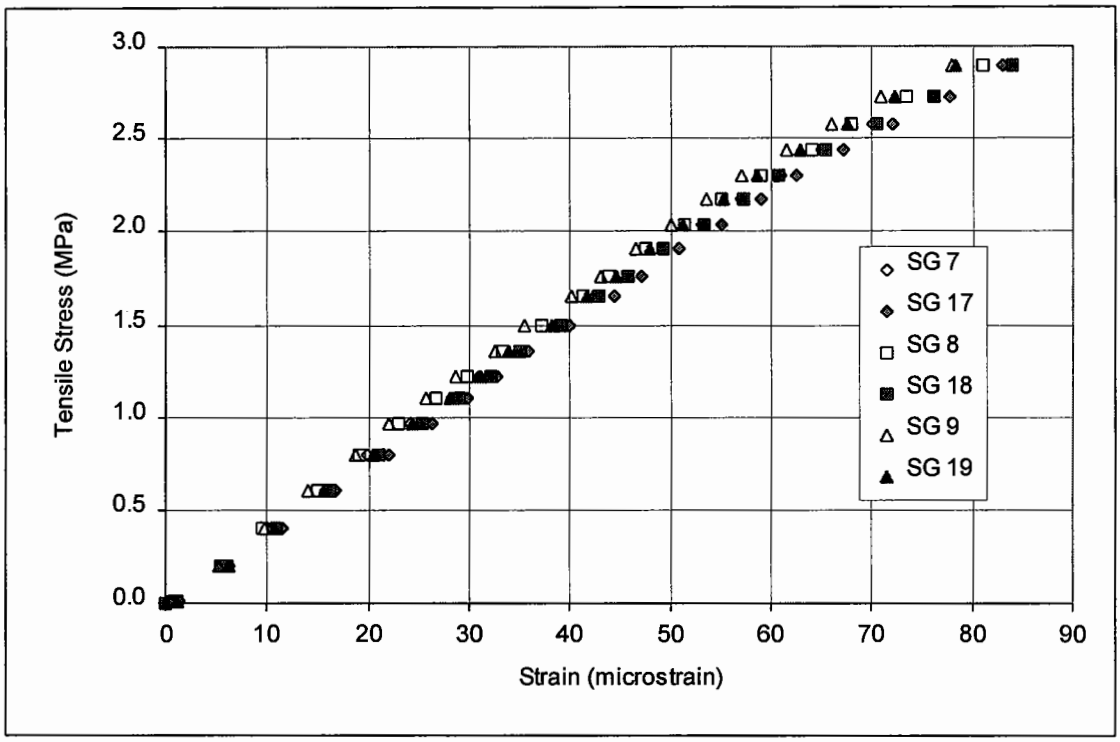

Figure 3.15. Comparison of strains at level 3 of faces A and C

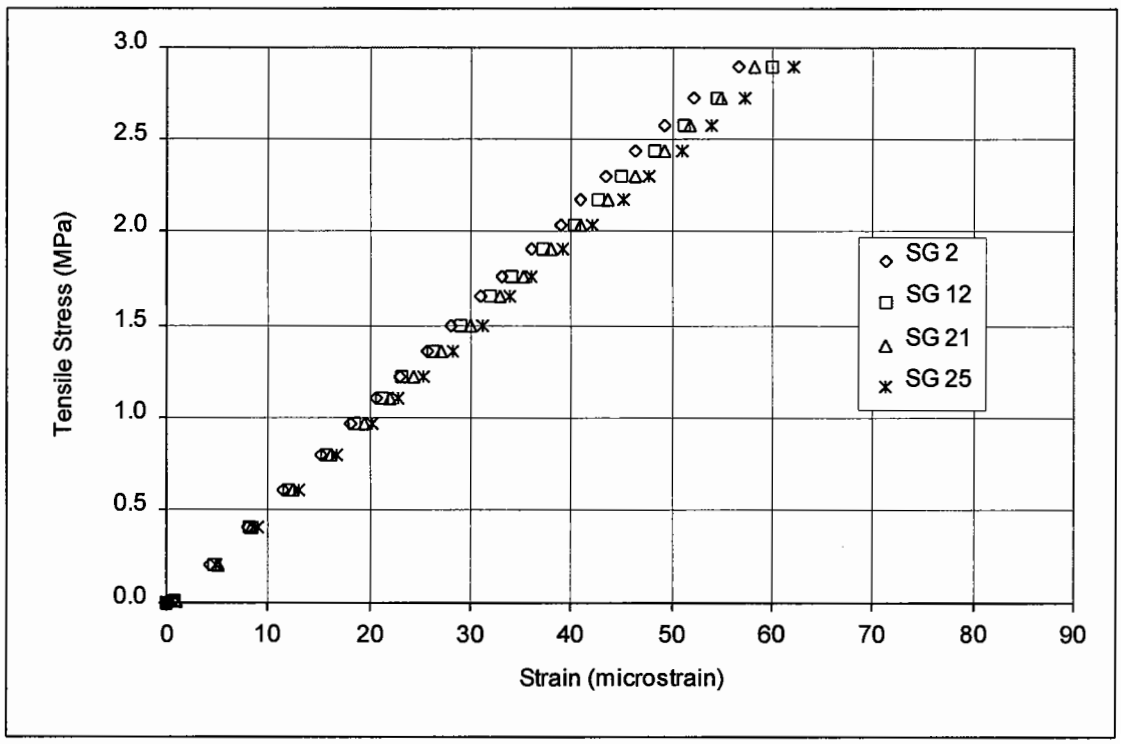

Figure 3.16. Comparison of strains at level 1 from the four faces

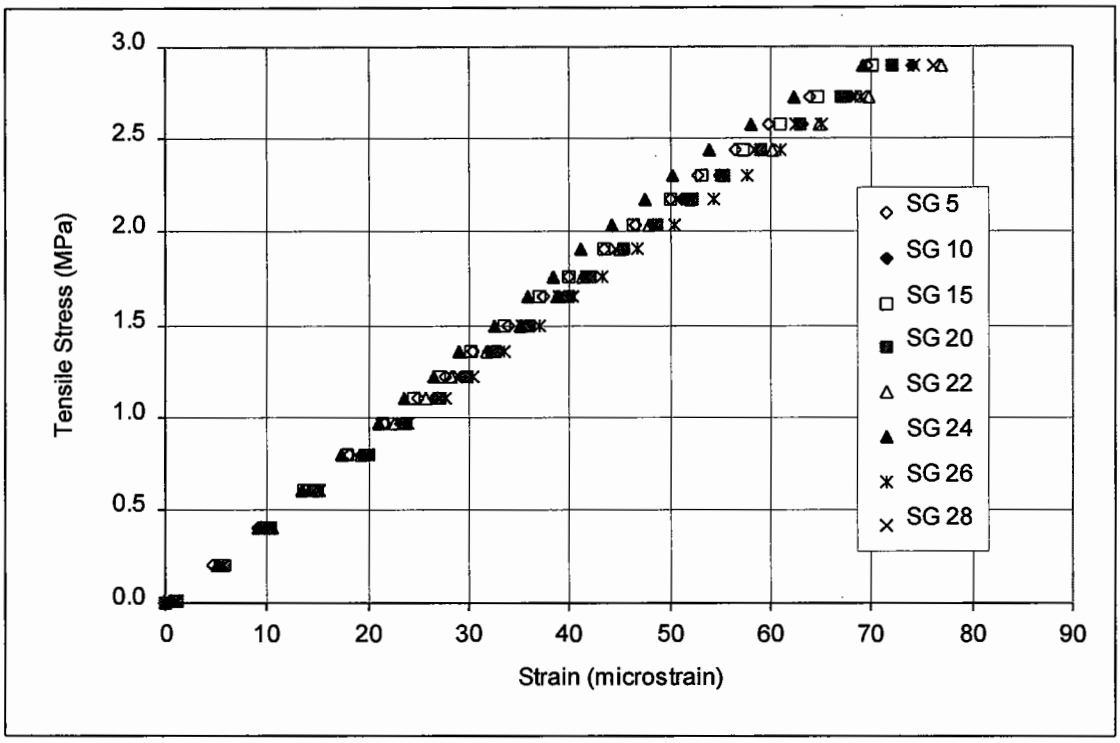

Figure 3.17. Comparison of strains at levels 2 and 4 from the four faces

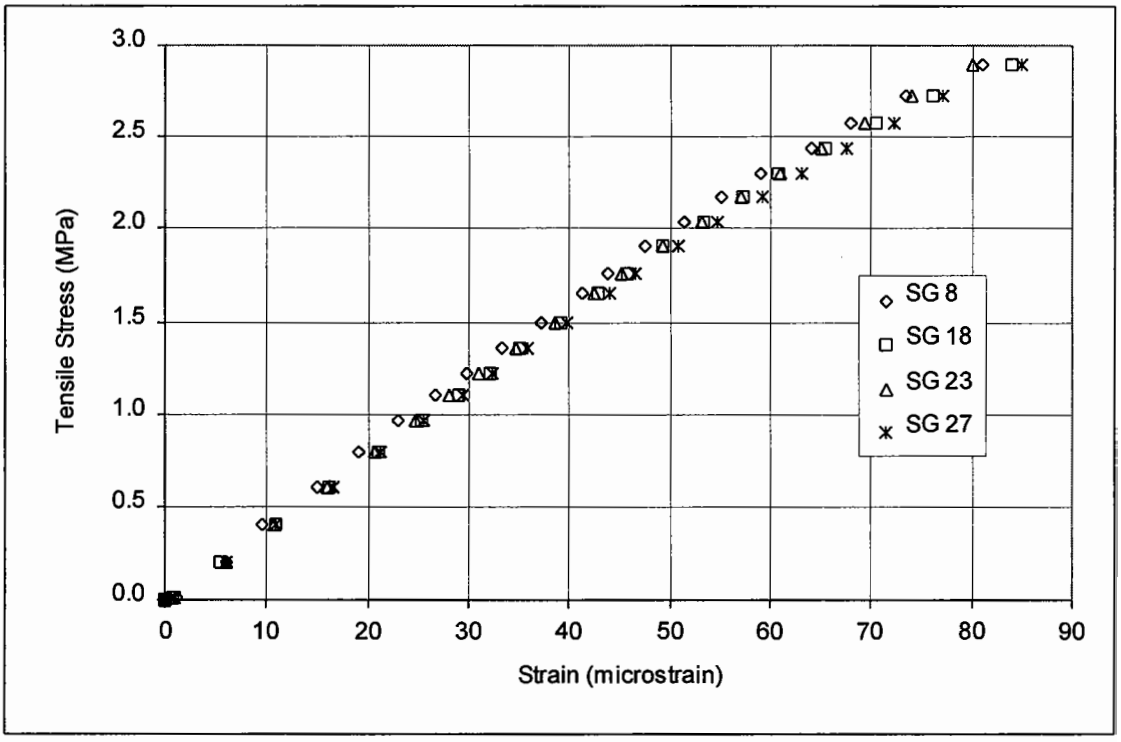

Figure 3.18. Comparison of strains at level 3 from the four faces

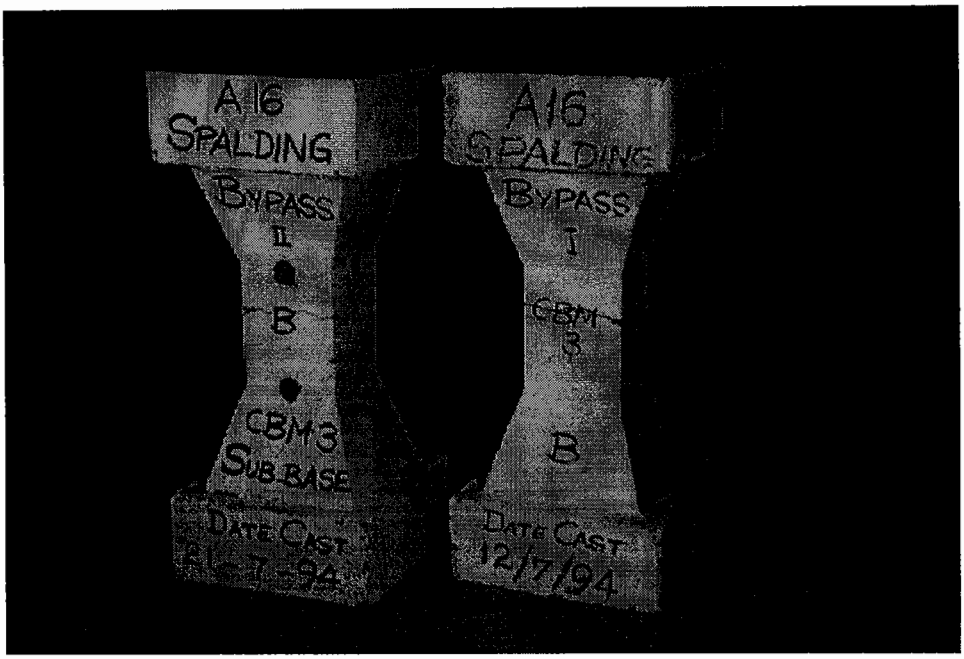

Figure 3.19. CBM specimens tested under direct tension

3.6 SUMMARY

The direct tensile test, developed in this project, provides a reasonably accurate measurement for the tensile strength and elastic stiffness of CBMs. The indirect tensile tests (flexural and cylinder splitting) overestimate in the magnitude of tensile strength due to unrealistic assumptions and complex stress distribution involved. A study of strain distribution has revealed that almost consistent strains are developed in the central part of the tensile specimen which is subjected to the most critical and uniform stress conditions. This is confirmed by the failure, within this part, of a majority of the CBM specimens tested under direct tension.

The lifting system used has been found satisfactory in applying an axial tensile force, by causing the occurrence of no (or negligible) flexural stresses in the specimen. The stress strain relationship under direct tension is linear almost up to failure, but that in compression is generally linear only for stress levels up to some proportion (say 60%) of the ultimate strength, after which it becomes non-linear.

Mechanical Properties of Cement Bound Materials

4.1 INTRODUCTION

A review of the properties of cement bound materials from previous research [Williams, 1986] demonstrates that, although the cube compressive strength is a useful indicator of the quality of a CBM for compliance purposes, for analytical pavement design information is needed about the properties which influence the development of stress and strain, and which govern the ability of a material to resist such effects. Properties such as elastic modulus (also termed elastic stiffness or stiffness in this thesis) of each pavement layer and the modular ratio of the adjacent layers have a significant effect on the stresses, generated by traffic, not only in the pavement layers, but also in the subgrade [Kolias and Williams, 1978]. Measurement of the effective moduli for different layers of a pavement structure is an important part of the analytical design procedure.

The significance of the tensile properties of CBMs, in relation to the onset of cracking and crack spacing in a CBM base is well known [Kolias and Williams, 1978; Bonnot, 1972]. A measurement of tensile strength is important for assessing the ability of a CBM to resist fatigue failure under repeated loading [Kolias and Williams, 1978]. Of various techniques, the direct tensile test system is generally believed to provide the truest measure of the tensile strength [Dempsey, 1984].

The problem with the tensile properties of CBMs is that they have been reported to be material sensitive [Kolias and Williams, 1978]. The elastic modulus for example is greatly affected by the type of aggregate [Williams, 1972], such that the modulus is higher at a given strength as the material processed more closely approaches a concrete quality aggregate. Another matter of concern is that the determination of tensile modulus from compressive data seems uncertain, as there is some conflicting evidence available regarding the relative values of moduli in tension and in

compression [Williams, 1986]. Some researchers [Metcalf, 1966; Bofinger, 1970; Wang and Huston, 1972] suggest that the moduli differ appreciably, whereas others have reported that they are equal [Kolias and Williams, 1978; Fossberg et al, 1972; Nair et al, 1972; Bonnot, 1972; Patankar and Williams, 1970; Larsen and Nussbaum, 1967].

Present research was, therefore, focused on the measurement of the structural properties of CBMs comprising various types of aggregate used in the UK. The tensile strength was measured through a direct tensile test (discussed in Chapter 3) and an indirect tensile (cylinder splitting) test. Stiffness was measured, in tension and in compression, from the tensile specimens. Stiffness in compression was also measured from standard cylinders. Poisson's ratio was measured from cylinders under static loading, and fatigue characteristics were determined under repeated loading in direct tension.

4.2 DESCRIPTION OF MATERIALS TESTED

The assessment of structural properties was carried out for different CBM categories, comprising a variety of crushed and uncrushed aggregates, produced in the laboratory and on construction sites. A description of these materials, termed A, B, C, D, E and F, is given in the following paragraphs.

A : Gravel Sand CBMs

An uncrushed silica gravel was blended with sand to produce a grading shown in Figure 4.1. The material was obtained from the Trent Valley, and was used to produce CBM3 to CBM6 mixes in the laboratory. The same material was utilized for a steel fibre reinforced (SFR) CBM5 (discussed in Chapter 6), and concrete mixes. Two concrete mixes were included in this study. The first one was concrete (i.e. cement, sand and coarse aggregate in the proportions 1:2:3), used on a trial basis to determine its tensile properties through the direct tensile test. The second mix was a cement plus sand (5.0 to 0.15 mm) mortar (1:4), which was used to investigate the strain distribution in the tensile specimens (discussed in Chapter 3).

B : Limestone CBMs

A crushed limestone aggregate, obtained from Dene quarry in Derbyshire, was reconstituted to attain a grading shown in Figure 4.1. This material was also used for preparing CBM3 to CBM6 mixes in the laboratory.

C : Flint Gravel Sand CBM : A11 Stumpcross, Cambridge

A crushed flint gravel blended with sand, used for the construction of a CBM2 sub-base on the A11 at Stumpcross, Cambridge, was the first element in the investigation into site produced CBMs. This material was obtained from the Thames Valley. The average grading from representative samples (collected on different days), is shown in Figure 4.2. Although the maximum aggregate size was 75mm, for making specimens particles of size larger than 20mm were removed (from the mix) due to the limitations of the size of tensile specimen (Figure 3.7 of Chapter 3).

D : Glacial Gravel Sand CBM : A16 Spalding Bypass

An uncrushed glacial gravel plus sand mix was used for a CBM3 sub-base on the A16 Spalding Bypass. This material was obtained from the Nene Valley. The maximum aggregate size was nominally 20mm. The average grading from different samples is shown in Figure 4.3. A particular feature of this material was the flaky shape of the gravel particles.

E : Limestone CBM : M4 & M49 SSC, Bristol

A crushed limestone aggregate was used for a CBM3 sub-base on the new M4 and M49 access routes to the Second Severn Crossing near Bristol. The maximum aggregate size of this material was 40mm. The average grading from the representative samples (collected on different days), is shown in Figure 4.4. For making specimens, the particles larger than 20mm were discarded for the reasons mentioned above.

F : Flint Gravel Sand CBM : A11 Wymondham Bypass, Norwich

A crushed flint gravel blended with sand was used for a CBM3 sub-base on the A11 Wymondham Bypass near Norwich. The maximum aggregate size was 40mm. The

material comprised washed coarse (40 to 5mm) and fine (below 5mm) aggregates. The average grading from the representative samples is shown in Figure 4.5. For specimens, the particles with size greater than 20mm size were removed.

A previous investigation [Kolias and Williams, 1978] into the structural properties of CBMs included two materials which fall within the grading limits for 20mm CBM3 to CBM6. These materials, termed 1 and 2, are shown in Figure 4.6 and are considered in this chapter for comparison purposes. Material 1 was a washed flint gravel aggregate from the Thames Valley, whereas material 2 was a reconstituted one produced by combining gravel aggregate with brickearth. The cement and water contents used for these materials were 5.55% and 6%, respectively, by weight [Kolias and Williams, 1978], which are approximately similar to those for materials D and F in the present research.

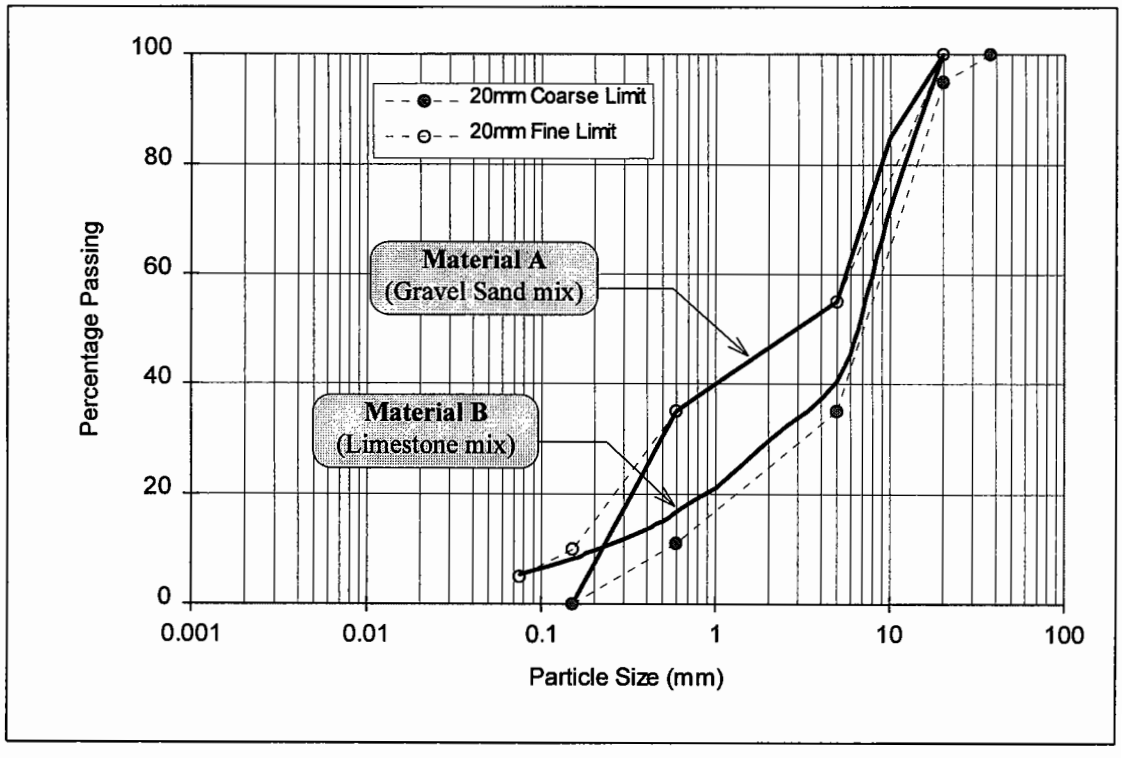

Figure 4.1. Gradings for gravel sand (Trent Valley) and limestone (Nene Valley) aggregate used for CBM3 to CBM6 mixes in the laboratory

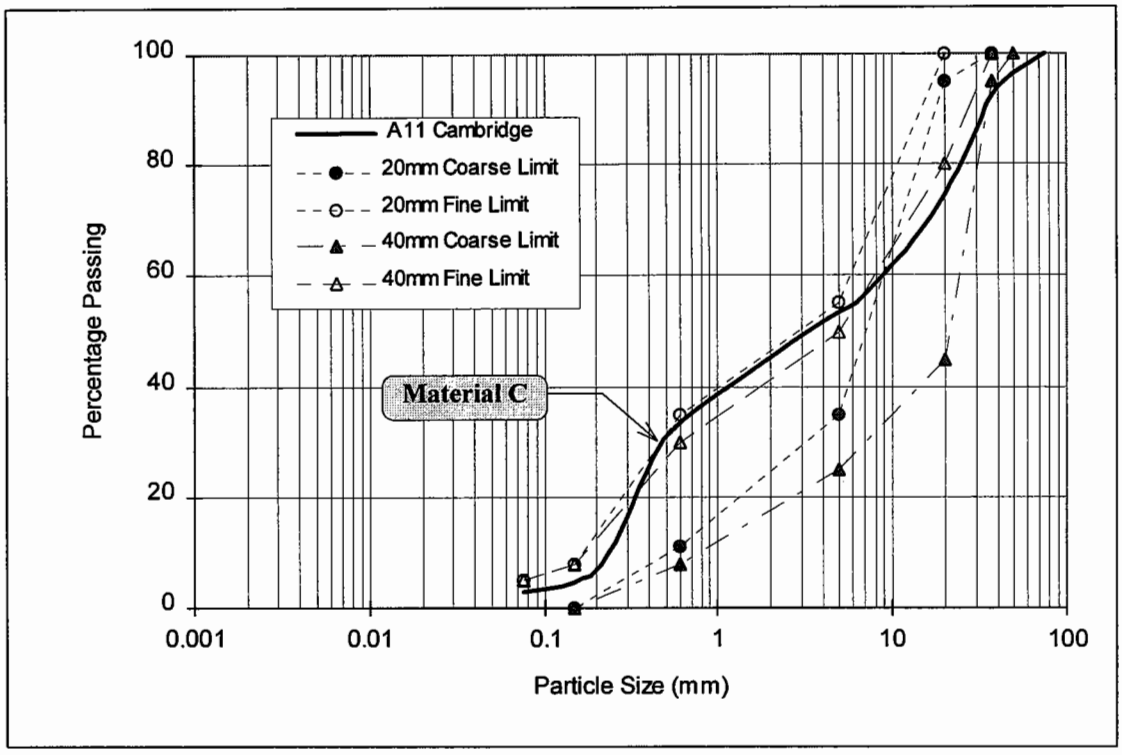

Figure 4.2. Grading for the crushed flint gravel plus sand aggregate, from Thames Valley, used on the A11 at Stumpcross, Cambridge

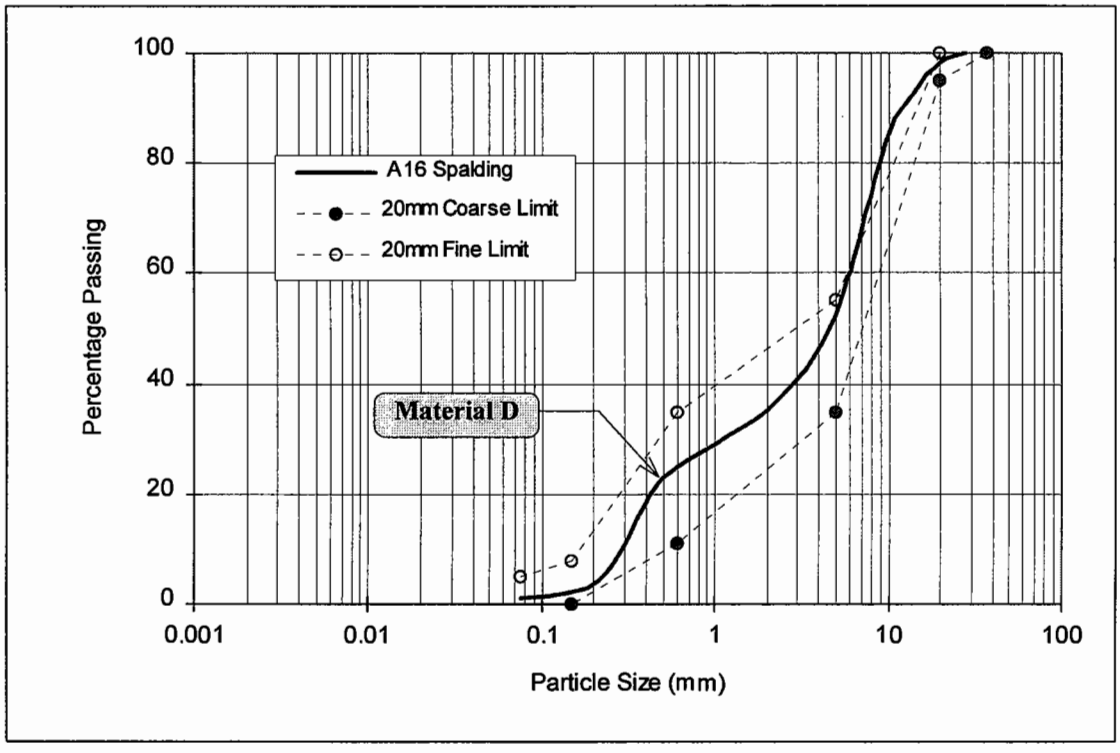

Figure 4.3. Grading for the uncrushed glacial gravel plus sand aggregate, from Nene Valley, used on the A16 Spalding Bypass

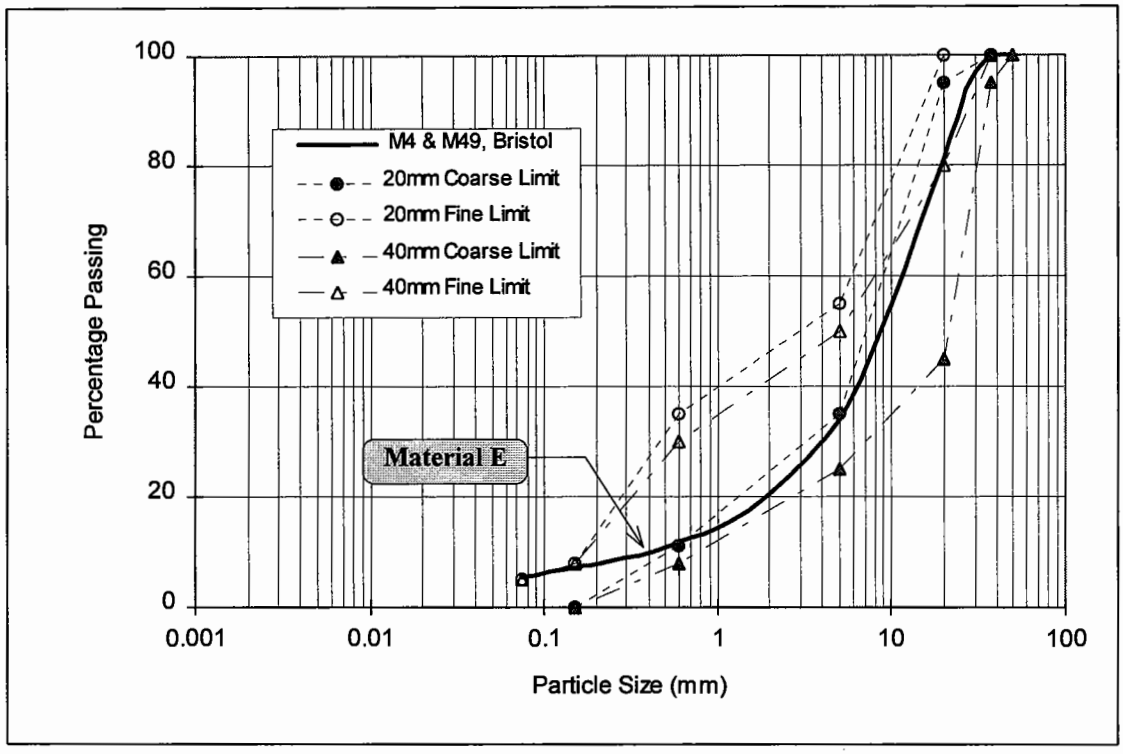

Figure 4.4. Grading for the crushed limestone aggregate used on the M4 and M49 Second Severn Crossing, Bristol

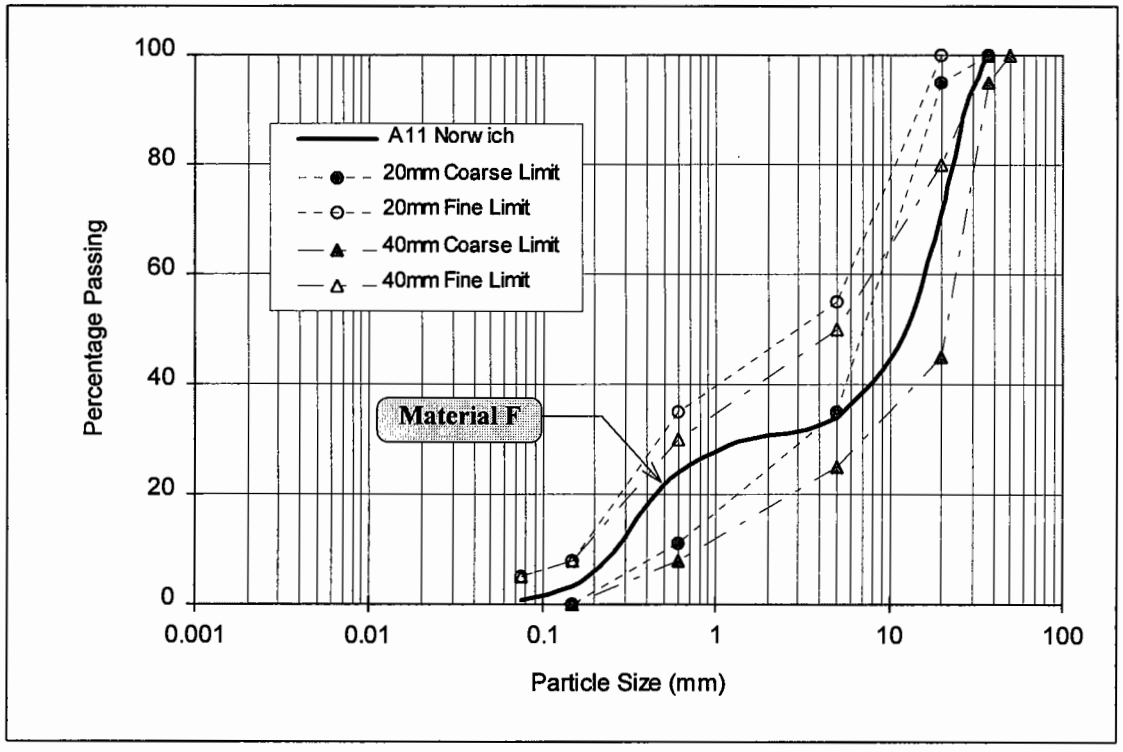

Figure 4.5. Grading for the crushed flint gravel and sand aggregate used on the A11 Wymondham Bypass, Norwich

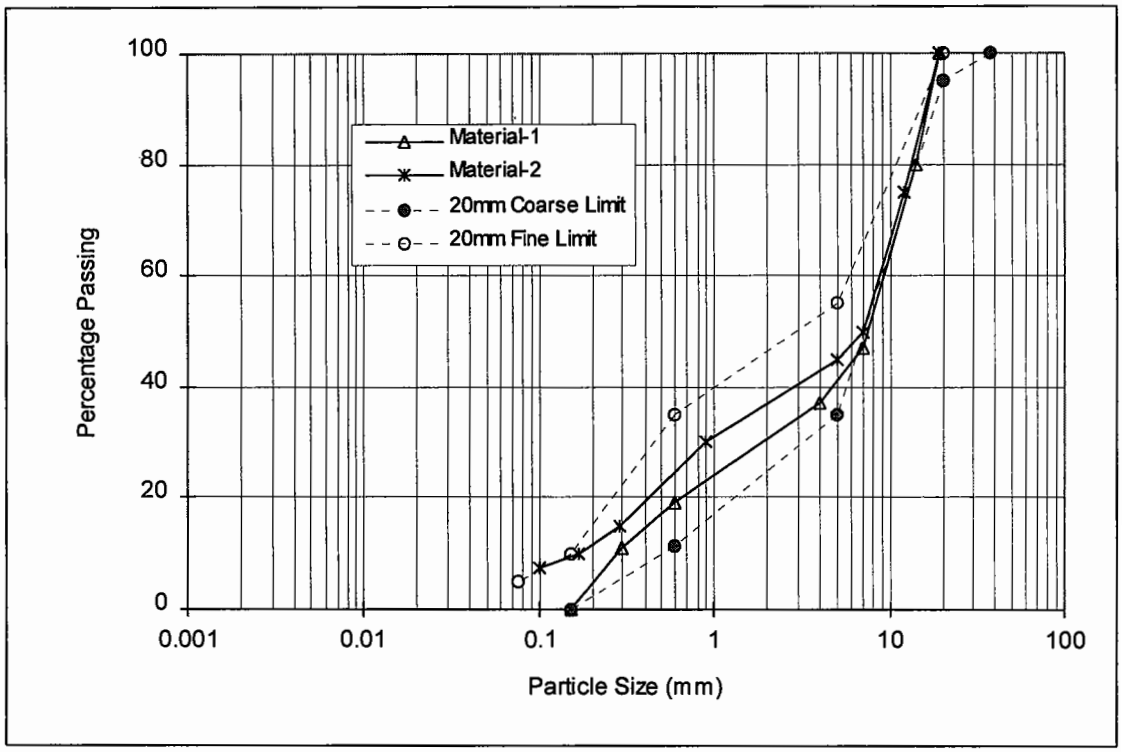

Figure 4.6. Gradings for the two previously researched materials (Kolias and Williams, 1978), which fall within the limits for 20mm CBM3 to CBM6.

4.3 STRENGTH AND ELASTIC STIFFNESS

4.3.1 Determination of Strength and Elastic Stiffness

The strength and elastic stiffness properties of CBM (and concrete) mixes were determined through a variety of tests, a brief description of which is given below.

Strength Properties

Compressive strength was determined from cubes (100mm) and standard cylinders (300mm × 150mm diameter). Tensile strength was measured through the direct tensile test. The indirect tensile strength, termed splitting strength, was determined from the cylinder splitting test [BS 1881: Part 117: 1983], performed on cylindrical specimens (150mm × 150mm diameter). All the CBM specimens were compacted, in the laboratory and on construction sites, using a vibrating hammer. The procedure for preparing, curing and testing of cubic specimens is given in Clause 4.2 of BS 1924: Part 2: 1990. The same procedure was used for cylinders. For the tensile specimens, however, the procedure is given in Chapter 3. The testing age was mainly 28 days, except for the 7 day cube compressive strength determination.

For concrete specimens, the vibrating table method was used for compaction. BS 1881: Part 108: 1983 and BS 1881: Part 110: 1983 describe the procedures for making concrete cubes and cylinders, respectively. The method of curing is given in BS 1881: Part 111: 1983.

Besides the prepared specimens, cores (150mm diameter) were also taken from the CBM pavements on the above mentioned sites. Some of the cores were tested for splitting strength, while the others were tested to determine their equivalent (estimated) in-situ cube strength. A method for the determination of the compressive strength of concrete cores is described in BS 1881: Part 120: 1983, according to which the estimated in-situ cube strength f_{ic} is calculated through the following relation:

$$f_{ic} = \frac{\mu}{1.5 + \left(1/\lambda\right)} \times f_{cc} \qquad (4.1)$$

where:

f_{ic} : estimated in-situ cube strength (N/mm^2)

μ : 2.3 for cores drilled vertically, or 2.5 for cores drilled horizontally

λ : ratio of the length (after end preparation) to diameter of core

f_{cc} : compressive strength of core (N/mm^2)

Elastic Stiffness

The elastic stiffness in tension and compression was measured from the tensile specimens by testing them under tension and compression, respectively (see Section 3.3 of Chapter 3), and was determined from the slope of the stress strain curve. The calculation of stiffness in tension E_t is based on the strain corresponding to a stress level of 50% of the tensile strength, whereas the stiffness in compression E_c corresponds to the magnitude of strain against a stress level of 30% of the compressive strength [Kolias and Williams, 1978]. This is because when a CBM is tested under direct tension, the stress strain relationship is linear almost up to failure. But in compression, the stress strain curve is generally linear for stresses below 60% of the ultimate strength. In this range, the stiffness is measured as a secant modulus corresponding to a particular stress level [Bonnot, 1972].

For comparison purposes, the stiffness in compression was also determined from cylinders (300mm × 150mm diameter), in accordance with the method described in BS 1881: Part 121: 1983. The magnitude of (secant) elastic modulus was calculated from the slope of the stress strain relationship as follows:

$$E_{cl} = \frac{\Delta\sigma}{\Delta\varepsilon} \qquad (4.2)$$

where E_{cl} is the elastic stiffness in compression from the cylinder. $\Delta\sigma$ and $\Delta\varepsilon$ are the differences in stress (N/mm^2) and strain, respectively, between a basic loading level of

0.5 N/mm^2 and an upper loading level of one-third of the cylinder compressive strength of a CBM [BS 1881: Part 121: 1983].

4.3.2 Presentation of Results

The study of CBMs from materials C to F involved making specimens from the plant mixed CBMs produced on the construction sites, transporting these specimens (covered with air-tight polyethylene bags), and then curing and testing them under laboratory conditions. For each site, more than one visit was necessary for the collection of specimens. On each visit, samples of the CBM mix and aggregate were collected to determine the mix water content and material grading, respectively. With visits on different days, some variation in the mix water content was noticed for each site, shown in column 5 (w.c. used) of Table 4.1.

The average results, summarized in Table 4.1, include the material description, mix design parameters, and average densities achieved from different types of specimens. A summary of the strength properties and elastic stiffness results is given in Tables 4.2 and 4.3. Each value of the cube compressive strength f_c (in Table 4.2) represents the average of five specimens for the laboratory produced CBMs, and from three to six specimens in the case of CBMs produced on sites. Cylinder compressive strength results are the average from a minimum of three specimens. Similarly, the tensile strength and elastic stiffness results (Table 4.3) represent the average values from a minimum of three specimens for the laboratory mixes, but the number of specimens varied (from one to three) for the site mixes. The splitting strength results are the average from four to eight specimens. The last column of Table 4.2 represents the category of CBM based on the results of the 7 day cube compressive strength attained, as a result of the mix design parameters used (columns 3 and 5).

Table 4.4 summarizes the average results of tests performed on cores (at 28 days), which included density measurements, following determination of equivalent (estimated) in-situ cube strength, and core splitting strength.

Table 4.1. Description of materials and density of specimens

Material	Description	Mix Parameters			Saturated Density of Specimens (kg/m^3)							
					Cubes (7 days)		Cubes (28 days)		Cylinders (28 days)		Tensile Specimens (28 days)	
		c.c. (%)	omc (%)	w.c. used (%)	density	st. dev.	density	st. dev.	density	st. dev.	density	st. dev.
A	Laboratory Mix (Trent Gravel Sand CBMs)	5.0	5.0	5.0	2357	9.8	2359	7.9	2341	6.7	2347	3.5
		5.5	5.1	5.1	2361	3.6	2368	11.3	2348	4.5	2352	5.1
		6.5	5.2	5.2	2394	12.2	2407	6.5	2384	7.3	2381	6.8
		7.0	5.2	5.2	2406	7.6	2413	8.0	2396	4.7	2392	7.4
B	Laboratory Mix (Dene Limestone CBMs)	3.6	4.3	4.3	2522	3.6	2521	3.0	2511	8.3	2507	6.4
		4.2	4.3	4.3	2520	6.8	2524	5.9	2516	5.8	2518	4.7
		5.0	4.35	4.35	2521	10.3	2524	6.9	2519	10.1	2524	9.5
		5.5	4.35	4.35	2531	7.2	2530	5.3	2522	3.9	2527	5.9
C	A11 Cambridge (CBM2)*	4.6	6.8	6.4	2385	3.4	2390	7.2	2378	5.8	2380	–
				7.0	2349	7.4	2354	10.6	2355	8.3	2357	–
D	A16 Spalding (CBM3)*	5.8	6.9	6.3	2493	3.8	2494	3.2	2471	6.5	2472	–
				7.5	2472	5.0	2477	4.1	2466	10.2	2461	–
E	M4 & M49, Bristol (CBM3)*	4.8	–	4.2	2546	4.9	2547	6.1	2540	5.8	2536	7.8
				5.1	2530	5.7	2528	3.1	2515	7.6	2514	6.9
F	A11 Norwich (CBM3)*	5.03	5.4	5.9	2414	6.9	2415	5.3	2384	9.7	2392	–
				5.4	2417	3.5	2416	2.5	2397	6.6	2407	11.2
A	SFR CBM5	6.5	5.2	5.2	2421	5.3	2423	7.3	2428	4.5	2427	3.6
	Concrete (1:2:3)	w/c = 0.530			2419	4.5	2420	3.7	2417	5.2	2422	5.5
	Cement Sand (C/S) mortar (1:4)	w/c = 0.525			2239	10.8	2234	2.5	2218	7.4	2225	8.5

Table 4.2. Summary of the compressive strength results

Material	Description	Mix Parameters			Cube Strength, f_c (N/mm^2)				Cylinder Strength, f_{cl} at 28 days (N/mm^2)		CBM Category[1]
		c.c. (%)	omc (%)	w.c. used (%)	7 day strength	7 day st. dev.	28 day strength	28 day st. dev.	strength	st. dev.	
A	Laboratory Mix (Trent Gravel Sand CBMs)	5.0	5.0	5.0	13.7	0.39	17.4	0.41	11.3	0.87	CBM3
		5.5	5.1	5.1	16.8	0.40	21.7	0.57	14.4	0.67	CBM4
		6.5	5.2	5.2	23.1	0.35	30.5	0.52	21.5	1.13	CBM5
		7.0	5.2	5.2	26.8	0.74	34.7	0.85	25.8	1.04	CBM6
B	Laboratory Mix (Dene Limestone CBMs)	3.6	4.3	4.3	13.0	0.44	17.9	0.50	12.2	0.98	CBM3
		4.2	4.3	4.3	16.7	0.38	22.5	0.53	15.6	0.77	CBM4
		5.0	4.35	4.35	24.2	0.41	31.0	0.49	22.3	1.02	CBM5
		5.5	4.35	4.35	27.5	0.52	35.3	0.43	28.1	0.67	CBM6
C	A11 Cambridge (CBM2)*	4.6	6.8	6.4	13.4	0.98	19.8	1.07	10.7	0.64	CBM3
				7.0	9.1	0.42	15.2	1.15	7.7	0.91	CBM2
D	A16 Spalding (CBM3)*	5.8	6.9	6.3	26.2	0.91	32.2	0.50	18.5	0.78	CBM6
				7.5	20.3	0.67	25.4	1.31	16.5	0.57	CBM5
E	M4 & M49, Bristol (CBM3)*	4.8	–	4.2	24.0	0.85	31.8	1.01	17.2	0.64	CBM5
				5.1	16.6	0.47	21.3	0.80	13.4	1.12	CBM4
F	A11 Norwich (CBM3)*	5.03	5.4	5.9	17.6	1.03	23.4	1.29	15.6	0.87	CBM4
				5.4	21.1	1.17	27.1	1.05	17.9	0.65	CBM5
A	SFR CBM5	6.5	5.2	5.2	24.7	0.66	32.3	0.80	24.4	0.47	CBM5
	Concrete (1:2:3)	w/c = 0.530			40.7	0.55	48.0	0.37	33.4	0.72	Concrete
	C/S mortar (1:4)	w/c = 0.525			39.0	0.40	46.0	0.64	31.2	1.20	Concrete

Note: [1] : Classification based on the CBM strength achieved

* : Contractor's target CBM grade on site

Table 4.3. Summary of the tensile strength and elastic stiffness results (at 28 days)

Material	CBM Description	w.c. used (%)	Tensile Specimens						Cylindrical Specimens			
			Direct Tensile Strength (N/mm^2)		Elastic Stiffness (GPa)				Splitting Strength (N/mm^2)		Elastic Stiffness (GPa)	
					Tension		Compression					
			f_t	st. dev.	E_t	st. dev.	E_c	st. dev.	f_{sp}	st. dev.	E_{cl}	st. dev.
A	CBM3	5.0	1.13	0.07	24.7	1.61	23.0	1.51	1.62	0.07	19.2	0.85
	CBM4	5.1	1.61	0.09	28.3	1.32	26.7	0.94	2.17	0.14	23.1	1.06
	CBM5	5.2	2.12	0.14	35.8	0.66	36.1	1.01	2.72	0.08	25.4	0.98
	CBM6	5.2	2.61	0.08	38.5	0.85	37.1	0.78	3.38	0.15	26.3	1.10
B	CBM3	4.3	1.53	0.06	29.5	1.02	28.3	0.83	2.02	0.07	23.2	2.01
	CBM4	4.3	2.02	0.05	33.6	0.53	34.7	1.07	2.67	0.09	25.5	0.85
	CBM5	4.35	2.48	0.09	36.8	1.61	35.4	1.64	3.32	0.11	27.4	1.64
	CBM6	4.35	3.07	0.17	40.2	0.75	38.7	1.72	4.0	0.09	30.1	1.93
C	CBM3	6.4	1.11	–	22.3	–	20.9	–	1.81	0.06	17.3	–
	CBM2	7.0	0.90	–	19.7	–	17.8	–	1.67	0.02	15.3	–
D	CBM6	6.3	1.78	–	29.3	–	28.2	–	2.35	0.04	18.5	–
	CBM5	7.5	1.34	–	28.6	–	27.8	–	2.08	0.03	16.5	–
E	CBM5	4.2	2.27	0.12	37.2	1.92	35.4	0.86	3.26	0.13	22.1	0.85
	CBM4	5.1	1.87	0.13	34.1	1.36	33.5	1.73	2.61	0.09	19.9	1.11
F	CBM4	5.9	1.42	–	30.2	–	29.3	–	1.81	0.10	23.1	–
	CBM5	5.4	1.73	0.12	31.7	1.52	32.5	1.84	2.16	0.07	25.2	1.23
A	SFR CBM5	5.2	2.82	0.04	36.3	1.06	36.6	0.79	3.76	0.10	25.9	1.35
	Concrete (1:2:3)	w/c	3.24	0.16	43.5	1.42	41.7	1.27	4.23	0.20	31.6	1.05
	C/S mortar (1:4)	w/c	3.16	0.07	40.5	0.76	39.3	1.56	4.06	0.08	30.1	1.32

Table 4.4. Average density, splitting strength and estimated in-situ cube strength of cores from different sites (at 28 days)

Material	Description	Core Test Results					
		Saturated density (kg/m^3)		Splitting strength (N/mm^2)		Estimated in-situ cube strength (N/mm^2)	
		density	st. dev.	f_{sp}	st. dev.	f_{ic}	st. dev.
C	A11 Cambridge	2254	14.2	1.31	0.09	12.3	2.71
D	A16 Spalding	2376	15.1	1.72	0.18	18.5	3.51
E	M4/M49, Bristol	2435	23.6	1.90	0.08	18.3	2.47
F	A11 Norwich	2317	13.3	1.35	0.17	16.6	3.25

4.3.3 Discussion of Results

Density Results

Table 4.1 shows that the maximum densities, even higher than for concrete, are obtained from materials B and E. This is because both B and E are crushed limestone, from different sources, with uniform grading (Figures 4.1 and 4.4). With well graded material, the void content is minimized and higher densities are attainable [Robnett and Thompson, 1969; Winterbaum, 1968]. Material D is denser than the other gravel aggregate mixes A, C and F, possibly due to a relatively more uniform grading of the glacial gravel sand aggregate (refer Figures 4.1, 4.2, 4.3 and 4.5), which might have helped to achieve a better packing of the particles under compaction. On the other hand, the densities obtained from materials A, C and F are comparable to those for materials 1 and 2 (Figure 4.6), for which the average densities are 2353 and 2360 kg/m^3, respectively, as reported by Kolias and Williams [1978].

The densities obtained from different shapes of specimen, that is cube, cylinder and tensile specimen, are almost similar. The core densities (Table 4.4) are, on average, 4 to 6% less than the prepared specimens (Table 4.1). The amount of scatter (standard deviation) in the density results is less for cubes, than for the tensile specimens and cylinders, by 7.5% and 10%, respectively. Both the tensile specimens and cylinders,

however, show more or less similar scatter, 2.5% less for the tensile specimens. But maximum scatter has been found in the core densities.

Variations in the Mix Water Content

Some variations in the mix water content were found on each site. Tables 4.2 and 4.3 show that the effect of a variation in the water content, at constant cement content, is more significant upon the strength properties than on the elastic stiffness results, such that a mix water content on the wet side of the optimum (omc) causes a reduction in the CBM strength, and hence alters the CBM grade (category), as shown in Table 4.2. The compensation of such a reduction in strength demands an extra amount of cement [Marais et al, 1973]. Indeed, a comparison of the mix parameters and strength properties of the site produced CBMs with those for the laboratory mixes indicates that a relatively higher cement content had been employed on these sites with respect to the target CBM grades. For such CBMs, which comprise coarse grained materials, a relatively denser mix with maximum strength can be achieved at a particular cement content if the mix water content used is slightly on the dry side of the optimum [Cauley and Kennedy, 1973]. The results in Table 4.2 confirm this finding.

Strength Results

The amount of scatter, on average, is similar for both direct tensile and splitting (indirect tensile) strength results (Table 4.3). For the site produced CBMs (materials C to F), the direct tensile strengths show slightly higher scatter. The results of cylinder compressive strength show approximately 18% more scatter than those for cube strength (Table 4.2). A relatively higher amount of variation in the cube strength results is noticeable for the site CBMs. The same applies to the estimated in-situ cube strength results in Table 4.4.

Table 4.3 shows that the tensile strength (direct and indirect) of CBMs comprising limestone aggregate is greater than the gravel sand CBMs. This demonstrates that the physical properties of an aggregate, that is surface texture and angularity, are more important than its inherent strength. Previous research [Cauley and Kennedy, 1973]

has shown that crushed rock aggregates with a rough surface texture and angularity develop a stronger bond with the cement paste, which leads to an increased tensile strength.

Williams [1986] reported that tensile strength is governed by the mode of failure of a CBM which largely depends on the aggregate strength and the amount of cement. The failure may occur through one of the following modes:

1. Fracture of cement paste
2. Fracture of aggregate
3. Failure of bond between the aggregate and cement paste
4. Failure of bond between coarse aggregate and mortar phase (cement-sand-water)

It has been noticed, during the present investigation, that modes 3 and 4 are dominant in CBM4 and below. The occurrence of mode 2 failure has been seen in CBM5 and CBM6 comprising crushed limestone aggregate. Mode 4 failure is typical of the flint gravel sand CBMs, perhaps due to the smooth surface texture of the flint gravel aggregate. These observations confirm that the failure mode, which is a function of the aggregate properties, is likely to influence the magnitude of tensile strength.

Tensile strength of CBMs also seems to be influenced by the aggregate grading. An analysis of the results (in Table 4.3) in the light of the gradings of materials A to F (Figures 4.1 to 4.5) shows that the higher tensile strength of the limestone CBM (materials B and E) may also be attributable to their relatively coarse grading. This type of increase in strength may be attributable to the relatively small surface area of the coarser aggregate particles, resulting in a proportionate increase in the cement paste [Catton, 1940].

The magnitude of both tensile and compressive strengths is sensitive to the degree of compaction, as it directly affects the mix density. Previous investigations [Williams, 1986; Kolias and Williams, 1978] have shown that a 5% shortfall in the degree of compaction reduces the tensile and compressive strengths of a CBM by as much as 40

to 50 percent. This seems to be the main reason for the lower values of core splitting strength (Table 4.4) compared to cylinder splitting strengths (Table 4.3) of the corresponding materials (C to F).

Another important factor which influences the strength properties is age of a CBM. In the present research, tensile strength was determined mainly at 28 days, and at 90 days only for CBM4 material of types A and B. From the average results, the 90 day tensile strengths for gravel sand CBM4 (material A) and limestone CBM4 (material B) were found to be 1.98 and 2.43 N/mm^2, respectively, indicating an increase of 20 to 23 percent, when compared to their 28 day tensile strengths (in Table 4.3). For more information, Kolias and Williams [1978] performed tension tests at different ages for CBMs with materials 1 and 2. Based on their results, the effect of age on the direct tensile strength, shown in Figure 4.7, is as follows:

- Tensile strength at 2 days is 34 percent of that at 28 days,
- Tensile strength at 7 days is 70 to 80 percent of that at 28 days,
- Tensile strength at 100 days is 13 to 19 percent greater than at 28 days.

From previous and present research, it is clear that the increase in tensile strength with age is heavily dependent on the material type and grade of a CBM. A relatively higher rate of increase in the tensile strength may be expected from CBM4 to CBM6, than from CBM1 to CBM3 categories.

To gain confidence in the values of tensile strength, presented in Table 4.3, it is important to compare these results with some previous research. The only available data on direct tensile testing of CBMs is from the work reported by Kolias and Williams [1978]. This work included a study of five materials with different gradings. From the view point of grading and mix design parameters, only two of these materials (1 and 2, Figure 4.6) can be roughly compared for their strength properties with materials used in this study (F and D respectively), although a direct comparison is not possible because the materials and mix properties are not exactly the same. The results of tensile strength for materials 1 and 2 are given in Table 4.5. By comparing

Tables 4.3 and 4.5, it is clear that the average tensile strengths of materials F and D are slightly higher than those of materials 1 and 2, respectively, even though the cement content for material F (Table 4.1) is 0.52% less than for material 1. Overall the results from present research compare well with the previous investigation.

Table 4.5. Tensile strength, and elastic stiffness of materials 1 and 2, at 28 days [Kolias and Williams, 1978]

Description	Mix Parameters		Direct Tensile Strength (N/mm^2)		Elastic Stiffness (GPa)	
	c.c. (%)	w.c. (%)	f_t	st. dev.	E_t	E_c
Material 1 (Flint gravel sand)	5.55	6.0	1.43	0.17	34.8	34.4
Material 2 (Gravel + brickearth)	5.55	6.0	1.17	0.04	35.7	33.5

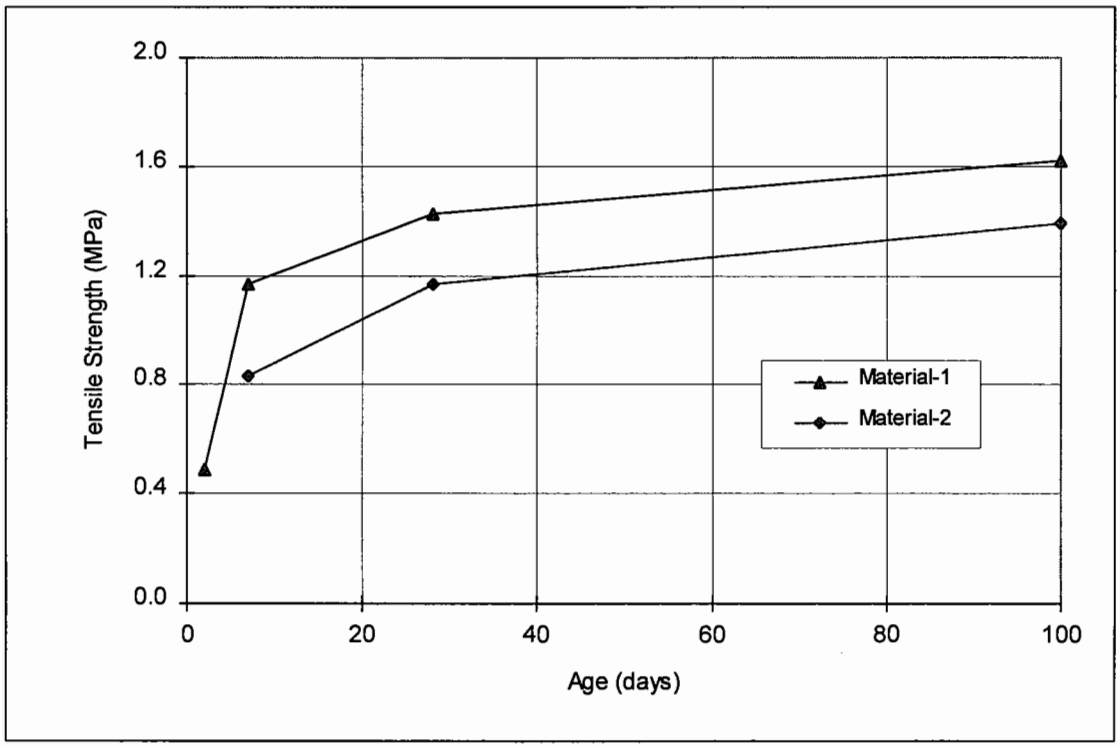

Figure 4.7. Effect of age on the direct tensile strength of CBMs [Kolias and Williams, 1978]

Elastic Stiffness Results

Table 4.3 shows that the values of elastic stiffness, E_t and E_c measured from the tensile specimens, in direct tension and in compression, are almost the same. This confirms earlier findings [Kolias and Williams, 1978] which were based on testing of prism specimens (101.6×101.6×254 mm), in tension and in compression (see Table 4.5). In contrast, the values of stiffness in compression E_{cl} measured from cylinders are comparatively less. The amount of scatter is reasonably small and approximately the same for stiffness results from both the tensile specimens and cylinders.

Regarding the difference between the E_c and E_{cl} results, previous research [Kolias and Williams, 1978] confirms that the stiffness in compression measured from cylinders (203.2mm × 101.6mm diameter) is almost 22% less than from prism specimens (101.6×101.6×254 mm) under compression. These prisms were used by Kolias and Williams [1978] to perform direct tension tests in their study. It appears that the difference between the values of E_c and E_{cl} may be due to a different distribution of stresses induced in the two types of specimens under compression, although further study is required to know the actual mechanism.

It can be seen from Table 4.3, that the magnitude of elastic stiffness increases with an increase in the CBM strength (from CBM3 to CBM6), and is dependent upon the aggregate type, because relatively higher values are found in the case of limestone CBMs, in comparison with the respective categories of gravel sand CBM. This finding is in agreement with previous study, as many researchers [Lofti and Witczak, 1985; Kolias and Williams, 1978; Mitchell et al, 1974; Bofinger, 1970, and Williams and Patankar, 1968] have reported that the elastic stiffness is a function of the type of aggregate, and is also influenced by the type of binder, binder content and degree of compaction. In addition, the stiffness of CBMs is affected by the type and quality of material processed, because at a given degree of compaction and CBM strength, the modulus of elasticity is the highest for CBMs with concrete quality aggregate and lowest for a fine silty or clayey stabilized material [Dempsey et al, 1984].

The effect of the type of binder on stiffness, although not investigated in the present work, was studied by Bonnot [1972] on two crushed gravel mixes, one treated with 3.5% cement content and the other with 15-20% granulated blast furnace slag plus 1% lime. The results of his work [Bonnot, 1972] show that the gravel-cement mix attained a stiffness of 17 and 26 GPa after 7 and 28 days, respectively, whereas the gravel-slag mix achieved a value of only 2 GPa at 7 days and 18 GPa after 90 days, although in the latter, the stiffness was still increasing after 90 days.

The effect of age on stiffness of the CBMs comprising materials 1 and 2, from a previous study [Kolias and Williams, 1978], is shown in Figure 4.8, suggesting that:

- Stiffness at 2 days is 55% of that at 28 days,
- Stiffness at 7 days is 87% of that at 28 days,
- Stiffness at 100 days is only 7.5% greater than the stiffness at 28 days.

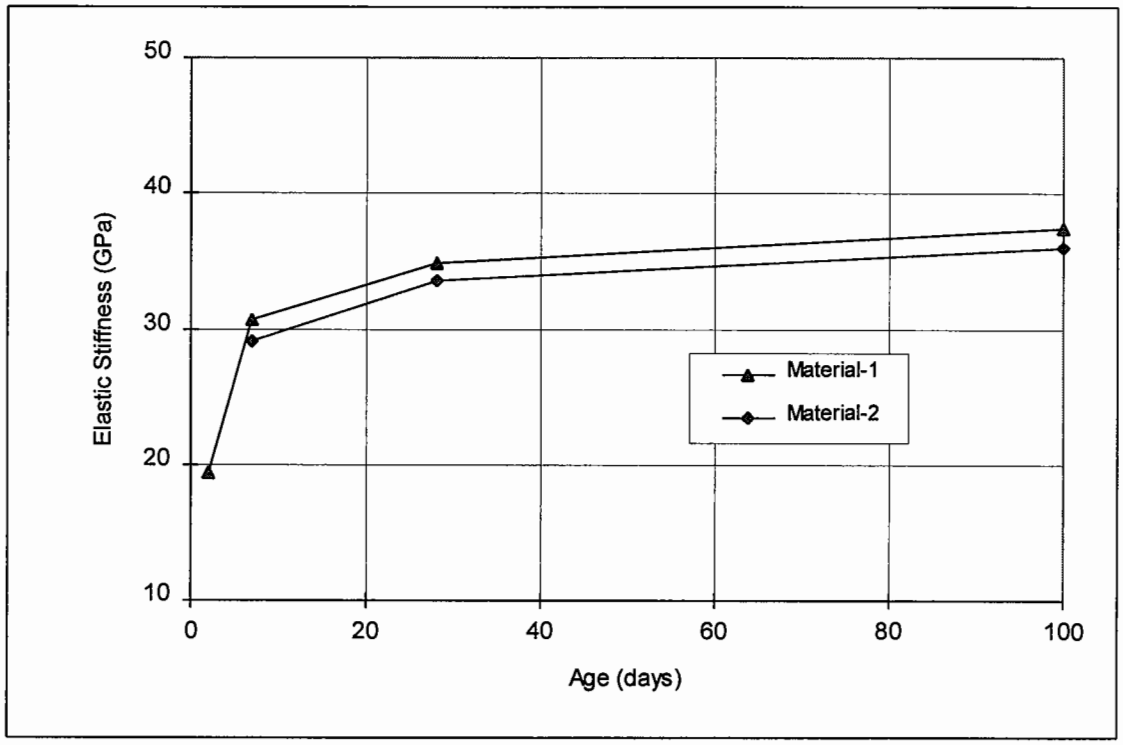

Figure 4.8. Effect of age on the elastic stiffness of CBMs [Kolias and Williams, 1978]

Similar findings were reported by Galloway et al [1979] for a high strength pavement quality concrete, namely that there is a noticeable increase in the magnitude of stiffness during the first 28 days, and afterwards it slows down, such that a further increase of 4 to 12 percent can be expected after a period of 10 years.

4.3.4 Interpretation of the Strength and Elastic Stiffness Results

The results of strength and elastic stiffness characteristics from various CBMs investigated have been expressed in the form of correlations, presented in Figures 4.9 to 4.21. In these correlations, discussed in two sub-sections, direct tensile strength and stiffness in tension have been selected as the main parameters, and are related to other strength and stiffness properties.

Correlations Between Strength Parameters

Direct Tensile Strength and Cylinder Splitting Strength

Although it is well established [Dempsey et al, 1984; Raad et al, 1977], that a direct tensile test provides the truest measure of tensile strength of a CBM, the determination of direct tensile strength involves a sophisticated test system and specimen instrumentation, which make it relatively difficult to use this test (in its present form) for compliance purposes. In contrast, the indirect tensile (cylinder splitting) test is attractive for the simplicity of making and testing simple cylindrical specimens, and also because in-situ specimens can be easily cored without damaging an actual pavement. The advantage of in-situ (cored) specimens makes this test even more attractive than a flexural test.

Despite these advantages, the cylinder splitting test overestimates the magnitude of tensile strength for the reasons mentioned in Section 3.2 (Chapter 3). Therefore, the determination of the tensile strength from cylinder splitting test data demands the establishment of an appropriate correlation between the direct tensile and splitting strengths. Such a relationship, shown in Figure 4.9, has been developed for the whole range of CBMs investigated, at 28 days, and is expressed by the following equation:

$$f_t = 0.75 f_{sp} \tag{4.3}$$

where:

f_t : direct tensile strength (N/mm^2)

f_{sp} : splitting strength (N/mm^2)

Figure 4.9 indicates that the above relation (Eq. 4.3) is applicable to various CBM grades involving different aggregates.

Direct Tensile Strength and Flexural Strength

Although flexural strength tests were not performed in this research, several relationships between direct tensile and flexural strength have been found in literature. Kolias and Williams [1978] reported the following relation based on the best fit line through a wide range of test results:

$$f_t = 0.53 f_b + 0.154 \tag{4.4}$$

In Eq. 4.4, f_b is flexural strength (N/mm^2). Besides this relationship, however, Kolias and Williams [1978] suggested that the following relation may be considered for practical purposes:

$$f_t = 0.6 f_b \tag{4.5}$$

Eq. 4.5 is in close agreement with the relationship recommended by Dempsey et al [1984], which is as follows:

$$f_t = 0.5 f_b \tag{4.6}$$

Other researchers [Pretorius and Monismith, 1971; Raad et al, 1977] have also reported that the flexural strength can be as much as twice the direct tensile strength, thus agreeing to Eqs. 4.5 and 4.6.

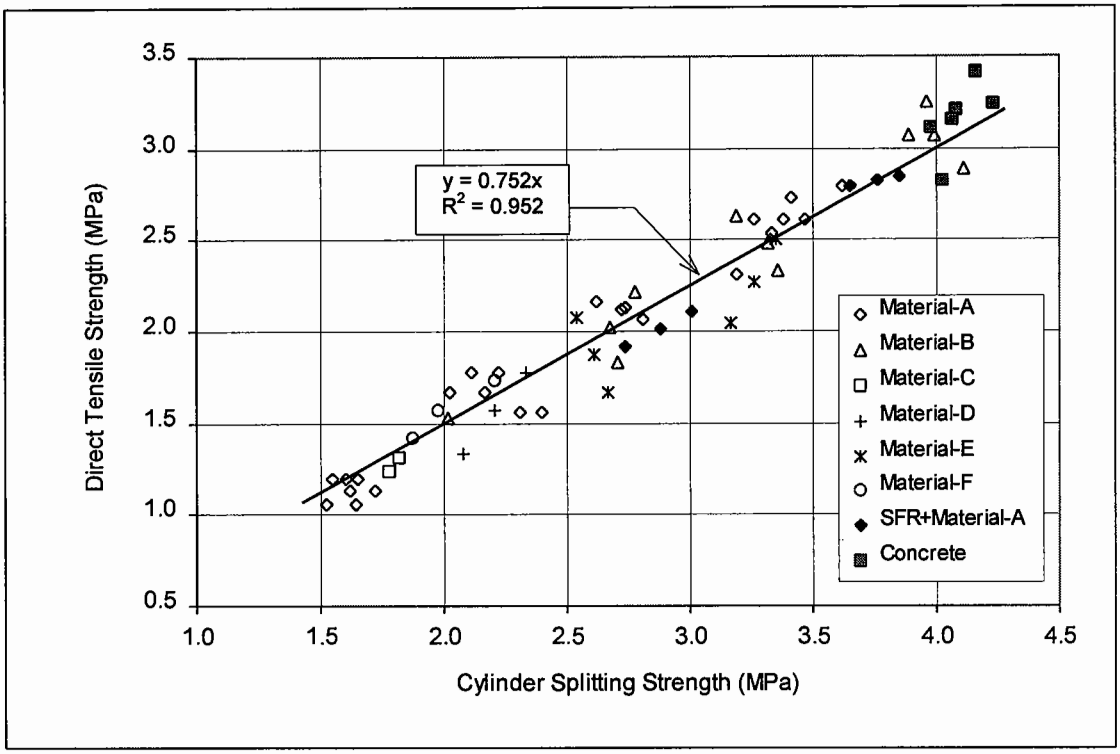

Figure 4.9. Relation between direct tensile strength and cylinder splitting strength at 28 days

Direct Tensile Strength and Compressive Strength

The direct tensile strength has been related to cylinder compressive strength f_{cl} at 28 days in Figure 4.10. This relationship is given by the following equation.

$$f_t = 0.1084 f_{cl} \tag{4.7}$$

This relation (Eq. 4.7) shows a good agreement with the results from Kolias and Williams [1978], also shown in Figure 4.10, who concluded that the direct tensile strength is one-tenth of cylinder compressive strength. The same finding is reported by Dempsey et al [1984].

In Figures 4.11 and 4.12, 28 day direct tensile strength has been related to 7 day and 28 day cube compressive strengths, respectively. These relations are as follows:

$$f_t = 0.0984 \times (f_c)_{7day} \tag{4.8}$$

and $$f_t = 0.0766 \times (f_c)_{28day} \tag{4.9}$$

where:

f_{cl} : cylinder compressive strength (N/mm^2)

f_c : cube compressive strength (N/mm^2)

Eqs. 4.8 and 4.9 indicate that, for CBMs, the 28 day direct tensile strength may be assumed approximately one-tenth of the 7 day cube compressive strength, or 7.7% of the 28 day cube strength.

Each of the Figures 4.10 to 4.12 indicates that most of the points for limestone CBMs (materials B and E), with relatively higher tensile strength, lie above the line, whereas the reverse is the case for gravel sand CBMs from materials A, D and F.

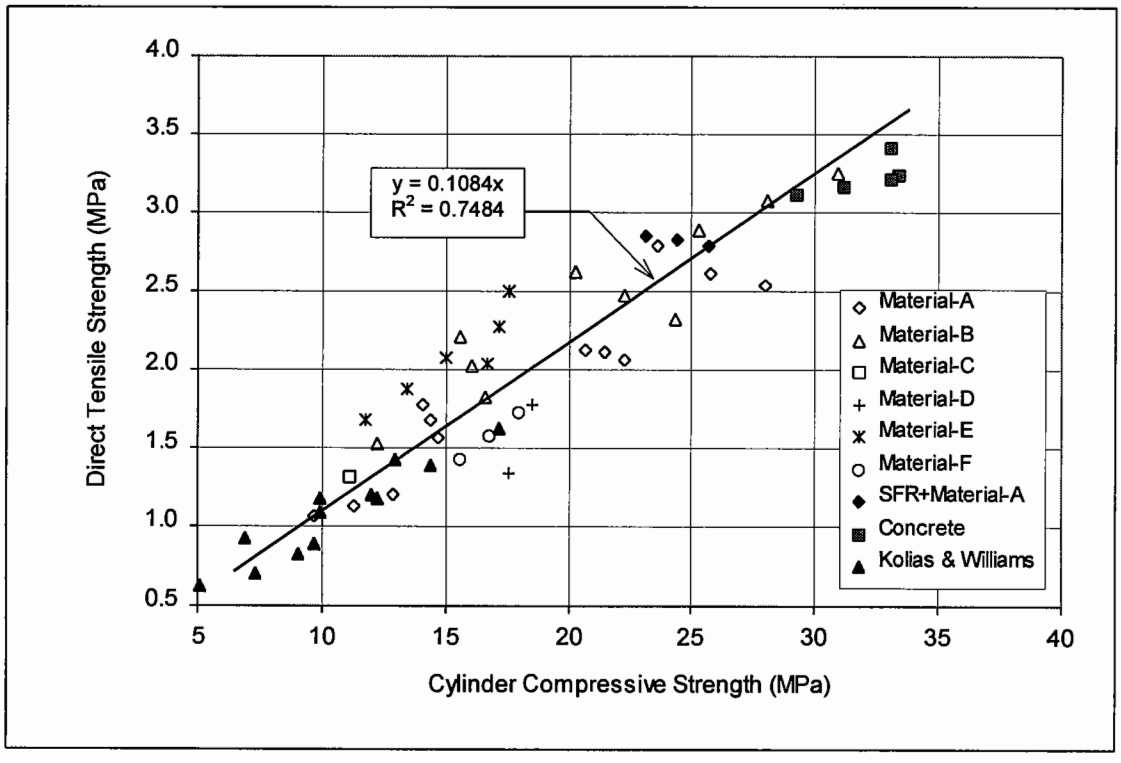

Figure 4.10. Relation between direct tensile strength and cylinder compressive strength at 28 days

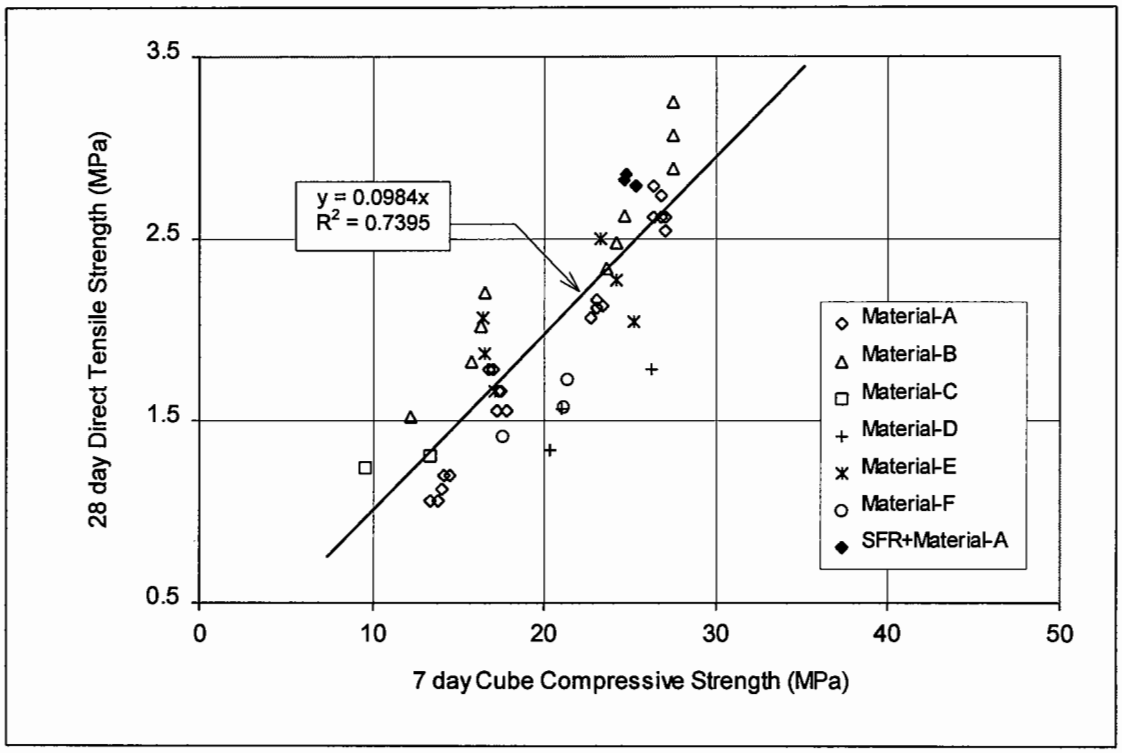

Figure 4.11. Relation between 28 day direct tensile strength and 7 day cube compressive strength

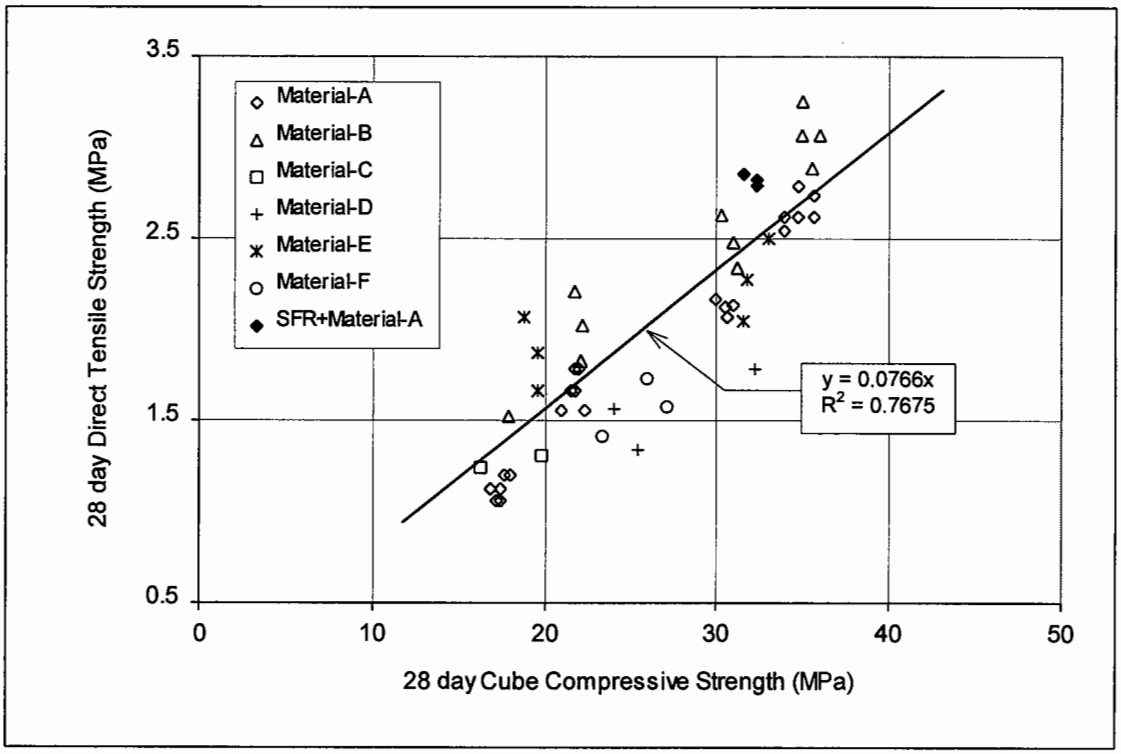

Figure 4.12. Relation between 28 day direct tensile strength and 28 day cube compressive strength

Cube Compressive Strength and Cylinder Compressive Strength

The rate of gain in CBM strength is relatively higher during the early stage after construction, and then it gradually slows down, such that the strength attained at 7 days is a significant proportion of the 28 day strength. Figure 4.13 shows a correlation between the 7 day and 28 day cube compressive strengths. The relation is as follows:

$$(f_c)_{7day} = 0.76(f_c)_{28day} \tag{4.10}$$

According to Kolias and Williams [1978], the measurement of compressive strength in isolation from the influence of platen restraint is only possible from specimens with a minimum ratio of 2:1 between the height and lateral dimension, such as cylinders (300 × 150 mm diameter). Therefore, for comparison purposes, the results of 28 day compressive strengths from both cylinders and cubes have been related in Figure 4.14. The relation is given by the following equation:

$$f_{cl} = 0.7801 \times (f_c) - 2.7068 \tag{4.11}$$

Eq. 4.11 represents the best fit line relationship. But for practical purposes, the average relationship, also given in Figure 4.14 may be used, suggesting that cylinder compressive strength is approximately 68% of the cube compressive strength. This finding compares well with the ratio of 66.6% recommended by Kolias and Williams [1978].

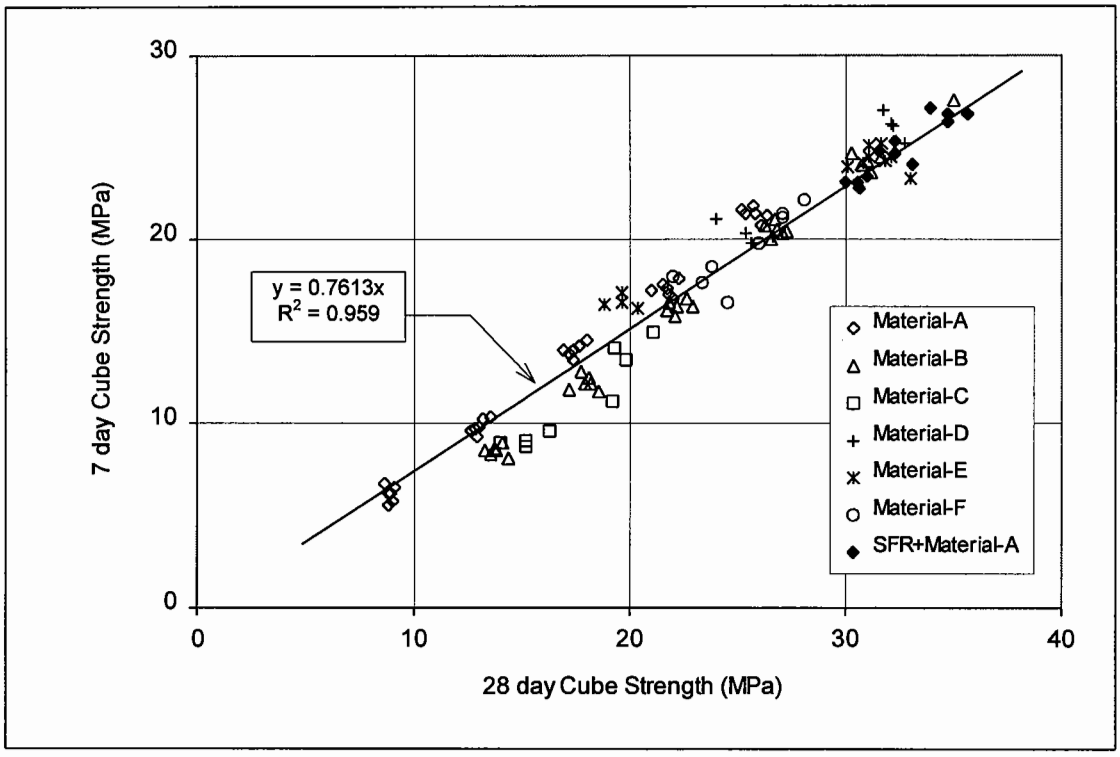

Figure 4.13. Relation between the 7 day and 28 day cube compressive strengths

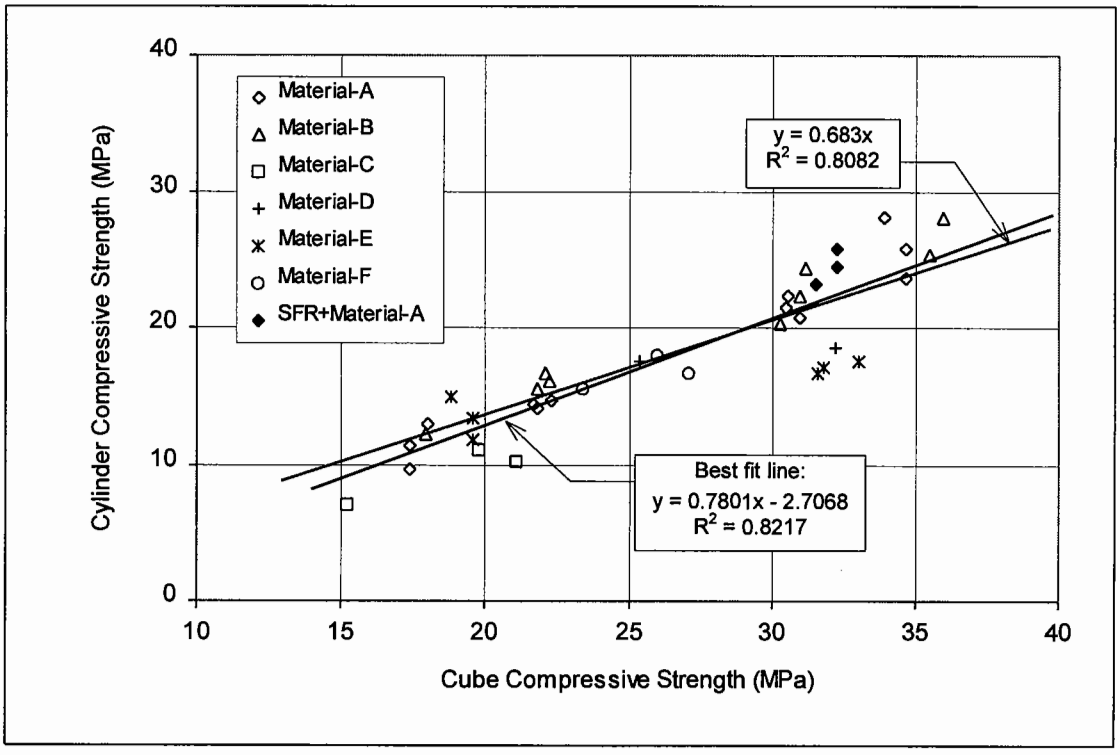

Figure 4.14. Relation between cylinder compressive strength and cube compressive strength at 28 days

Strength Parameters from Cores and Prepared Specimens

Some variations in the magnitude of strength parameters, measured from the prepared specimens (described in Table 4.1) and cores taken from the actual pavements, have been noticed. The results of estimated in-situ cube strength and splitting strength from cores are related to cube compressive strength and cylinder splitting strength (in Tables 4.2 and 4.3), respectively, at 28 days. The resulting correlations, shown in Figures 4.15 and 4.16, are as follows:

$$f_{ic} = 0.5208 f_c + 3.7668 \tag{4.12}$$

$$(f_{sp})_{core} = 0.4547 \times (f_{sp})_{cylinder} + 0.5311 \tag{4.13}$$

where f_{ic} : estimated in-situ cube strength (N/mm^2)

Besides the best fit line relations given by Eqs. 4.12 and 4.13, the average correlations shown in Figures 4.15 and 4.16 indicate that f_{ic} is approximately 67% of the cube compressive strength, and core splitting strength is approximately 68% of the cylinder splitting strength from the prepared specimens (150mm × 150mm diameter). It appears that the lower value of the core splitting strength is possibly due to the following reasons:

- The lower core densities (Table 4.4), which were found to be 4 to 6 percent less than those of cylinders (Table 4.1).
- Day to day variations (by small amount) in aggregate grading and mix water content, which are likely to occur in the CBM mix on sites, and influence the strength properties.

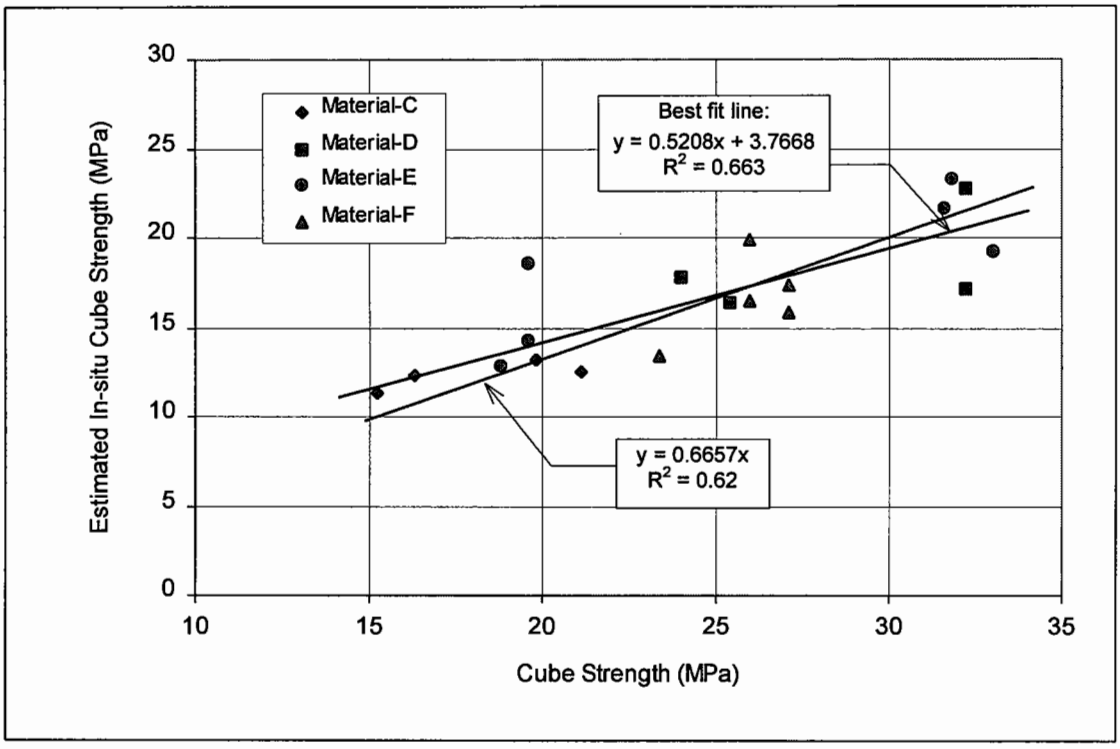

Figure 4.15. Relation between estimated in-situ cube strength (from cores) and cube compressive strength at 28 days

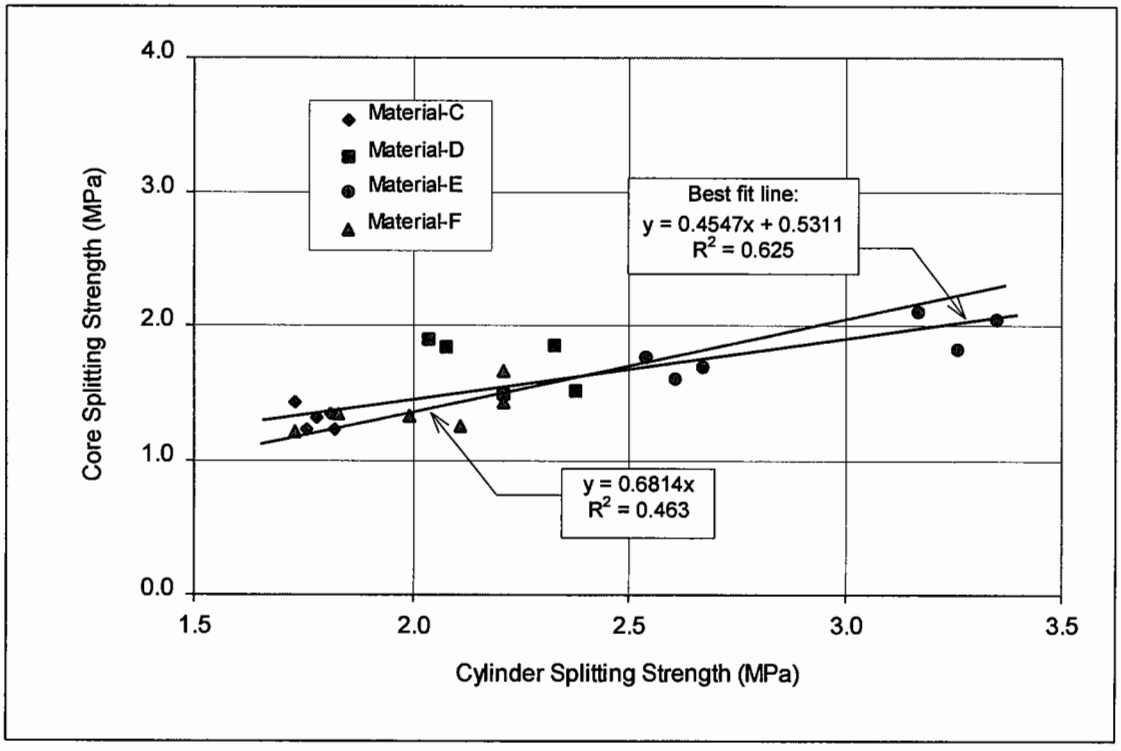

Figure 4.16. Relation between core splitting strength and cylinder splitting strength at 28 days

Correlations of Stiffness and Strength Properties

The stiffness in direct tension has been related to different strength and stiffness parameters in the correlations shown in Figures 4.17 through 4.21.

Elastic Stiffness in Tension and Compression

The values of elastic stiffness in tension E_t and compression E_c measured from tensile specimens are compared in Figure 4.17, and are in agreement with the results of a previous investigation [Kolias and Williams, 1978], also shown on this figure. The relationship thus obtained follows the line of equivalence. In contrast, Figure 4.18 shows a different relationship between the stiffness in tension and stiffness in compression measured from cylinders E_{cl}. This relation is as follows:

$$E_t = 1.1774 \times (E_{cl}) + 5.0278 \qquad (4.14)$$

where:

$E_t = E_c$: stiffness from tensile specimen (GPa)

E_{cl} : stiffness in compression from cylinder (GPa)

Eq. 4.14 is in close agreement to the results of a previous study [Kolias and Williams, 1978], also shown in Figure 4.18. By combining both the present and previous research data (Figure 4.18), an average correlation has been found, which seems rather more appropriate for practical purposes. This relation is given by the following equation:

$$E_t = 1.374 \times (E_{cl}) \qquad (4.15)$$

Stiffness in Tension and Direct Tensile Strength

Figure 4.19 indicates that, for the range of CBMs investigated, a reasonable relationship exists between the elastic stiffness and direct tensile strength. Although the results from the previous investigation [Kolias and Williams, 1978] do not fall under this correlation, due to their lower tensile strength and higher stiffness values,

they show a more or less similar trend with almost similar scatter. The correlation found in this study is as follows:

$$E_t = 16.584 \times \ln(f_t) + 21.6 \tag{4.16}$$

Stiffness in Tension and Compressive Strength

A previous study [Kolias and Williams, 1978] has reported that there is no unique relationship between the elastic stiffness and compressive strength data. However, to obtain a general idea of the magnitude of stiffness from the results of compressive strength, the stiffness in tension at 28 days has been related to 28 day cylinder compressive strength in Figure 4.20, and to cube compressive strengths at 7 and 28 days in Figure 4.21. The resulting correlations are approximate, with the amount of scatter shown, and are given by:

$$E_t = 14.524 \times \ln(f_{cl}) - 9.03 \tag{4.17}$$

$$E_t = 15.569 \times \ln(f_c)_{7day} - 14.404 \tag{4.18}$$

$$E_t = 17.159 \times \ln(f_c)_{28day} - 23.64 \tag{4.19}$$

Figure 4.20 indicates that the relation given by Eq. 4.17 is in a reasonable agreement with the results of previous research [Kolias and Williams, 1978], which show a very similar trend, but with slightly more scatter. On the other hand, the relationships given by Eqs. 4.18 and 4.19 compare well with those suggested by Brown [1979], and by Williams and Patankar [1968]. The relation, between stiffness and cube compressive strength, given by Brown [1979] is as follows:

$$E = 0.7 f_c + 20.5 \tag{4.20}$$

Williams and Patankar [1968] suggested the following relationships, presented by Williams [1986], between electro-dynamic modulus E_d determined through resonance tests and cube compressive strength for the British CBMs. For the purposes of

correlations, they divided CBMs into two main groups based on their 7 day cube compressive strength f_c, such that:

- For CBMs with 7 day f_c = 7 to 20 N/mm^2 (i.e. CBM2 to CBM5), the relation is:

$$E_d = 16.8 f_c^{1/4} \tag{4.21}$$

- For CBMs with 7 day f_c < 7 N/mm^2 (i.e. below CBM2), the relation is:

$$E_d = 4 f_c \tag{4.22}$$

Williams [1986] related the static and electro-dynamic moduli through the following equation:

$$E_c = \frac{6}{7} E_d \tag{4.23}$$

where:

E_d : electro-dynamic modulus (GPa)
E_c : static modulus measured in compression (GPa)

Of these, Eqs. 4.20 and 4.21 show a reasonable agreement with Eqs 4.18 and 4.19, because all of these are applicable to more or less similar range of CBM strength. Equation 4.22, however, is only applicable to relatively weak CBMs. Other researchers [Dempsey et al, 1984; Otte et al, 1982] have also suggested some relationships between stiffness and cube compressive strength, but they provide much lower values of the stiffness for CBMs under investigation.

Stiffness and Flexural Strength

Although no correlation between the CBM stiffness and flexural strength has been developed in this study, a review of literature shows that the relation suggested by Brown [1979] is more appropriate. This relation is based on the results of CBM properties presented by Williams [1972], and is as follows:

$$E = 7.125 f_b + 20.5 \tag{4.24}$$

where $f_b = 0.1 f_c$ (4.25)

The results of Kolias and William's investigation [1978] confirm that the relation in Eq. 4.24 can be satisfactorily used. However, Dempsey et al [1984] suggested a relation, between flexural strength and cube strength, as $f_b = 0.2(f_c)$ in contrast with that given in Eq. 4.25.

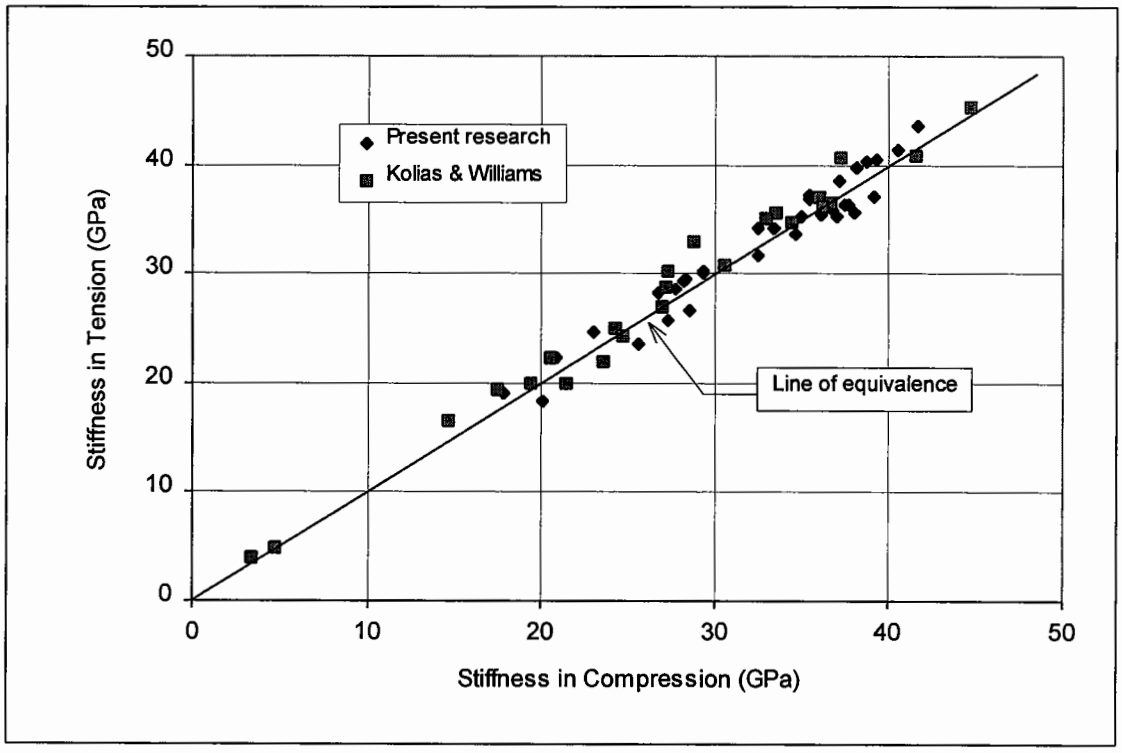

Figure 4.17. Stiffness in tension and in compression measured from tensile specimens

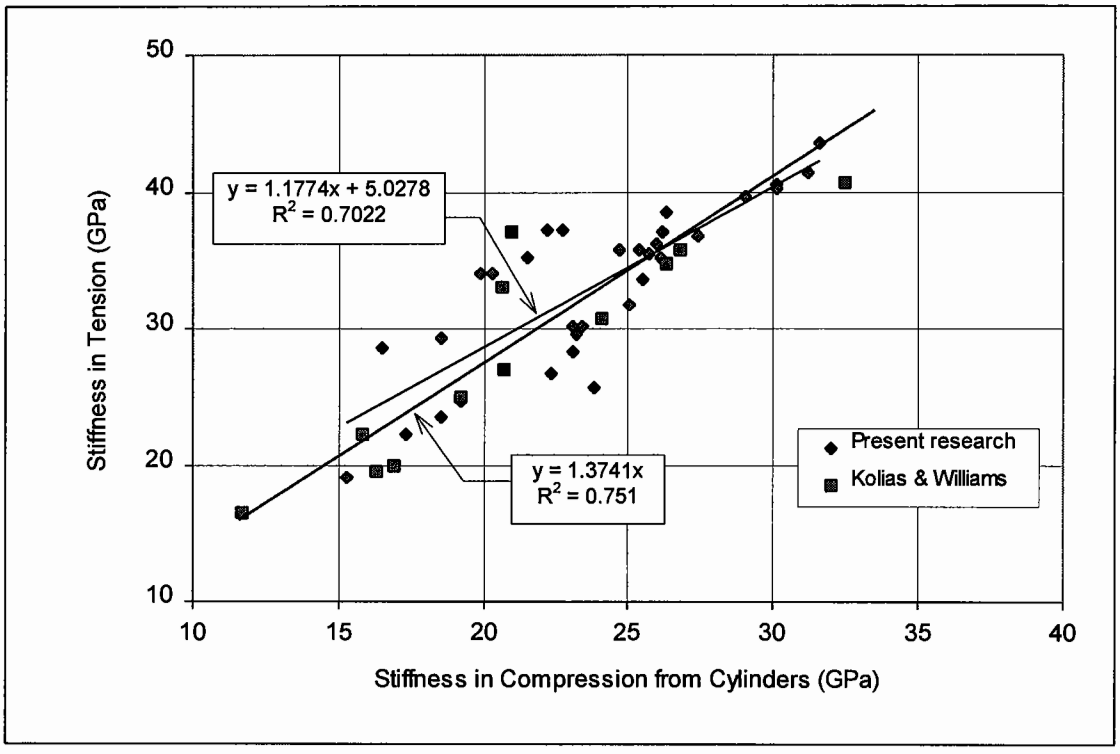

Figure 4.18. Stiffness in tension versus stiffness in compression from cylinders

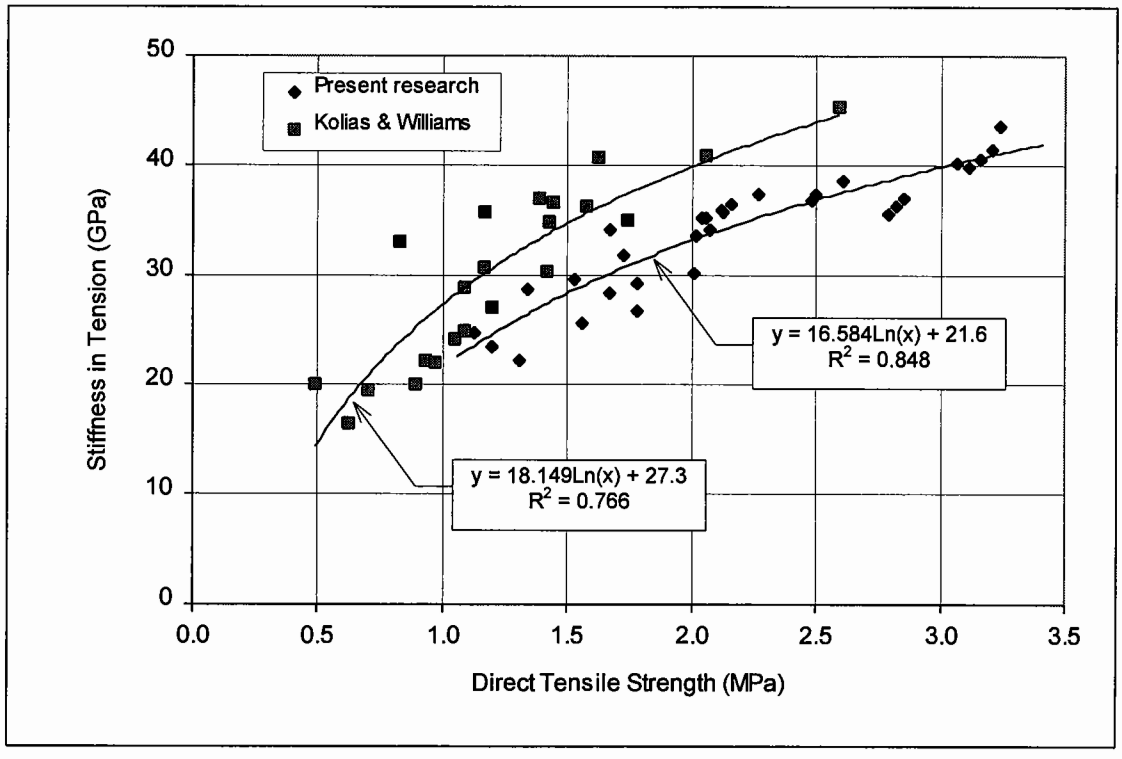

Figure 4.19. Relation between stiffness in tension and direct tensile strength

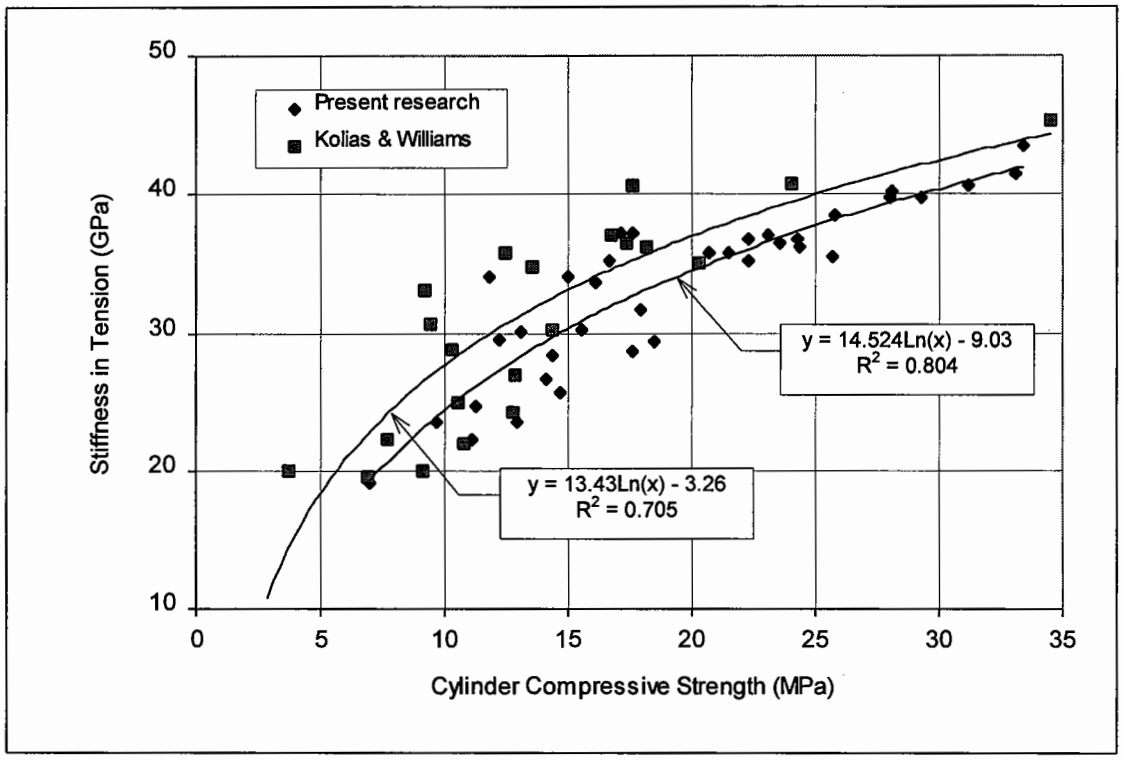

Figure 4.20. Relation between stiffness in tension and cylinder compressive strength

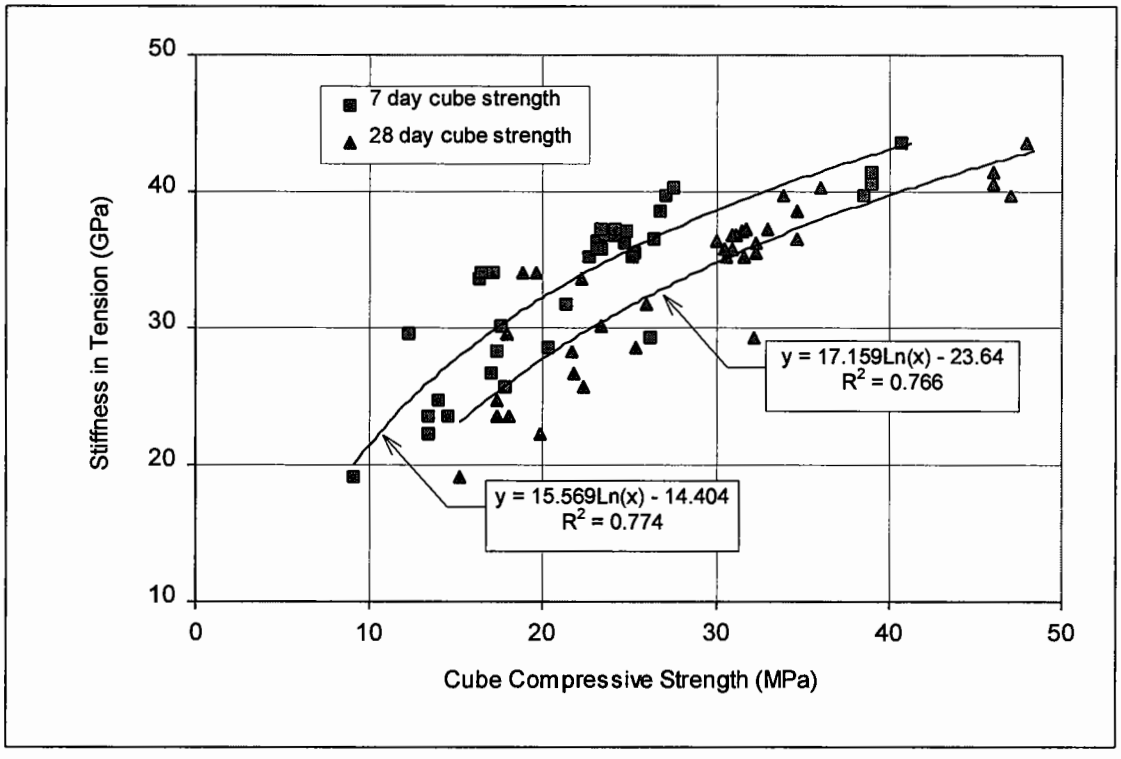

Figure 4.21. Relation between stiffness in tension and cube compressive strength

4.4 POISSON'S RATIO

Poisson's ratio of cement bound materials is used as an important input parameter in pavement analysis. It can be determined through static and dynamic methods. In the static method, it is measured as the ratio of lateral to longitudinal (along the load axis) strains developed during the static compression testing of a standard cylinder. The dynamic method involves calculation of Poisson's ratio from resonance frequency and pulse velocity measurements from CBM beam specimens.

In the present research, Poisson's ratio was determined through static compression tests performed on CBM cylinders (300mm × 150mm diameter). Lateral and longitudinal deformations were recorded through Linear Variable Differential Transformers (LVDTs). The longitudinal deformation was measured over the middle 100mm distance. The calculation of Poisson's ratio is based on the strains at one-third of the ultimate load [Kolias and Williams, 1978], because of the dependency of its magnitude on applied stress level [Obi, 1972]. Figure 4.22 shows the relationships between lateral and longitudinal strains for CBMs comprising materials A to F. Specimens were stressed up to 30 to 40 percent of the ultimate load, depending on the CBM strength and loading capacity of the testing machine. The values of Poisson's ratio are given in Table 4.6.

The Poisson's ratios for materials 1 and 2 investigated by Kolias and Williams [1978], and for various materials reported by other researchers, are given in Table 4.7. It can be seen that the values of Poisson's ratio for gravel sand CBMs (materials A, C, D and F) in Table 4.6 compare well with materials 1 and 2 in Table 4.7. This may be because the aggregate type, aggregate grading, and mix design parameters involved are more or less similar for these materials. Similar values have been reported by Dempsey et al [1984] for a cement stabilized granular material (see Table 4.7).

Table 4.6 indicates that Poisson's ratio for limestone CBMs (materials B and E) is slightly higher than the gravel sand CBMs, which may be due to a relatively lower cement content used [Obi, 1972] in the limestone CBMs. Fine grained stabilised

materials have relatively higher values of Poisson's ratio (Table 4.7). But lower values have been reported [Obi, 1972] for CBMs involving relatively coarse aggregate and high cement content, and at lower levels of applied stress during testing.

Table 4.6. Poisson's ratio measured from CBMs comprising materials A to F

Material	Description	Poisson's ratio, ν	
		Range	Average
A	Gravel sand CBM3 to 6	0.14 - 0.16	0.15
B	Dene Limestone CBM3 to 6	0.19 - 0.21	0.20
C & F	Flint gravel sand CBM2 to 5	0.15 - 0.18	0.165
D	Glacial gravel sand CBM4 to 6	0.16 - 0.19	0.175
E	Limestone CBM4 & 5	0.20 - 0.24	0.22

Table 4.7. Poisson's ratio for different materials reported by other researchers

Material description	Poisson's ratio, ν	Researcher
CBMs with granular aggregate (materials 1 and 2 in Figure 4.6)	0.15 - 0.20	Kolias & Williams, 1978
Fine grained soil cement	0.33	
Gravel cement mixture	0.10 - 0.15	Bonnot, 1972
Lean concrete (with primary cracking)	0.20	Brown, 1979
Lean concrete (with secondary cracking)	0.30	
Cement stabilized granular material	0.10 - 0.20	Dempsey et al, 1984
Cement stabilized fine grained material	0.15 - 0.35	
Lime-fly ash material	0.10 - 0.15	
Lime stabilized soil	0.15 - 0.33	

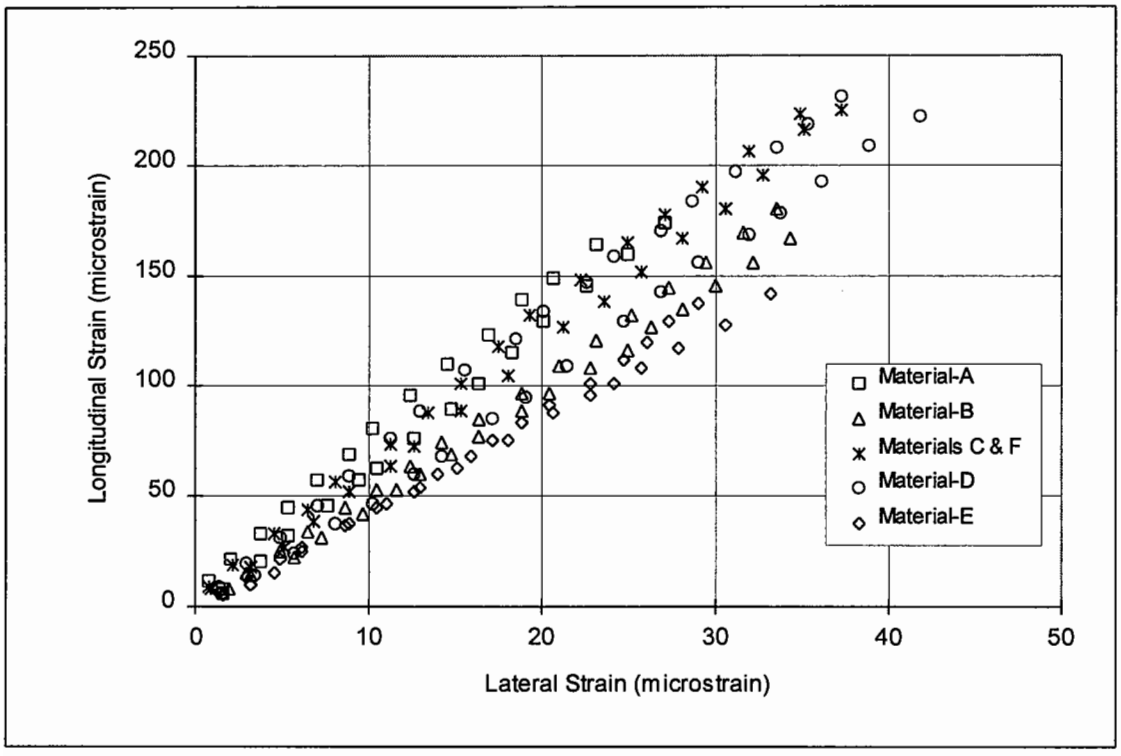

Figure 4.22. Relationship between the lateral and longitudinal strains for CBMs comprising materials A to F.

4.5 FATIGUE BEHAVIOUR

4.5.1 General

Cement bound materials are susceptible to fatigue cracking [Brown, 1979], and the phenomenon of cracking in a CBM pavement is the result of repeated application of stress [Kesler, 1953]. A knowledge of the performance of CBMs under repeated loading is of critical importance because, as a consequence of their relatively high modulus, they develop significantly high tensile stresses under the combined influence of traffic and thermal loading [Kolias and Williams, 1978].

The fatigue properties of CBMs (or concrete) exposed to pure tensile stresses have not been studied extensively, although from the point of view of assessing the susceptibility of a structure to cracking under repeated loading the behaviour of concrete under tension is important [RILEM Committee 36-RDL, 1984]. Some

limited fatigue tests in direct tension were carried out on lean concrete by Kolias and Williams [1978], but the response of CBMs with different types of aggregate needs to be studied.

Fatigue strength data are frequently expressed in terms of the nominal static strength determined from tests carried out at a loading rate which is much less than the rate at which load is applied in the fatigue tests [Galloway and Raithby, 1973]. The results are presented in terms of an S-N (stress ratio - number of cycles on logarithmic scale) diagram. It is usual to refer to fatigue strength at a very large number of cycles, such as 10 millions [Neville, 1995].

An S-N curve is usually plotted for maximum applied stresses either at a given minimum stress level, or for a constant range between the maximum and minimum stresses [RILEM Committee 36-RDL, 1984], or for a constant mean stress level [Suresh, 1994]. Most researchers [Kesler, 1953; Raithby and Galloway, 1974; Nanni, 1992] have studied fatigue of concrete with respect to a constant minimum stress.

For fatigue testing, particularly in direct tension or flexure, a minimum stress level (greater than zero) is always kept on the specimens to eliminate the possibility of any impact loads being applied to the specimen [Kesler, 1953; Raithby and Galloway, 1974].

4.5.2 Factors Influencing Fatigue Strength

Of various variables influencing the fatigue performance, the following are the most important [Raithby and Galloway, 1974; Galloway and Raithby, 1973; Neville, 1995; Kesler, 1953; Assimacopoulos et al, 1959]:

- Age and moisture condition of a CBM at the time of test
- Rate (or frequency) of loading
- Maximum stress level, f_{max}
- Stress range, $\Delta f = f_{max} - f_{min}$, where f_{min} is the minimum stress level

The fatigue performance is dependent on the age and moisture condition of concrete at the time of test [Raithby and Galloway, 1974]. The fatigue strength increases with age, but reduces if the concrete is in a saturated state [Kolias, 1975; Raithby and Galloway, 1974]. Also the fatigue strength increases with an increase in the specimen density [Kolias, 1975].

The effect of rate of loading was investigated by Galloway and Raithby [1973]. They found that, up to 20 Hz, the loading frequency has no effect on the fatigue performance of concrete. Other researchers [Murdock, 1960; Assimacopoulos et al, 1959] have reported that the frequency, at least within the range 1.2 to 33 Hz, does not affect the resulting fatigue strength. This applies to fatigue in compression, flexure, and in splitting tension [Tepfers, 1979], suggesting that the failure mechanism may be the same [Neal and Kesler, 1968].

The effect of stress range has been demonstrated by Neville [1995], through the modified Goodman diagram, indicating that, for a given number of cycles, the smaller the stress range applied the higher the fatigue strength. On the other hand, for a constant minimum stress level, an increase in the stress range increases the maximum stress level, and leads to a decreased fatigue strength [Assimacopoulos et al, 1959].

4.5.3 Laboratory Study of Fatigue of CBMs

Present research included an investigation into the fatigue characteristics of two types of CBM4, comprising gravel sand (material A) and limestone (material B) aggregates. For this purpose, a number of tensile specimens were prepared from each type of CBM4, and were subjected to repeated loading under direct tension. The specimens were in a dry condition, and were tested at 90 days. A uniform sinusoidal loading frequency of 10 Hz was selected, a function of the sensitivity and control of the test system.

Most testing was performed by varying the stress range applied at a constant mean stress level (f_{mean}) of 50% of the static tensile strength f_t of each of the two CBMs. The mean stress is defined as $f_{mean} = 0.5\times(f_{max} + f_{min})$, as illustrated on next page.

For the specimens tested at a maximum stress of 100% of the tensile strength, the mean stress was selected at 60% to avoid proximity to zero load. Specimens with a maximum applied stress of 60% or 65% of the f_t, were tested at a lower mean stress level of 35%, but failure was not recorded in any such case.

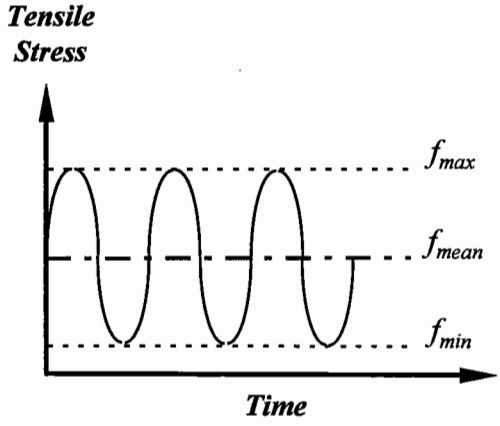

During testing, the maximum and minimum limits of the stress range used, and uniformity of the sinusoidal loading, were frequently monitored through an oscilloscope. The number of cycles was recorded automatically. Testing was continued up to 10 million cycles, and even up to 15 million cycles for a few of the specimens that did not fail. The fatigue strength data for both types of CBM4 are presented in Figure 4.23 in terms of the maximum stress ratio applied.

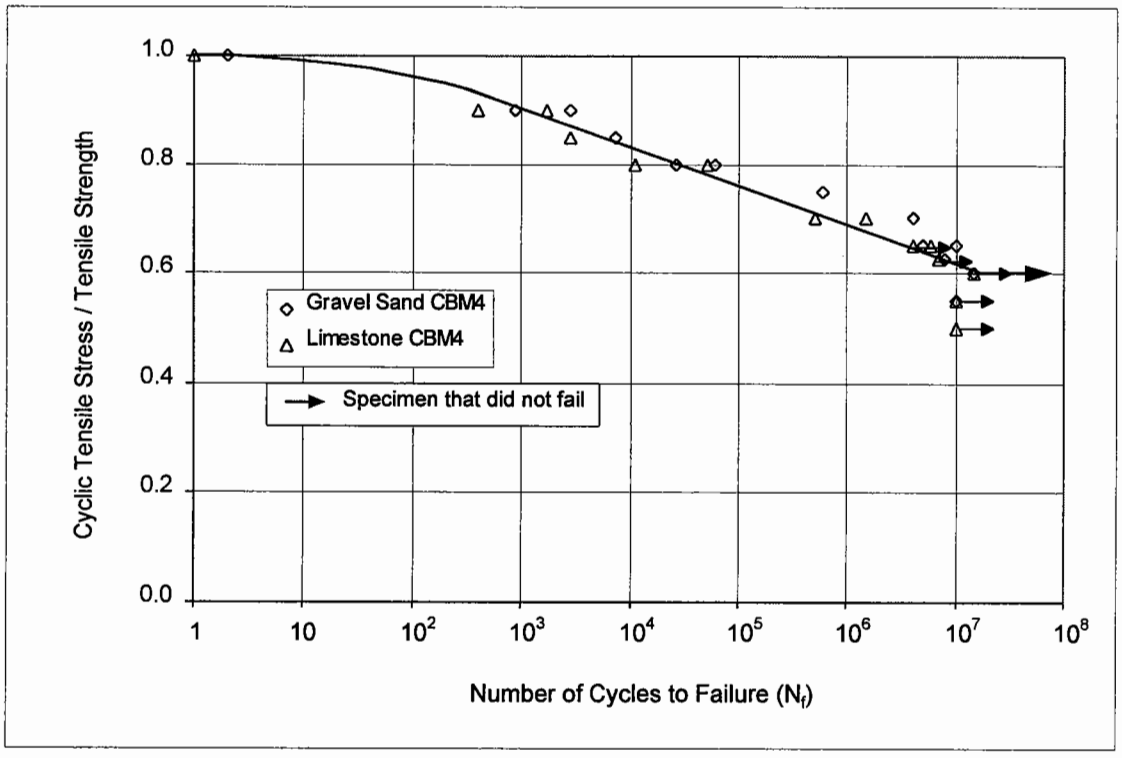

Figure 4.23. Fatigue characteristics for gravel sand and limestone CBM4

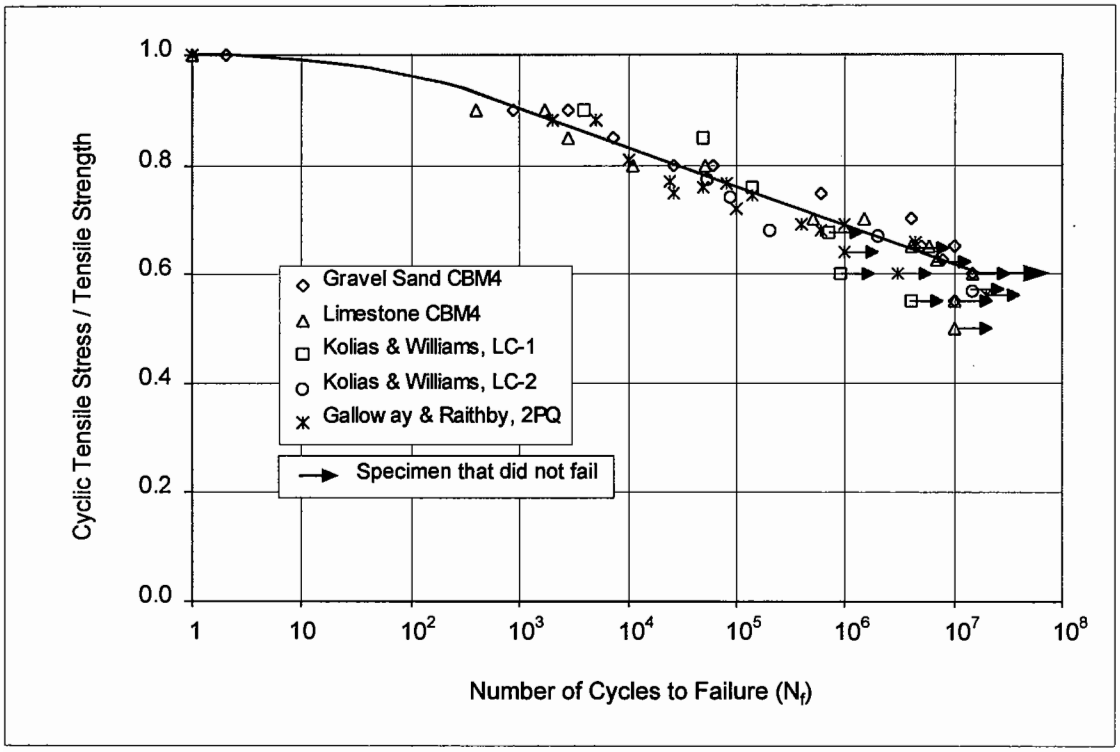

Figure 4.24. Fatigue relationships from present and previous research
(where: LC-1 & 2 : two lean concretes, and 2PQ : two pavement quality concretes)

4.5.4 Discussion and Interpretation of Fatigue Results

The best fatigue relationship, for comparison purposes, is the one recommended by Brown [1979], which includes fatigue strength results for two relatively weak CBMs (lean concrete) tested under direct tension [Kolias and Williams, 1978], and for pavement quality concrete tested in flexure [Galloway and Raithby, 1973]. In both cases, the same type of constant amplitude sinusoidal loading, in which the minimum load was kept approximately zero, was used. Superimposed on these results are the fatigue relationships for the two types of CBM4 in Figure 4.24, indicating that there is a general agreement, although different techniques have been used in each case and different mean and minimum stress ratios applied.

It can be seen from Figure 4.24 that the fatigue relationship remains almost the same for CBMs of different strengths, as well as for concrete, and for various test techniques. This is because the fatigue strength has been normalised by expressing it in terms of the corresponding static strength. The distribution of stress, which is

different for the two test systems, has no effect on results as these are set out in non-dimensional form [RILEM Committee 36-RDL, 1984]. Generally speaking, the ratio of fatigue strength to static strength is independent of the water/cement ratio, the cement content, type of aggregate, and age at loading because these factors affect both the static and fatigue strength in the same manner [Neville, 1995]. As strength increases with age, fatigue strength both in compression and in flexure also increases [Tepfers, 1979]. Therefore, the important point is that, at a given number of cycles, fatigue failure occurs at the same fraction of the ultimate strength, and is thus independent of the magnitude of this strength, whether in compression, in flexure or in splitting tension [Galloway et al, 1979], and of the age of concrete [Murdock, 1960]. However, some tests have shown an increase in fatigue life with age [Raithby and Galloway, 1974].

Figure 4.24 confirms that, for CBM3 and higher, a fatigue strength of 60% is an appropriate endurance limit, also suggested by Brown [1979], for design purposes, and is given by the following relation:

$$\frac{f}{f_t} = 0.6 \tag{4.26}$$

where:

f : cyclic tensile stress applied (N/mm^2)

f_t : static tensile strength of CBM (N/mm^2)

For comparison purposes, fatigue strengths of 60% and 55% have been reported, after one million load cycles in direct tension, corresponding to two materials [Kolias and Williams, 1978] which are more or less similar to a CBM3 and CBM2, respectively. Kolias [1975] reported a fatigue strength of 50 to 60% of the static tensile strength for a CBM after 10 million cycles. The fatigue strength values of 64 to 72% (for 10 million cycles) have been reported for concrete in flexure by Galloway et al [1977], but a value of 55% of the static strength has also been suggested [Shi et al, 1993]. By comparison, in compression, the fatigue strength of concrete was reported to be between 60 and 64% after the same number of cycles, whereas a value of 55% has

also been quoted [Nelson et al, 1988]. For a gravel-cement mixture, Bonnot [1972] obtained a fatigue strength of 50% of the static tensile strength after one million cycles.

Based on the results of this study, presented in Figure 4.24, the straight line part of the fatigue relationship can be expressed by the following equation (with R^2 value of 94.5%):

$$\frac{f}{f_t} = 1.11 - 0.03 \times \ln(N_f) \tag{4.27}$$

or

$$\ln(N_f) = 36.2 - 32.6(f/f_t) \tag{4.28}$$

where:

N_f : number of load cycles to failure

Eq. 4.28 can be used to determine the fatigue lives at stress levels higher than the fatigue strength of 60%. This equation can be compared with the relationship given by Brown [1979], which is also applicable for stress levels higher than the fatigue strength (of 60%), and is as follows:

$$\ln N_f = 17.2 - 13.2(f/f_t) \tag{4.29}$$

Eq. 4.28 compares well with Eq. 4.29 at higher stress levels, but gives relatively higher lives at lower stress levels. In both the cases, however, the endurance limit is the same, i.e. a fatigue strength of 60% (see Eq. 4.26).

4.5.5 Mechanism of Fatigue Failure

It is believed [Horii et al, 1992; Kolias, 1975] that fatigue failure is attributed to the development of slowly propagating internal microcracks, which originate both at the cement matrix - aggregate interface and in the cement paste itself [RILEM Committee 36-RDL, 1984], or at existing cracks or flaws in concrete. A propagating fatigue crack will occasionally be arrested when it reaches an aggregate particle and the process will be repeated until, finally, the rate of release of strain energy is sufficient to overcome the remaining cohesive forces and thus fracture occurs [Kolias, 1975]. Assimacopoulos et al [1959] reported that fatigue failure in the specimens tended to occur in the cement paste and at the surface of bonding between aggregate and paste, rather than in the aggregate itself.

Shah and Chandra [1970] used ultrasonic pulse velocity measurements to detect the occurrence and rate of growth of the internal microcracks in concrete specimens subjected to fatigue loading. They found that for stress levels of 70% and below, during which failure in general did not occur, there was a fairly stable and relatively small rate of crack growth, as the ultrasonic velocity decreased at a fairly stable rate. In contrast, at the stress levels of 80% and higher, during which specimens generally failed, they found a faster rate of crack growth, because a sharp rate of decrease in the pulse velocity was recorded.

Murdock [1960] expressed the view that the deterioration of bond between the cement paste and aggregate is responsible for fatigue failure. Tests in the present study have shown that fatigue specimens had fewer broken aggregate particles than specimens which failed in a static test. These findings are in agreement with previous work [Assimacopoulos et al, 1959], thus suggesting that the failure at the aggregate-paste interface is probably dominant in fatigue [Neville, 1995].

4.6 CONCLUSIONS

The investigation into the mechanical characteristics of various grades of CBM with different aggregates demonstrates the following conclusions:

1. The strength properties of a CBM are more sensitive to variations in the mix water content and the degree of compaction, at a given cement content, than the elastic stiffness.
2. Tensile strength is heavily influenced by the aggregate type and grade of a CBM. Physical properties of an aggregate, such as surface texture and angularity, are more important than its inherent strength. Use of crushed aggregate with a rough surface texture increases the tensile strength for a given CBM grade.
3. Tensile strength is sensitive to aggregate grading, degree of compaction, age at testing, and mode of failure of a CBM. An increase of 20 to 23 percent can be expected in the tensile strength at 90 days, for CBM3 to CBM6, compared to that at 28 days.
4. Elastic stiffness increases with an increase in the CBM strength, following the sequence from CBM2 to CBM6, and is a function of the type and quality of the aggregate.
5. The elastic stiffnesses in direct tension and in compression are equal, for the whole range of CBMs investigated, and are likely to be sensitive to stress strain distributions attained in different shapes of specimen under loading.

6. The inter-relationships of the strength properties demonstrate that:
   - The direct tensile strength is 75% of cylinder splitting strength (with almost similar scatter for both), and 11% of cylinder compressive strength.
   - The 28-day direct tensile strength is one-tenth of the 7-day cube compressive strength, but 7.7% of the 28-day cube compressive strength.
   - Cylinder compressive strength is 68% of the cube compressive strength.
   - Cube compressive strength at 7 days is 76% of that at 28 days.
   - The estimated in-situ cube strength, measured from cores, is approximately equal to 67% of the cube compressive strength from prepared specimens.
   - The core splitting strength is 68% of the splitting strength of prepared cylinders.

7. The elastic stiffness can be related to various strength parameters. The correlations, presented in this research, relate stiffness in tension with direct tensile strength, cylinder compressive strength, and cube compressive strength.
8. Poisson's ratio of a CBM is a function of the aggregate grading and cement content. Values in the range 0.14 to 0.19 have been found for gravel sand CBMs, whereas for CBMs with limestone (and relatively less cement) the values are slightly higher in the range 0.19 to 0.24.
9. Fatigue behaviour, in direct tension, of two types of CBM4 comprising uncrushed gravel sand and crushed limestone aggregates, is similar when the results are expressed in terms of a S-N (stress ratio - number of cycles) diagram. For both the CBMs, a fatigue strength of 60% is an appropriate endurance limit (for 10 million cycles). In general, this fatigue strength is applicable to CBM3 and higher grades.
10. The ratio of fatigue strength to static strength is independent of the type of aggregate, cement content, age at loading, and testing method, as the fatigue failure occurs at the same fraction of the ultimate strength at a given number of cycles.

Controlled Cracking of Cement Bound Bases

5.1 INTRODUCTION

The problems with cement bound base roads have generally stemmed from the tendency for discrete cracks within the base to propagate through bituminous surfacing layers, giving rise to maintenance concerns. This does not lead to immediate pavement failure so long as these cracks are sealed and maintained, because primary cracking (transverse cracks due to thermal contraction and shrinkage effects) hardly reduces the strength of the pavement. The problem is that traffic causes deterioration of these primary cracks through shear movement of the crack faces, and, in some cases, also induces longitudinal wheel-path cracks. This phenomenon (termed secondary cracking) is the actual mechanism of failure in such pavements and it is most likely to occur if water is allowed into the pavement through unsealed primary cracks. Thus, propagation of primary cracks through the bituminous surfacing, though it may start as a major maintenance problem, can lead eventually to pavement failure.

Controlled cracking [Shahid et al, 1995; Shahid, 1996; Shahid and Thom, 1996a and 1996b], also termed precracking, of a cement bound base is a simple and inexpensive technique for dealing with this problem. It is similar to the concept of joint formation in rigid pavements, and aims to deliberately induce frequent cracks in the CBM base due to shrinkage and thermal stresses. The cracks thus formed will be of minimum width and have maximum load transfer capacity due to superior aggregate interlock. The controlled crack width can be potentially useful in limiting the movement at cracks and therefore the tensile stresses generated within the bituminous layer [Colombier and Marchand, 1993]. In consequence, with a controlled cracking system, it may be possible to minimize the thickness of bituminous layer required to counter reflective cracking. Also the use of expensive modified bituminous mixes, designed to resist the tensile stresses accompanying the crack movement, may be avoided [Colombier and Marchand, 1993].

The concept is that a CBM base still provides a high quality support for the bituminous surfacing but does not incur the penalty of early reflective cracking, and associated maintenance concerns. To check the validity of this technique, two full scale site trials were performed in the UK, in 1994/95, by involving CBMs with two different aggregates of considerably different thermal coefficients. The performance of controlled cracking system was then evaluated through a laboratory study and field investigation comprising a visual examination, coring survey and Falling Weight Deflectometer (FWD) testing.

5.2 DESCRIPTION OF SITES AND TRIALS

Two full scale site trials of controlled cracking were carried out, in the UK, to investigate the response of two different CBMs, having different thermal characteristics, a major factor influencing the crack pattern. These trials were not set up as long term performance trials, since the upper pavement was to be rigid. A description of the sites and trials is as follows:

5.2.1 M4 Second Severn Crossing, Bristol

A trial section on the new M4 access route to the Second Severn Crossing consisted of a 150 mm thick CBM layer, with a minimum 7 day cube compressive strength of 10 MPa, involving a crushed limestone with 40 mm maximum aggregate size. This trial section was 120 metres long on a 12 metre wide carriageway. The construction took place in December 1994 when the air temperature was 12°C.

For comparison purposes, data was also collected from an adjoining section of M4 pavement and another similar pavement, without controlled cracking, constructed as part of the new M49 access route, also an element of the Second Severn Crossing scheme. The CBM material was the same in each case.

5.2.2 A11 Wymondham Bypass, Norwich

The A11 Wymondham Bypass trial section comprised a 150 mm thick CBM layer, with the same cube compressive strength requirement as on the M4, involving a

crushed flint gravel of 40 mm maximum aggregate size blended with sand. This trial section was 140 metres long on a 12 metre wide carriageway and was constructed in July 1995 when the air temperature was 22°C.

All of the above mentioned pavement carriageways were subjected to construction traffic during the course of their investigation.

5.3 THE PROCESS OF CONTROLLED CRACKING

A brief description of the process of controlled cracking [Shahid et al, 1995; Shahid, 1996] is as follows:

1. In fresh CBM, laid by a slipform paver, create 10 mm wide transverse slots at 3 m intervals to approximately half the layer depth. For this purpose, a simple manually controlled device is used, consisting of a small vibrating plate having a vertical cutting blade attached at its base (Figure 5.1).
2. Introduce emulsified bitumen into the slots before compaction is commenced. The emulsion serves two purposes; it creates a weak zone in the CBM layer and helps the shrinkage cracks to be accurately located.
3. Close the slots at the time of compaction through rolling as usual, thereby restoring the integrity of the layer as the slot faces are pushed back together (Figure 5.2).
4. Complete the entire process within two hours of mixing the CBM.

5.4 VISUAL ASSESSMENT OF SITE TRIALS

The CBM pavements of the M4 and M49 Second Severn Crossing were not overlaid until June 1995, and similarly the A11 Wymondham Bypass was left until the end of September 1995. This allowed a direct investigation of the CBM pavements to be performed. The sites were regularly inspected to investigate the influence of the two aggregate types upon the crack pattern in the CBM pavements. Visual inspection of cracks was carried out, not only inside the trial sections, but also on the adjacent lengths of the A11 and M4 pavements, in addition to the M49 pavement.

Figure 5.1. Process of controlled cracking in a cement bound layer

Figure 5.2. A slotted CBM layer before and after compaction

5.4.1 Induced Cracking

Two months after construction, the slot marks were identifiable on the trial section of the M4 Second Severn Crossing, but in none of them could a crack be visually detected. However, coring at the slot locations revealed that 40% of the slots had developed cracks, throughout the entire thickness of the CBM layer (Figure 5.3). The crack width was found to be ≤ 0.25 mm.

In contrast, one month after construction, distinctly visible cracks were found at slot locations on the trial section of the A11 Wymondham Bypass. By taking cores, from the slot locations, it was disclosed that 90% of the slots had developed cracks through the entire layer thickness. The crack width was ≤ 0.5 mm. However, no other cracks could be identified between the positions of the induced cracks on either trial section.

5.4.2 Natural Cracking

Cracking occurred naturally, due to shrinkage and thermal contraction, on pavement lengths outside the trial sections of both the M4 Second Severn Crossing and A11 Wymondham Bypass, as well as on the M49 pavement. The width of these cracks varied from 1.0 to 2.0 mm on the A11 CBM pavement, whereas on the M4 and M49 it was between 1.0 and 3.0 mm. The natural cracking on the A11 was more frequent than on the M4 or M49. Table 5.1 shows a comparison of the crack spacing obtained from the two sites. The difference between the cracking pattern on the two sites is attributable to the different thermal properties of the two CBM types.

5.5 LABORATORY INVESTIGATION

Strength properties of the two CBMs were measured in the laboratory. For this purpose, specimens were prepared on each site, from the materials at the time of construction, and transported to the laboratory. The tensile strength was measured through a direct tensile test (Chapter 3). Table 5.2 shows the results of cube compressive strength and tensile strength for both types (flint gravel sand and limestone) of CBMs, and indicates that although the cube compressive strength of flint gravel sand CBM is 80% of that for limestone CBM, the corresponding value for tensile strengths is only 69%.

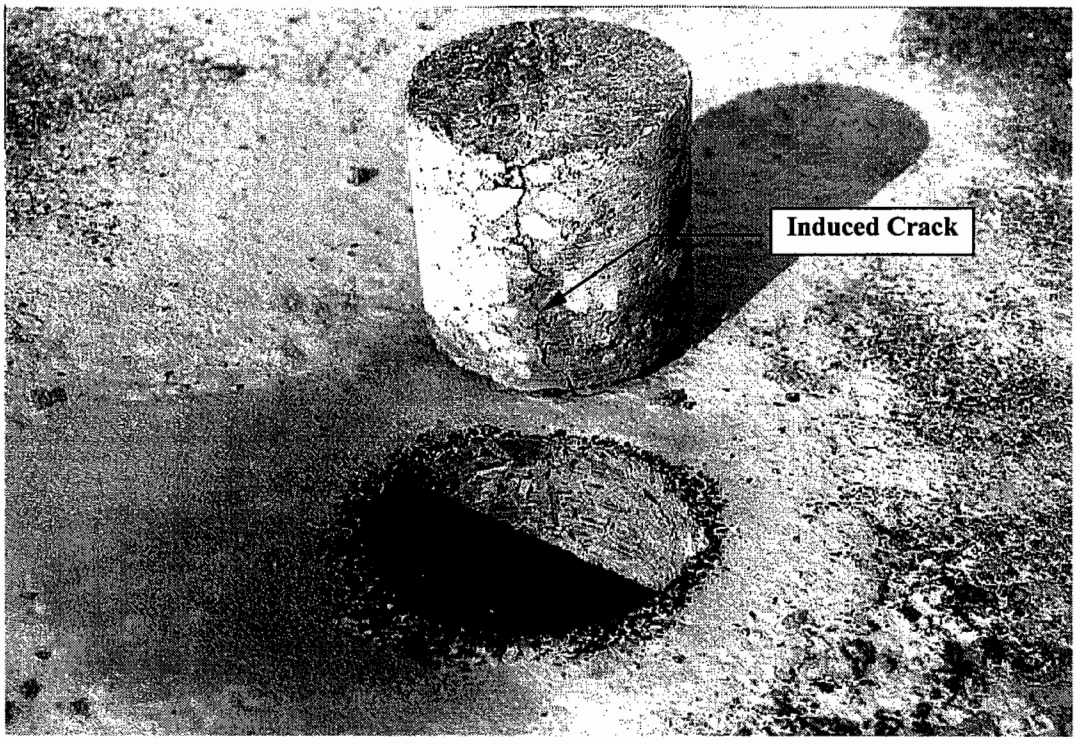

Figure 5.3. Core taken from a slot on the M4 Second Severn Crossing trial section

Table 5.1. Natural crack spacing observed from the two sites

	Natural Crack Spacing (m)	
Spacing between	A11 (Flint gravel sand CBM)	M4 and M49 (Limestone CBM)
Crack 1 and 2	10	12
Crack 2 and 3	9	20
Crack 3 and 4	13	23
Crack 4 and 5	8	15
Crack 5 and 6	12	22
Crack 6 and 7	11	18
Crack 7 and 8	7	16
Crack 8 and 9	9	27
Crack 9 and 10	6	19
Crack 10 and 11	10	13
Crack 11 and 12	11	24
Crack 12 and 13	8	17
Average spacing	9.5	18.8

The in-situ tensile strength of both CBMs was determined through indirect tensile (splitting strength) tests on cores taken from both sites. Cores were taken both from slot locations and from elsewhere. While testing of the cores taken from the uncracked slots, the load was applied diametrically along the average plane of the bitumen emulsion film. Table 5.3 gives a summary of the average values of results, and indicates that the indirect tensile strength at slotted zones is 46% and 50% of the intact CBMs comprising flint gravel sand and limestone aggregate respectively, even where no crack has formed. This implies that the slotted zones are always likely to crack, in preference to other locations, due to shrinkage in the first instance and due to traffic at a latter stage.

Table 5.2. Comparison of the average strength properties of CBMs from both sites

Description of Site	Saturated Density (to refusal) (kg/m^3)	Cube Compressive Strength, f_c		Direct Tensile Strength, f_t at 28 days (N/mm^2)
		7 days (N/mm^2)	28 days (N/mm^2)	
M4	2540	24.0	31.8	2.27
A11	2415	19.3	25.3	1.57

Note: Each value of cube compressive strength represents the average of six specimens.
Each value of direct tensile strength represents the average of 2 to 3 specimens.

Table 5.3. Average splitting strength of cores taken from uncracked slots and intact CBM

Description of Site	Cores from Uncracked Slots		Cores from Intact CBM	
	Saturated Density (kg/m^3)	Splitting Strength (N/mm^2)	Saturated Density (kg/m^3)	Splitting Strength (N/mm^2)
M4	2417	0.88	2435	1.90
A11	2329	0.67	2317	1.35

5.6 FIELD INVESTIGATION

5.6.1 Load Transfer

Falling weight deflectometer [DoT, HD 29/94, 1994] testing was performed to investigate the load transfer efficiency of both induced and natural cracks (Figure 5.4). The load transfer efficiency was expressed in terms of the differential deflection measured 50 mm either side of the induced or natural crack. The load was applied at a distance of 0.55 m from the crack. For comparison purposes, differential deflections were also measured from the intact CBM. All values of deflections and pressures were normalized to a load of 44 kN.

Figures 5.5 and 5.6 show a comparison between the results of differential deflection measured across natural cracks, induced cracks and from the intact CBM on both sites. Figure 5.6 includes measurements across natural cracks for the M49 rather than the M4, because of the availability of more data on the M49. The same limestone CBM was used for both. It can be seen from Figures 5.5 and 5.6 that the induced cracks have much better load transfer, that is smaller differential deflection, than natural cracks. This is attributed to better aggregate interlock at the induced cracks. The magnitude of this aggregate interlock is heavily dependent on the crack width [Shahid et al, 1996; Bondt and Saathof, 1993; Colombier et al, 1993], and is expected to play an important role in determining the structural performance of a pavement [Scarpas et al, 1993] under trafficking.

Since the width of natural cracks is 2 to 4 times greater than that of controlled cracks, there will be an increased amount of shear slip under traffic. A repeated action of this shear slip might be expected to cause accelerated damage of the crack faces, and lead to a further reduction in load transfer. Figure 5.7 illustrates the effect using the average magnitudes of shear slip across an induced and natural crack on the A11 Wymondham Bypass.

A summary of the average magnitudes of the differential deflection measured from the intact CBM, induced cracks and natural cracks, for both sites, is given in Table 5.4, which indicates that the average differential deflection at natural cracks on the A11 is relatively higher than those of the natural cracks on the M49. This may be attributable to a significant difference in the physical properties of the aggregates, used on the two sites, and tensile strengths of the resulting CBMs. The limestone aggregate with a rough surface texture, is likely to develop a relatively stronger bond with cement matrix, thus providing a higher degree of shear resistance across the crack faces, and leading to a relatively lower differential deflection. In contrast, the average differential deflection at the induced cracks is almost the same for both trial sections (Table 5.4), although the number of induced cracks was twice on the A11.

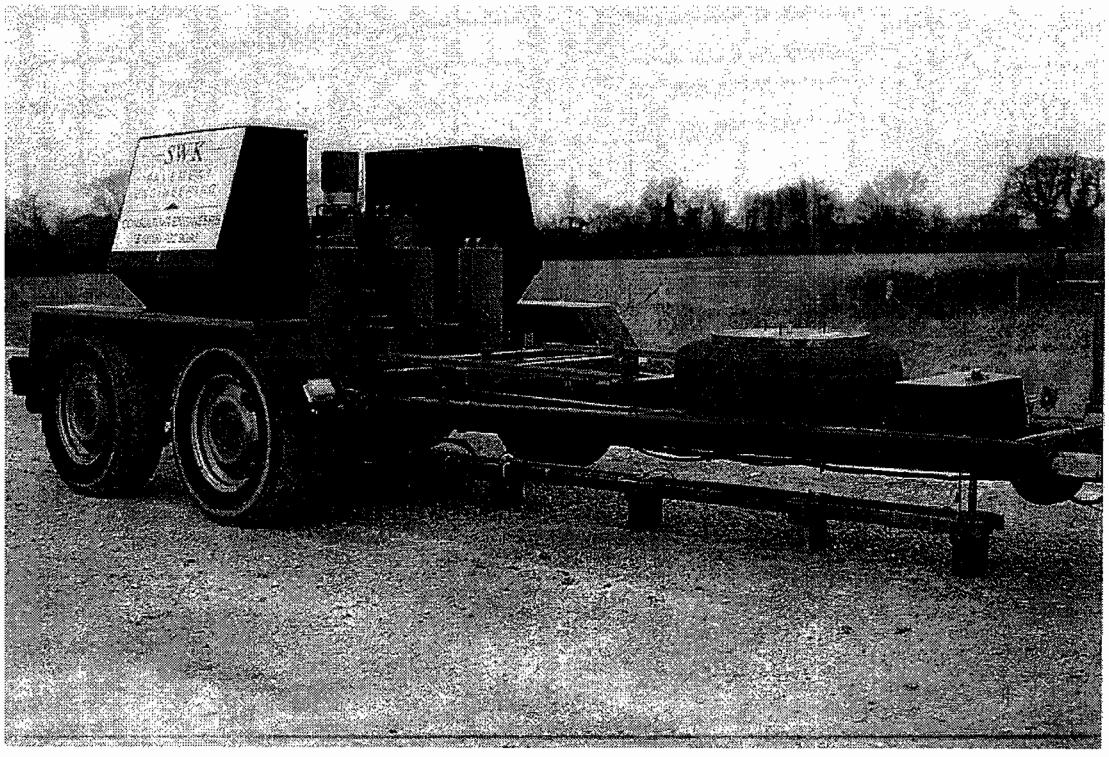

Figure 5.4. Falling Weight Deflectometer survey

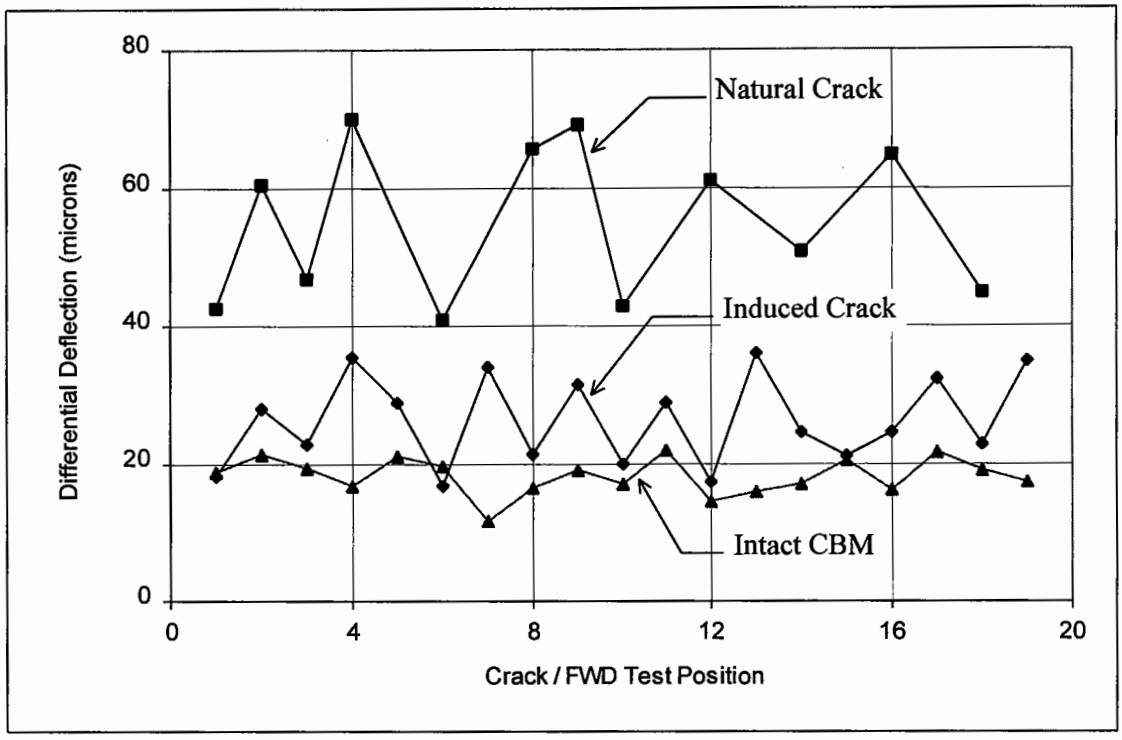

Figure 5.5. Differential deflections measured across natural cracks, induced cracks and from intact CBM on the A11 Wymondham Bypass

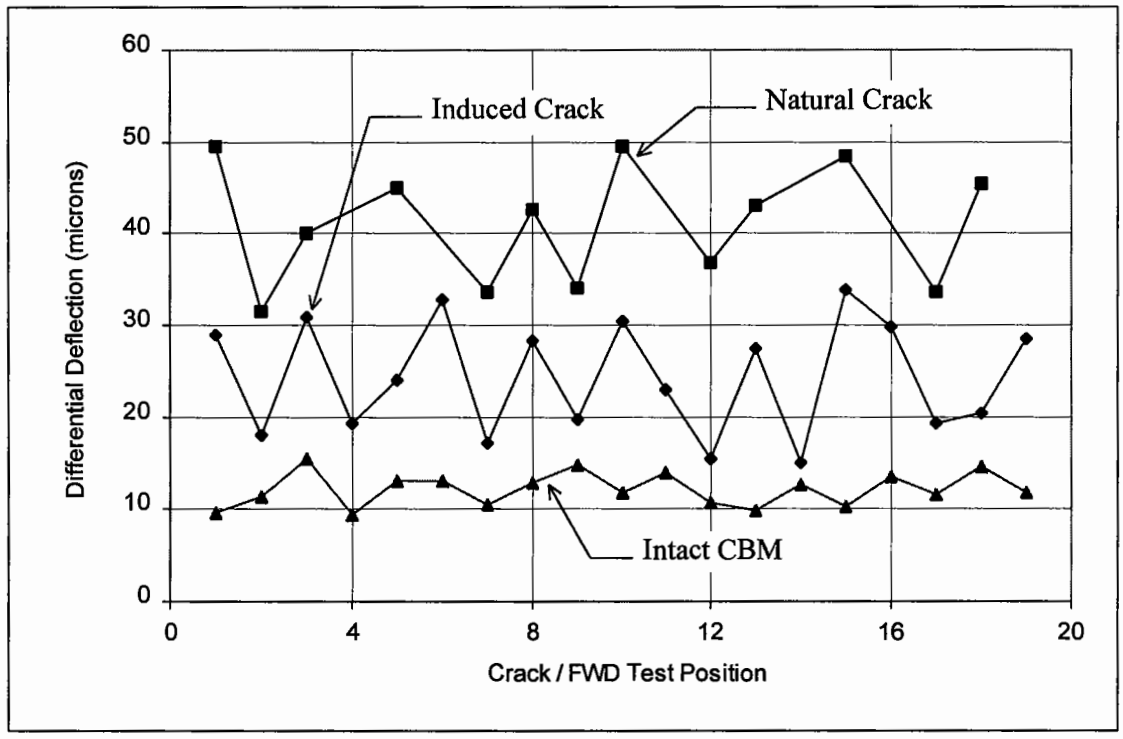

Figure 5.6 Differential deflections measured across natural cracks on the M49, induced cracks and the intact CBM on the M4 Second Severn Crossing

Table 5.4. Summary of the average values of differential deflection at induced cracks, natural cracks and on intact CBM.

Description of Site	Average Differential Deflection (microns)		
	Intact CBM	Induced Cracks	Natural Cracks
A11 Wymondham Bypass	18.0	26.3	54.7
M4 Second Severn Crossing	12.2	24.3	—
M49 Second Severn Crossing	11.5	—	41.0

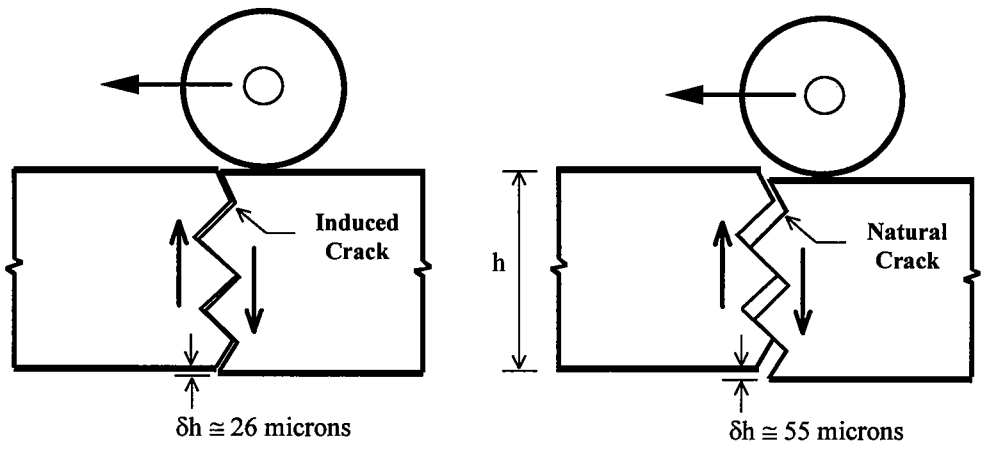

Figure 5.7 Shear slip across an induced and natural crack on the A11 pavement

5.6.2 In-situ Stiffness Modulus

The in-situ stiffness of the CBM layer was determined from FWD data through a back-analysis computer programme (Brown et al, 1987). For each site, two sets of data were back-analyzed, i.e. for FWD pulses applied 550 mm from cracks (or slots) and on intact CBM in between the cracks (or slots). For comparison purposes, FWD data was analyzed from within both trial sections and outside them, as well as on the M49 site. Table 5.5 presents a summary of the stiffness modulus results and indicates that the stiffness drop associated with controlled cracking is almost negligible in comparison with that of natural cracking.

The average values of the in-situ stiffness moduli measured from: the trial sections on the A11 and M4, the adjacent sections on the A11 and M4 without controlled cracking, and from the M49 CBM pavement, are given in Table 5.6. The difference between the stiffnesses for the A11 and M4 pavements is expected due to different types of aggregates. However, the higher stiffness from the M49 may be due to the difference in mix proportion, material grading, or due to a relatively greater thickness of the CBM used. One point is clearly known that the age of the M49 pavement was approximately three times that of the M4 at the time of test.

Table 5.5. Ratio of the in-situ stiffnesses at induced and natural cracks to that of the intact CBM.

Description of Site	Ratio of the In-situ Stiffnesses (%)	
	Induced cracks and intact CBM	Natural cracks and intact CBM
A11 Wymondham Bypass	84.0	52.3
M4 Second Severn Crossing	89.3	56.4
M49 Second Severn Crossing	—	55.1

Table 5.6. In-situ stiffness modulus at induced cracks, natural cracks, and intact CBM

Description of Site	Average In-situ Stiffness (MPa)		
	Induced Cracks	Natural Cracks	Intact CBM
A11 Wymondham Bypass	18050	11250	21500
M4 Second Severn Crossing	22950	14500	25700
M49 Second Severn Crossing	—	17250	31300

5.7 INTERPRETATION OF RESULTS

5.7.1 Cracking Pattern

As mentioned in Section 5.4, transverse cracks were induced at 90% of the slots on the A11 trial section, in comparison with 40% of the slots on the M4 trial section. This variation in cracking pattern may be due to a significant difference between the magnitudes of the following two important properties of the two CBM pavements:

- Thermal expansion coefficient
- Tensile strength

Since the thermal coefficient for a flint gravel sand CBM is much higher (almost twice) than for a limestone CBM (Table 1.8, Chapter 1), therefore the A11 pavement is more susceptible to thermal shrinkage under a given temperature drop. Moreover, tensile strength of the flint gravel sand CBM is less (69%) than that for the limestone CBM (Table 5.2). As a result, the magnitude of temperature drop to cause fracture, which is affected by both the thermal coefficient and tensile strength, is much smaller for a flint gravel sand CBM base compared to a limestone CBM. The temperature drop causing fracture (ΔT_f) can be calculated through the following equation:

$$\Delta T_f = \frac{f_t}{E\alpha} \tag{5.1}$$

where:

ΔT_f : temperature drop causing fracture of the CBM base (^oC)

f_t : tensile strength of a CBM base (N/mm^2)

E : elastic modulus of a CBM base (N/mm^2 or MPa)

α : coefficient of thermal expansion, with values of 13×10^{-6} and 7×10^{-6} per ^oC [Bonnell and Harper, 1950] for flint gravel sand and limestone CBMs, respectively.

It is clear from Eq. 5.1 that the thermal drop to cause fracture is directly related to tensile strength (which is lower for flint gravel sand CBM), and inversely related to the coefficient of thermal expansion (which is higher for flint gravel sand CBM). Thus the A11 pavement will develop much higher shrinkage strain under a given temperature drop, and would be expected to crack more easily.

5.7.2 Crack Spacing

The spacing of controlled cracking is directly related to crack width. The amount of change in length δl, for a CBM section of length L, under a temperature drop ΔT, is given by the following relation:

$$\delta l = L\alpha\,\Delta\mathrm{T} \tag{5.2}$$

This change in length δl is equal to the opening or closing of the cracks and, from Eq. 5.2, it is obvious that δl increases with crack spacing L, and is also affected by the magnitude of thermal coefficient of expansion.

5.8 EFFECTIVENESS OF CONTROLLED CRACKING

The performance of controlled cracks has been measured in various ways. It has been shown that zones of weakness are formed giving the material locally only 50% of its intrinsic tensile strength. This has been shown to generate cracks in practice, particularly in the high thermal expansion coefficient gravel sand CBM. These cracks have been found to give excellent load transfer in comparison with naturally occurring cracks on adjacent sections, such that the effective stiffness modulus of the layer is hardly reduced. The expected benefits from such a system, in comparison with a CBM base road without controlled cracking are as follows:

- Thermal expansion and contraction cause very little horizontal movement at each crack (refer Eq. 5.2).
- Traffic loading causes very little relative vertical movement at each crack (refer FWD results).
- The combination implies greatly reduced reflective cracking (see Chapter 8).

- Pavement design can therefore allow a substantial reduction in the thickness of bituminous surfacing (refer Chapter 8).

There remains a key issue for pavement design, which is crack deterioration under traffic loading. This has been the subject of separate laboratory based wheel tracking experiments, which are described in Chapter 7. These wheel tracking experiments have also included a study of reflective crack generation. The effectiveness of controlled cracking in CBM bases has been studied analytically in Chapter 8.

In France, precracking is included in the recommendations for the construction of roadbases incorporating hydraulic binders [SETRA, 1990]. From 1988 to 1992, precracking has been carried out over more than 40 sections in France (nearly 100 km length) and one in Spain. In each case, slotting had been performed throughout the entire depth of CBM base. In addition, eight reference sections were also constructed without precracking. Several types and thicknesses of wearing courses were used on different sections. A systematic monitoring programme was applied to all sites in order to establish the results in terms of the number of transverse cracks reflecting to the surface. It is reported [Colombier et al, 1993] that the benefit of precracking has been a saving of 50 to 60 mm of the bituminous overlay (Figure 5.8), which would otherwise be required to prevent or delay reflective cracking. According to Colombier et al [1993], precracking may replace the use of crack-resistant modified bituminous wearing courses.

One important point is that since, in the French precracking technique, slotting was performed through the entire depth of a CBM base, the induced cracks are likely to generate a relatively higher differential deflection. In this relation, an average value of 50 microns has been reported [Colombier et al, 1993], but no mention of the type of CBM and applied pressure has yet been found. On the other hand, with the controlled cracking system (described in this chapter), the average differential deflections of 26.3 and 24.3 microns (refer Table 5.4) have been recorded from flint gravel sand and limestone CBMs under an applied pressure of 620 kPa. These values are, in fact, only a little higher than those measured on the intact CBM. It seems that the performance

of the controlled cracking system, described in this chapter, may be better than the above mentioned French precracking, but the absence of data makes the comparison difficult.

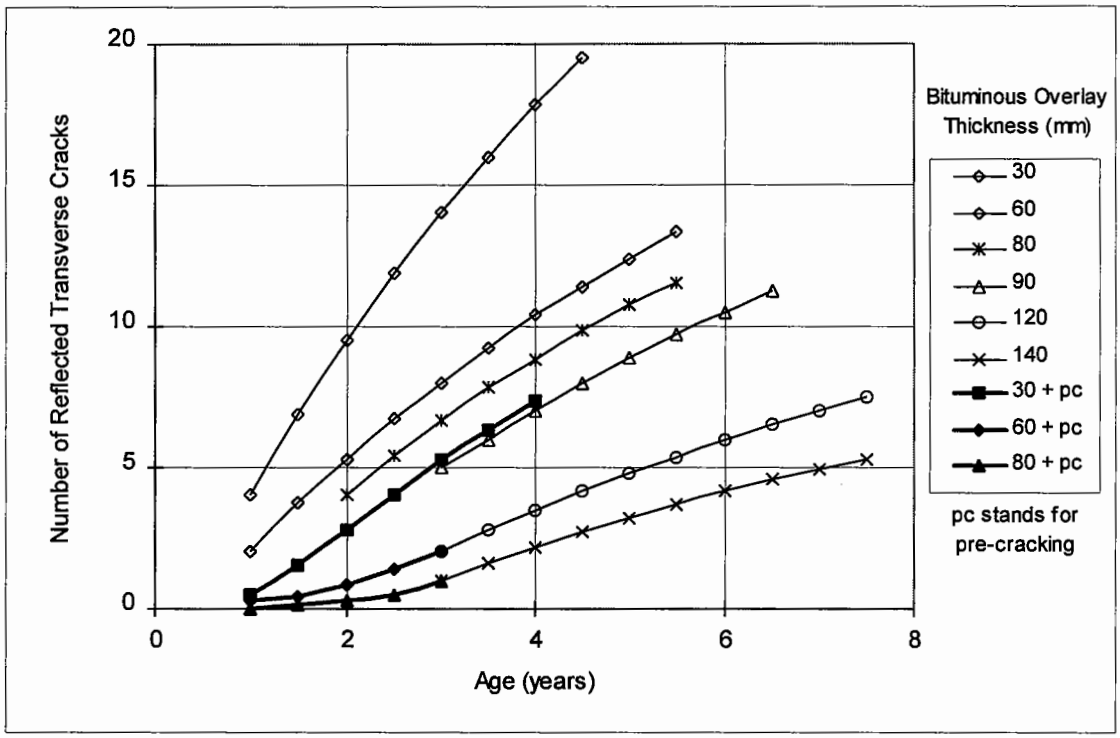

Figure 5.8 Number of reflected transverse cracks per 100 m section, with and without precracking, as a function of the thickness of bituminous overlay and age of the underlay [Colombier et al, 1993].

5.9 PRACTICAL IMPLEMENTATION

The practical significance and effectiveness of controlled cracking of CBM bases have convinced other research organizations to look into more detailed aspects of this system and road industries to implement this technique in construction. Relating to this subject, Transport Research Laboratory (TRL) is carrying out further long term performance trials of controlled cracking in CBM bases, overlaid by bituminous surfacing, on behalf of the UK Highways Agency [Research Focus, 1996].

Regarding practical implementation, Road Management Group Joint Venture (RMG JV) is currently working on a Design Build Finance and Operate (DBFO)

project on the A1(M), from Alconbury to Peterborough (22 km length), where the controlled cracking system is being used to induce primary cracking in a CBM4 roadbase, which is being overlaid by a slightly reduced bituminous thickness, compared to the that recommended in HD 26/94 [DoT, DMRB Vol. 7, 1994].

5.10 CONCLUSIONS

Based on two trial pavements incorporating controlled cracking of CBM layers, assessed before being overlaid, the following conclusions have been drawn:

- Controlled cracking system described successfully led to the formation of regular transverse cracks in CBM bases.
- Controlled cracking resulted in crack widths of less than 0.5 mm, whereas the width of natural cracks was found to be typically more than 1.0 mm.
- The induced cracks have greatly superior load transfer characteristics (as measured by the FWD) to those of the natural cracks.
- The performance data suggests that the improvement is due to better aggregate interlock between the crack faces.
- The effective stiffness modulus of CBM at a controlled crack location was found to be only marginally less than that of the intact material. This was not the case at naturally occurring cracks.
- The expectation is that controlled cracking will have significant benefit in reducing reflective crack development.

Steel Fibre Reinforced Cement Bound Bases

6.1 INTRODUCTION

This chapter presents innovative research aimed at preventing the propagation of cracks in a CBM base through a bituminous surfacing, by using steel fibre reinforcement in the CBM. The performance of CBMs has been investigated with reference to the influence of 1% steel fibre reinforcement (by volume) upon direct and indirect tensile strength, compressive strength, elastic stiffness, load versus deformation characteristics, and post-cracking behaviour.

The development of controlled cracking system (discussed in Chapter 5) and other precracking techniques [Verhée, 1996; Jofre et al, 1996] is an advanced step indeed in flexible composite pavement technology. With this development, the problem of widely spaced primary cracking potentially with poor load transfer, which is quite serious for many existing composite pavements, can now be tackled during construction and therefore need not adversely influence the performance of a CBM base. Secondary (longitudinal) cracking is a matter of concern and is wholly attributable to traffic [Brown et al, 1993; Williams, 1986]. Longitudinal cracking, which is the most damaging form of distress, occurs due to the tensile failure of a cement bound base, and is mainly related to the following factors [Williams, 1986; Shahid, 1994]:

- Tensile strength of a CBM
- Thickness of a CBM base
- Stiffness of support
- Condition of transverse cracks

For a relatively weak CBM, say a gravel sand CBM3 having a lower tensile strength, the current Highways Agency's thickness requirement is over 200mm for

'indeterminate' pavement design [DoT, HD 26/94, 1994]; that is a sufficiently strong design to avoid longitudinal cracking. This thickness can be difficult to compact satisfactorily [Powell et al, 1984], causing a further reduction in the tensile strength and a greater risk of secondary cracking. In contrast, a stronger CBM is more resistant to tensile failure, but gives rise to the occurrence of occasional but relatively wide transverse cracks (under uncontrolled conditions) allowing greater differential movement at each crack, lower load transfer and earlier reflective cracking [Bondt and Saathof, 1993].

Steel fibre reinforcement in CBMs is intended to overcome the problems of both primary and secondary cracking. Present research has shown that, in the case of a steel fibre reinforced CBM base, the cracks are much finer than those in a non-reinforced CBM base and, in the laboratory, deteriorate less under traffic loading. These cracks provide a much superior load transfer, indicating that the fibre reinforcement can contribute significantly towards the crack's shear resistance [Holmgren, 1985]. This improved load transfer, which is manifested as a reduced differential vertical movement, should logically lead to a considerable reduction in reflective cracking. As far as the cost of steel fibres is concerned, it can be argued that the difference between the unit costs of the SFR and non-reinforced CBMs may well be offset by an appreciably reduced thickness of bituminous surfacing [Williams, 1986].

6.2 CBMS FOR STEEL FIBRE REINFORCEMENT

Steel fibre reinforcement has been used only in the high strength CBMs (Table 2.2 of Chapter 2) for the following reasons:

- High strength CBMs provide sufficiently strong material to hold the steel fibres across cracks, because they contain a greater amount of cement paste (due to their relatively high cement content) which plays an important role in developing a strong bond between steel fibres and the CBM matrix.
- The cracks in a high strength CBM are less likely to deteriorate under trafficking.

As stated above, it is the higher strength values that are likely to benefit most.

6.3 INVESTIGATION OF STEEL FIBRE REINFORCED CBMS

An investigation has been carried out into the mechanical characteristics of a steel fibre reinforced (SFR) gravel sand CBM5. Specimens were prepared for a variety of tests, from nominally identical mixes, with and without steel fibre reinforcement. All specimens were stored and tested under similar conditions.

6.3.1 Mix Design of SFR CBM

The mix design for a CBM requires the determination of a cement content and an optimum water content corresponding to a desired cube compressive strength. As discussed in Section 2.4 (Chapter 2), the mix design parameters are highly sensitive to variations in aggregate type and grading. Therefore, for this study, a 20 mm gravel sand aggregate was used whose grading has been shown in Figure 2.5. The effect of fibres with other aggregate gradings is an area requiring further study. A mix design criterion is also established (in Chapter 2), from which the amount of cement and the optimum water content were derived. For the SFR CBM5, the fibres were considered as part of the aggregate volume.

Dramix steel fibres ZP 30/0.5 and ZL 30/0.5 (collated and loose respectively) were used in separate batches of the mix. All these fibres have hook shaped ends. The designations 30/0.5 represent the aspect ratio of the fibres, defined as the fibre length divided by the equivalent fibre diameter. The amount of the steel fibres added into each batch of the mix was 1.0% by volume of the compacted specimens. Although this may be a relatively high fibre content, it was intended to ensure that the effect of fibres could be clearly evaluated in this preliminary investigation. If benefits are clear, then lower and potentially more economic levels of fibre reinforcement can be researched, together with alternative lengths and shapes of fibres.

6.3.2 Mixing Process

Batching of ingredients was performed by mass. For mixing, the following procedure was adopted to attain a uniform dispersion and prevent balling of steel fibres in the CBM matrix:

1. Steel fibres were added to aggregates of size greater than 600 microns, and dry mixing was performed, over one minute for loose fibres but two minutes for collated fibres, in a pan type concrete mixer.
2. The rest of the aggregates plus cement were then added, and dry mixing was continued over a further one minute.
3. The addition of water was gradual and followed by three minutes wet mixing.

The resulting mixes involving the two fibre types were visually identical in achieving dispersion of the fibres. This was confirmed by comparative test results showing similar specimen properties. The feasibility of mixing fibres into a CBM on a commercial scale is one of the subjects of ongoing research at Nottingham, in collaboration with industry.

6.3.3 Specimen Preparation

A brief description of the element test specimens prepared from the SFR and non-reinforced gravel sand CBM5 is as follows:

- Cubes (100 mm)
- Cylinders (300 mm × 150 mm diameter)
- Cylinders (150 mm × 150 mm diameter)
- Tensile specimens (refer Figure 3.7 in Chapter 3)

All these specimens were compacted using a vibrating hammer. The procedure of preparing, curing and testing of cubic specimens is given in Clause 4.2 of BS 1924: Part 2: 1990. The same procedure was used for cylinders. The tensile specimens were prepared, cured and tested according to a procedure described in Chapter 3.

In addition, roller compacted slabs (1100×900×80 mm) were prepared of several different CBM mixes, including SFR and non-reinforced gravel sand CBM5. These slabs were produced for testing in a wheel tracking facility, and are discussed in Chapter 7.

6.4 RESULTS AND DISCUSSION

6.4.1 Compressive Strength

Compressive strength results, obtained from a number of cubes (100 mm) and standard cylinders (300 mm × 150 mm diameter), are given in Tables 6.1 and 6.2 respectively. Cubes were tested at 7 and 28 days, whereas cylinders were tested only at 28 days. The average results of cube compressive strength, for SFR and non-reinforced CBM5 (Table 6.1), indicate that the steel fibre reinforcement has no significant influence upon the magnitude of the cube compressive strength. The CBM density also remains almost unaffected. The increase of 1 to 2% in the CBM density (from all specimens) is purely attributable to the relatively high specific gravity of steel. These results of cube compressive strength and density of the SFR CBM are in accordance with expectations [ACI Committee 544.2R, 1988].

In contrast, Table 6.2 shows that the steel fibre reinforcement of 1.0% has increased the cylinder compressive strength by nearly 12%, which seems to be in reasonable agreement with the results of a previous study by Nanni and Johari [1989], who reported an increase of more than 10% after testing cylindrical specimens cored from a trial section on site. Both these findings are in comparison with ACI Committee Report [544.4R, 1988], according to which the increase in cylinder compressive strength of a steel fibre reinforced concrete ranges from negligible, in most cases, to 23% when the fibre content is 2% by volume.

From Tables 6.1 and 6.2, it appears that the performance of steel fibre reinforcement is influenced by the mode of failure which is controlled by the specimen shape. The failure of cylinders, under a compressive force, is actually caused by tensile stresses which are developed, in a lateral direction, inside the specimen under a wedge action at the ends. Since the presence of steel fibres alters the failure mode by making the CBM a pseudo-ductile material [ACI Committee 544.2R, 1988; Nanni and Johari, 1989], the cylinder compressive strength is therefore increased.

Table 6.1. Average cube compressive strength of gravel sand CBM5, with and without steel fibre reinforcement.

Description of CBM	7 days			28 days		
	Density (kg/m^3)	Cube Strength (N/mm^2)		Density (kg/m^3)	Cube Strength (N/mm^2)	
		f_c	st. dev.		f_c	st. dev.
SFR CBM5	2421	24.7	0.66	2423	32.3	0.80
Non-reinforced CBM5	2394	23.1	0.35	2407	30.5	0.52

Table 6.2. Average cylinder compressive strength of gravel sand CBM5, with and without steel fibre reinforcement.

Description of CBM	Specimen Density (kg/m^3)	28 day Cylinder Compressive Strength (N/mm^2)	
		Strength, f_{cl}	st. deviation
SFR CBM5	2425	24.4	0.47
Non-reinforced CBM5	2384	21.5	1.13

6.4.2 Tensile Strength

The tensile strength of SFR and non-reinforced CBM5 was determined at 28 days through direct tensile and indirect tensile (cylinder splitting) tests. Both the tests are described in Chapter 3. The average results have been summarized in Table 6.3, indicating that the direct tensile strength (on average) is 76% of the indirect tensile strength, agreeing with the relationship established in Chapter 4.

The tensile strength is a very important characteristic of CBMs, affecting crack development, propagation and deterioration [Bonnot, 1972]. In contrast, the cube compressive strength is not a reliable indicator of any of the properties of CBMs relating to pavement performance [Brown et al, 1993]. This is particularly important

for SFR CBMs, in which the cube compressive strength remains almost unaffected by the fibre reinforcement, whereas the tensile strength is increased by a substantial amount (Table 6.3), as follows:

- Increase in the direct tensile strength = 33%
- Increase in the indirect tensile strength = 38%

Other research [ACI Committee 544.4R, 1988] has shown that steel fibre reinforcement of 0.6, 0.9 and 1.2 percent (by volume) increases the shear strength of concrete by 22, 35 and 42 percent, respectively.

Table 6.3. Average values of direct and indirect tensile strength for gravel sand CBM5, with and without steel fibre reinforcement.

Description of CBM	Direct Tensile Strength (f_t)			Indirect Tensile Strength (f_{sp})		
	Density (kg/m^3)	Strength (N/mm^2)		Density (kg/m^3)	Strength (N/mm^2)	
		f_t	st. dev.		f_{sp}	st. dev.
SFR CBM5	2427	2.82	0.04	2425	3.76	0.10
Non-reinforced CBM5	2381	2.12	0.14	2390	2.72	0.08

6.4.3 Elastic Stiffness

The elastic stiffness was measured from the tensile specimens because the relatively uniform stress conditions obtained during a direct tensile test are thought to give the most suitable conditions for measuring elastic stiffness of CBMs [Brown et al, 1993; Bonnot, 1972]. The tensile specimens were also tested in compression, mainly to compare the magnitudes of stiffness under tension and compression. Both the SFR and non-reinforced CBM5 specimens were tested, at 28 days, in accordance with the procedure described in Chapter 3.

The stress strain relationships for SFR and non-reinforced gravel sand CBM5, shown in Figures 6.1 and 6.2 respectively, are effectively linear up to a substantial proportion of the ultimate strengths under tension and compression. The calculation of elastic stiffness in tension E_t and in compression E_c is based on the magnitudes of strain corresponding to stress levels of 50% of the tensile strength and 30% of the compressive strength [Kolias and Williams, 1978] respectively. The average values of stiffness in Table 6.4 indicate that steel fibre reinforcement has a negligible effect on the elastic stiffness of CBMs.

Table 6.4. Average elastic stiffness under direct tension and compression from a gravel sand CBM5, with and without steel fibre reinforcement.

Description of CBM	Stiffness in tension E_t (MPa)	Stiffness in compression E_c (MPa)
SFR CBM5	36250	36650
Non-reinforced CBM5	35800	36100

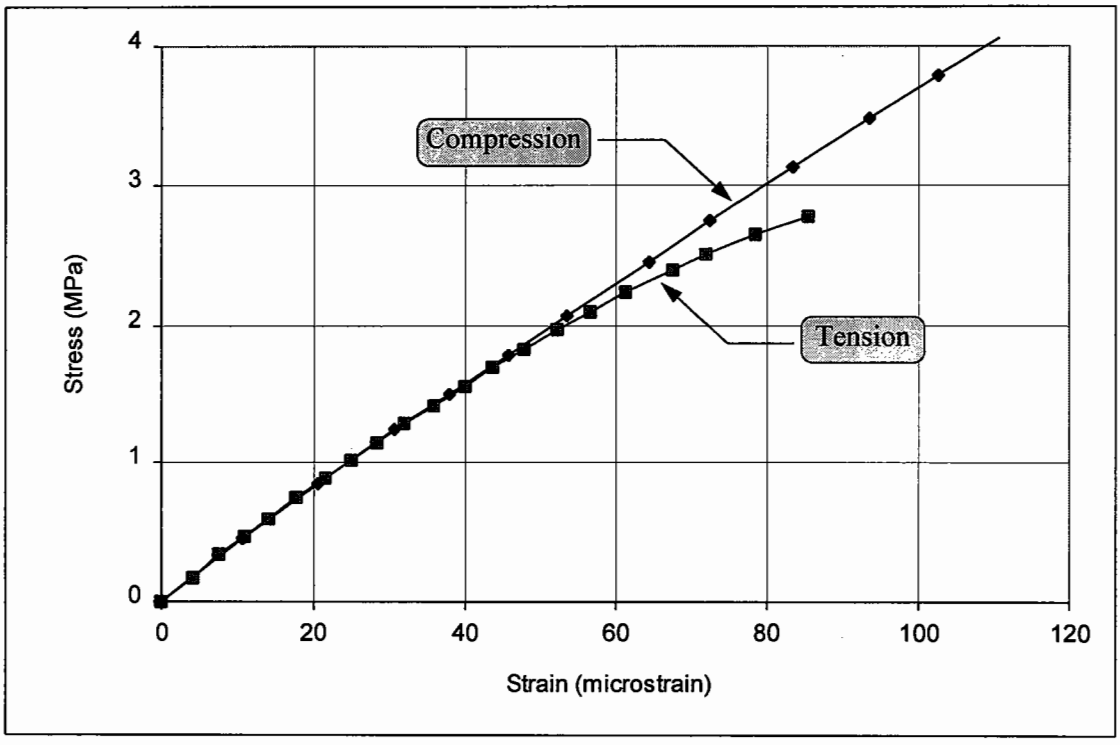

Figure 6.1. Stress strain relationships for a steel fibre reinforced CBM5 tensile specimen subjected to direct tension and compression.

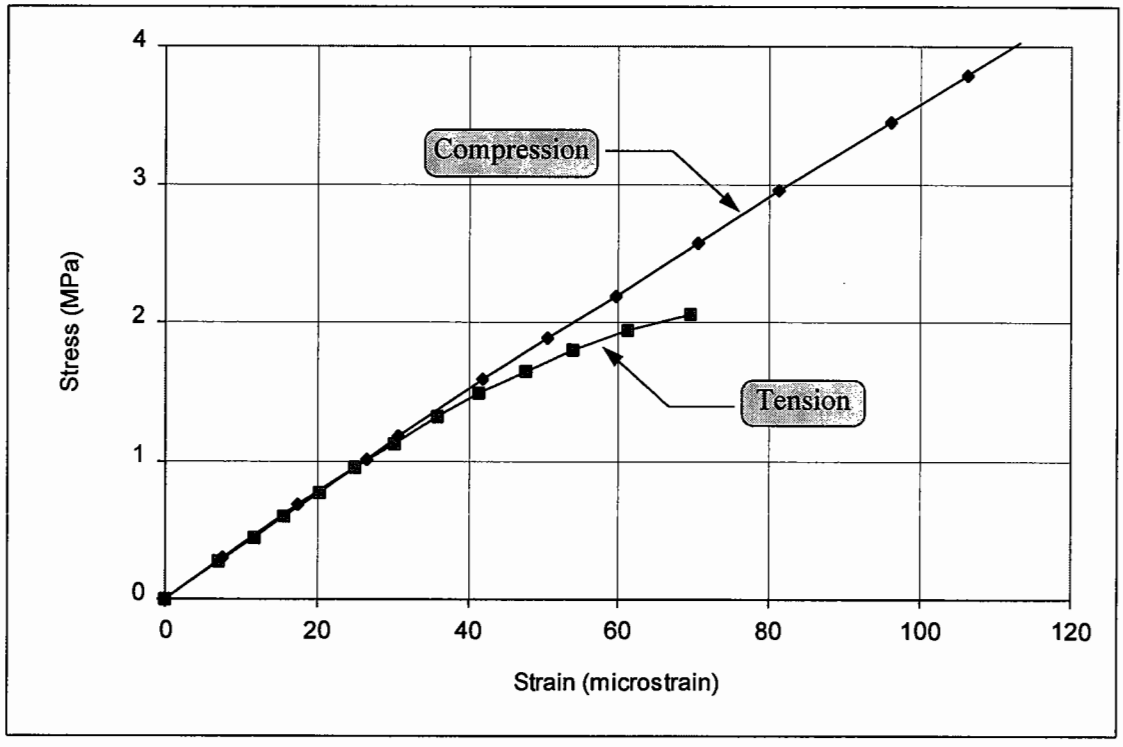

Figure 6.2. Stress strain relationships for a non-reinforced CBM5 tensile specimen subjected to direct tension and compression.

6.4.4 Load Deformation Relationship

The full load versus deformation relationships for SFR and non-reinforced CBM5 were obtained by indirect tensile testing of cylindrical specimens (150 mm × 150 mm diameter). This test has been in use to assess pavement materials for many years [Yoder and Witczak, 1975], and is generally applicable [Nanni, 1988] to obtain the functional parameters, used for evaluating the performance of SFR CBMs, presently derived from the conventional flexural test.

The preparation of specimens for testing was quite simple. On each end of the specimen, two mutually perpendicular axes were marked and a LVDT was attached, along the horizontal axis, over a 90 mm gauge length at the middle (Figures 6.3 and 6.4). For testing, the specimen was centrally placed in the testing machine via a frame, so that the LVDTs on both ends were horizontal (Figure 6.5).

Testing of specimens and recording of data were controlled automatically through a computer. The load rate was set at 0.033 N/mm^2 per second [BS 1881: Part 117: 1983]. After two preloading cycles of up to 0.57 N/mm^2, the test was continued for the SFR CBM5 specimens until an average deformation of 5 mm was obtained. For non-reinforced CBM5, however, the test was stopped when the specimen failed at its ultimate strength.

The load deformation relationships for non-reinforced CBM5 specimens, shown in Figure 6.6, are linear nearly up to failure. A typical average magnitude of the ultimate load reached by the CBM5 specimens, under indirect tension, is 96 kN (a stress of 2.72 N/mm^2), corresponding to an approximate deformation of 12 microns. The rate of increase in deformation is absolutely constant up to a load level of 90 kN. This seems to be the starting point for microcracks which gradually increase in width on further loading and ultimately lead to major cracks [ACI Committee 544.1R, 1982], thus causing failure of the specimen.

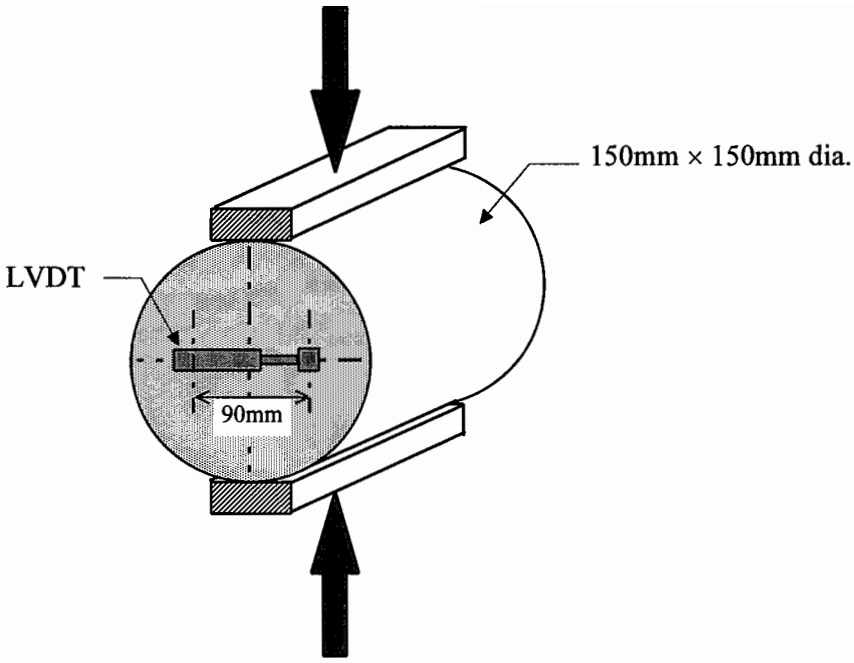

Figure 6.3. Load versus deformation test arrangement

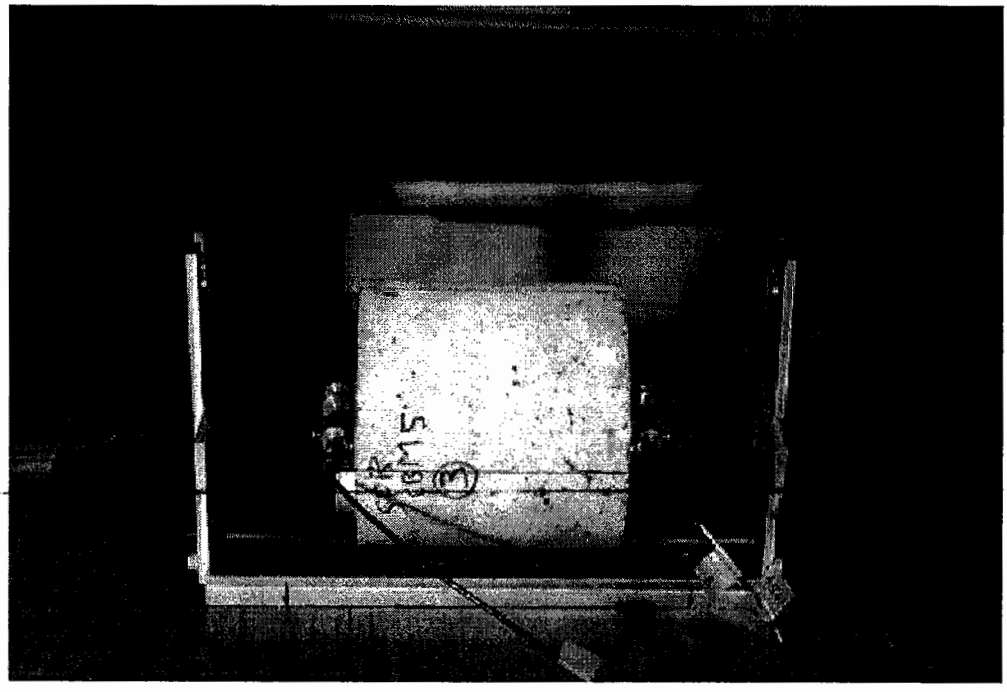

Figure 6.4. Instrumentation of specimen

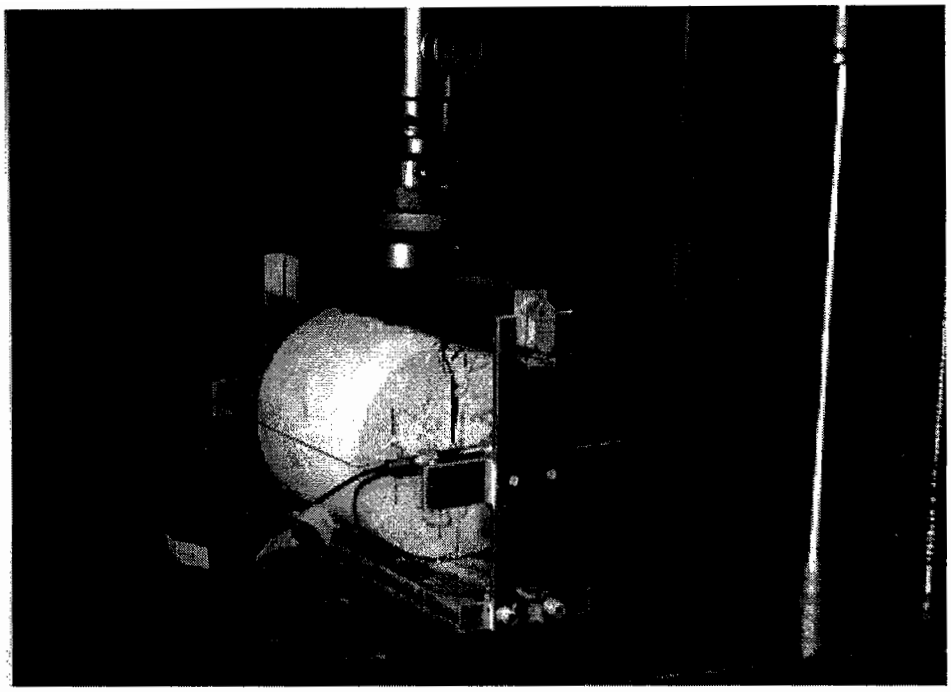

Figure 6.5. Testing of fibre reinforced CBM5 specimen

The failure mechanism is interestingly different in the case of steel fibre reinforced CBM5, for which the load deformation curves (Figure 6.7) are practically linear up to a load level of 100 kN. From this point, the rate of deformation gradually increases, on further loading, till the specimen attains its maximum strength. Unlike the case of a non-reinforced CBM, the SFR CBM does not fail at first cracking and is still capable of withstanding a considerable magnitude of load while it undergoes a significant deformation (refer Figure 6.5). This type of failure mechanism is a typical characteristic of SFR CBM and represents a substantial increase in toughness. This mechanism is also indicative of the fictitious ductility [Nanni and Johari, 1989] of the SFR CBM specimens.

Relating to the performance of a SFR CBM pavement, two important parameters can be derived from Figure 6.8 (which is an enlarged scale version of Figure 6.7 up to 1000 microns):

- The stress level at which the load deformation curve becomes non-linear, is defined as "First Crack Strength", sometimes referred to as the elastic limit [ACI Committee 544.1R, 1982] of the SFR CBM composite, based on the assumption that both the CBM and the steel fibres behave elastically up to this load. This is approximately equivalent to the tensile strength of unreinforced CBM.
- The highest point in the load deformation relationship is termed the "Ultimate Strength" of the SFR CBM, and is strongly dependent upon the fibre performance [Nanni, 1988].

This confirms that the first crack strength is not significantly influenced by the fibre reinforcement [Nanni, 1988]. Therefore, it can be concluded that the first crack strength of the SFR CBM (Figure 6.8) is almost equal to the failure strength of a non-reinforced CBM (Figure 6.6). The ultimate strength of the SFR CBM is increased by typically 38% due to the fibre reinforcement.

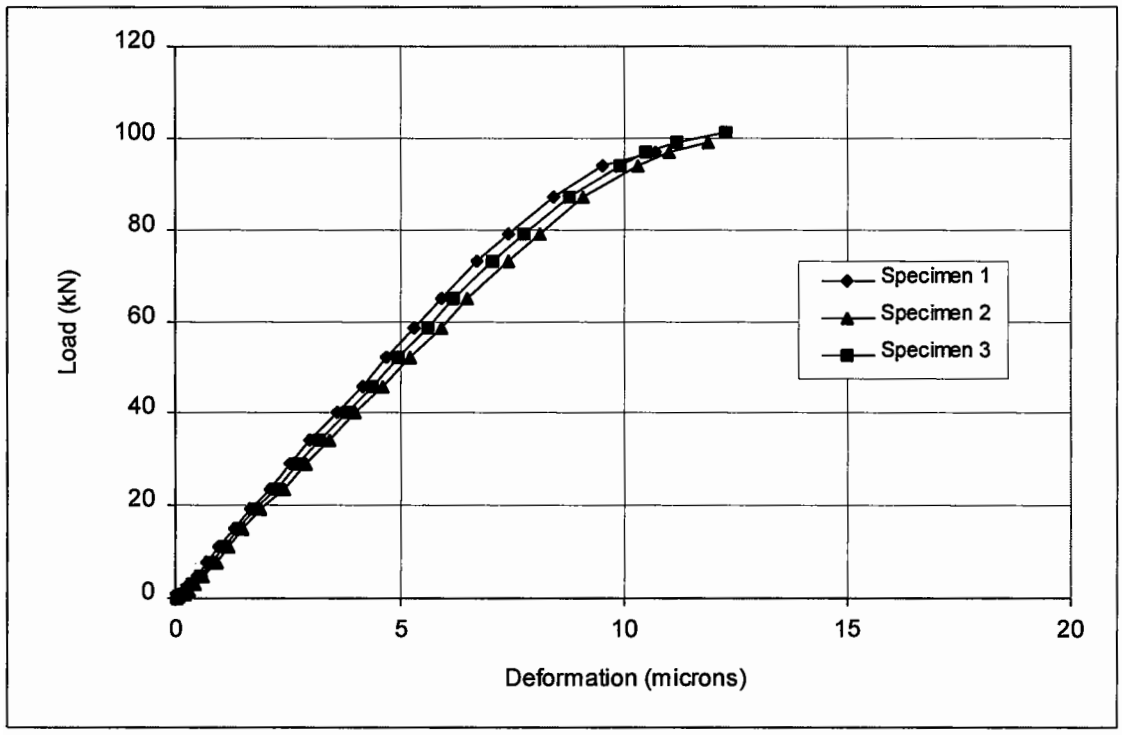

Figure 6.6. Load deformation relationships for non-reinforced CBM5 specimens.

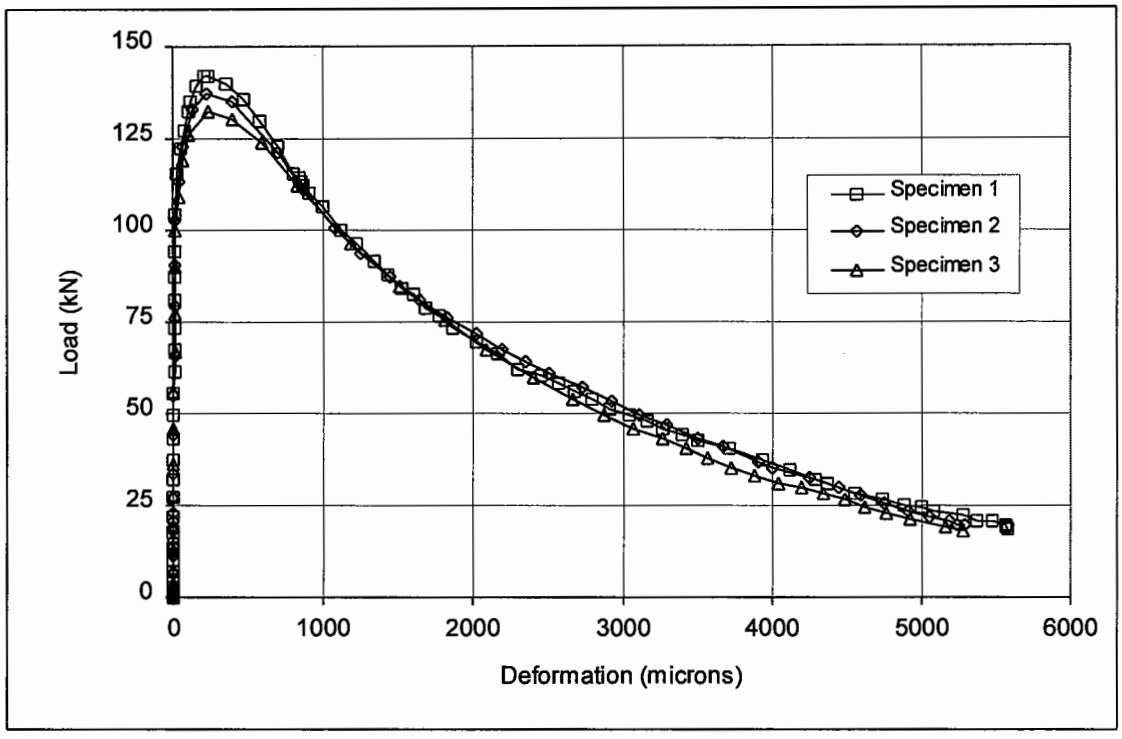

Figure 6.7. Typical load deformation relationships for steel fibre reinforced CBM5 specimens.

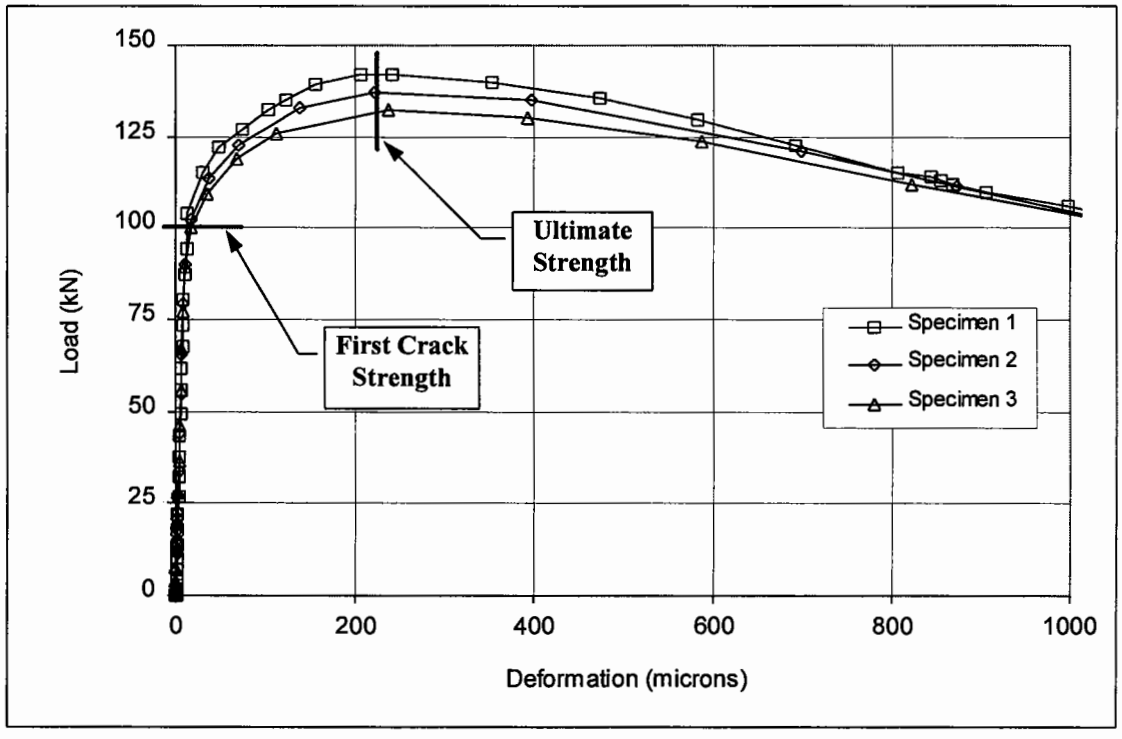

Figure 6.8. Load deformation relationships for steel fibre reinforced CBM5 specimens.

6.4.5 Toughness

Toughness is an important parameter in evaluating the performance of steel fibre reinforcement in CBMs. It is a measure of the energy absorption capacity of a material and is used in characterizing the material's ability to resist fracture when subjected to static, dynamic or impact loads [ACI Committee 544.2R, 1988]. Toughness is measured by the area under the load deformation curve. By roughly comparing the areas under the load deformation curves, in Figures 6.6 and 6.7, it can be seen that the toughness of a non-reinforced CBM is almost negligible compared to that of a SFR CBM, in which case the very large amount of energy is absorbed in debonding (see Figure 6.9) and stretching of the steel fibres [ACI Committee 544.1R, 1982]. Thus, with the inclusion of steel fibres, a composite material with pronounced post-cracking pseudo-ductility [Williams, 1986; Nanni and Johari, 1989] can be produced, which is expected to demonstrate improved fatigue response [Nanni, 1992].

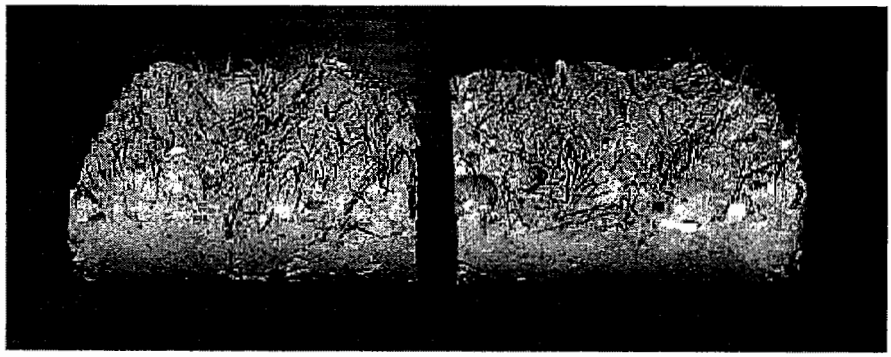

Figure 6.9. Steel fibres bonded in a gravel sand CBM5 mix

6.4.6 Post Cracking Behaviour

This is one of the most important aspects affecting pavement life. Figures 6.6 to 6.8 illustrate the greatly increased toughness of SFR CBM compared to unreinforced, which may be expected to inhibit crack propagation rates, although this has not been investigated here. However, of key significance is the load transfer across a crack, and that has been tested directly by running a wheel over slabs of precracked, SFR and

non-reinforced CBM5. The slabs were bedded on 60 mm sand, overlying a thin rubber mat, simulating a subgrade soil. The applied wheel load was 5 kN, and the test is considered to represent a one third scale pavement. The test system is described in detail in Chapter 7.

Some of the results, closely related with this chapter, are presented in Figure 6.10 in terms of the maximum differential vertical movement across the crack as the wheel passes, which illustrate that a very considerable improvement in load transfer and reduction in deterioration rate can be achieved by steel fibre reinforcement.

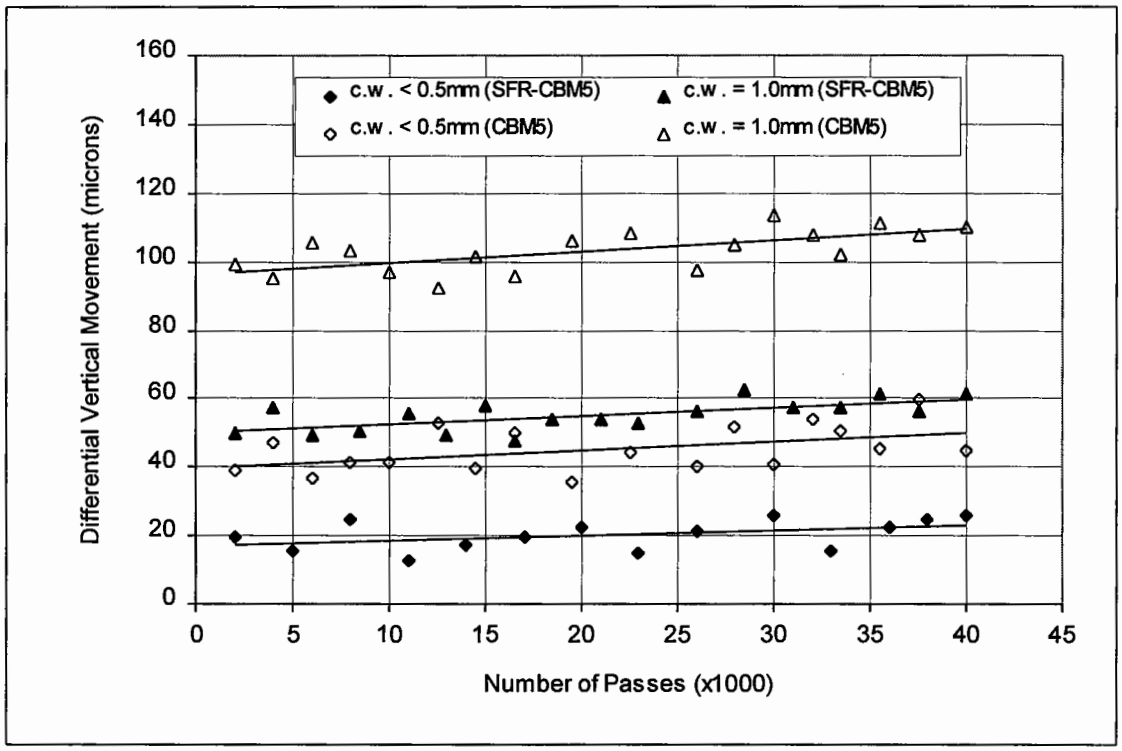

Figure 6.10. Load transfer across cracks induced in SFR and unreinforced gravel sand CBM5 slabs subjected to traffic (c.w. stands for crack width)

6.5 PRACTICAL SIGNIFICANCE

In practice, all cement bound bases suffer from transverse primary cracking, controlled or uncontrolled, at an early stage after their construction. The width of these cracks is of critical importance, because aggregate interlock, which is greatly influenced by crack width [Bondt and Saathof, 1993], plays an important role in the structural performance [Scarpas et al, 1993] of a pavement under trafficking. Although presented in Chapter 7, a recent series of slab tests with different crack widths has clearly shown that the greater the crack width, the higher the differential vertical movement, implying reduced load transfer (see Figure 6.10). The expected practical consequence of the reduced load transfer is increased reflective cracking.

Steel fibre reinforcement in CBMs is expected to be of great help in keeping the crack width to a minimum. First crack strength, which is almost equal to the failure strength of a non-reinforced CBM, corresponds to the beginning of cracking in the SFR CBM. It is in the form of microcracks, which can hardly be visually detected at this stage, and is only deduced from the load deformation relationship (Figure 6.8). Further loading has been observed gradually to increase crack widths but as stresses increase, only a slight increase in crack width would logically be expected before another crack is generated elsewhere in the layer. The result should be several very narrow cracks with almost no loss of load transfer at each. This expectation will be thoroughly investigated in a project which has now started at the University of Nottingham.

Steel fibre reinforcement also contributes directly towards the durability of a CBM base by increasing the shear resistance of cracks, because it is generated both by aggregate interlock and fibre reinforcement [Holmgren, 1985]. Its increased tensile strength would also directly improve resistance to longitudinal crack development.

Further slab tests (reported in detail in Chapter 7) have proved that a smaller crack width, leading to reduced differential vertical movement at cracks [Shahid, 1996; Bondt and Saathof, 1993], effectively delays crack propagation through an overlying bituminous layer. Since the cracks in the SFR CBM base are likely to be of an

extremely small width, but have a high shear capacity, they will not permit excessive differential vertical movement, and the improved crack control and fibre micro-dowel action across the cracks will enhance load transfer capacity [Nanni and Johari, 1989]. Therefore, the risk of reflective cracking should be substantially reduced and there is the possibility of using reduced thicknesses of bituminous surfacing and CBM base in the design of composite pavements.

6.6 CONTINUATION OF RESEARCH

Based on the recommendations made in PGR 96016 [Shahid et al, 1996], a research proposal, dated: 04 February 1997, was sent to EPSRC (Engineering and Physical Sciences Research Council) to support further research on SFR CBMs. With the consent of the Highways Agency (UK Department of Transport), a three year research project has been awarded to the University of Nottingham, which has been started from September 1997. This project will have a significant input and collaboration from: Bekaert S.A. (Belgian based fibre manufacturer) and Bekaert Building Products (in the UK), Sitebatch (Contracting) Ltd., Scott Wilson Pavement Engineering Ltd., and the Highways Agency. The project will include a detailed study into the effects of various fibre contents, with different aspect ratios, upon the performance characteristics of SFR CBMs comprising different aggregate types and gradings. Full scale site trials are also included in the research programme to look at the practical aspects.

6.7 CONCLUSIONS

The following conclusions have been drawn based on this research:

- Steel fibre reinforcement at 1% by volume causes an increase of 33% in the direct tensile strength of cement bound materials. In contrast, the cube compressive strength is negligibly affected, but the cylinder compressive strength is increased by 12%.
- The magnitudes of elastic stiffness, under direct tension and compression, are equal and unaffected by fibre reinforcement.
- The "first crack strength" corresponds to the onset of cracking in SFR CBM. The "ultimate strength" for a CBM5 having 1% steel fibre content, from indirect tensile testing, is typically 38% greater.
- The cracks in a SFR CBM base are initially observed to be of negligible width. The expected insitu results, following material shrinkage, is a relatively large number of tightly closed cracks.
- Steel fibre reinforcement may prevent reflective cracking in flexible composite pavements, because crack propagation through a bituminous surfacing has been shown to be dependent upon the degree of relative movement at cracks in the CBM base which, in the case of SFR CBM, is restricted both by their small width and increased shear resistance imparted by the fibres.
- The increased tensile strength of the SFR CBMs can provide extra safety against longitudinal cracking.
- Steel fibre reinforcement in CBM bases has the potential of introducing an economic and durable structural design, for flexible composite pavements, by minimizing the thicknesses of bituminous surfacing as well as the CBM base.

Load Transfer Investigation of Cracks in CBM Bases

7.1 INTRODUCTION

Recent research has led to several advances in pavement materials and methods in the field of flexible composite pavements. Two of these are controlled cracking of cement bound bases and steel fibre reinforced cement bound bases, described in Chapters 5 and 6, respectively. The effectiveness of controlled cracking systems, in the early years following construction, has been proved to be satisfactory in several countries [Shahid and Thom, 1996a and 1996b; Jofre et al, 1996], but the long term performance of this technique is still unknown. The current DBFO (Design Build Finance and Operate) project at the A1(M) Alconbury to Peterborough is one of those making use of this technique and for which data relating to long term performance could be highly beneficial. Likewise, although the laboratory investigation into the mechanical properties has clearly indicated benefits associated with steel fibre reinforced CBM bases, these remain qualitative and do not provide confidence about the long term performance.

In order to translate the benefits of these techniques (controlled cracking and steel fibre reinforcement in CBM bases) into pavement life predictions, a new laboratory test system has been developed and used, in this study, for assessing long term performance of the two methods. This is aimed at investigating the load transfer characteristics of a crack, induced in a CBM base, under traffic. The load transfer has been shown to be dependent on aggregate interlock, a function of the crack width [Bondt and Saathof, 1993], and is likely to be affected by the physical properties of aggregate, CBM thickness, and CBM strength.

Model pavement (scaled down pavement) tests have been performed, on CBM slabs subjected to repeated applications of a stress representative of the traffic on a real road, to characterize the performance of different categories of CBM, comprising two

different aggregates, with varying crack width. This study was intended to establish relationships between load transfer, crack width and CBM strength. A limited number of tests was also performed to investigate the influence of these parameters upon the rate of propagation of a crack in a CBM base into a bituminous surfacing.

7.2 DESCRIPTION OF CBM SLABS

Several slabs, each with dimensions 1100×900×80 mm, were prepared from different categories of CBM comprising uncrushed gravel sand and crushed limestone aggregate. Some of the slabs were prepared from steel fibre reinforced CBM5 (with gravel sand and limestone aggregate) to determine the influence of the steel fibre reinforcement upon the load transfer performance of a crack. A description of the CBMs, used for making slabs, is as follows:

1. Gravel sand CBM3
2. Gravel sand CBM4
3. Gravel sand CBM5
4. Steel fibre reinforced (SFR) gravel sand CBM5

5. Limestone CBM3
6. Limestone CBM4
7. Limestone CBM5
8. Steel fibre reinforced (SFR) limestone CBM5

Both materials (gravel sand and limestone) used for this study are the same as discussed in Chapter 2, with gradings shown in Figures 2.5 and 2.6. Mix design for CBMs involving these materials is described in Section 2.4. In the case of SFR CBM slabs, Dramix steel fibres having a hook-ended shape were used with a fibre content of 1.0% by volume. For reasons of availability of fibres, Dramix ZP 30/0.5 (30mm length) steel fibres were used in the SFR gravel sand CBM5 slab, whereas Dramix ZC 60/0.8 (60mm length) were used in the SFR limestone CBM5 slab, although this change of the fibre size was not desirable from the view point of making a comparison between the performance of CBM5 comprising two types of aggregate.

7.3 PREPARATION OF CBM SLABS

Slabs were prepared by using a pedestrian type vibrating roller. For this purpose, a rigid (steel) frame mould with inside dimensions of 1100×900×80 mm, shown in Figure 7.1, was used, which was constructed from four pieces of mild steel (MS) 80×38×6 mm channel section. The mould was assembled and placed over a smooth waterproof (visaform) sheet which was placed on even ground. A metal strip (1000×20×3 mm) was used to act as a crack inducer. This strip was placed transversely at the middle of the mould by sliding through slots provided in the longer sides of the mould.

The quantity of the CBM mix required for each slab was calculated from the mould volume and the target CBM density. Mixing of the ingredients was performed in one batch, and the entire bulk of the CBM mix was placed into the mould. The surface was levelled, and compaction was started with passes of a static roller, followed by the addition of vibrations.

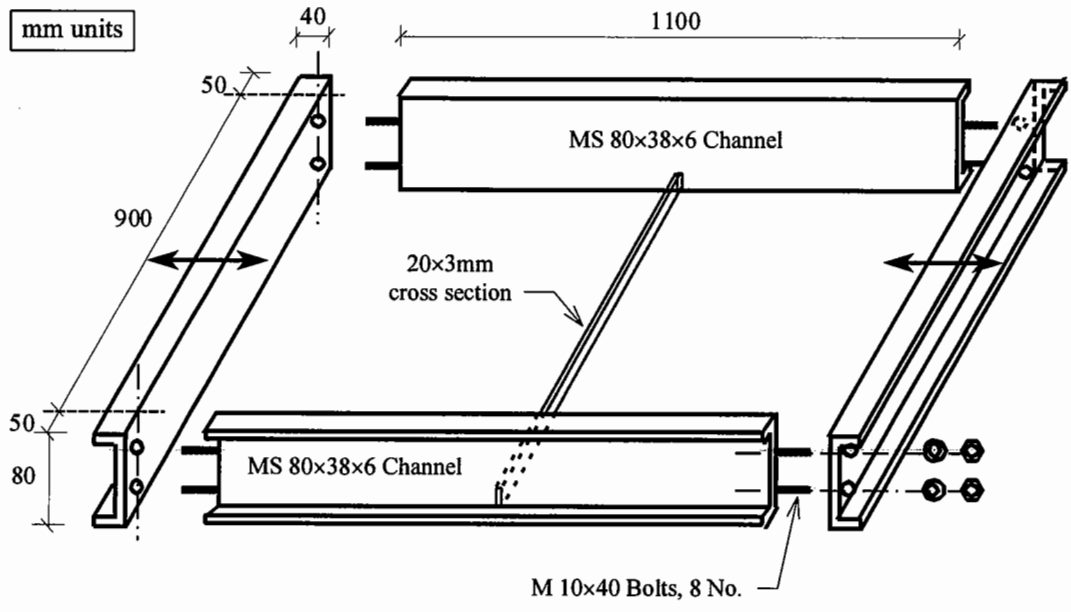

Figure 7.1. Steel frame mould used for casting of CBM slab

Finally, compaction was stopped with a few static roller passes when the required thickness of the slab (surface level with the top edges of the mould) was achieved. The slab was properly covered with a ploye thylene sheet. After 24 hours, the mould was removed and the slab was cured for 28 days before testing. During the curing period, the slab was kept covered with wet matting and further covered with ploye thylene sheet.

After the curing period, the slab was lifted up and positioned over two thin wooden pieces (900×200×18 mm) placed transversely, underneath the slab and on either side of the crack inducing slot, with a sufficient gap (400 mm) in between. Inside this gap, a sheet of hardboard (900×300×8 mm) was inserted. Now another piece of solid wood (900×90×90 mm) was placed transversely over the slab, such that the crack inducing slot, at the bottom of slab, was right underneath. An impact force was applied at the centre of this wooden piece to crack the slab along the slot. The hardboard (900×300×8 mm), underneath the slot, helped to provide a damping surface to secure the crack faces from damage. By using this procedure, a crack with uneven and natural faces (Figure 7.2) was successfully induced in each slab.

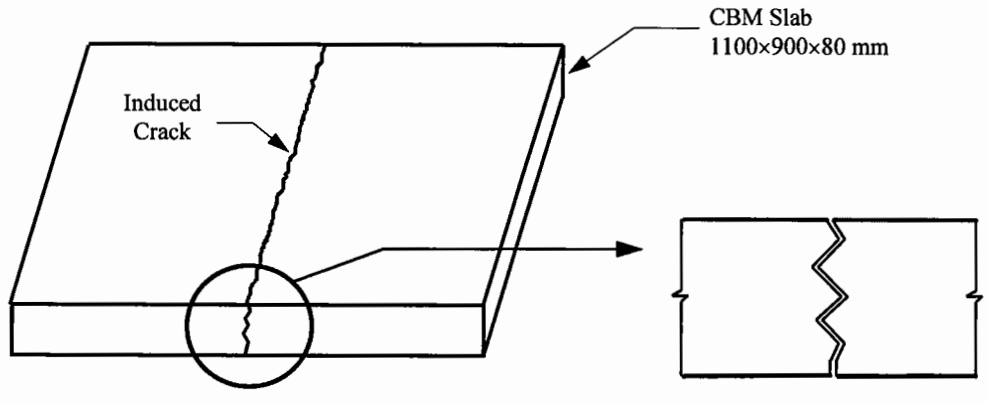

Figure 7.2. CBM slab with an induced crack

7.4 TESTING EQUIPMENT

The investigation of load transfer was based on the measurement of differential vertical movement across the faces of a crack induced, in a CBM slab, perpendicular to the direction of traffic. For this purpose, an equipment known as the 'slab test facility' was used (Figure 7.3). This equipment was originally developed to investigate the performance of grid reinforcement in asphalt pavements [Brown et al, 1985], and was found suitable for accelerated testing of model pavements on an experimental bases. The slab test facility is an electrically controlled apparatus that uses a hydraulic supply to apply pressure through a pneumatic tyred wheel (0.46m diameter), which runs over a CBM slab. A description of the working principle of this apparatus is given in Report No. 3 on "grid reinforcement for asphalt pavements" [Brown et al, June 1985]. The maximum load capacity of this machine is limited to 5.0 kN, and the test conditions are inevitably slightly different from those of a real pavement structure, but it can still be used to obtain sufficiently accurate and meaningful results.

The test system in the laboratory was a model pavement structure, approximately on 1/3 scale (Figure 7.5), designed through a computer programme based on multilayer linear elastic analysis to produce stress conditions in the CBM slab similar to those of a 200 mm CBM base subjected to a 40 kN standard wheel load in the real case.

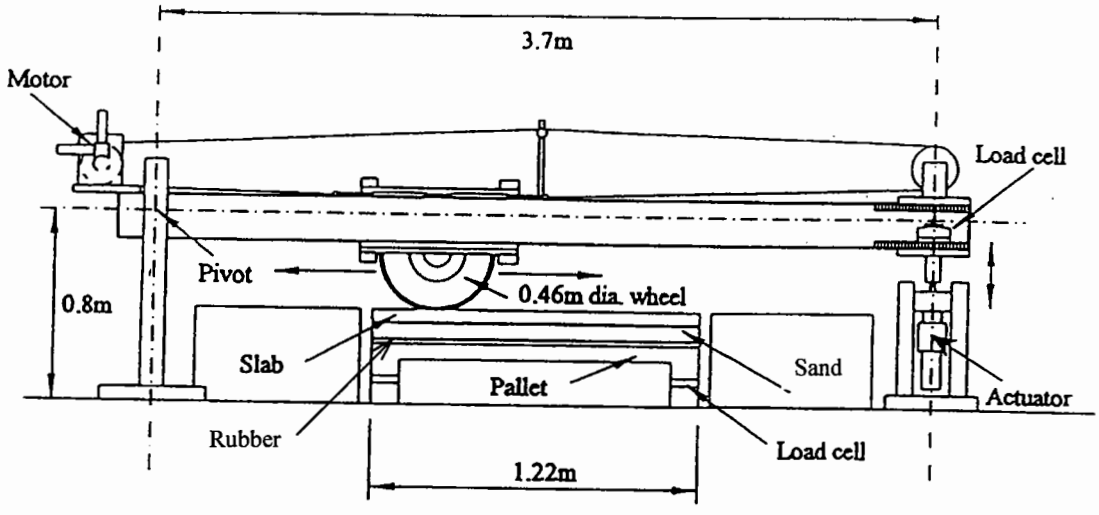

Figure 7.3. Slab Test Facility

7.5 TESTING PROCEDURE

The rigid frame, used as a mould, was re-assembled in such a way that the inside dimensions became 1100×910×80 mm. Vertical extensions were provided to the shorter sides (910 mm long) of the frame by rigidly fixing MS 50×60×6 mm angles as shown in Figure 7.4a. These (shorter) sides were intended to provide smooth vertical faces, and were used as restraints against the longitudinal displacement of the slab ends during trafficking.

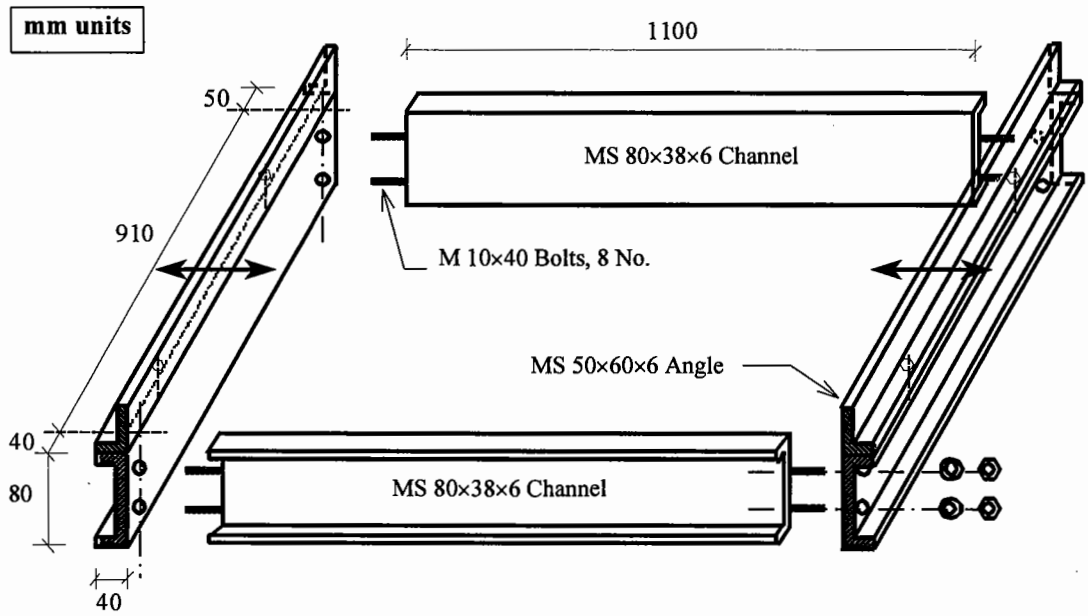

Figure 7.4a. Rigid (steel) frame assembly used for holding a CBM slab during testing

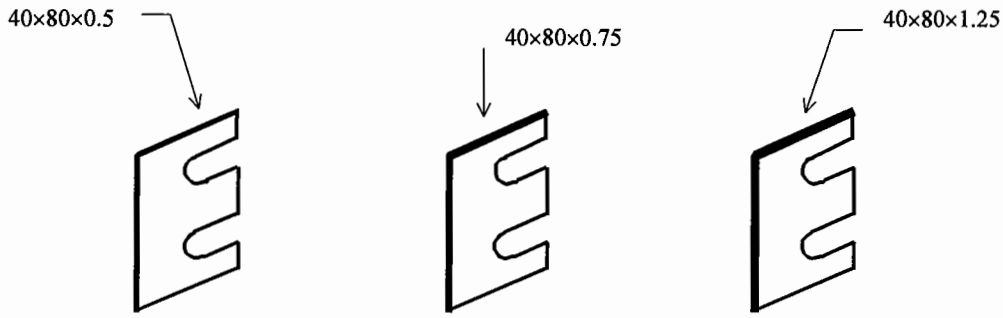

Figure 7.4b. Shape and size of steel plates (to be inserted into the frame joints) used to control different crack widths.

The frame was placed on a steel pallet (Figure 7.5). The longer sides (1100 mm) of the frame were clamped to the pallet, whereas the shorter ones were kept unclamped and adjustable through 10×40mm bolts, such that they could be moved in and out, as illustrated in Figure 7.4a.

The experimental setup for the model pavement structure is shown in Figure 7.5. The slab were bedded on 60 mm sand, overlying a thin rubber mat, simulating a subgrade soil. The longer side ends of slab were kept unrestrained, because the difference between the frame width (910 mm) and slab width (900 mm) provided a 5mm clearance along both (longer) sides of the slab. This clearance was intended to allow free vertical movement at the crack under trafficking. The shorter ends of the slab, in contact with the frame, were further provided with MS 40×40×4 mm angles to stop excessive vertical movement of the slab ends. These angles were positioned inverted over the slab ends via 1.5mm thick rubber seats, and were fixed to the frame through long vertical bolts (8×90mm).

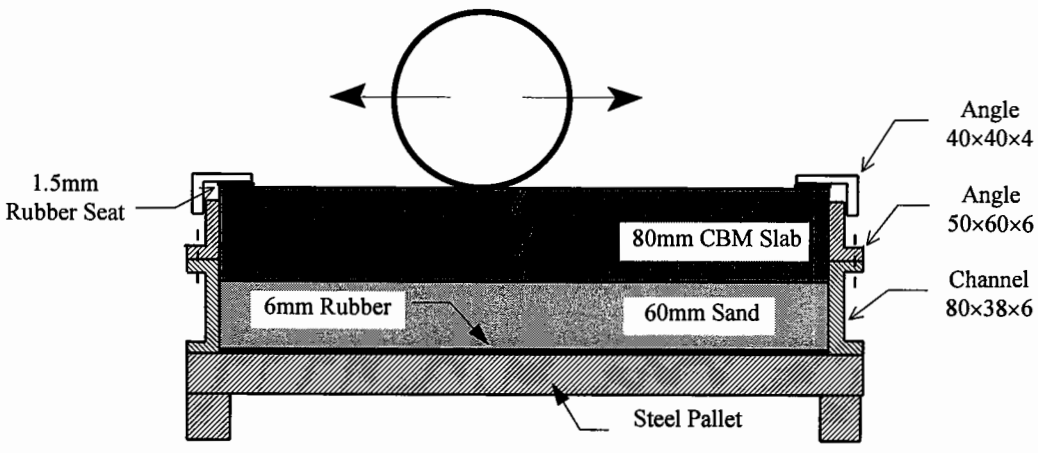

Figure 7.5. Model Pavement Structure

The load transfer investigation was carried out in the following four stages corresponding to four different widths of the induced crack. The crack width is defined as the average opening of a crack.

- Stage 1: Crack width ≤ 0.5 mm
- Stage 2: Crack width ≅ 1.0 mm
- Stage 3: Crack width ≅ 1.5 mm
- Stage 4: Crack width ≅ 2.5 mm

During each stage, the crack width was kept constant and the slab was subjected to 40,000 wheel passes (approximately). The reciprocating motion of the 5 kN loading wheel was set, at a speed of 40 passes per minute, to cover the central 900 mm length along the centreline of slab, such that there was a 100 mm clear space on either end of the wheel-track length. The width of the wheel-track was 100 mm. All slabs were trafficked under similar test conditions.

The crack width was controlled by means of three sets of 40×76 mm steel plates with 0.5, 0.75 and 1.25mm thickness. Each set consisted of four plates of similar thickness. The shape of these plates is shown in Figure 7.4b. While increasing or decreasing the crack width, the inverted angles were first removed from the slab. To increase the crack width, say by 1.0 mm, the shorter frame sides (910 mm) were slightly moved out and the 0.5 mm (thick) steel plates were inserted into the four joints of the frame. The frame joints, containing the plates, were tightened back. The two halves of the (cracked) slab were then moved outwards to come in contact with the frame ends, thus generating an increased crack opening by 1.0 mm in the middle. The crack width remained unchanged as long as the position of shorter sides of the frame was not disturbed. The same procedure was repeated with other combinations of the metal plates to generate other crack widths (of 1.5 and 2.5 mm). Before the insertion of steel plates into the frame joints, or for the closed crack conditions, the crack width was assumed to be ≤ 0.5 mm.

7.6 INSTRUMENTATION AND RECORDING OF DATA

Under trafficking, the vertical deflections were measured on either side of the crack. For this purpose, two LVDTs 'A' and 'B' (Figure 7.6) were positioned vertically at an offset of 50 mm from the edge of the wheel-track, and were mounted on a rigid support which was kept independent of the CBM slab and wheel settings. A third LVDT 'C' was attached horizontally, across the crack, at the neutral axis depth on the side of the CBM slab. This LVDT was used to measure the horizontal crack movement due to traffic loading. All the LVDTs were calibrated with reference to the data acquisition system used.

Different positions of the wheel, along the track length, were calibrated against voltage. Three wheel positions, that is at left crack face, crack centre, and right crack face, were important in relation to the maximum deflections during testing. Left crack face refers to a position of the wheel just left of the crack, without any direct contact on the right side. Similarly, right crack face corresponds to a position when the entire wheel contact is just right of the crack. The respective values of voltage were recorded, so that any of the wheel positions could be accurately identified (or read) through the data acquisition system during the test.

As a starting point, zero readings of the LVDTs were recorded before the application of wheel load. During testing, the magnitude of applied wheel load and number of passes were monitored from the control system of the slab test facility. Readings of the vertical and horizontal deflections were taken at frequent intervals of traffic (or time). For both directions of the reciprocating wheel motion (leftward and rightward), deflections were measured corresponding to each of the three wheel positions (left crack face, crack centre, and right crack face).

The magnitudes of differential vertical deflection (or shear slip) were calculated, as the difference of readings from LVDTs 'A' and 'B', for each of the two wheel positions on either side of the crack, and the higher of the two values was selected for further analysis. In contrast, the reading of horizontal deflection (or crack opening),

recorded from LVDT 'C', was found to be maximum when the wheel position was right at the crack centre.

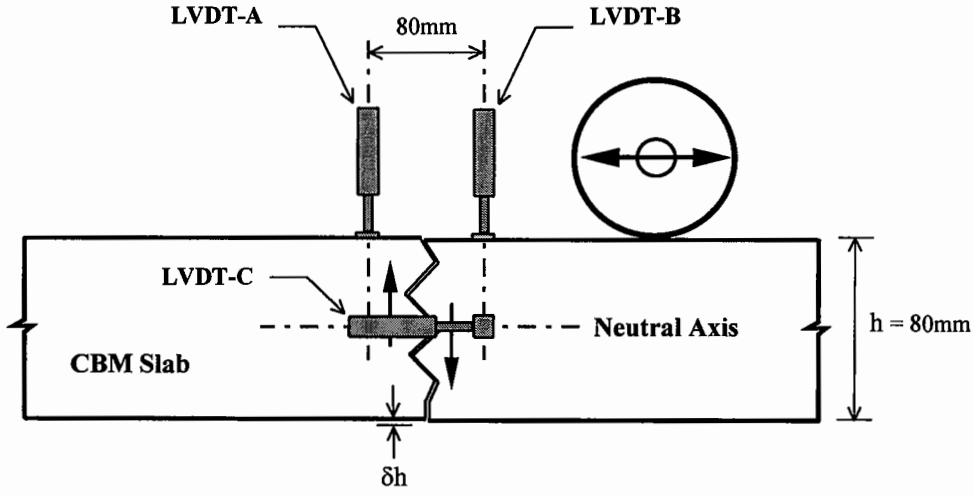

Figure 7.6. Instrumentation of CBM slab during testing

7.7 RESULTS AND DISCUSSION

7.7.1 General

The assessment of load transfer is based on the measurement of the magnitude of differential vertical movement across the induced crack under trafficking. In addition, horizontal movement of the crack under traffic loading was also measured. However, the effect of thermal action upon horizontal crack movement was not considered in this small scale laboratory study. Both the differential vertical and horizontal movements are related to load transfer performance [Bondt and Saathof, 1993] of a crack, induced naturally or artificially (by controlled cracking), and have been considered in this study to characterize different CBMs.

The effect of crack width upon load transfer (or differential vertical movement) of a crack is quite significant, and has been studied through FWD testing on a real CBM pavement in this work [Chapter 5, or Shahid et al, 1995; Shahid, 1996]. However, the long term performance of different widths of cracks, in CBM bases of different strengths, under repeated loading is unknown. It was hoped that the results of this investigation would provide this information. The model pavement system, in the laboratory, was designed to attain stress conditions similar to those in a real CBM base before it is overlaid by bituminous surfacing. During testing, the CBM slabs (with induced crack) were directly subjected to repeated load applications. The results from this investigation are given in the following sections.

7.7.2 Differential Vertical Movement Results

The results of differential vertical movement across a crack induced in the (uncrushed) gravel sand CBM3, CBM4, and CBM5 slabs are shown in Figures 7.7 to 7.9, respectively. Figure 7.10 shows the results for a SFR gravel sand CBM5. Each of these figures indicates a comparison of the values of differential vertical movement, for the respective CBM slab, at four different widths of the induced crack. For comparing load transfer properties of CBMs comprising two different aggregates, Figures 7.11 to 7.14 show the results of differential vertical movement across a crack

induced in the crushed limestone CBM3, CBM4, CBM5, and SFR limestone CBM5 slabs, respectively, tested under similar conditions to those for the gravel sand CBMs.

In general, Figures 7.7 to 7.14 demonstrate the following points:

- The magnitude of differential vertical movement (or shear slip) increases with an increase in crack width.

- Minimum differential vertical deflection and hence maximum load transfer is noticeable at a crack width ≤ 0.5 mm. Such a crack width is attainable through controlled cracking (discussed in Chapter 5).

- Overall, the differential vertical deflections are found to be higher in the case of gravel sand CBMs compared to limestone CBMs. This may be attributable to aggregate shape, which is round in the case of gravels, but angular for limestone aggregate.

- The effect of CBM strength upon differential vertical movement is very small from CBM3 to CBM4 (Figures 7.7 & 7.8, and 7.11 & 7.12), but slightly greater in the case of CBM5 (Figures 7.9 and 7.13) suggesting that an improvement in the load transfer may be expected at increased CBM strength.

- Steel fibre reinforcement has shown a positive effect in reducing the amount of differential vertical deflection, leading to a consequent increase in the load transfer by a significant amount compared to an unreinforced CBM. A comparison of Figure 7.10 with Figure 7.14 indicates that the performance of longer steel fibres (ZC 60/0.8) used in SFR limestone CBM5 is much superior to that of the shorter fibres (ZP 30/0.5) used in SFR gravel sand CBM5, even allowing for the difference between the aggregates.

7.7.3 Horizontal Crack Movement Results

This horizontal movement was, in fact, in the form of a wedge shaped opening of the crack, because the crack closes in the upper half and opens in the lower half of the

CBM base, due to downward deflection of the crack faces under traffic loading. The horizontal crack movement was therefore measured, as an average relative value, at the neutral axis depth of the CBM slab.

The results of horizontal crack movement for gravel sand CBM3, CBM4, and CBM5 slabs, are shown in Figures 7.15 to 7.17, respectively. Figure 7.18 shows the results for SFR gravel sand CBM5. Similarly, Figures 7.19 to 7.21 show the results of horizontal crack movement for crushed limestone CBM3, CBM4, and CBM5, respectively, and for SFR limestone CBM5 the results are shown in Figure 7.22. Each figure presents a comparison of the horizontal crack movements at four different crack widths.

From Figures 7.15 to 7.22, the following general points are clear:

- The magnitude of horizontal crack movement, under traffic loading, shows an increase with an increased crack width. Minimum horizontal movement is attained at crack width ≤ 0.5 mm.

- Figures 7.15 to 7.17 and 7.19 to 7.21, indicate that the effect of CBM strength upon horizontal crack movement is almost insignificant.

- Steel fibre reinforcement has led to a significant reduction in the horizontal crack movement (Figures 7.18 and 7.22). The shorter fibres (ZP 30/0.5) used in gravel sand CBM5 have shown satisfactory performance, that is with almost negligible deterioration, as long as the crack width is not more than 1.0 mm (Figure 7.18), within the traffic range tested. But for greater crack widths (1.5 and 2.5 mm), there is an increasing trend in the magnitude of horizontal movement, indicating some deterioration, possibly due to stretching or pulling out of the fibres. On the other hand, the longer fibres (ZC 60/0.8) used in limestone CBM5 have shown a considerably higher level of performance (Figure 7.22).

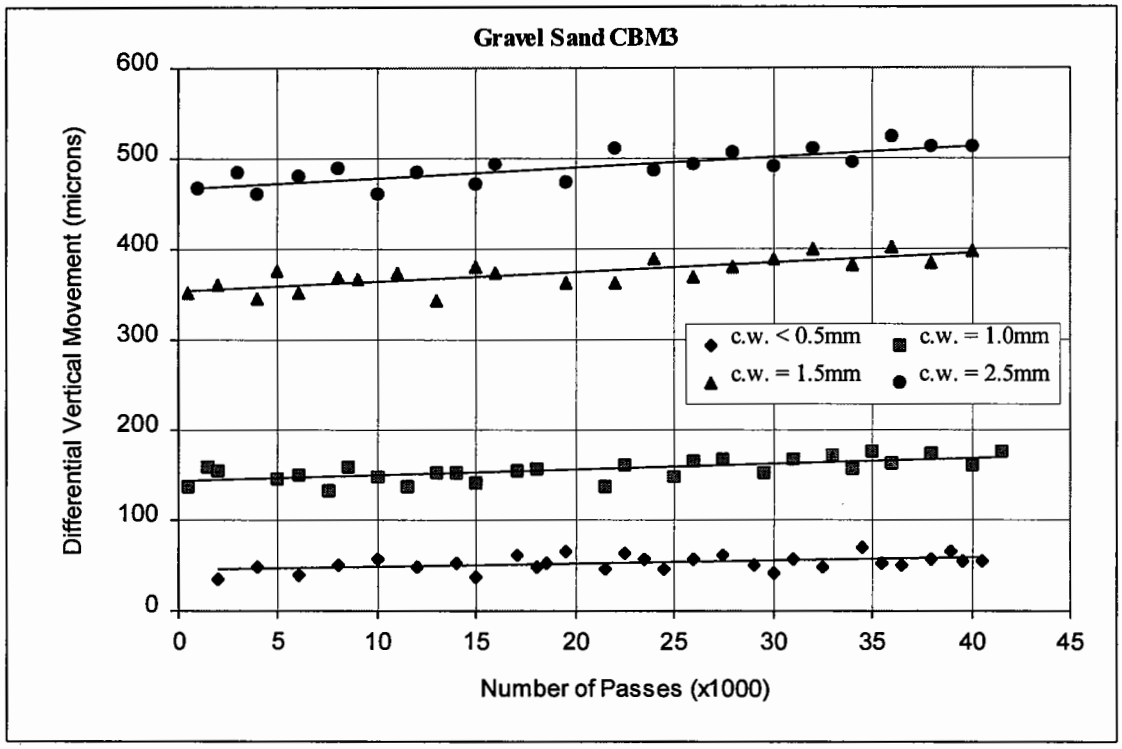

Figure 7.7. Differential vertical movement across different widths of a crack in a gravel sand CBM3 slab.

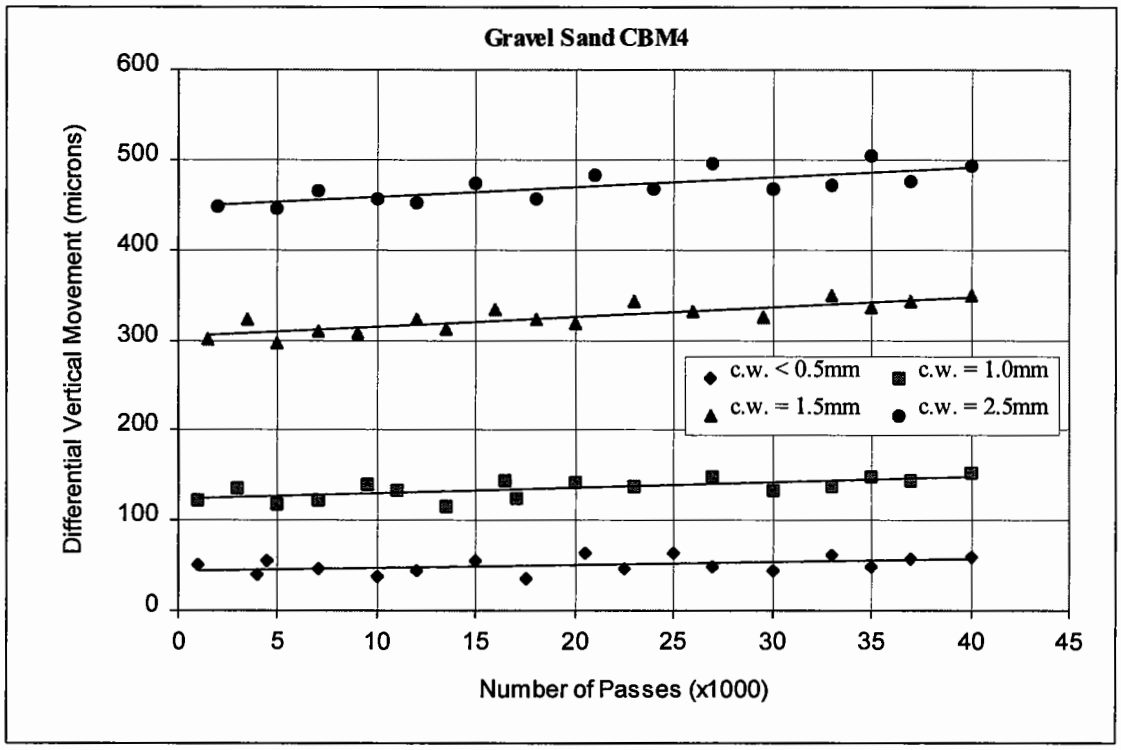

Figure 7.8. Differential vertical movement across different widths of a crack in a gravel sand CBM4 slab.

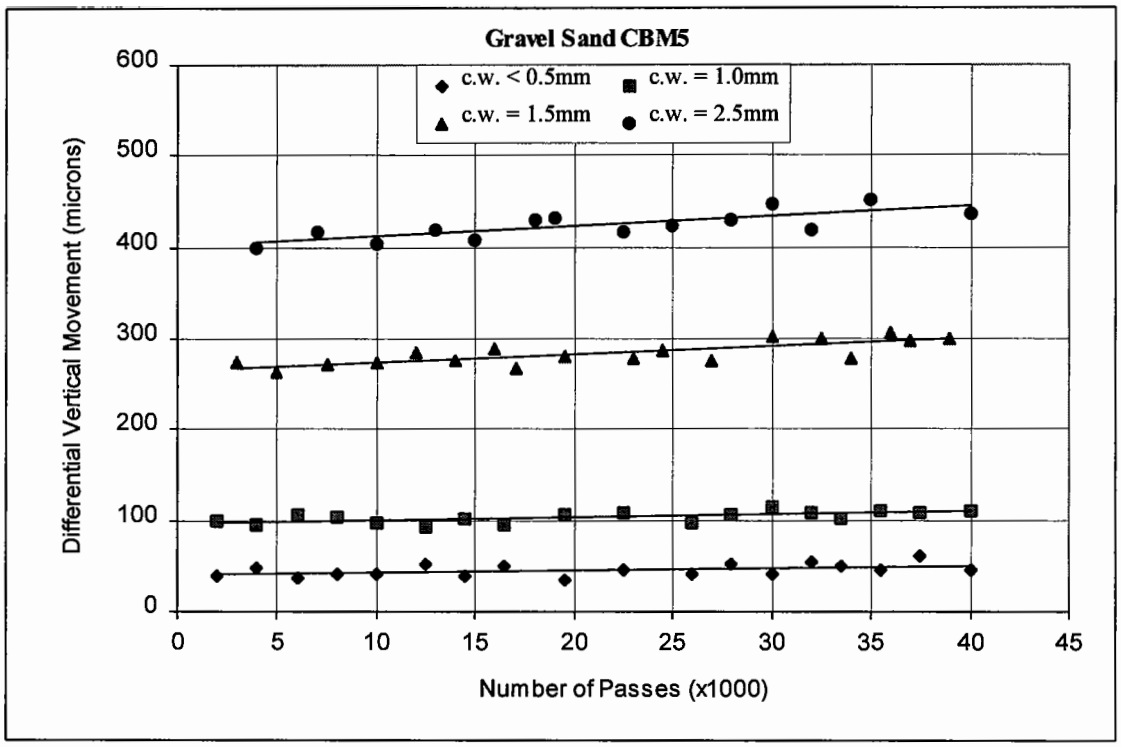

Figure 7.9. Differential vertical movement across different widths of a crack in a gravel sand CBM5 slab.

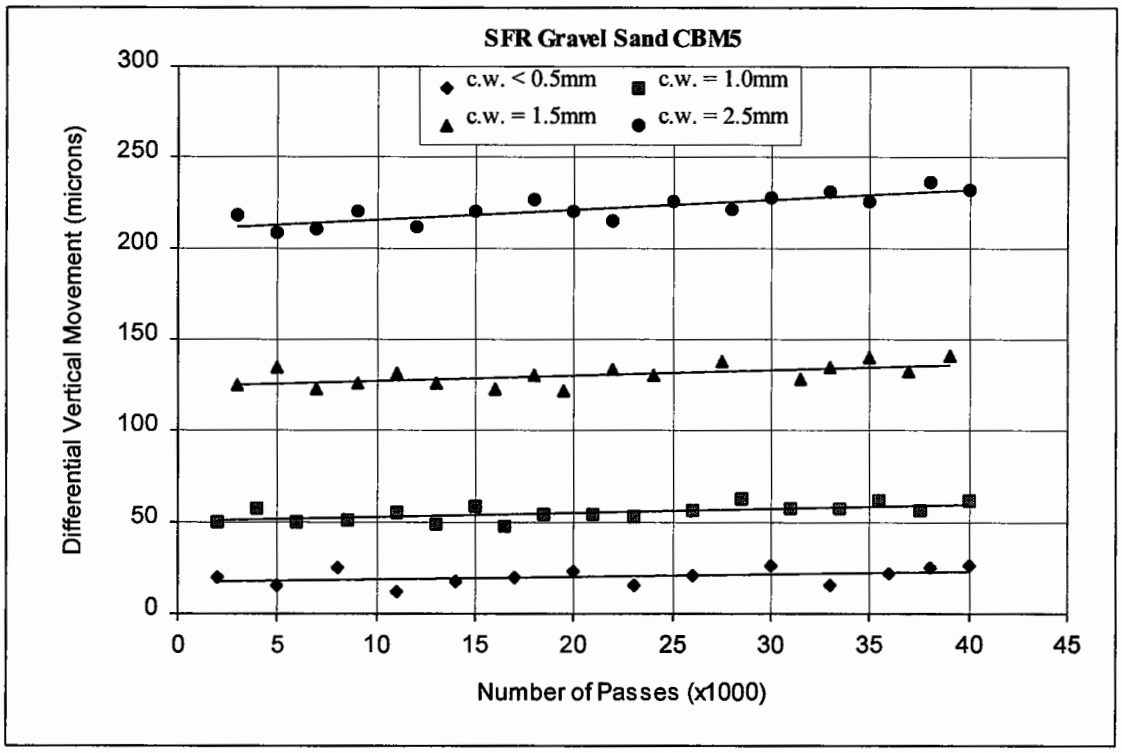

Figure 7.10. Differential vertical movement across different widths of a crack in a steel fibre reinforced gravel sand CBM5 slab.

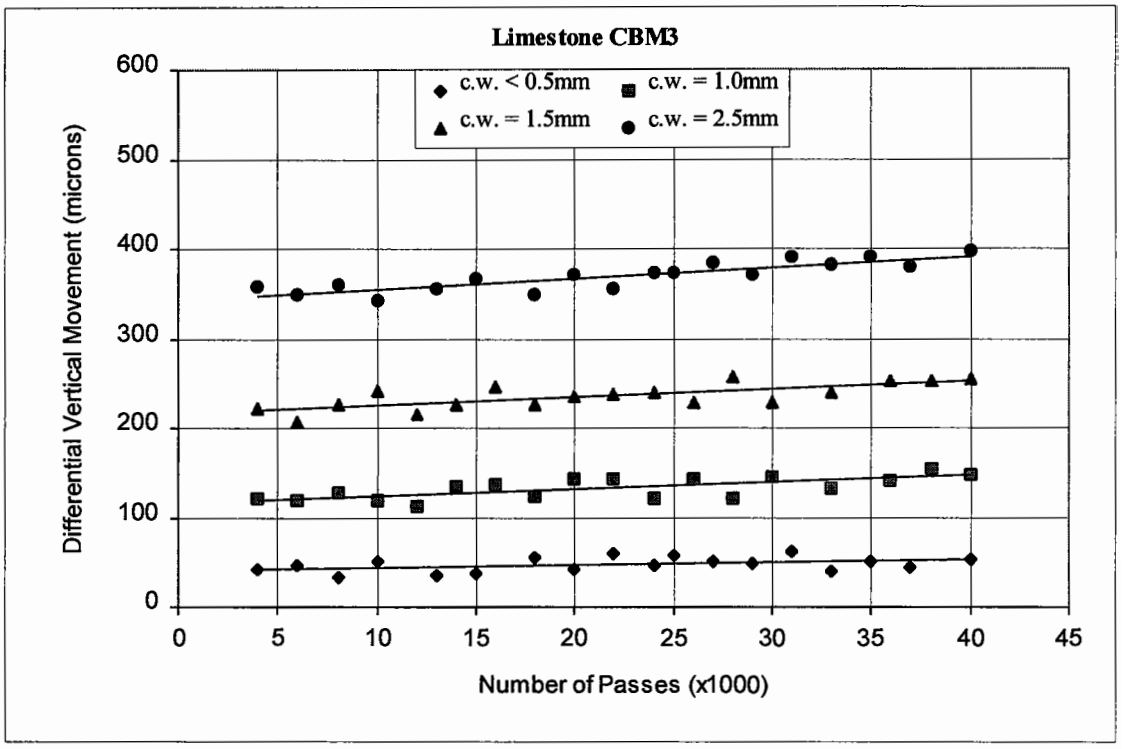

Figure 7.11. Differential vertical movement across different widths of a crack in a limestone CBM3 slab.

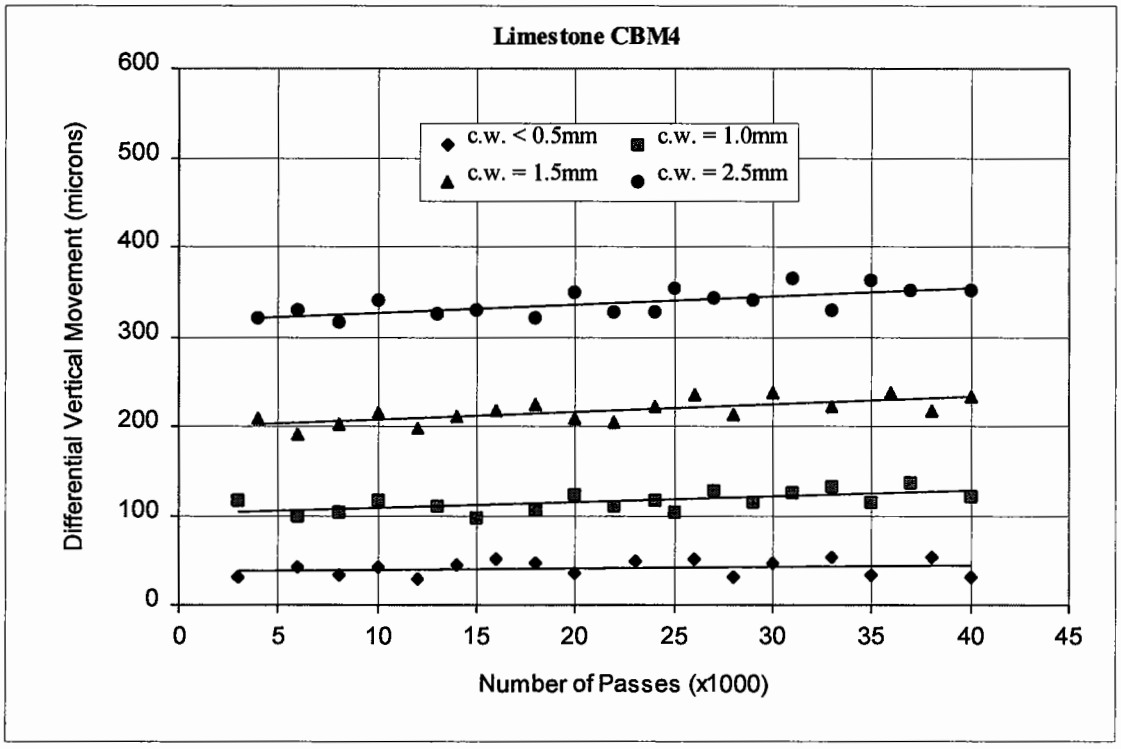

Figure 7.12. Differential vertical movement across different widths of a crack in a limestone CBM4 slab.

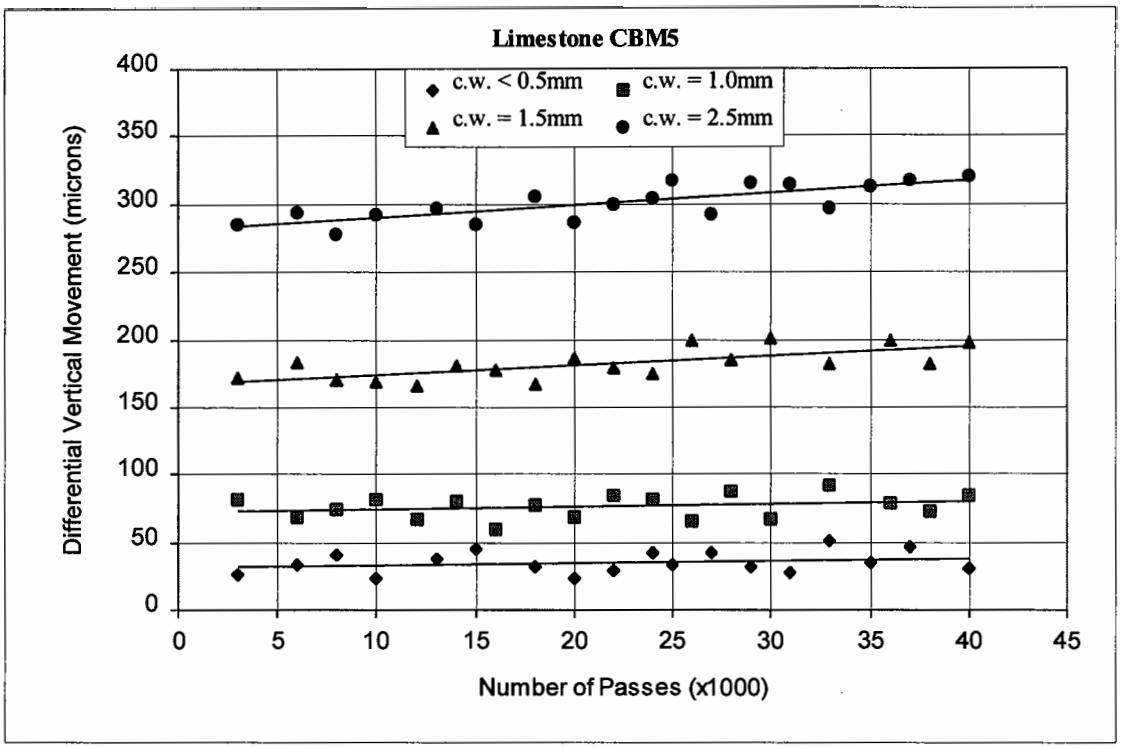

Figure 7.13. Differential vertical movement across different widths of a crack in a limestone CBM5 slab.

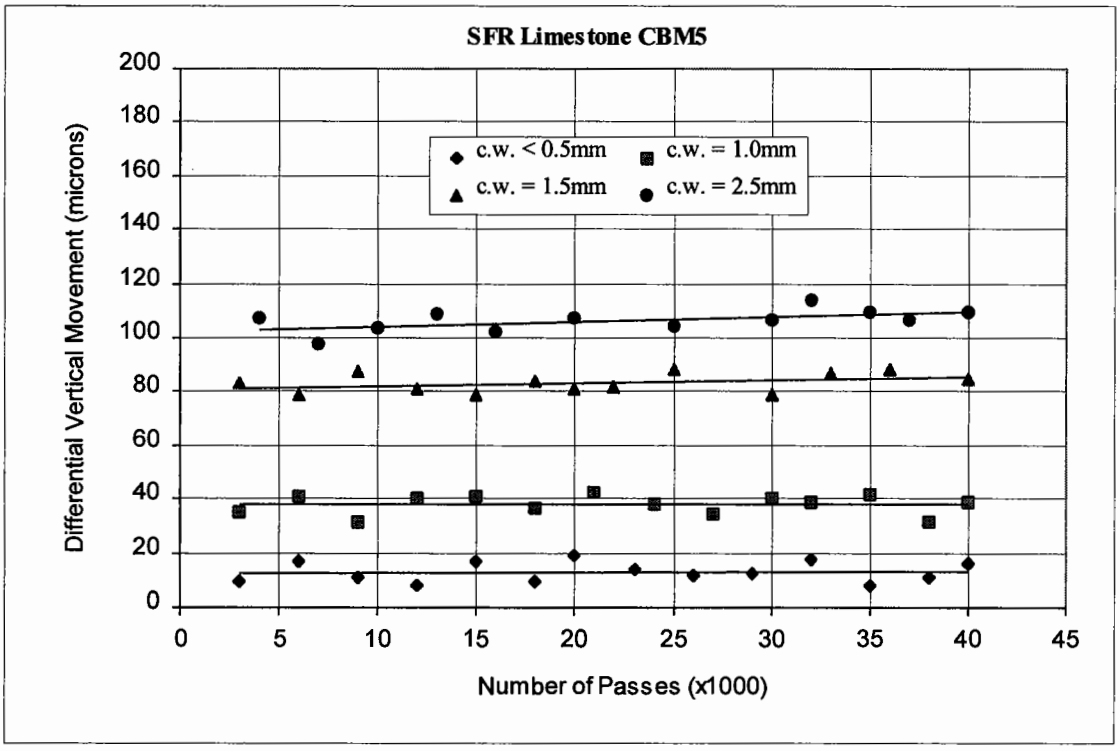

Figure 7.14. Differential vertical movement across different widths of a crack in a steel fibre reinforced limestone CBM5 slab.

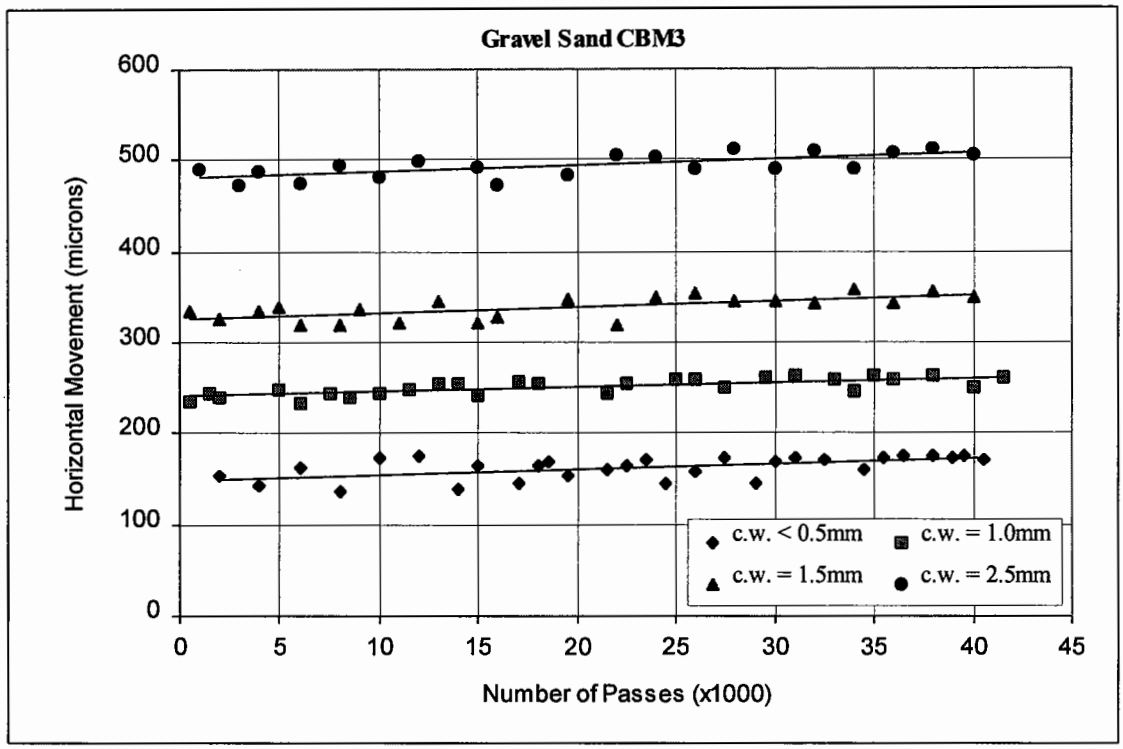

Figure 7.15. Horizontal movement across different widths of a crack in a gravel sand CBM3 slab

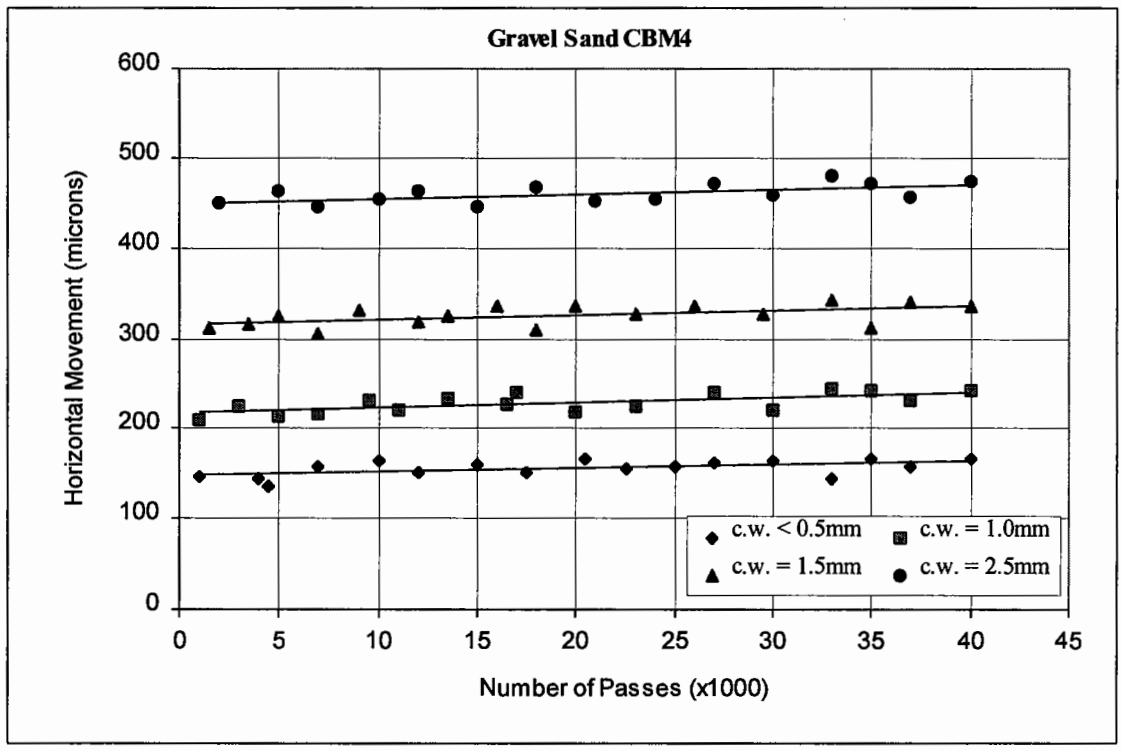

Figure 7.16. Horizontal movement across different widths of a crack in a gravel sand CBM4 slab

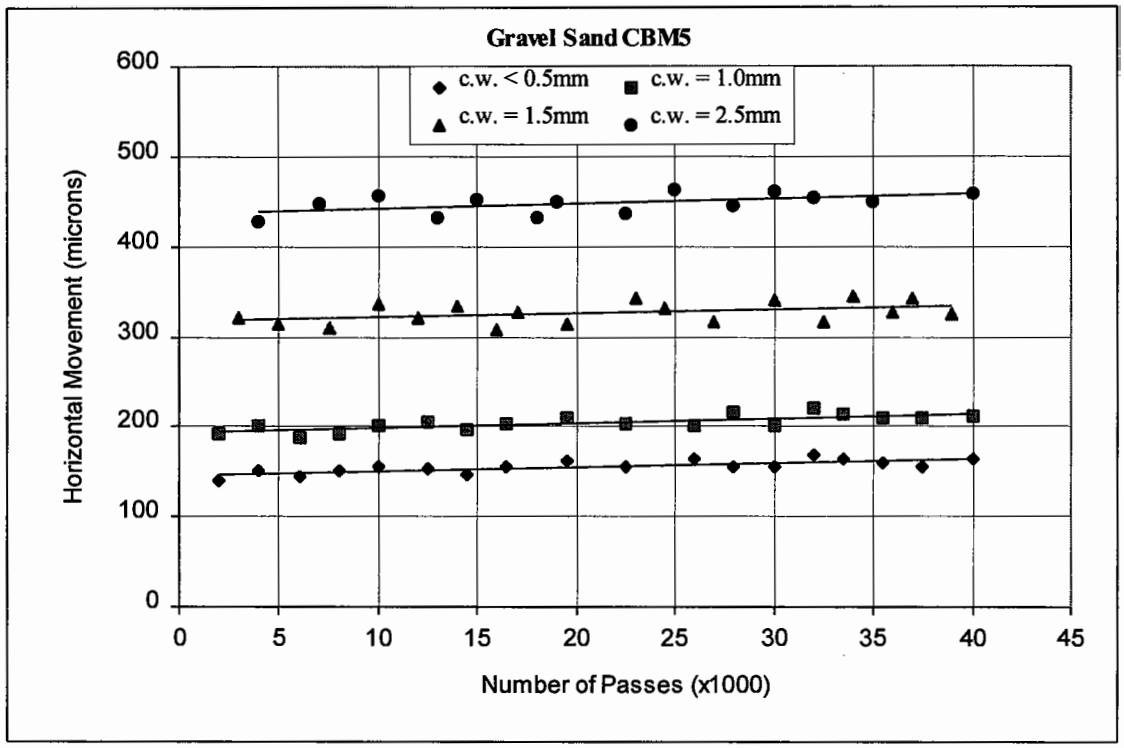

Figure 7.17. Horizontal movement across different widths of a crack in a gravel sand CBM5 slab

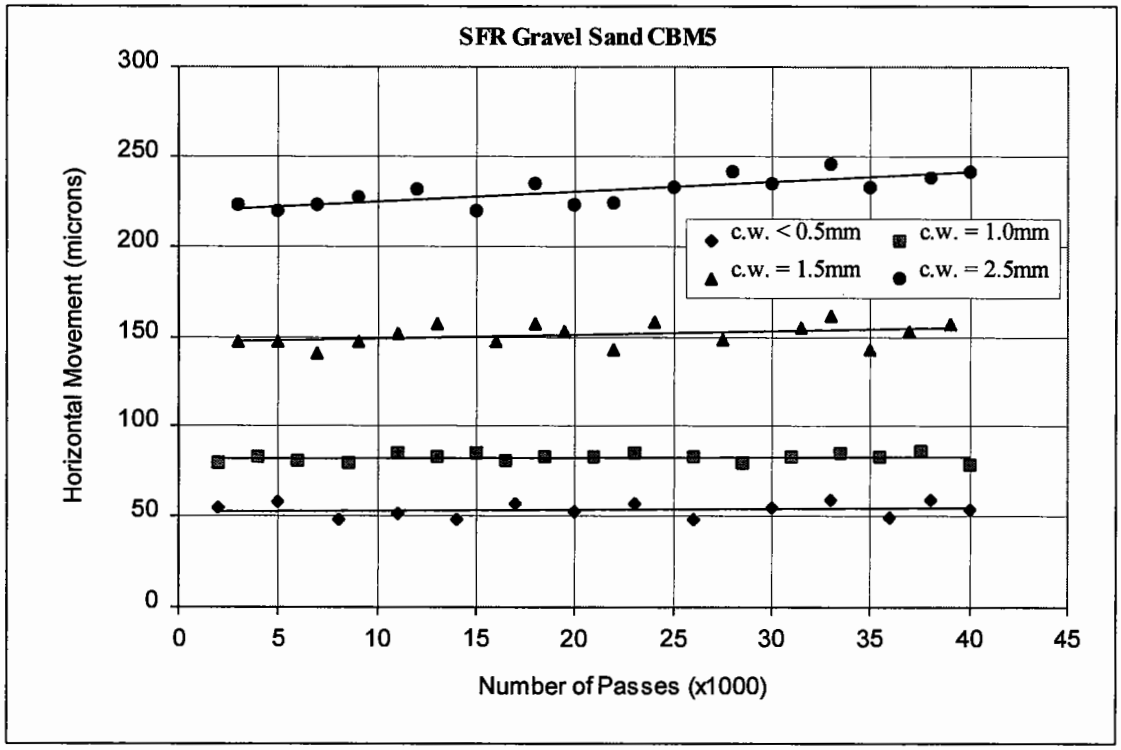

Figure 7.18. Horizontal movement across different widths of a crack in a steel fibre reinforced gravel sand CBM5 slab

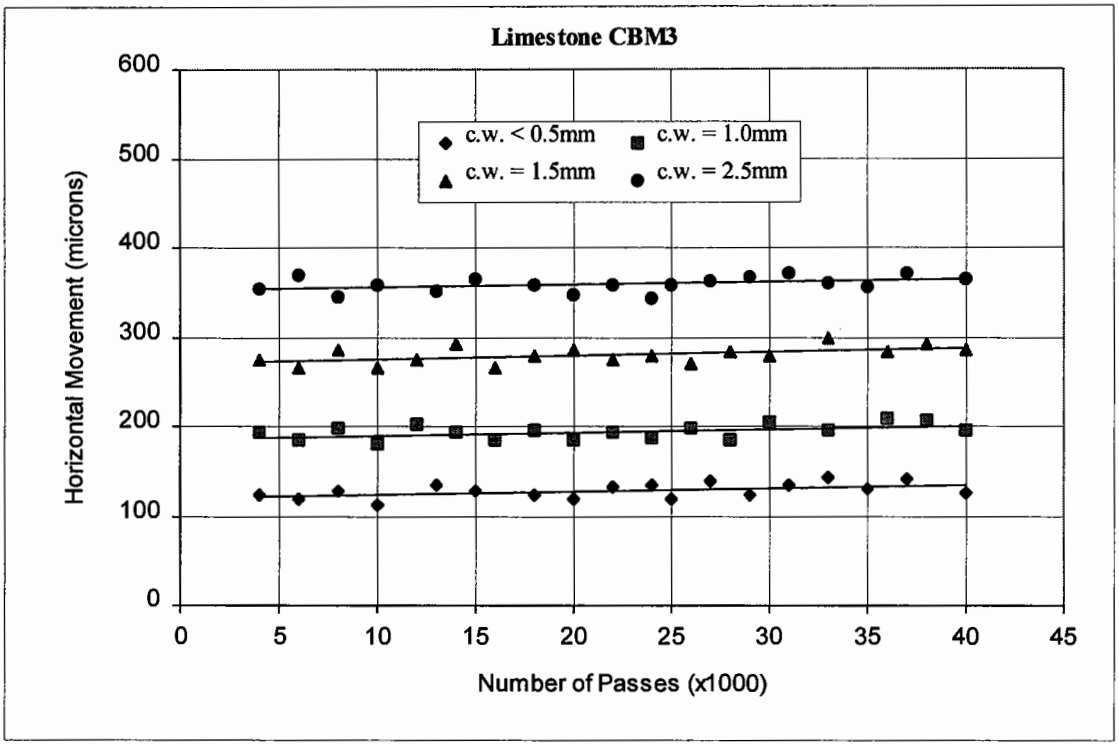

Figure 7.19. Horizontal movement across different widths of a crack in a limestone CBM3 slab

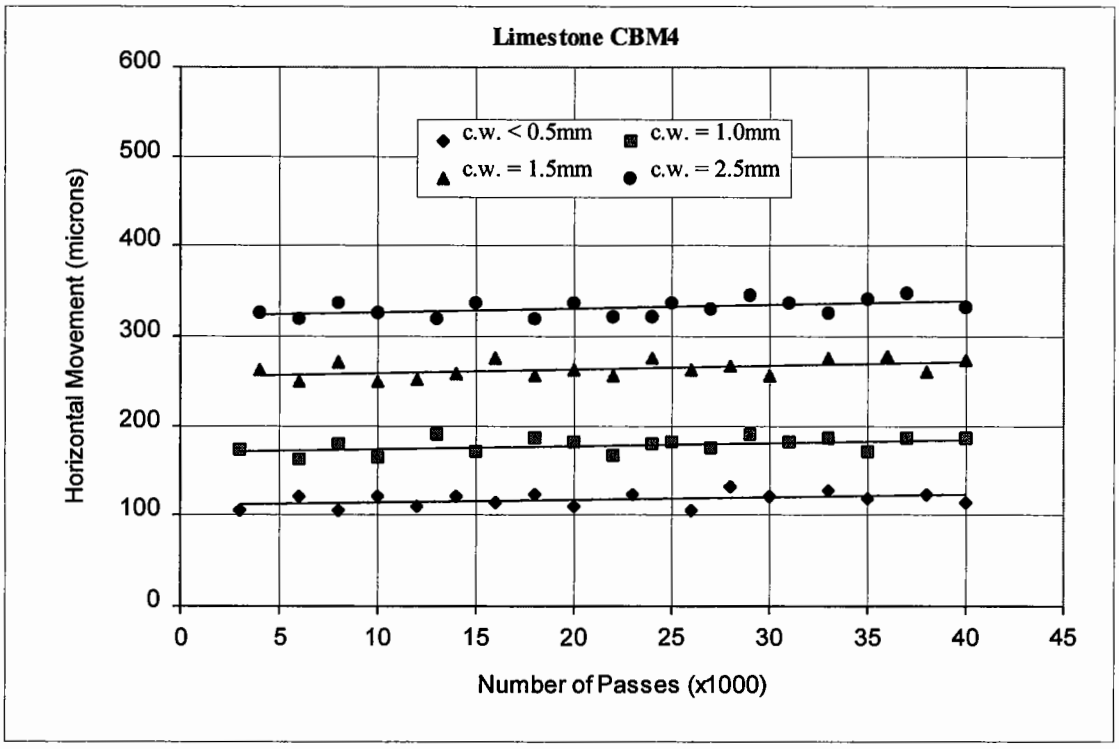

Figure 7.20. Horizontal movement across different widths of a crack in a limestone CBM4 slab

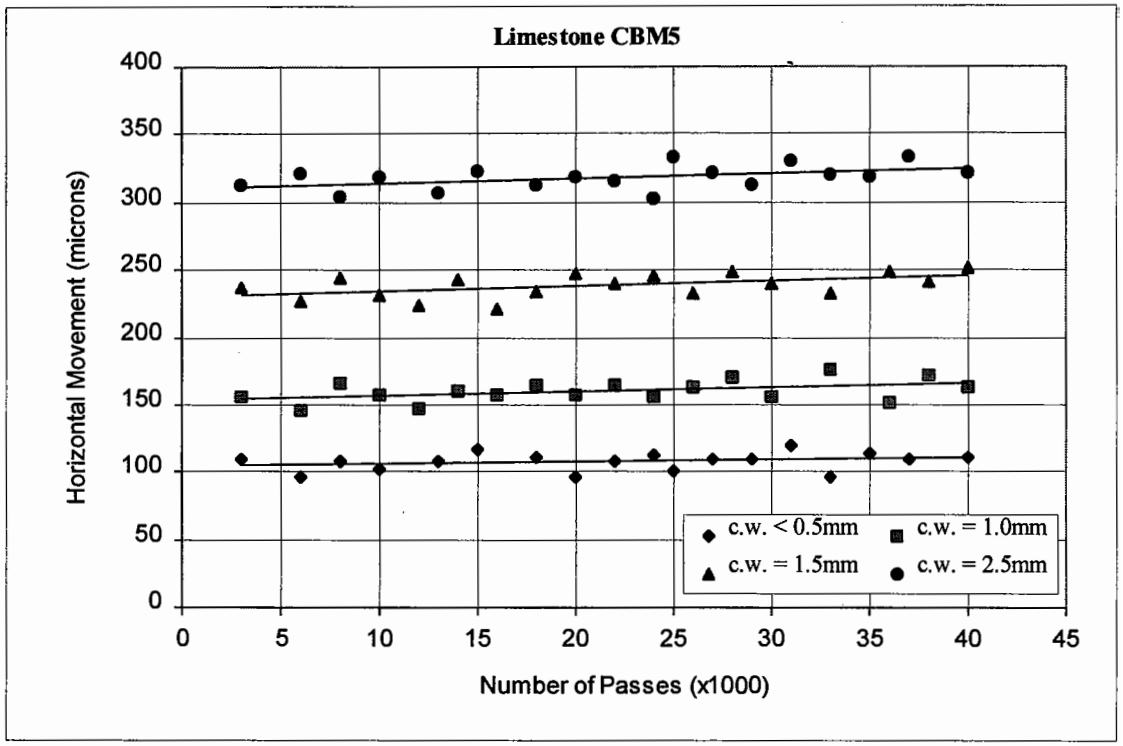

Figure 7.21. Horizontal movement across different widths of a crack in a limestone CBM5 slab

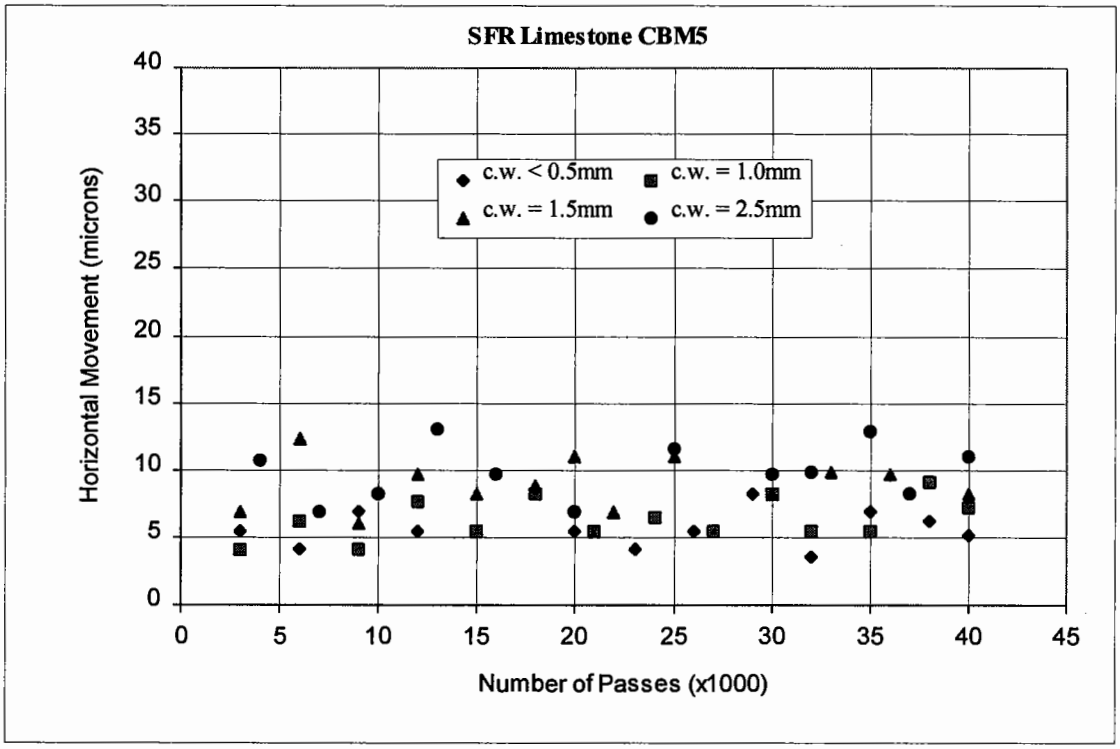

Figure 7.22. Horizontal movement across different widths of a crack in a steel fibre reinforced limestone CBM5 slab

7.7.4 Interpretation of Results

The results of differential vertical and horizontal crack movement for various categories of gravel sand and limestone CBMs are summarized in Tables 7.1 and 7.2, respectively. These tables show the average values and amount of variation of the crack movement results with respect to different crack widths. The results of crack movement, presented in Figures 7.7 to 7.22, are expressed in the form of approximate relationships in Tables 7.3 and 7.4 for gravel sand and limestone CBMs, respectively.

It can be seen from Tables 7.1 and 7.2 that the average values of crack movement (differential vertical and horizontal), generally decrease from CBM3 towards CBM5 for both the gravel sand and limestone CBMs, suggesting that the load transfer capability of material improves from CBM3 to CBM5.

In Figures 7.7 to 7.14, the slope of any of the relationships represents the rate of degradation of material at the crack faces due to repeated traffic loading. This slope is likely to be dependent on two factors, CBM strength and crack width. The slope is generally higher for relatively weaker CBM categories, and at greater crack widths for both the gravel sand and limestone CBMs (refer Tables 7.3 and 7.4). The degradation of cracks, during trafficking, causes an increased amount of differential vertical movement [Bondt and Saathof, 1993], thus impairing the quality of load transfer. By comparing Figures 7.7 to 7.10 with Figures 7.11 to 7.14, it appears that the crack deterioration rate is slightly less for each category of the limestone CBMs than the respective category of gravel sand CBMs. It is also known that the tensile strength for a limestone CBM is higher than a gravel sand CBM for the same compressive strength (refer Chapter 4). From this, it seems that the higher tensile strength of the limestone CBMs is possibly responsible for their lower rate of damage to the crack faces.

Tables 7.3 and 7.4 indicate that the rate of crack deterioration (i.e. slope of line) is much lower for SFR CBMs. In particular, the lowest rate of crack damage is found in the case of SFR limestone CBM5, which may be for two reasons: first the relatively

higher tensile strength of the limestone CBM, and second the relatively stronger bond which is expected between the crushed limestone aggregate (compared to round shaped gravel) and longer steel fibres. Also the longer fibres may have provided a stronger bridging action. From this discussion, it appears that one important factor influencing crack deterioration rate is the tensile strength of a CBM.

The situation is different in the case of horizontal movement of the crack. It can be seen from Figures 7.15 to 7.17 and 7.19 to 7.21, that the slope of the relationships shows a small rate of increase in the horizontal crack movement during trafficking. This slope varies for different CBM categories (refer Tables 7.3 and 7.4). Regarding the rate of crack degradation, there appears to be different mechanisms for weak and strong CBMs. To understand these mechanisms, it is important to remind here that the crack tends to close, under traffic loading, in the upper half of the CBM base. Under this action, significantly high compressive stresses are produced in this zone. These have been analysed using a computer programme 'CAPA' (discussed in Chapter 8), based on finite element method [Scarpas et al, 1996]. These stresses are sufficiently high to crush a relatively weak CBM, which consequently leads to a progressive increase in the horizontal crack movement. This is in agreement with the visual inspection of the slabs tested, during this investigation. Each slab was examined, at the end of its testing, for any loose material left underneath due to crack damage caused by traffic. Indeed, the relatively weak CBMs (gravel sand CBM3, CBM4, and limestone CBM3) showed a comparatively greater amount of loose particles. On the other hand, for relatively stronger CBMs, the compressive stresses are not high enough to damage the CBM (by crushing), but may cause a slow deterioration of the aggregate interlock until the magnitude of the horizontal crack movement reaches a maximum. However, after some degradation of the crack, it is expected that no further increase in the horizontal movement is likely to occur [Bondt and Saathof, 1993] in relatively stronger CBMs.

By comparing Figures 7.15 to 7.17 with Figures 7.19 to 7.21, it can be seen that the values of horizontal movement and rate of crack degradation are higher for gravel sand CBMs than those for the limestone CBMs. This is possibly due to the

considerable difference between the aggregate types and tensile strengths for the two types of CBM.

Steel fibre reinforcement has shown significantly improved performance in limiting not only the differential vertical, but also horizontal crack movement. However, the performance of longer steel fibres (ZC 60/0.8) in the crushed limestone CBM5 (Figure 7.22) has been found to be much superior to that of the shorter fibres (ZP 30/0.5) used in uncrushed gravel sand CBM5 (Figure 7.18).

From the results shown in Figures 7.10, 7.14, 7.18 and 7.22, and from the relationships given in Tables 7.3 and 7.4, it can be summarized that the steel fibre reinforcement in a CBM5 produces a relatively strong composite material with improved load transfer characteristics, provided that the crack width is not greater than 1.0 mm. The improved load transfer performance of this composite material may be due to the increased shear capacity of cracks [Holmgren, 1985], which is contributed by both aggregate interlock and the fibre reinforcement, in comparison with a non-reinforced CBM.

Table 7.1. Summary of the differential vertical and horizontal movements of the induced crack in gravel sand CBMs.

CBM	Crack width (mm)	Number of Passes	Crack Movement (microns)					
			Differential Vertical Movement			Horizontal Movement		
			85%tile	15%tile	Average	85%tile	15%tile	Average
CBM3	0.5	40500	62	45	52	173	145	162
	1.0	41500	167	142	155	261	242	251
	1.5	40000	390	353	374	349	321	338
	2.5	40000	511	471	491	508	480	493
CBM4	0.5	40000	61	41	50	164	146	156
	1.0	40000	146	123	135	242	218	228
	1.5	40000	343	308	325	336	311	325
	2.5	40000	492	452	470	471	449	460
CBM5	0.5	40000	52	39	45	163	148	155
	1.0	40000	109	96	103	213	195	204
	1.5	39000	301	273	284	341	314	326
	2.5	40000	436	408	423	459	433	447
SFR CBM5	0.5	40000	25	15	20	58	48	54
	1.0	40000	59	50	55	85	80	82
	1.5	39000	137	124	131	157	145	151
	2.5	40000	230	212	222	240	223	230

Table 7.2. Summary of the differential vertical and horizontal movements of the induced crack in crushed limestone CBMs.

CBM	Crack width (mm)	Number of Passes	Crack Movement (microns)					
			Differential Vertical Movement			Horizontal Movement		
			85%tile	15%tile	Average	85%tile	15%tile	Average
CBM3	0.5	40000	56	39	47	136	118	128
	1.0	40000	145	120	132	202	184	194
	1.5	40000	252	223	236	288	269	280
	2.5	40000	387	353	370	367	349	359
CBM4	0.5	40000	50	31	41	123	107	117
	1.0	40000	127	103	115	186	169	178
	1.5	40000	234	203	216	276	254	264
	2.5	40000	353	323	338	340	321	332
CBM5	0.5	40000	43	27	35	113	99	107
	1.0	40000	85	67	76	168	153	160
	1.5	40000	199	169	182	248	229	238
	2.5	40000	316	286	301	326	309	318
SFR CBM5	0.5	40000	17	10	13	7	4	6
	1.0	40000	41	34	38	8	5	6
	1.5	40000	88	79	83	11	7	9
	2.5	40000	110	103	106	12	8	10

Table 7.3. Approximate relationships derived from differential vertical and horizontal crack movement results for gravel sand CBMs.

CBM	Crack width (mm)	Relationship	
		Differential Vertical Movement (Figures 7.7 to 7.10)	Horizontal Movement (Figures 7.15 to 7.18)
CBM3	0.5	$y = 0.3501x + 44.22$	$y = 0.5681x + 148.61$
	1.0	$y = 0.6357x + 142.55$	$y = 0.5200x + 240.61$
	1.5	$y = 1.0420x + 353.83$	$y = 0.6958x + 324.78$
	2.5	$y = 1.1583x + 467.27$	$y = 0.6788x + 479.59$
CBM4	0.5	$y = 0.3001x + 43.98$	$y = 0.3630x + 148.41$
	1.0	$y = 0.6017x + 123.39$	$y = 0.5924x + 216.98$
	1.5	$y = 1.0951x + 303.92$	$y = 0.4911x + 315.98$
	2.5	$y = 1.1194x + 446.52$	$y = 0.5167x + 449.19$
CBM5	0.5	$y = 0.2553x + 39.84$	$y = 0.4767x + 144.98$
	1.0	$y = 0.3196x + 96.52$	$y = 0.5612x + 192.15$
	1.5	$y = 0.8685x + 265.29$	$y = 0.4403x + 316.68$
	2.5	$y = 1.0813x + 400.43$	$y = 0.5461x + 435.58$
SFR CBM5	0.5	$y = 0.1581x + 16.60$	$y = 0.0619x + 52.22$
	1.0	$y = 0.2482x + 49.91$	$y = 0.0321x + 81.76$
	1.5	$y = 0.3075x + 124.41$	$y = 0.2170x + 146.33$
	2.5	$y = 0.5648x + 209.81$	$y = 0.5455x + 218.90$

Note: 'y' is crack movement in microns; 'x' is Number of passes in 1000's.

Table 7.4. Approximate relationships derived from differential vertical and horizontal crack movement results for limestone CBMs.

CBM	Crack width (mm)	Relationship	
		Differential Vertical Movement (Figures 7.11 to 7.14)	Horizontal Movement (Figures 7.19 to 7.22)
CBM3	0.5	$y = 0.3107x + 40.36$	$y = 0.3985x + 118.91$
	1.0	$y = 0.7420x + 116.53$	$y = 0.3548x + 186.23$
	1.5	$y = 0.9152x + 216.12$	$y = 0.4213x + 271.05$
	2.5	$y = 1.2335x + 342.61$	$y = 0.3163x + 351.75$
CBM4	0.5	$y = 0.1897x + 36.95$	$y = 0.2731x + 111.17$
	1.0	$y = 0.6339x + 101.29$	$y = 0.3510x + 170.71$
	1.5	$y = 0.8754x + 197.76$	$y = 0.4043x + 255.29$
	2.5	$y = 0.9209x + 317.83$	$y = 0.3931x + 322.95$
CBM5	0.5	$y = 0.1898x + 30.91$	$y = 0.1546x + 103.88$
	1.0	$y = 0.1976x + 72.01$	$y = 0.3425x + 152.68$
	1.5	$y = 0.6960x + 166.76$	$y = 0.3966x + 229.86$
	2.5	$y = 0.9016x + 280.79$	$y = 0.3562x + 310.26$
SFR CBM5	0.5	$y = 0.0247x + 12.47$	—
	1.0	$y = 0.0163x + 37.70$	—
	1.5	$y = 0.1177x + 80.87$	—
	2.5	$y = 0.1906x + 102.14$	—

Note: 'y' is crack movement in microns; 'x' is Number of passes in 1000's.

7.8 STUDY OF REFLECTIVE CRACKING

7.8.1 Introduction

A limited study was carried out to investigate the effect of a Dense Bitumen Macadam (DBM) layer, laid over a CBM base, upon the load transfer characteristics of a crack induced in the CBM base. A 20mm DBM basecourse material was selected for this purpose, the specification of which is given in BS 4987: Part 1: 1993.

Mix design parameters of this DBM were chosen such that a relatively weak and brittle material could be obtained. Such a material was expected to crack due to fatigue at a relatively low number of wheel passes, thus accelerating the experiment. A conventional 100Pen bitumen binder was used. The binder content and void content used for this mix were as follows:

Binder Content: 4.1% by mass of oven dried aggregate. The binder content for a typical 20mm DBM is 4.7±0.6% by mass [BS 4987: Part 1: 1993].

Void Content: 6%, which is within the range 4 to 8% for a typical 20mm DBM [BS 4987: Part 1: 1993].

7.8.2 Preparation of Specimens

A slab (1000×900×60mm) was prepared from 20mm DBM mix by using a rigid (steel) frame mould, fixed over a smooth (visaform) sheet which was placed on an even surface. For compaction purposes, a pedestrian type vibrating roller was used. The DBM slab was left inside the mould for nearly three weeks to allow for some binder hardening. The mould was then removed and the slab was sawn to divide it into four pieces of dimensions shown in Figure 7.23.

The three 1000×250×60mm pieces (termed DBM beams) were used for load transfer study, whereas the fourth one (1000×150×60mm) was utilized to core 9 specimens (100mm diameter). These specimens were tested to measure the elastic stiffness and fatigue characteristics of the DBM mix.

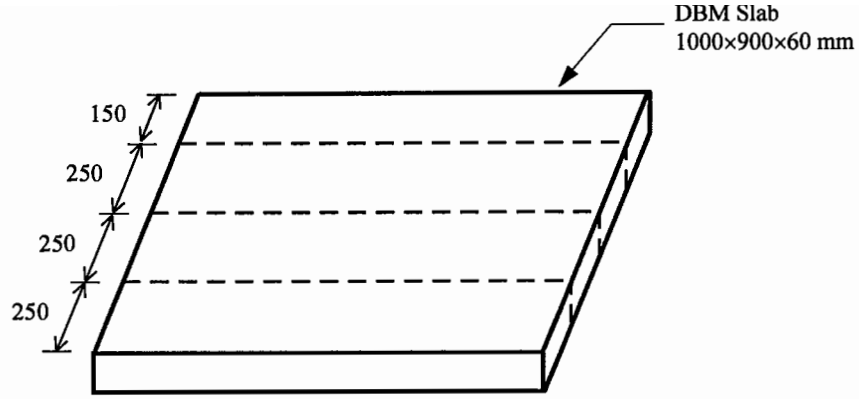

Figure 7.23. Size and sub-division of the 20mm DBM slab

7.8.3 Properties of the 20mm DBM

The mechanical properties of the 20mm DBM were determined from the core specimens (60mm thickness × 100mm diameter). Elastic stiffness was measured in the Nottingham Asphalt Tester (NAT) [Brown et al, 1995] according to the method described in BS DD213: 1993. The average values for density and stiffness of this material were as follows:

Average Density: 2360 kg/m^3

Average (NAT) Stiffness: 1890 MPa

Fatigue characteristics were obtained through the Indirect Tensile Fatigue Test (ITFT), described in Read's doctoral thesis [1996]. The fatigue line of this DBM mix is given in Figure 7.24, for which the calculation of the maximum initial horizontal tensile strain is based on the following relation [Read, 1996]:

$$\varepsilon_{max} = \frac{\sigma_{max}}{E}(1+3\nu) \qquad (7.1)$$

where:

ε_{max} : maximum initial horizontal tensile strain at the centre of the specimen

σ_{max} : maximum horizontal tensile stress at the centre of the specimen (kPa)

E : stiffness modulus (kPa)

ν : Poisson's ratio of the material

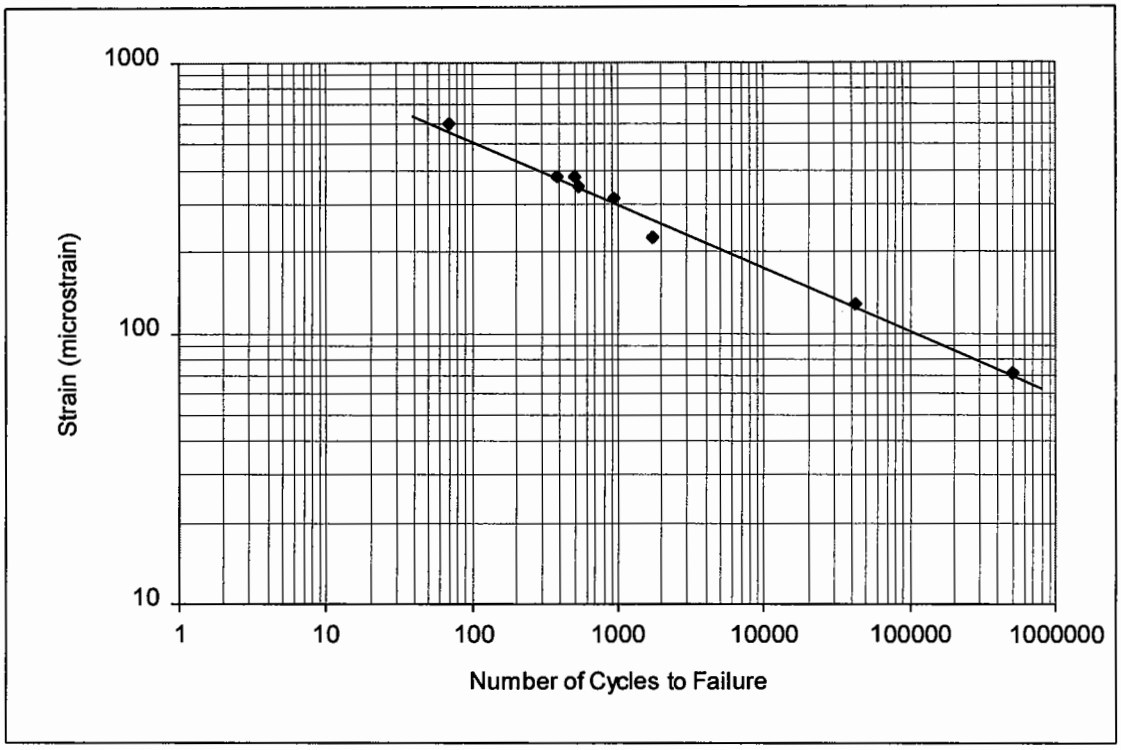

Figure 7.24. Fatigue characteristics for the 20mm DBM

7.8.4 Experimental Setup

For this study, the experimental setting and instrumentation of the CBM slab were the same as described in Sections 7.5 and 7.6. The system for recording of data was also the same. After the CBM slab was properly setup with the intended width of the transverse crack (in the middle), one of the three DBM beams (1000×250×60 mm) was positioned centrally over the CBM slab along its length, such that the DBM beam was right underneath the wheel during trafficking.

The DBM beam was strongly bonded to the CBM slab. For this purpose, the contact surfaces of both the CBM slab and DBM beam were brushed with hot bitumen (100Pen), and then stuck together. To allow for settling of bond, some dead weight was placed over the entire surface of the DBM beam, and left for at least 2 days. The dead weight was then removed, and two purpose built clamps were fixed at a distance of 250mm from either end of the beam (Figure 7.25). The middle 500mm length of the beam was unclamped, but bonded via the hot bitumen to the CBM slab. This part

of the beam extended half the distance (250mm) on either side of the transverse crack induced in the CBM slab. A photograph of this experimental setting is shown in Figure 7.25.

During testing, the DBM beam was subjected to repeated application of wheel loading, the magnitude of which was the same as in the case of direct trafficking on the CBM slab. The vertical and horizontal deflections were still measured directly from the CBM slab. In this case, LVDTs 'A' and 'B' were positioned vertically on either side of the crack, in the CBM slab (refer Figure 7.6), but at an offset of 30mm from the edge of the DBM beam. The third LVDT 'C' was attached horizontally, across the crack, at the neutral axis depth, as mentioned earlier in Section 7.6. This study was carried out at an average temperature of 18°C.

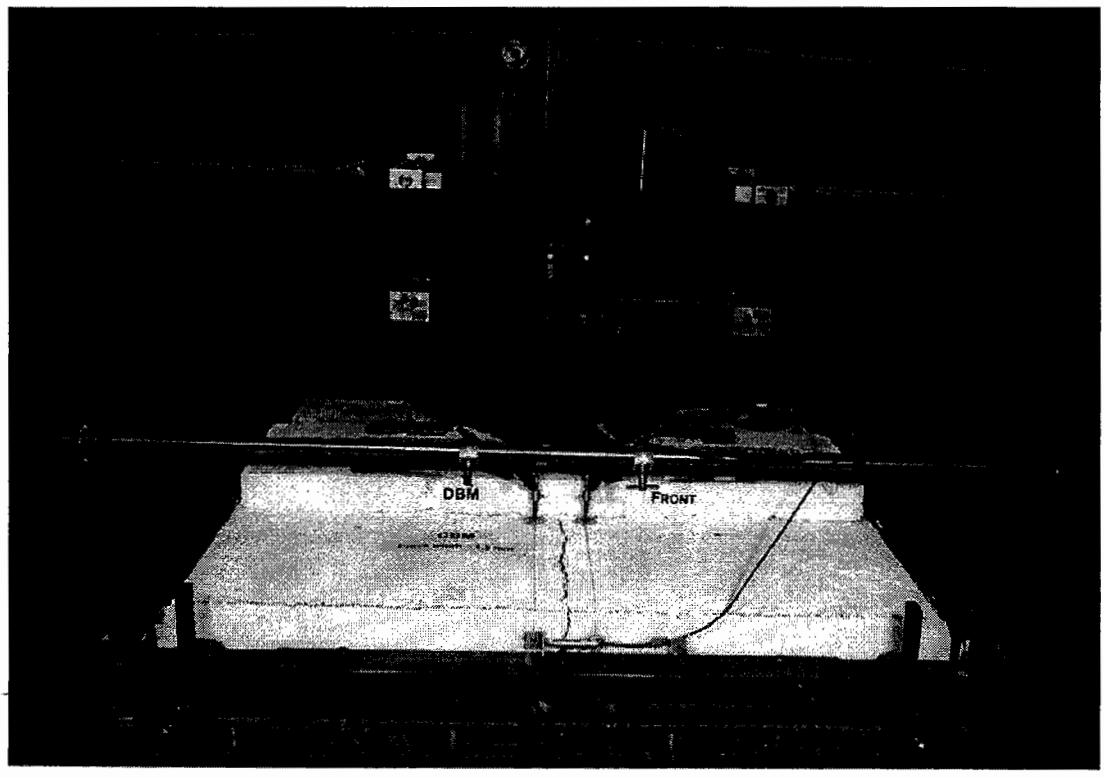

Figure 7.25. Experimental setting with 20mm DBM beam over a CBM slab

This study involved three combinations, using DBM surfacing over two categories of limestone CBM. The following three cases were investigated:

Case 1: 20mm DBM beam (1000×250×60 mm) over
a limestone CBM5 slab with a width of the induced crack ≤ 0.5 mm

Case 2: 20mm DBM beam (1000×250×60 mm) over
a limestone CBM5 slab with a width of the induced crack = 1.5 mm

Case 3: 20mm DBM beam (1000×250×60 mm) over
a limestone CBM4 slab with a width of the induced crack = 1.5 mm

7.8.5 Results and Discussion

The results of differential vertical and horizontal movement of a crack induced in the crushed limestone CBM slabs, overlaid by a 60mm thick surfacing of 20mm DBM, are shown in Figures 7.26 to 7.28, and Figures 7.29 to 7.31, respectively. A summary of these results is given in Table 7.5.

The effect of the DBM surfacing upon the load transfer of a crack, in the CBM base, can be seen by comparing the crack movement results before and after the surfacing is laid. A comparison of Figures 7.26 and 7.27 with Figure 7.13 indicates that the differential vertical movements, across both widths (0.5 and 1.5mm) of a crack in the limestone CBM5, have decreased (as is obvious) after the surfacing is laid. A similar situation can be seen by comparing Figure 7.28 with Figure 7.12 for a 1.5mm crack in the limestone CBM4. Likewise, a reduction in the horizontal crack movement, after the surfacing is laid, is obvious from a comparison of Figures 7.29 and 7.30 with Figure 7.21 for limestone CBM5, and Figure 7.31 with Figure 7.20 for limestone CBM4.

Table 7.5 indicates that, for the same crack width and surfacing thickness, the crack movements are found to be relatively higher for the limestone CBM4 than for CBM5.

The amount of reduction in the differential vertical and horizontal movements, due to the bituminous surfacing, can be calculated by comparing Table 7.5 with Table 7.2 for the respective CBMs and crack widths.

Table 7.5. Differential vertical and horizontal movements of a crack induced in the limestone CBM slabs, overlaid by a 60mm layer of 20mm DBM.

CBM	Crack width (mm)	Number of Passes	CBM Crack Movement (microns)					
			Differential Vertical Movement			Horizontal Movement		
			85%tile	15%tile	Average	85%tile	15%tile	Average
CBM5	0.5	270000	24	13	19	27	15	21
CBM5	1.5	160000	70	55	63	78	69	74
CBM4	1.5	125000	90	74	83	114	109	111

The results shown in Figures 7.26 to 7.31, are expressed in the form of approximate relationships in Table 7.6, from which the degradation of a crack in limestone CBM5 is found to be insignificant when the crack width is ≤ 0.5mm. This agrees with visual examination during the experiment. The testing for this particular case was continued up to 270,000 wheel passes. During this trafficking, a crack initiated from the surface and propagated to half the depth (35 mm) of the bituminous surfacing. This crack is shown in Figure 7.32 by marking a black line along its side. In contrast, a certain rate of deterioration can be seen (Figures 7.27 and 7.28) for both the limestone CBM5 and CBM4 at a crack width of 1.5mm. This point is also supported by visual observation, because this (1.5mm) crack propagated throughout the DBM (beam) thickness after 125,000 passes in the case of the CBM4 slab, and after 160,000 passes for CBM5 slab. In both cases, a crack initiated from the top of the surfacing (refer Figure 7.33), almost above the crack in the CBM slab, and propagated downward nearly to mid-depth. Another crack then initiated from the bottom of the surfacing and started propagating towards the surface. This second crack dominated and joined the first crack almost at mid-depth in one case, whereas in the other case the second (bottom) crack reflected to the surface at a short distance from the first crack.

Table 7.6. Relationships derived from the results of differential vertical and horizontal movement of a crack in the limestone CBM slabs, overlaid by a 60mm layer of 20mm DBM.

CBM	Crack width (mm)	Relationship	
		Differential Vertical Movement (Figures 7.26 to 7.28)	Horizontal Movement (Figures 7.29 to 7.31)
CBM5	0.5	$y = 0.0024x + 18.56$	$y = 0.0041x + 19.98$
CBM5	1.5	$y = 0.0535x + 59.01$	$y = 0.0181x + 72.35$
CBM4	1.5	$y = 0.1010x + 76.13$	$y = 0.0109x + 110.39$

Note: 'y' is crack movement in microns; 'x' is Number of passes in 1000's.

From the above results and discussion, it seems that the magnitudes of differential vertical and horizontal movements across a 0.5mm crack in the limestone CBM5 may be small enough to prevent reflective cracking in the long term, provided that the thickness of bituminous surfacing is appropriately designed. On the other hand, the movements resulting from a crack width of 1.5mm or above, are likely to generate sufficiently high tensile strains in the same thickness of the bituminous surfacing to cause premature reflective cracking.

The pavement system, shown in Figure 7.25 was studied analytically by using a simplified modelling approach, described in Chapter 8, to predict fatigue life under traffic loading. In this study, the three cases discussed earlier (see Section 7.8.4), and another situation for a SFR limestone CBM5 slab (overlaid by bituminous surfacing) were modelled. In each case, tensile strain was calculated in the bituminous layer at a location directly above the crack in the CBM slab. The magnitude of strain was then used in a fatigue relationship to determine pavement life.

Following the regression analysis procedure described by Read [1996], the ITFT fatigue relationship, shown in Figure 7.24, can be expressed by the following equation:

$$N_i = 2.9 \times 10^{13} \times (\varepsilon)^{-4.2271} \qquad (7.2)$$

In Eq. 7.2, N_i is the number of load applications to crack initiation [Read, 1996], ε is tensile strain (microstrain). The values 2.9×10^{13} and -4.2271 represent constants determined through regression analysis of the fatigue results (Figure 7.24).

Eq. 7.2 gives fatigue life to crack initiation. To determine the pavement life to failure N_f, the value of N_i has to be multiplied by an appropriate shift factor for crack propagation time. The value of the shift factor for a typical 20mm DBM is 6.4 [Read, 1996]. The results of the analytical study are shown in Table 7.7 for the various situations modelled. The calculated values of N_f (Table 7.7) are comparatively greater than the experimental results (Table 7.5). This is possibly due to the following two main reasons:

- The sub-structure of the experimental pavement system was modelled with an equivalent foundation modulus of 50 MPa/m.
- The shift factor (for crack propagation time to failure) used actually correspond to a typical 20mm DBM with binder content of 4.7% by mass [Read, 1996; BS 4987: Part 1: 1993], whereas the binder content used in the present mix was less (4.1%), which would have increased the crack propagation rate.

Instead of looking at the absolute magnitudes of life, given in Table 7.7, it is rather more important to notice the significantly improved performance which is attributable to the 0.5mm width of crack in the CBM base. Similarly, it is interesting to find the even more enhanced performance of the SFR CBM base compared to the unreinforced ones.

Table 7.7. Predicted fatigue life to crack initiation and failure conditions of the experimental pavement structure with limestone CBM base

Description	Crack width (mm)	Bituminous layer (mm)	Tensile strain (microstrain)	N_i ($\times10^6$)	N_f ($\times10^6$)
CBM5	0.5	60	85.9	0.1937	1.240
CBM5	1.5	60	114.0	0.0586	0.375
CBM4	1.5	60	116.1	0.0542	0.347
SFR CBM5	0.5	60	68.2	0.5129	3.282

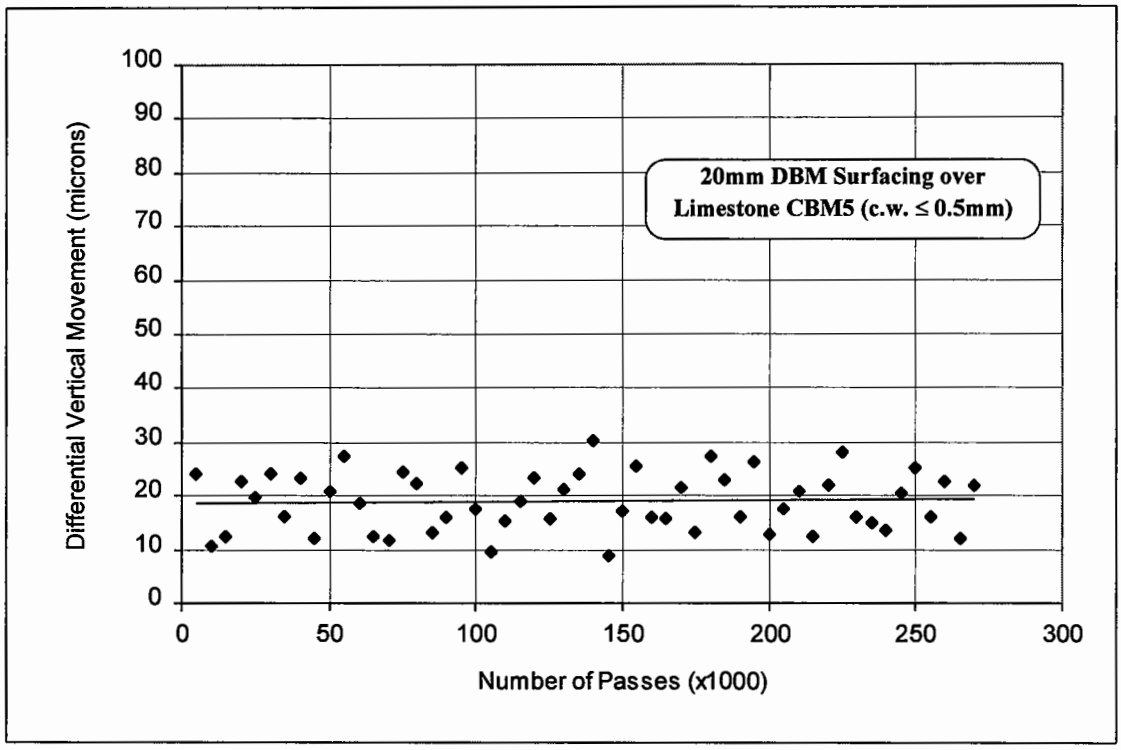

Figure 7.26. Differential vertical movement across a 0.5mm crack induced in a limestone CBM5 slab, after it was overlaid by a 60mm layer of 20mm DBM.

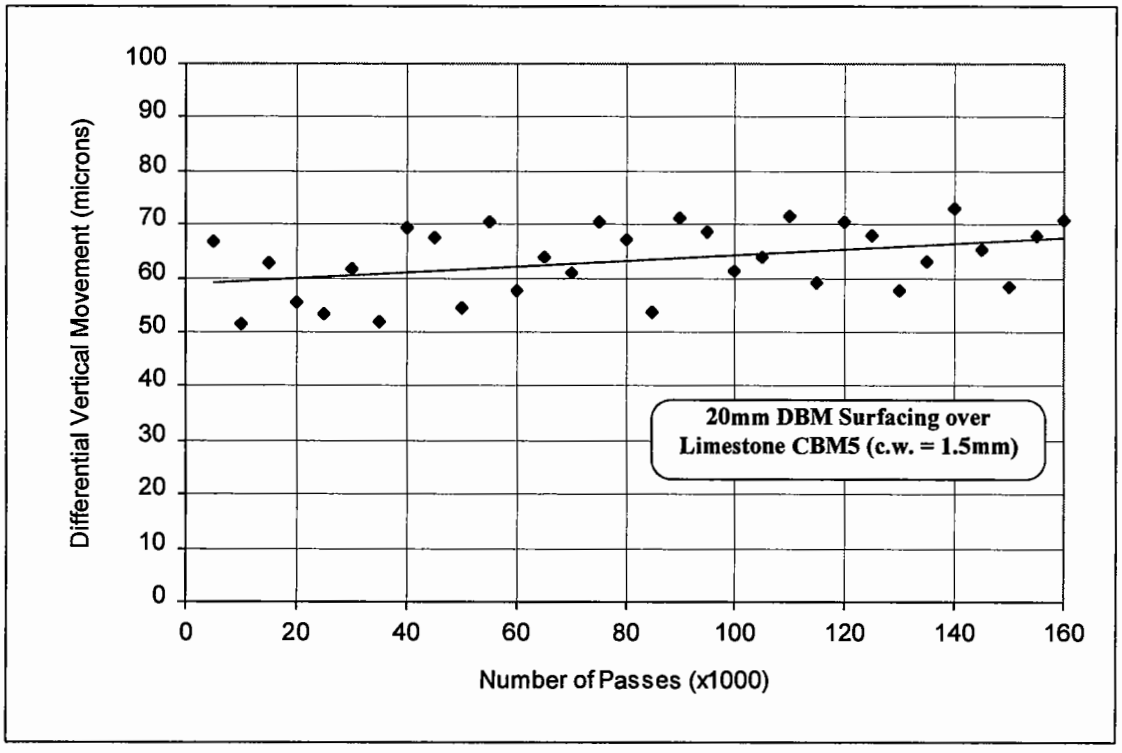

Figure 7.27. Differential vertical movement across a 1.5mm crack induced in a limestone CBM5 slab, after it was overlaid by a 60mm layer of 20mm DBM.

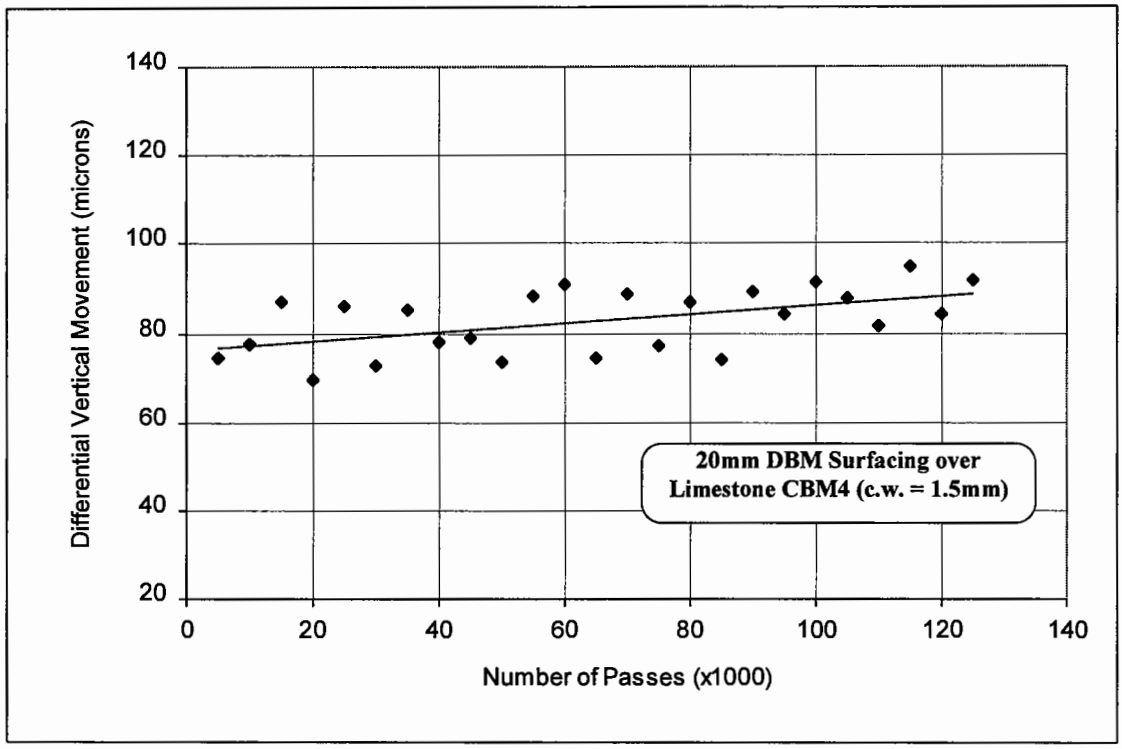

Figure 7.28. Differential vertical movement across a 1.5mm crack induced in a limestone CBM4 slab, after it was overlaid by a 60mm layer of 20mm DBM.

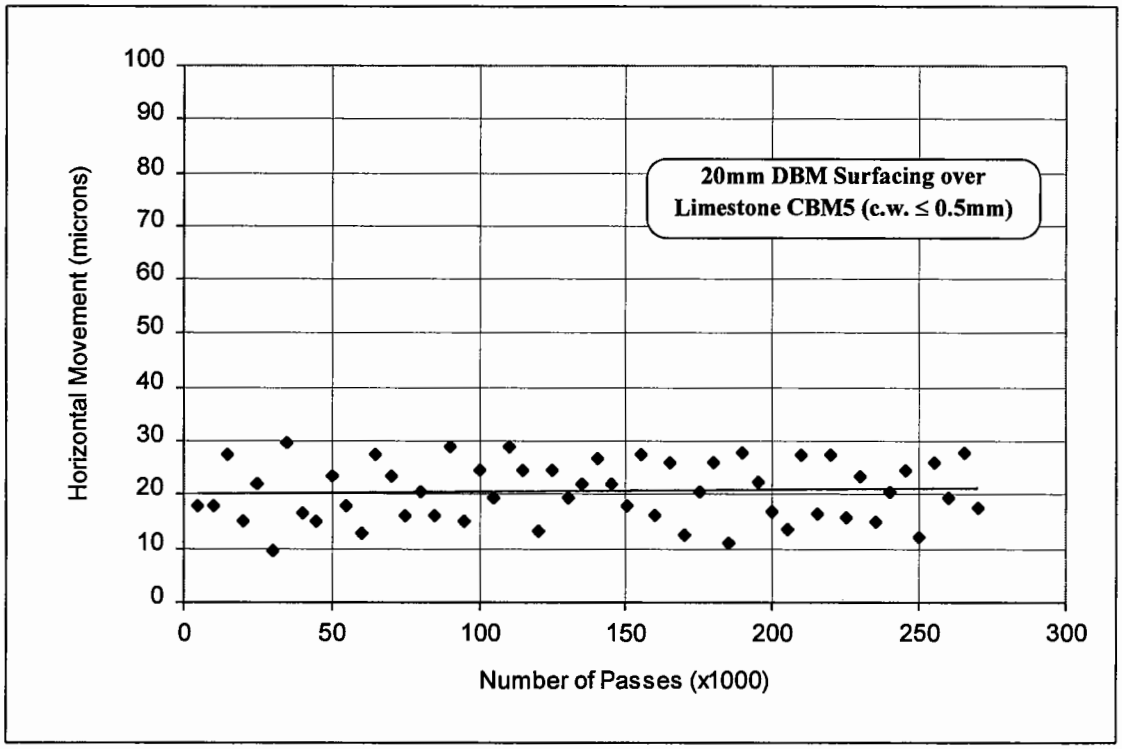

Figure 7.29. Horizontal movement at a 0.5mm crack induced in a limestone CBM5 slab, after it was overlaid by a 60mm layer of 20mm DBM.

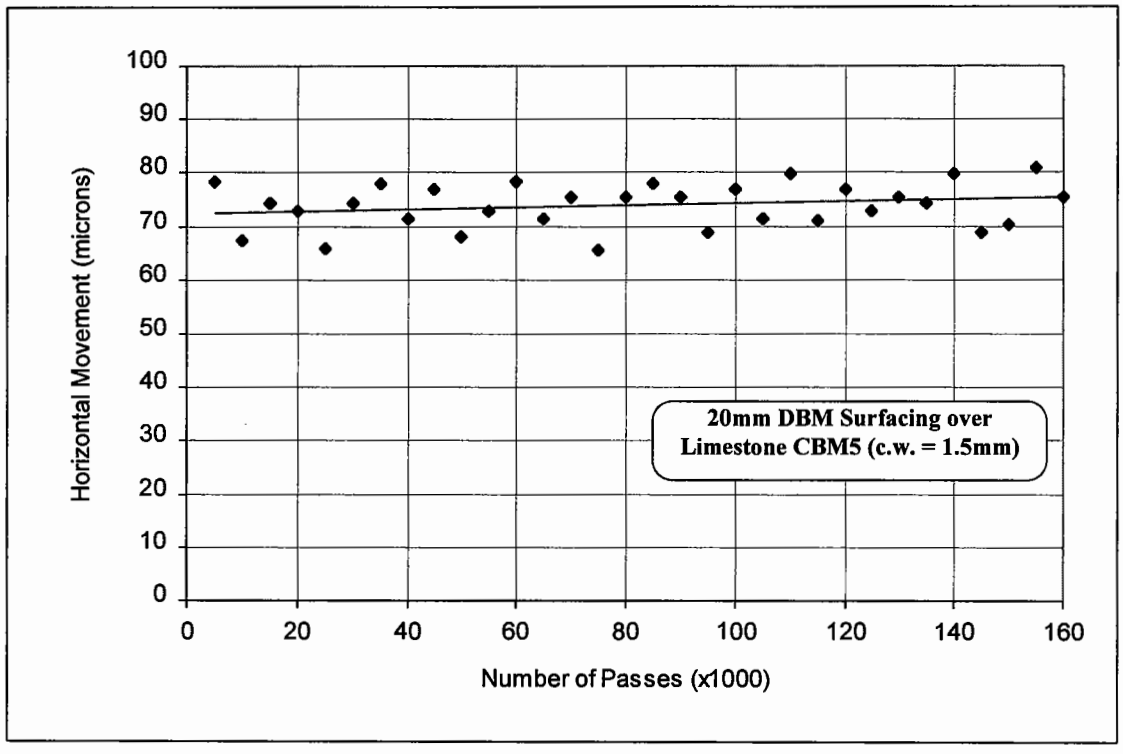

Figure 7.30. Horizontal movement at a 1.5mm crack induced in a limestone CBM5 slab, after it was overlaid by a 60mm layer of 20mm DBM.

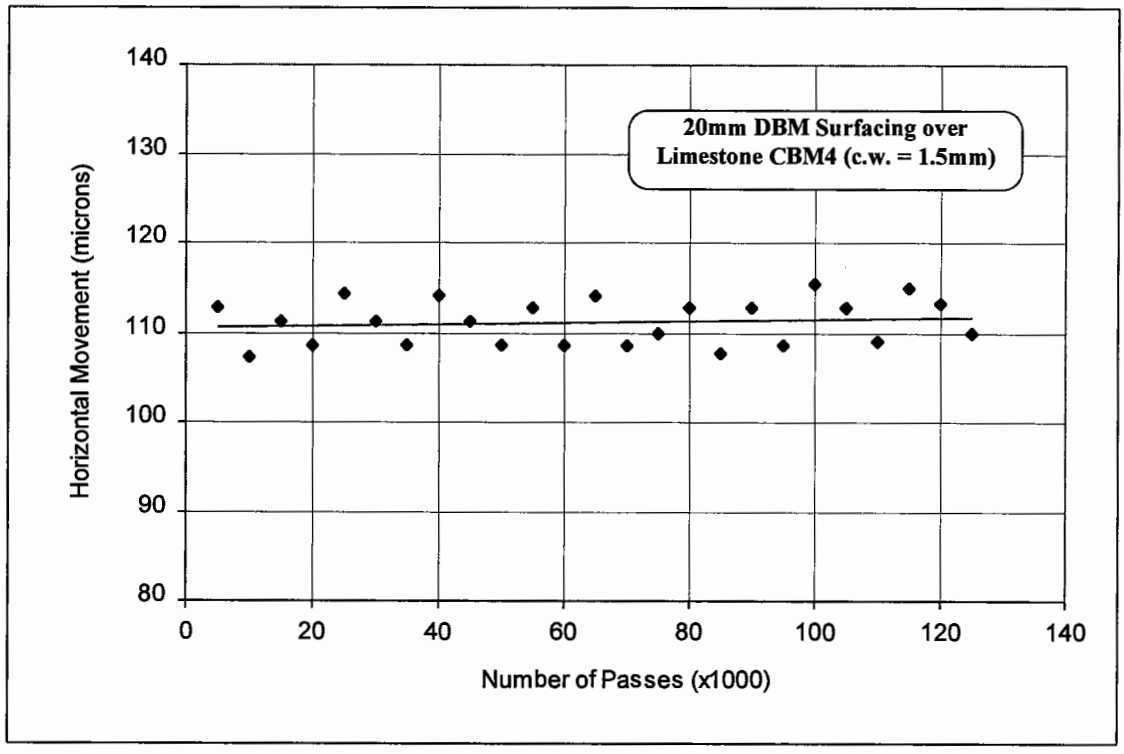

Figure 7.31. Horizontal movement at a 1.5mm crack induced in a limestone CBM4 slab, after it was overlaid by a 60mm layer of 20mm DBM.

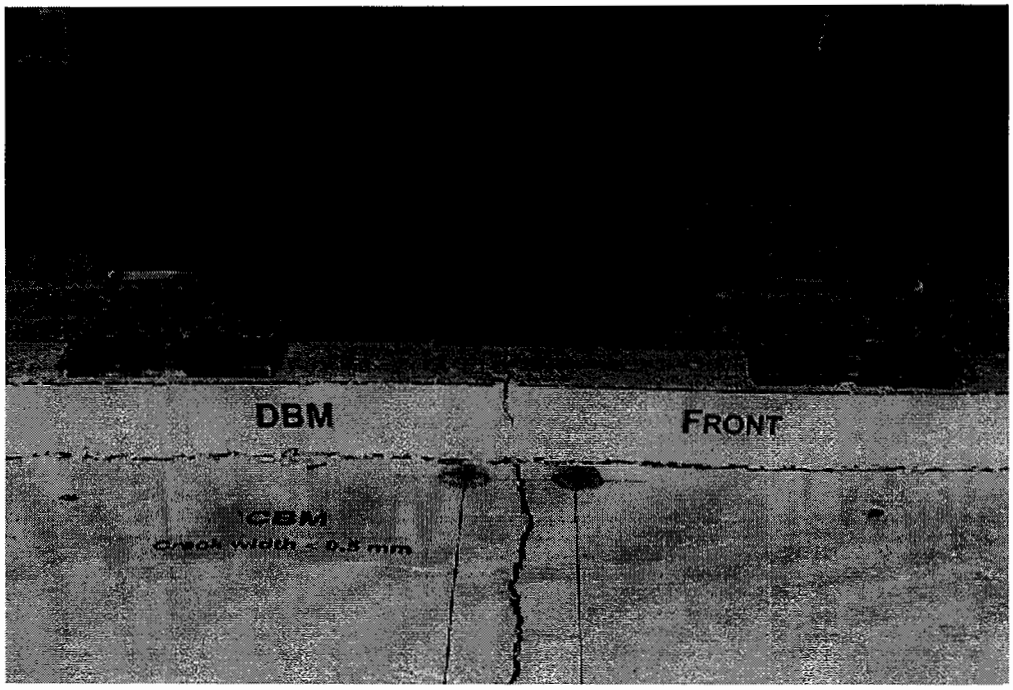

Figure 7.32. Cracking in the 60mm bituminous surfacing as a result of the movements at a 0.5mm wide crack in the limestone CBM5 base

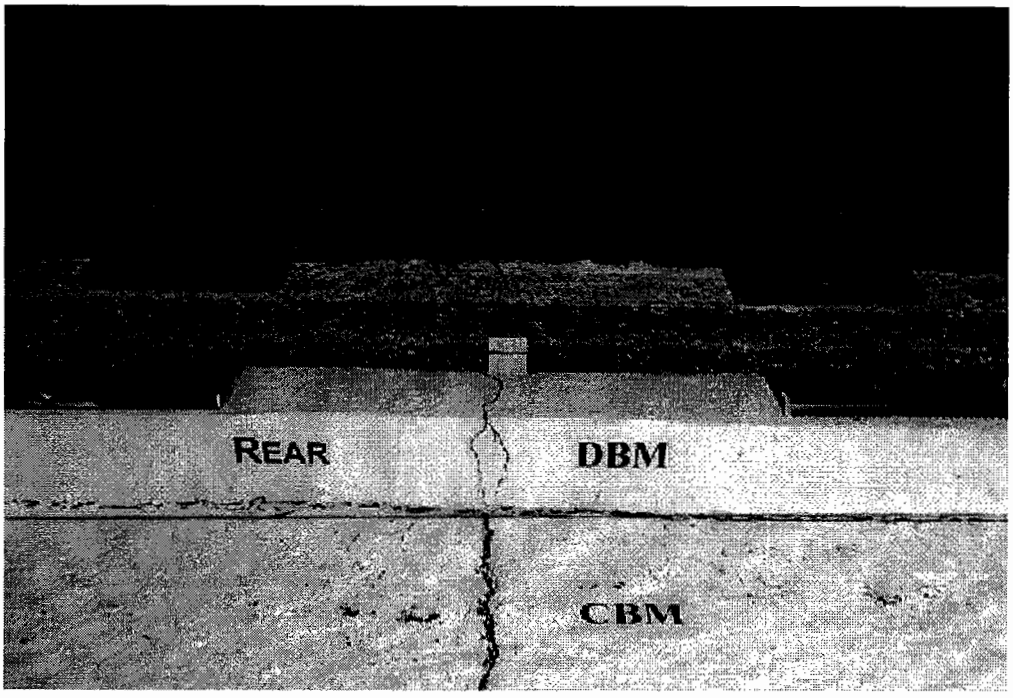

Figure 7.33. Cracking in the 60mm bituminous surfacing as a result of the movements at a 1.5mm wide crack in the limestone CBM5 base

7.9 SIGNIFICANCE OF THE LOAD TRANSFER TEST SYSTEM

The test system, presented in this chapter, can be used as a useful tool to characterize various categories of CBMs by investigating their long term performance, under repeated applications of a wheel load, with reference to the influence of the following important parameters upon the load transfer capability of cracks:

1. Type of aggregate: shape, strength, and grading
2. Strength of a CBM
3. Thickness of a CBM base
4. Width and shape of crack
5. Traffic
6. Steel fibre reinforcement: by varying fibre content, aspect ratio, fibre shape.

Further research is suggested to study the effect of aggregate grading, CBM thickness, shape of the crack, and the variables involved in steel fibre reinforcement.

7.10 CONCLUSIONS

Based on the results of research, presented in this chapter, the following conclusions have been drawn:

- The magnitudes of differential vertical and horizontal movement, under traffic loading, increase with an increase in crack width. Minimum crack movement and hence maximum load transfer is found at a crack width ≤ 0.5mm.

- The amount of crack movement (vertical and horizontal) is influenced by the shape of aggregate, and is higher for a round shaped gravel sand CBM, compared to a crushed limestone CBM, for a given crack width.

- The load transfer is a function of the CBM strength and improves from lower to higher CBM categories.

- The crack degradation, due to traffic loading, is a function of the tensile strength of a CBM and crack width. The rate of degradation is found to be higher for CBMs with relatively low tensile strength, and at greater crack widths.

- Steel fibre reinforced CBMs have shown a significant improvement in load transfer performance by limiting both the differential vertical and horizontal movements at the induced crack. Also crack degradation rate is found to be much lower, compared to unreinforced CBMs.

- The longer steel fibres (ZC 60/0.8), used in a limestone CBM5, have shown comparatively better load transfer than the shorter fibres (ZP 30/0.5), used in a gravel sand CBM5. However, further research is suggested to study the effect, on the load transfer, of different aggregates for the same fibre type and CBM grade.

- Crack propagation through a bituminous surfacing is greatly influenced by the magnitude of differential vertical movements of a crack, a function of its width, in the CBM base. The crack generally initiates from the top of the bituminous surfacing, almost above the crack in the CBM base, and progresses downward. Another crack is then initiated at the bottom, which propagates upward, and dominates the first one.

- The degradation of a crack in a limestone CBM5, overlaid by a bituminous surfacing, is found to be insignificant when the crack width is $\leq$ 0.5mm. At a greater crack width (1.5mm) the crack deterioration is likely to be relatively higher for weaker CBMs.

- The results of an analytical study suggest an improved performance, against the occurrence of reflective cracking, for a 0.5mm width of crack in a limestone CBM5 base, and an even more enhanced performance for the case of a SFR limestone CBM base.

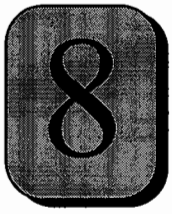

Analytical Modelling and Design Implication

8.1 INTRODUCTION

Although the field and laboratory investigations into controlled cracking, and the laboratory study of steel fibre reinforcement in cement bound bases have clearly indicated benefits associated with these techniques, relating to an improved CBM base design, these remain qualitative. In order to incorporate these benefits into predictions of pavement life, the behaviour of a flexible composite pavement has to be modelled. Although the subject of detailed analytical modelling and design development is recommended for future research, a brief analytical study has been included in this chapter to show the practical implications and benefits of the (above mentioned) advanced techniques.

The analysis and design of a flexible composite pavement with a cracked CBM base has been a complex problem. This is because the discontinuities caused by cracks (controlled or uncontrolled) render inappropriate the application of conventional methods based on continuous layered linear elastic analysis.

This chapter presents the application of two techniques for analytical modelling of a pavement structure with a cracked CBM base. One of these is based on a simplified approach [Thom, 1997], and the other involves the use of a finite element program CAPA [Scarpas et al, 1996a]. For each, the input parameters used are the performance characteristics investigated in this study through laboratory and site testing. It has been shown that, by using these techniques, the structure of a flexible composite pavement with controlled or uncontrolled cracks in the CBM base can be effectively modelled to predict reflective crack development and/or pavement life under thermal expansion and contraction effects and traffic loading.

8.2 SIMPLIFIED APPROACH

This approach is based on simplified analytical models which have been developed at the University of Nottingham [Thom, 1997] to predict reflective crack development, due to thermal and traffic loading. This section introduces the techniques which have been developed for traffic loading effects, because for CBM base roads with cracks induced at 3 m centres, it is the traffic loading rather than thermal loading which is usually predicted to be more critical. The cracking mechanism modelled is shown (in a simplified form) in Figure 8.1. The parameters required in the analysis are:

- Load (kN)
- Surfacing layer thickness (mm)
- Surfacing modulus (MPa)
- Equivalent foundation modulus (MPa/m)
- Load transfer efficiency (kPa/mm)

Of these, the first three need no explanation. The equivalent foundation modulus represents a simplification of the foundation layers often used in concrete pavement analysis. The load transfer efficiency is the subject which has already been discussed in Chapter 7. It is assumed that a linear relationship exists between shear stress across the crack faces and shear slip (differential vertical movement). The author is aware that this has been supported by recent FWD tests at varying load levels on a UK major road site. The direct output of the analysis is "tensile strain in the bituminous surfacing", although this can be related to pavement life or to crack propagation rate depending on the fatigue model used. An alternative approach which would be equally possible is to calculate "stress intensity factors" for use in the Paris law [Paris and Erdogan, 1963; Francken, 1993] for crack propagation.

As examples, the following two situations have been modelled for a CBM base pavement with a controlled cracking system:

a) A standard UK design [DoT, HD 26/94, 1994] for over 20 million standard axles (msa), that is 200 mm of bituminous layer over 250 mm of CBM base.

A design using controlled cracking to give similar life.

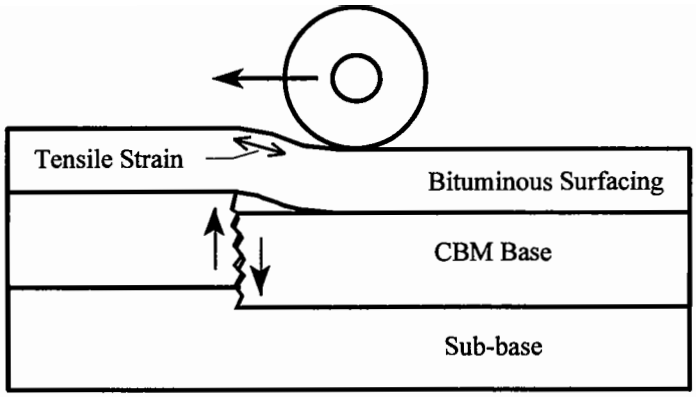

Figure 8.1. Model of a flexible composite pavement

The load used is a standard axle, giving a 40 kN wheel load. The equivalent foundation modulus is taken as 90 MPa/m, suggested [Mayhew and Harding, 1987] as equivalent to a crushed rock sub-base over a 5% CBR subgrade. A bituminous surfacing modulus of 4000 MPa is intended to be typical of standard materials at around 20°C. A load transfer efficiency of around 600 to 900 kPa/mm for the controlled cracking case is based on the field investigation in the present research and recent FWD tests. A value of 80 kPa/mm for the standard design represents an open crack with little load transfer capability. The results are as follows:

a) Standard design with 200 mm surfacing $\Rightarrow$ 76.1 microstrain in surfacing
b) Controlled cracking with 130 mm surfacing $\Rightarrow$ 73.7 microstrain in surfacing

In this instance, the saving indicated is at least 70 mm of bituminous surfacing, which would, if accurate, certainly be worth the effort required to produce the controlled cracking in the first place. However, this assumes that the CBM crack does not deteriorate significantly, and a higher shear stress (95 kPa) is calculated across the crack in case (b), compared with 78 kPa for case (a), as a consequence of the thinner bituminous layer. The effect of this stress on a crack is the subject of (ongoing) further research. The aim of the above examples is to give a comparison with a standard design, not to predict pavement life absolutely.

8.2.1 Pavement Life

To determine pavement life, the tensile strain (calculated above) can be used in a fatigue relationship. For bituminous materials, the fatigue relationship is generally expressed as given by the following equation (Eq. 8.1). This model gives the fatigue life to crack initiation [Read, 1996]:

$$N_i = k_1(\varepsilon)^{k_2} \tag{8.1}$$

where:

N_i : number of load applications to crack initiation (in the ITFT)

ε : tensile strain (microstrains) in the bituminous layer

k_1, k_2 : constants which are dependent on the bituminous mixture.

The values of material constants k_1 and k_2 for four different materials, determined through laboratory tests [Read, 1996], are given in Table 8.1. The materials include a conventional 20mm DBM (Dense Bitumen Macadam), a 28mm DBM (50Pen), a conventional 30/14 HRA (Hot Rolled Asphalt), and a SBS (Styrene Butadiene Styrene) modified 30/14 HRA.

For the determination of pavement life up to failure N_f, the value of N_i (from Eq. 8.1) needs to be multiplied by certain factors as shown in the following relation [Read, 1996]:

$$N_f = N_i \times (1.1) \times (20) \times SF_{cp} \tag{8.2}$$

In Eq. 8.2, N_f is the number of load applications to failure. The two factors 1.1 and 20 are given by Brunton [1983] to take into account the effects of lateral wander and rest periods between the load applications, respectively. SF_{cp} is the shift factor for crack propagation time to failure, and can be calculated by using a method described by Read [1996] in his doctoral thesis. For explanation, the factor of lateral wander is involved because the whole amount of traffic on a road does not follow a single (line) path. The rest periods are the time gaps between consecutive applications of wheel

loads, and are important as they allow time for cracks (in a bituminous layer) to heal, and stresses and strains to relax due to the viscous flow of the bitumen [Read, 1996]. The occurrence of the healing phenomenon is possible even on a very heavily trafficked road, when it is not subjected to frequent loading during night time.

Table 8.1. Material constants for different bituminous mixtures [Read, 1996]

Material	k_1	k_2
30/14 HRA	5.926×10^{13}	–3.788
20mm DBM	6.057×10^{13}	–4.032
28mm DBM (50Pen)	2.445×10^{13}	–3.922
30/14 HRA SBS Modified	1.294×10^{15}	–4.149

8.3 FINITE ELEMENT MODELLING

Analytical modelling of a pavement structure, with cracks induced in the CBM base, is also possible through a PC based finite element program 'CAPA' [Scarpas et al, 1993; Scarpas et al, 1996a]. Cracks introduce physical discontinuities in the otherwise homogeneous (assumed for engineering analysis purposes) body of the pavement. This phenomenon renders inappropriate the application of conventional continuum based layered analysis methods for studying stresses and strains [Scarpas et al, 1993]. The concept used in CAPA is that the discontinuity introduced by the cracks leads to the development of high tensile stress concentrations in the bituminous surfacing at a location over the tip of a crack in the CBM base (or an old existing pavement). These stresses lead to the mechanism of crack initiation and propagation into the surfacing. The mechanism assumes that the crack initiates from the base of the bituminous layer either at a location directly above the crack in the CBM (Figure 8.2a), which is realistic when the wheel position is centrally over the crack, or it can initiate from a location offset from the crack in the CBM (Figure 8.2b) [Scarpas et al, 1996a].

In CAPA, because of the generality of the finite element method, important parameters such as arbitrary geometry, boundary conditions, loading and interlayer bonding can be specified. Constitutive modelling is within the framework of the

theory of elasticity. Numerically integrated eight noded quadrilateral elements are used to model geometry of the pavement layers through a powerful mesh generator available within the CAPA program. Further details and other applications of the program can be found elsewhere [Scarpas et al, 1993, Scarpas et al, 1996a and 1996b; Gaarkeuken et al, 1996].

Cracks in the body of the pavement can be simulated by disconnecting the nodes of elements on either side of the crack propagation path (Figure 8.3). The crack region is subjected to shear and normal stresses under traffic loading. The magnitude of the compressive force normal to the crack face enables the friction mechanism to be developed at the crack interface [Tassios and Scarpas, 1987], shown in Figure 8.4, thus contributing to aggregate interlock. The phenomenon of load transfer is, therefore, modelled in CAPA by incorporating special crack interface elements (Figure 8.4) with appropriate values of normal stiffness D_{nc} and shear stiffness D_{ss}, which can be determined through laboratory experiments.

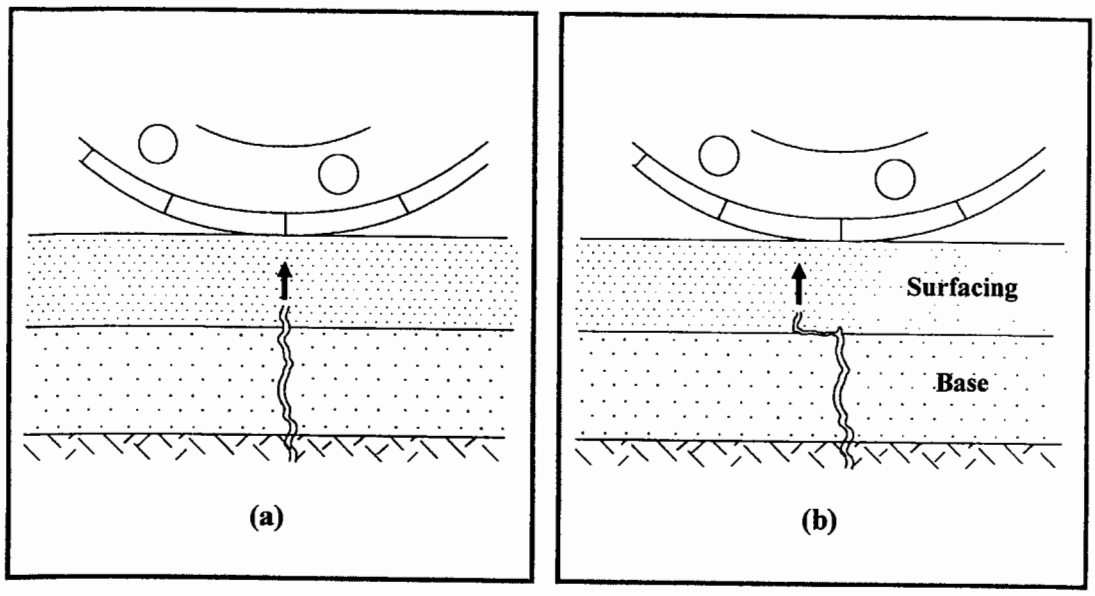

Figure 8.2. Mechanism of cracking in the bituminous layers [Scarpas et al, 1996]

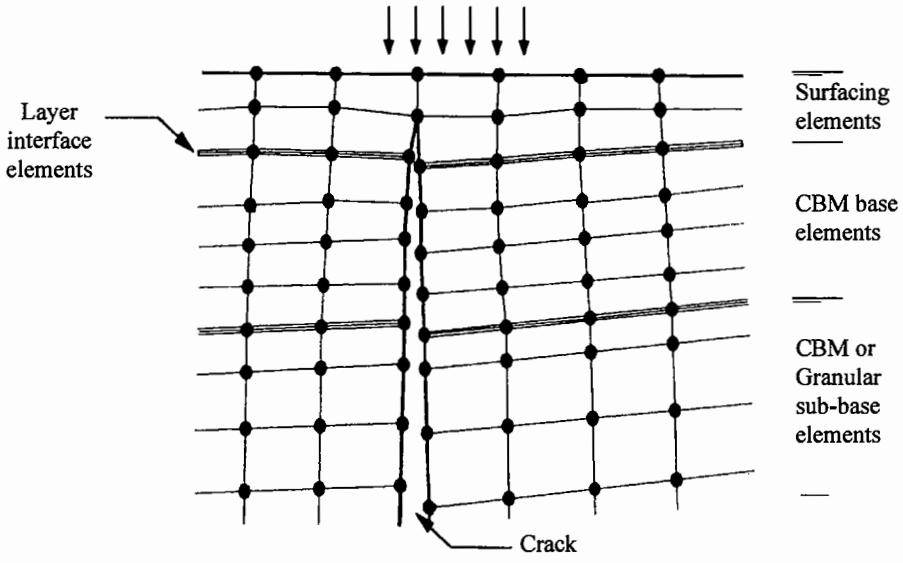

Figure 8.3. Finite element simulation for a crack in the pavement structure [Scarpas et al, 1996]

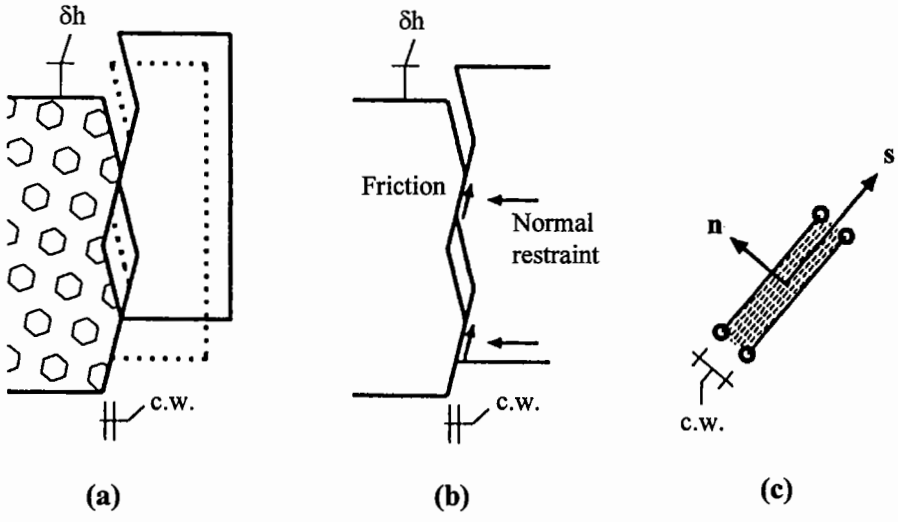

Figure 8.4. Crack interface idealization [Scarpas et al, 1993]

The successive layers in a pavement are seldom rigidly bonded to each other. Depending on the materials and construction methods used, some magnitude of interlayer slip is generally expected to occur. CAPA has the facility to model interlayer bonding by introducing interface elements of very small thickness (say 1mm) with certain values of normal stiffness D_{ni} and shear stiffness D_{tt}. It is reported

[Scarpas et al, 1996a] that the value of D_{tt} may range from 0.5 to 5.0 (MPa/mm). The value of D_{ni} , however, is equal to that of the stiffness of the interface material.

The parameters required in the analysis are:

- General mesh data: configuration of the elements, pavement layer thicknesses (mm), location and width of cracks (mm), boundary conditions
- Crack interface characteristics: smooth crack or aggregate interlock simulation
- Load transfer characteristics of crack, D_{nc}, D_{ss} (MPa/mm)
- Interface (interlayer bond) characteristics, D_{ni}, D_{tt} (MPa/mm)
- Overlay reinforcement properties (if applicable)
- Load characteristics: point load, distributed load, thermal load or any combination
- Elastic modulus (MPa), Poisson's ratio, and density (kg/m^3) of each pavement layer, that is bituminous surfacing, CBM base, granular (or CBM) sub-base, and subgrade.
- Thermal coefficients for materials in different layers of interest.
- Temperature difference (^oC) for different layers.

Within the context of the finite element method, crack extension requires a series of successive analyses, in each of which the mesh is progressively modified manually by disconnecting the nodes of elements on either side of the crack propagation path. In CAPA, an incorporated remeshing technique allows the system to automatically propagate the crack into the finite element mesh, starting from the initial cracked pavement configuration which is specified as input by the user. Meanwhile, the system computes, for each increment of the crack propagation, the necessary stress intensity factors at the crack tip.

Once the stress intensity factors are known, it is possible to compute the number of load repetitions necessary for the crack in the finite element mesh to propagate a distance Δc (MN in Figure 8.5) by using the Paris law [Scarpas et al, 1996a]:

$$\frac{dc}{dN} = A \times (K_{eq})^n \tag{8.3}$$

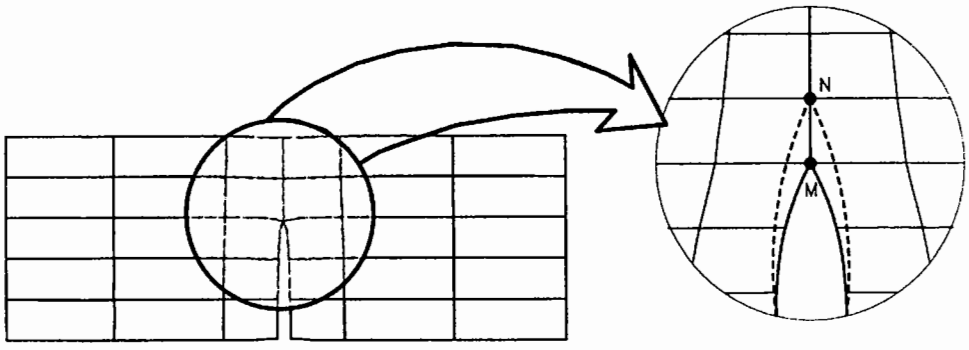

Figure 8.5. Crack propagation mechanism [Scarpas et al, 1996]

In Eq. 8.3, dc/dN is the crack growth rate. K_{eq} represents the equivalent stress intensity. The parameters 'A' and 'n' are material constants which can be determined from experimental measurements.

For the evaluation of Paris law parameters, a specimen is tested under cyclic loading in three or four point bending to determine the relation between the number of load repetitions (N) and crack opening displacement. The process of crack propagation in the same specimen, under monotonic load increments, is modelled by means of CAPA, to determine the corresponding stress intensity factors. The results of dc/dN and K are plotted on a double logarithmic graph. Then parameter 'n' is the slope of the curve, and 'A' is given by the intersection point on the dc/dN axis.

The K_{eq} can be calculated from the K_I and K_{II} (mode I and mode II) stress intensity factors through the following relation [Gaarkeuken et al, 1996]:

$$K_{eq} = K_I \cos^3(\theta/2) - 3K_{II} \cos^2(\theta/2)\sin(\theta/2) \tag{8.4}$$

where θ is the angle of crack extension (radians), and is calculated through iterations by using the following equation [Gaarkeuken et al, 1996]:

$$K_I \sin\theta + K_{II}(3\cos\theta - 1) = 0 \tag{8.5}$$

8.3.1 Modelling Examples

The pavement structure modelled in CAPA is shown in Figure 8.6. As examples, six different situations have been modelled including a standard UK design [DoT HD 26/94, 1994] for over 20 msa. In each case, the CBM base has been considered to be cracked (controlled or uncontrolled). Table 8.2 shows the materials properties used in the analysis, and Table 8.3 gives a description of the various pavement structures modelled.

The standard wheel load was simulated by placing a normally distributed load of 0.707 MPa at a location next to the crack in the CBM base (Figure 8.6). Only one load position was studied in these examples, although other positions at different distances from the crack axis need to be analysed, for a detailed study, in order to find out the most critical case. Thermal loading has not been considered in this study, as the length of the pavement structure modelled is only 3 metres. Figure 8.7 shows the general finite element mesh and boundary conditions for one of the various cases modelled.

Two crack widths, i.e. 0.5mm for controlled cracking and 1.5mm for natural cracking in a CBM base, have been modelled. These are accompanied by appropriate values of load transfer characteristics D_{ss} and D_{nc}. Shear stiffness (D_{ss}) values of 0.9 and 0.08 MPa/mm have been used corresponding to the situations for controlled and natural cracking, respectively, and are based on the information obtained from the FWD tests performed on different sites in this study. For the normal stiffness (D_{nc}), a value of 10000 MPa/mm was thought to be suitable from the view point of analysis.

An interface (interlayer bond) of 1.0 mm thickness has been included between any two of the top three pavement layers. The properties of this layer in terms of normal stiffness (D_{ni}) and shear stiffness (D_{tt}) have been used in the analysis. The value of D_{tt} used is 1.0 MPa/mm for the interface between the two CBM layers, and between the bituminous and CBM layers [Gaarkeuken et al, 1996]. For the interface between the CBM and granular layers, the value used is 1.5 MPa/mm, assuming a slightly higher friction in this case. For D_{ni} a value of 4000 MPa/mm was considered to be appropriate in modelling.

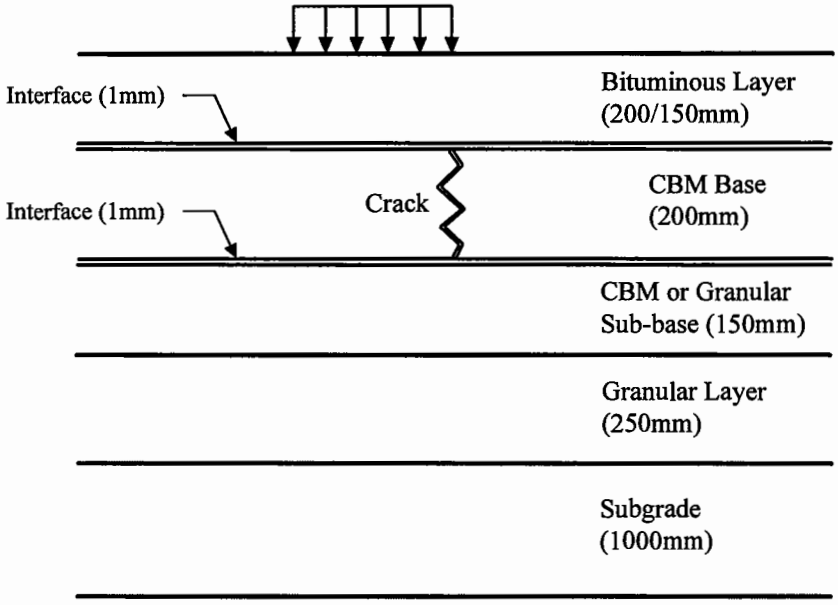

Figure 8.6. Pavement structure modelled in CAPA

Table 8.2. Material properties used for the pavement models

Pavement Layer	Material Description	Stiffness (MPa)	Poisson's Ratio
Surfacing	Bituminous	4000	0.4
Base	CBM4	20000	0.15
Upper Sub-base	CBM2	10000	0.2
	Granular	150	0.3
Lower Sub-base	Granular	100	0.3
Subgrade	Soil	50	0.45

Table 8.3. Description of the pavement structures modelled in CAPA

Description	Pavement Layer Thickness (mm)					
	Controlled Cracking				Natural Cracking	
	Case 1	Case 2	Case 3	Case 4	Case 5	Case 6
Surfacing	200	150	200	150	200	150
Base (CBM4)	200	200	200	200	200	200
Sub-base (CBM2)	—	—	150	150	—	—
Sub-base (Granular)	150	150	—	—	150	150
Granular	250	250	250	250	250	250
Subgrade	1000	1000	1000	1000	1000	1000

In these analyses, stress intensity factors K_I and K_{II} were determined through CAPA. Then by using Eqs. 8.4 and 8.5, K_{eq} was calculated. The number of load applications for each increment of crack propagation was computed from Eq. 8.3. The sum of the load applications from all crack propagation increments represented the life of a pavement until the occurrence of reflective cracking. The results are shown in Table 8.4. It is vitally important to note here that the results presented are based on assumed values for the Paris law parameters ($A = 1\times10^{-7}$ and $n = 4$) used in Eq. 8.3. These values were used by Gaarkeuken et al [1996] in their analysis for the case of a Dutch road (A50). It is therefore recommended that, for further research, the values for 'A' and 'n' should be determined from experimental measurements.

The main objective of the results shown in Table 8.4 is to compare the performance of various types of pavement structure, rather than the absolute values of pavement life. The performance of Case 2, with controlled cracking in the CBM4 base and overlaid by a 150mm surfacing layer, has been found to be much superior to Case 5 which is a standard design (200mm surfacing over 200mm CBM4 base) with uncontrolled cracking. The pavement structures with an upper CBM2 sub-base (Cases 3 and 4) have shown better performance compared to those with a granular sub-base.

It appears that a saving of around 50 to 70mm of bituminous surfacing (as mentioned in Section 8.2) is likely to result from the use of controlled cracking in CBM base. However, the actual amount of the saving in thickness can vary and is dependent on the pavement structure.

Table 8.4. Pavement life until the occurrence of reflective cracking

Pavement Structure	Life (msa)
Case 1	55.8
Case 2	36.7
Case 3	76.2
Case 4	43.0
Case 5	31.0
Case 6	15.7

Besides the analytical calculations, graphically controlled presentation facilities available in CAPA enable to concentrate on the design aspects rather than on data handling and reduction. With these facilities, multicolour screen and hard copy plots of stresses and deformations can be obtained. For example, Figure 8.8 shows deformation (on a magnified scale) of a flexible composite pavement structure when the wheel load position is over the centre of a crack in CBM base. Figure 8.9 shows a situation modelled, when the position of wheel load is next to the crack in the CBM. In addition, the phenomenon of propagation of the crack, in a CBM base, through bituminous surfacing (upper seven rows of elements) can be seen in Figure 8.9. In this particular case, the crack propagation has progressed up to 5th increment (i.e. 5th row of elements). The crack propagation phenomenon is also illustrated in Figure 8.10, which indicates the progress of the crack up to 3rd increment.

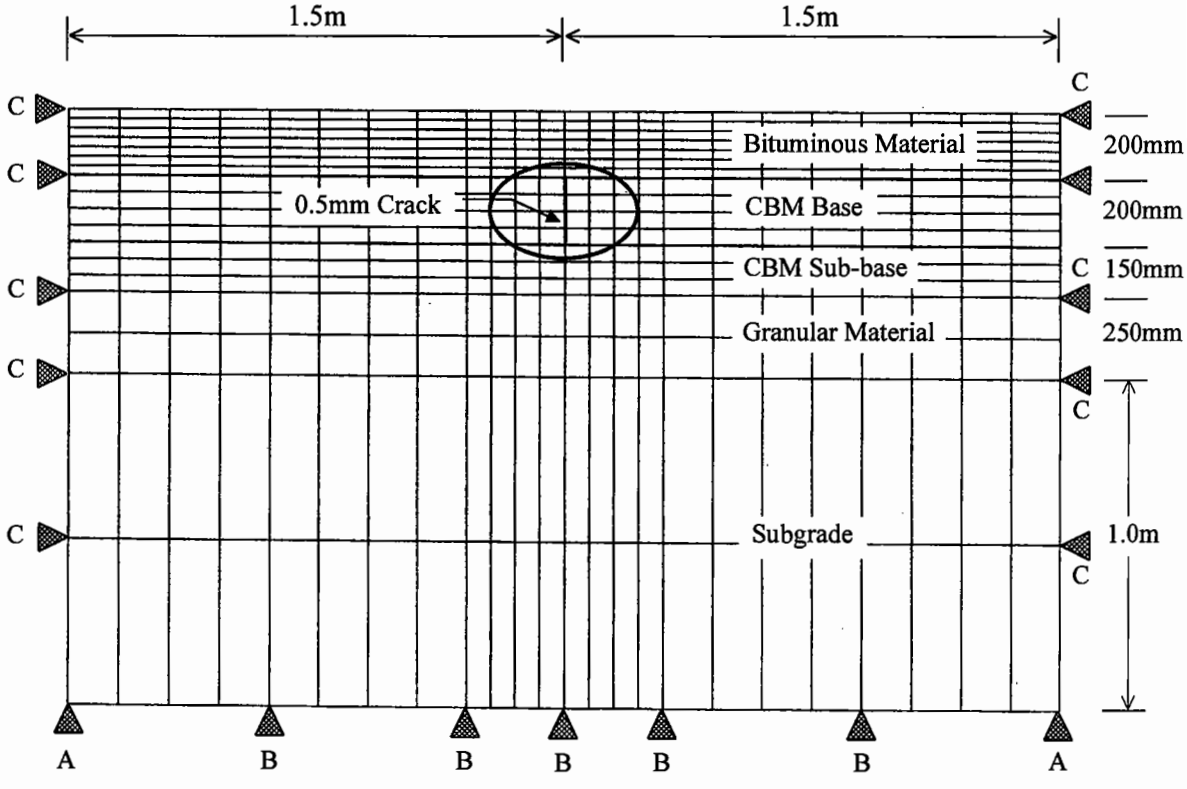

Figure 8.7. Finite element mesh for the pavement structure modelled

Boundary Conditions
Support **A** (Hinge) : Both vertical and horizontal displacements restrained
Support **B** (Roller) : Vertical displacement restrained
Support **C** (Roller) : Horizontal (outward) displacement restrained

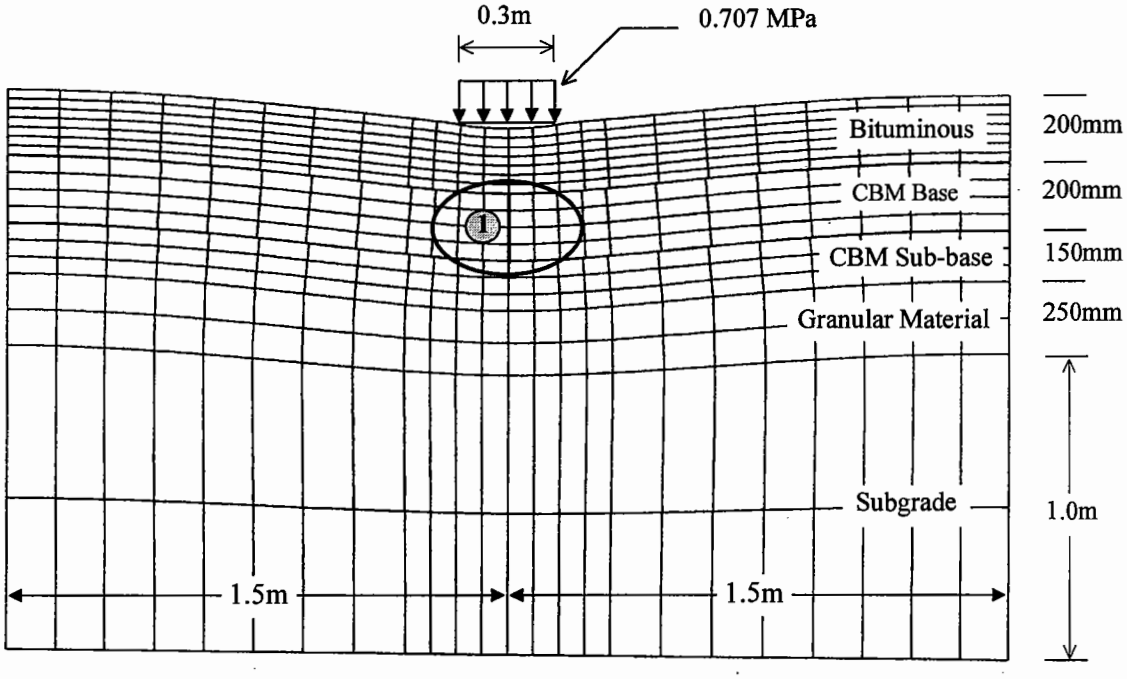

Figure 8.8. Graphical representation of the (deformed) pavement structure, when the position of wheel load is over the centre of a crack in CBM base

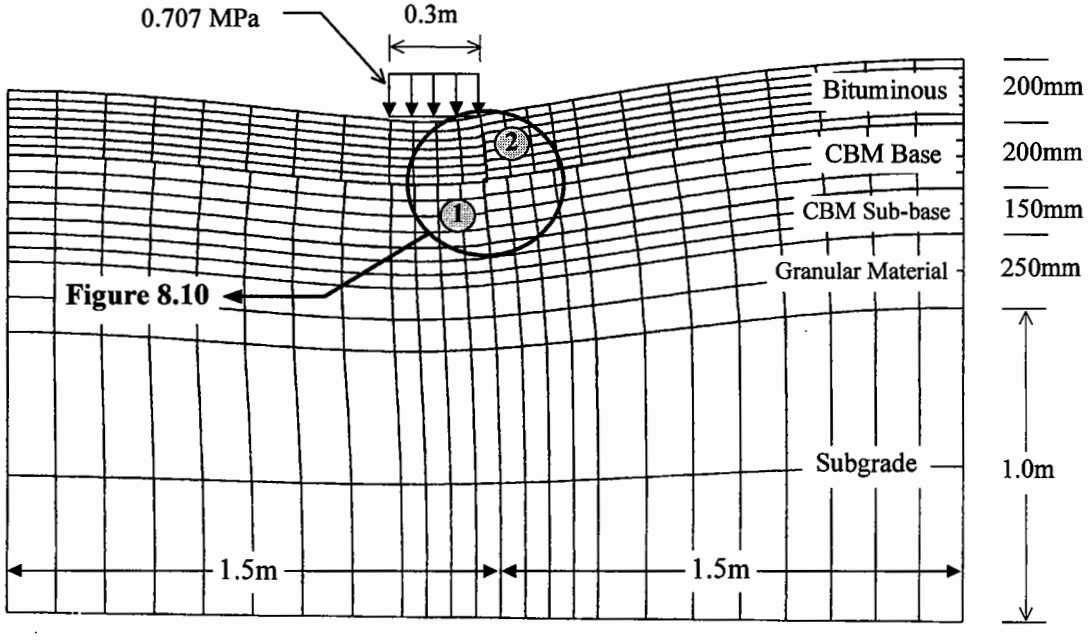

Figure 8.9. Graphical representation of the (deformed) pavement structure, when the position of wheel load is on one side of the crack in CBM base

(1) Controlled (0.5mm) or uncontrolled (1.5mm) crack in CBM base

(2) Propagation of the crack in a CBM base through bituminous surfacing elements

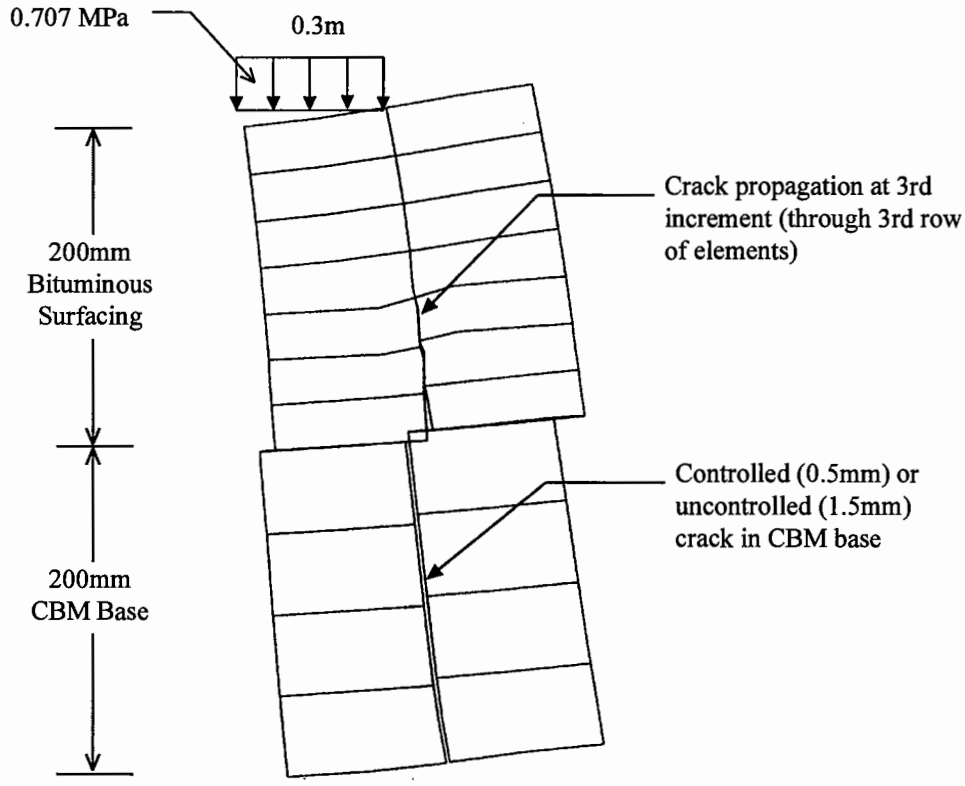

Figure 8.10. Finite element modelling of crack propagation through bituminous surfacing (as a result of the movement of the crack in CBM base)

8.4 DESIGN PROCEDURE

The various stages which should logically be considered in the analysis of a flexible composite pavement, are shown in the flow diagram (Figure 8.11). Pavement design implies an iterative use of the analysis procedure.

The fracture characteristics for various pavement layers demand careful attention in the design procedure. In particular, the thickness of a CBM base should be carefully selected to ensure that the combination of maximum tensile stresses due to thermal and traffic loading do not exceed the fatigue strength. If the tensile stresses are higher, the base may crack under a single load application. Similarly, the thicknesses of the various components need to be suitably selected to ensure that critical stresses and strains are maintained within limits.

Traffic load characteristics need to be considered, such as vehicle or aircraft loading, axle and wheel loads, spacing of dual tyres, their configuration, and contact pressure. All these parameters are important to calculate stresses.

Temperature distribution with depth influences thermal stresses which may be developed in various pavement layers. The stiffness of a bituminous material is dependent on temperature, which in turn influences the magnitude of stresses, due to traffic loads, being transmitted into the CBM base.

Subgrade properties should be carefully determined. Stiffness modulus of a subgrade can be directly assessed by using recently developed in-situ measuring devices [Shahid et al, 1997; Fleming et al, 1995; Brown (A.J.), et al, 1993], or it can be roughly estimated from CBR through the following relation [DoT, HD 25/94, 1994], which is only valid for CBR values between 2 to 12%:

$$E = 17.6 \times (CBR)^{0.64} \tag{8.6}$$

In Eq. 8.6, E is stiffness modulus (MPa). Poisson's ratio for subgrades ranges from 0.5 [Brown et al, 1987; Mitchell and Monismith, 1977] for saturated clays to 0.35 [Mitchell and Monismith, 1977] for sands. A value of 0.3 is recommended for a typical granular material by the Highways Agency [DoT, HD 25/94, 1994]. Small changes in the values of Poisson's ratio for subgrade do not show a significant effect upon the stresses developed in the upper layers. From a number of structural analyses, it has been shown [Mitchell and Monismith, 1977] that for a decrease in the subgrade's Poisson's ratio from 0.5 to 0.3, the tensile strains in a cemented base reduce by not more than 10 percent.

Depending on the performance characteristics of materials, in different layers, the final design would be selected and must be checked for the occurrence of reflective cracking by using at least one of the techniques described in this chapter.

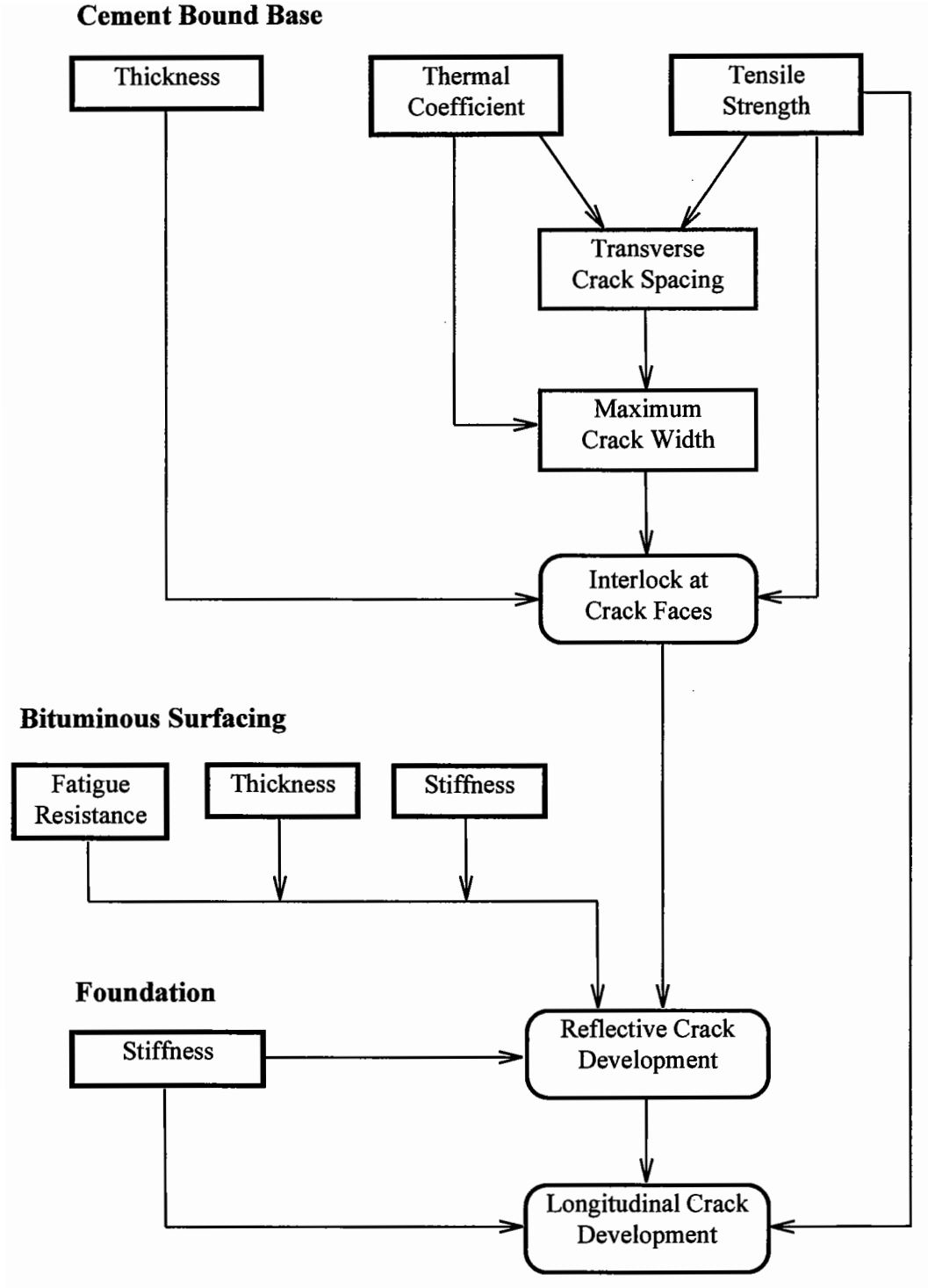

Figure 8.11. Flow diagram for flexible composite pavement analysis

8.5 SUMMARY

Two techniques have been presented for analytical modelling of a pavement structure with a cracked (controlled or uncontrolled) CBM base, to predict reflective crack development and/or pavement life under traffic and thermal loading. The first one is based on a simplified approach, and gives the magnitude of tensile strain in the bituminous surfacing over the crack tip. This strain can be related to pavement life by using a fatigue model. The second one is based on a finite element program CAPA, and involves a relatively greater number of variables. The main output results include the magnitudes of stress intensity factors for several increments of crack propagation, and the values for stress (tensile and compressive) and deformation corresponding to any selected elements. The stress intensity factors can be related to pavement life before the occurrence of reflective cracking through the appropriate crack propagation models. In both the techniques, the key role of the load transfer characteristics of cracks in the CBM base is dominant in the phenomenon of reflective crack development.

The results of analytical modelling suggest the following important points:

- Both the techniques presented can be used satisfactorily to predict the occurrence of reflective crack in pavements.
- Controlled cracking in a CBM base has the potential to reduce around 50 to 70mm of bituminous thickness. The actual amount of saving in thickness may vary depending on the pavement structure.
- A pavement structure with a CBM base over a CBM sub-base has shown a relatively improved performance in delaying reflective cracking, for a given bituminous surfacing thickness, compared to that with a granular sub-base.

In the flexible composite pavement design, for avoiding traffic induced cracking, the thickness of a CBM base should be carefully selected to ensure that the combination of the maximum tensile stresses due to thermal and traffic loading does not exceed the fatigue strength.

9 Conclusions and Recommendations

9.1 CONCLUSIONS

A summary of the main conclusions drawn from the literature review (Chapter 1) and the experimental work presented in this thesis is as follows:

9.1.1 Cracking in Cement Bound Base Roads (Literature : Chapter 1)

Shrinkage in a cement bound base is caused by the combined effect of hydration of cement, drying of a CBM, the amount of temperature drop, and thermal properties of aggregate. Maximum shrinkage stresses are developed during an early stage of 40 to 100 hours after construction. The stresses are highly localized on the exposed surface, and decrease sharply with depth.

Cracking occurs when the stresses, induced by shrinkage and traffic, exceed the tensile strength of a CBM base. It can be divided into two types. Primary cracking, which appears in the form of transverse cracks due to shrinkage and thermal effects, initiates at the weakest locations in a CBM layer. Crack spacing ranges from 3 to 50 metres depending on the CBM type and strength. Secondary cracking is the occurrence of longitudinal wheel-path cracks due to traffic loading, and includes the deterioration of primary cracks. This cracking is responsible for a significant reduction in the stiffness (i.e. elastic modulus) of a CBM base, and substantial damage to the structural integrity of a pavement. Under excessive relative horizontal and vertical movements, the cracks in a CBM base propagate through the bituminous surfacing, thus allowing the ingress of water, and leading to early failure of the pavement structure.

9.1.2 Sensitivity of the Mix Design for CBMs (Chapter 2)

The mix design of a cement bound material (CBM) is found to be particularly sensitive to variations in water content and aggregate grading. In particular, a mix

water content on the wet side of optimum is a matter of serious concern, because a very small increase, such as 0.5% above the optimum, is enough to cause a significant reduction in the strength properties for gravel sand CBMs (CBM3 and above). Limestone CBMs, however, are found to be comparatively less sensitive to such small variations, suggesting that the reduction in strength due to increased water content may be a function of the cleanliness of aggregate. This reduction of strength is possibly due to the loss of cement paste which is pumped out of the wetter mixes under vibration. The amount of escaped paste is, however, too small to affect the CBM density. From an economic aspect, with increased water content, a CBM mix requires a higher cement content, for a given strength.

A change in the cement content directly affects the CBM strength, but its effect on density is less significant. The amount of compactive effort, at optimum water content, is relatively greater for a crushed limestone CBM, than for a gravel sand CBM to achieve their respective target densities.

9.1.3 Direct Tensile Test (Chapter 3)

The direct tensile test, described in this research, provides a reasonably accurate measurement for the tensile strength and elastic stiffness of CBMs. The indirect tensile tests (flexural and cylinder splitting) overestimate the magnitude of tensile strength due to unrealistic assumptions made and the complex stress distribution involved. A study of strain distribution in the direct tensile test has shown that the central part of the specimen is subjected to the most critical, but also uniform, stress conditions, developing relatively consistent strains. This is also confirmed by the failure, within this part, of a majority of the CBM specimens tested under direct tension.

The lifting system, developed for this test, has been found to be satisfactory in applying an axial tensile force without causing the occurrence of flexural stresses in the specimen. The stress strain relationship under direct tension is linear almost up to failure, but that in compression is generally linear only for a stress level up to some proportion of the ultimate strength, after which it becomes non-linear.

9.1.4 Mechanical Properties of CBMs (Chapter 4)

The strength properties of CBMs are found to be sensitive to variations in mix water content and degree of compaction, for a given cement content, to a greater degree than the elastic stiffness. Tensile strength is strongly dependent on the aggregate type, aggregate grading, degree of compaction, cement content, and age of a CBM. Physical properties of an aggregate, such as surface texture and angularity, are more important than its inherent strength. For a given cement content, the use of a crushed aggregate leads to an increased tensile strength.

The inter-relationships of strength properties indicate that the direct tensile strength is, on average, 75% of the cylinder splitting strength, and 11% of the cylinder compressive strength. The 28 day direct tensile strength is one-tenth of the 7 day cube compressive strength, or 7.7% of the 28 day cube strength. The cylinder compressive strength is 68% of the cube compressive strength. The ratio between the cube compressive strengths at 7 and 28 days is 76%. The estimated in-situ cube strength measured from cores is approximately 67% of the cube compressive strength from prepared specimens. The core splitting strength is 68% of the splitting strength measured from the prepared cylindrical specimens.

Elastic stiffness is a function of the type and quality of aggregate, and increases with an increase in the CBM strength. The values of stiffness in tension and in compression are equal. The elastic stiffness can be related to various strength properties. The correlations, presented in this thesis, relate the stiffness in tension with direct tensile strength, cylinder compressive strength, and cube compressive strength.

Poisson's ratio is a function of the aggregate grading and cement content. The values range from 0.14 to 0.19 for gravel sand CBMs, and from 0.19 to 0.24 for limestone CBMs (with relatively less cement). Fatigue behaviour of CBMs (grade CBM3 and above), in direct tension, indicates that a fatigue strength of 60% of the static tensile strength may be considered as the endurance limit (for 10 million cycles). The ratio of fatigue strength to static strength is independent of the type of aggregate, cement content, age at loading, and testing method.

9.1.5 Controlled Cracking of CBM Bases (Chapter 5)

The controlled cracking system, described in this thesis, successfully led to the formation of regular transverse cracks in CBM bases of widths less than 0.5 mm, whereas the width of natural cracking was found to be typically more than 1.0 mm. The induced cracks showed greatly superior load transfer characteristics (measured by the Falling Weight Deflectometer) to those of the natural cracks. The effective stiffness modulus of CBM at a controlled crack location was found to be only marginally less than that of the intact material. This was not the case with naturally occurring cracks. The performance data suggests that the improvement is due to better aggregate interlock between the crack faces. The expectation is that controlled cracking will have significant benefit in reducing reflective crack development.

9.1.6 Steel Fibre Reinforced CBM Bases (Chapter 6)

A study of steel fibre reinforcement at 1% (by volume) has shown an increase of 33% in the direct tensile strength of CBMs. The cube compressive strength is negligibly affected, but the cylinder compressive strength is increased by 12%. The magnitudes of elastic stiffness, under direct tension and compression, remain equal and unaffected by the fibre reinforcement.

In steel fibre reinforced (SFR) CBM, the "first crack strength" corresponds to the onset of cracking. The "ultimate strength" for a CBM5 with 1% steel fibre content, from indirect tensile testing, is typically 38% greater. The cracks in a SFR CBM are initially observed to be of negligible width, and the expected in-situ result, following material shrinkage, is a relatively large number of tightly closed cracks.

Steel fibre reinforcement is expected to prevent reflective cracking in flexible composite pavements, because crack propagation through a bituminous surfacing has been shown to be dependent on the degree of relative movement at cracks which, in the case of SFR CBM, is restricted. At the same time, the increased tensile strength of the SFR CBMs can provide extra safety against longitudinal cracking, thus demonstrating the potential of introducing an economic and durable structural design,

for flexible composite pavements, by minimizing the thicknesses of bituminous surfacing as well as the CBM base.

9.1.7 Load Transfer Characteristics of Cracks in CBM Bases (Chapter 7)

The load transfer at cracks is a function of the CBM strength and improves from lower to higher CBM categories. Under traffic loading, the magnitude of both the differential vertical and horizontal movements increases with an increase of the crack width, and is also influenced by the shape of aggregate. Crack degradation, due to repeated loading, is a function of the tensile strength of a CBM and crack width. The deterioration rate is found to be higher for CBMs with relatively low tensile strength. Steel fibre reinforced CBMs have shown a significantly improved load transfer, with a reduced amount of (vertical and horizontal) crack movement, and reduced crack degradation.

Crack propagation through a bituminous surfacing is greatly influenced by the amount of differential vertical and horizontal movement of the crack in the CBM base. The crack initiates from the top of the bituminous surfacing, almost above that in the CBM, and progresses downward. Thereafter, another crack is initiated at the bottom, which propagates upward, and sometimes dominates the first one. Although the differential vertical and horizontal movements across a crack in the CBM base are significantly reduced after a bituminous surfacing is laid, but the degradation rate remains sensitive to its width.

9.1.8 Analytical Modelling and Design Implication (Chapter 8)

The two techniques presented, one based on simplified analytical models and the other based on a finite element program CAPA, are found to be capable of modelling a pavement structure with a cracked (controlled or uncontrolled) CBM base, to predict reflective crack development and/or pavement life under traffic and thermal loading.

The results of analytical modelling suggest that controlled cracking in a CBM base has the potential to reduce the thickness of bituminous surfacing approximately in the range 50 to 70mm. The actual amount of reduction in thickness may vary depending

on the pavement structure. This is because among the various pavement structures modelled, for a given surfacing thickness, a pavement with a CBM base over a CBM sub-base has shown a relatively better performance in delaying reflective cracking, compared to that with a granular sub-base.

9.2 RECOMMENDATIONS

Based on the experience and evidence presented in this thesis, the following recommendations are made:

9.2.1 Improved Analytical Design for Flexible Composite Pavements

In pavement technology, particularly in the field of flexible composite pavements, new construction techniques, such as controlled cracking and steel fibre reinforcement in cement bound bases, have been developed and, to some extent, investigated for their long term performance. The missing element, required to permit optimised implementation of these methods, is a rational pavement design approach which would predict realistic pavement failure modes.

It is, therefore, strongly recommended that a rationally based set of pavement performance models, leading to an economic design method for flexible composite pavements, be developed by making use of the fundamental material properties which can be specified using performance related tests. Many of the building blocks are already in place for this development in the materials research presented in this thesis. But in order to complete the remainder of the process, a comprehensive analysis needs to be carried out before the design stage. Experience from real roads should also be studied. Modelling will involve the sensible use of crack propagation equations to predict the life of a pavement before the occurrence of reflective cracking. One of the useful tools which can be used for analytical modelling would be the finite element program CAPA. The guiding principle will be that the models should be fundamentally based, that is to say they should take into account each actual way in which pavements deteriorate.

9.2.2 Shear Resistance at Cracks

Further laboratory and field work is required, particularly regarding shear resistance due to 'interlock' across controlled cracks in real pavements, as well as scaled down pavement tests. The main reason is that the occurrence of reflective cracking depends on interlock at the induced cracks in a CBM base, in addition to other factors, such as: asphalt stiffness, thickness and fatigue resistance, and foundation stiffness. The interlock depends on the CBM strength, thickness and crack opening, itself a function of crack spacing and thermal expansion coefficient.

As a guideline, in addition to laboratory specimens, in-situ (beam or cube) specimens could be sawn from CBM roadbases at typical controlled crack locations, which would make the investigation realistic. These specimens should be subjected to repeated stress applications of different magnitudes. The testing should be continued up to some millions of cycles. The important parameters, which need to be recorded in relation to number of load repetitions, will include: magnitude of the interlock shear resistance, rate of damage, and relative differential movement at the induced crack.

9.2.3 Study of Reflective Cracking

The study of reflective cracking, presented in Chapter 7 of this thesis, involved the use of a single thickness from one type of DBM material. Using the same test system, further investigation is recommended to determine the effects of different thicknesses and types of bituminous surfacing, including polymer modified asphalt, upon the rate of crack propagation. This study needs to include different widths of crack induced in CBM slabs comprising crushed and uncrushed aggregate.

The experimental data, in combination with the information from full scale field trials currently being carried out by the Transport Research Laboratory on behalf of the Highways Agency, can then be analysed to develop pavement life prediction models before the occurrence of reflective cracking.

9.2.4 Mechanism of Fatigue Cracking

The fundamental mechanism involved in fatigue cracking of CBM under direct tension is not very clear. Further work is needed to study this mechanism, and the aspects of strain accumulation when the specimens are subjected to repeated loading in tension. The best fatigue test system is now available in the form of a direct tensile test. The measured properties could then be incorporated into mathematical models of fatigue behaviour.

9.2.5 Mechanical Properties of CBMs with Slag/Fly-ash/Lime

Slag, fly-ash and lime are extensively used in France, in varying proportions, as a part-replacement to cement in hydraulically bound roadbases of relatively low strength, roughly up to a CBM3 grade after a few weeks. The use of these materials is cost effective, and is also advantageous for environmental reasons. There is quite a high potential for using these materials in different proportions and combinations to replace some proportion of cement (may be in the range 1 to 3%), depending on the type of material processed, in UK CBMs. Besides saving cement, the use of these materials can also reduce primary shrinkage of CBMs.

A detailed investigation would be needed to evaluate the effects of using varying proportions and combinations of slag, fly-ash and lime upon the mix design for CBMs with different aggregate types and gradings. The next stage should include a detailed study of the resulting mechanical characteristics under static and repeated loading, particularly the stress strain behaviour under direct tension.

References

ACI 209R-92, "Prediction of creep, shrinkage, and temperature effects in concrete structures," ACI Manual of Concrete Practice Part 1: Materials and General Properties of Concrete, Michigan, 1994.

ACI Committee 544.1R., "State of the art report on fibre reinforced concrete," American Concrete Institute, Detroit, May 1982, Reapproved 1986, pp 9-30.

ACI COMMITTEE 544.2R., "Measurement of properties of fibre reinforced concrete," American Concrete Institute, Detroit, Nov./Dec. 1988, pp 583-593.

ACI COMMITTEE 544.4R., "Design considerations for steel fibre reinforced concrete," American Concrete Institute, Detroit, Sept./Oct. 1988, pp 563-580.

Alberola, R. and Gordillo, J., "Treatment of cracks in semi-rigid pavement: cold microsurfacing with modified bitumen emulsion and fibres: Spanish experience," Proc. Second International RILEM Conference on Reflective Cracking in Pavements, Liege, 1993, pp 282-289.

Anagnos, J.N., Kennedy, T.W. and Hudson, W.R., "Evaluation and prediction of tensile properties of cement treated materials," Research Report No. 98-8, Centre for Highway Research, University of Texas at Austin, Oct. 1970.

Andrews, W.P., "Soil-cement roads," 3rd edition, Cement and Concrete Association, Slough, 1955.

Assimacopoulos, B.M., Warner R.F. and Ekberg, C.E., "High speed fatigue tests on small specimens of plain concrete," Journal Prestressed Concrete Institution, September 1959, pp 53-70.

ASTM Standards C 150-94, "Specifications for Portland Cement," 1994.

ASTM Standards C 496-90, "Test for splitting tensile strength of cylindrical concrete specimens," 1990.

Bernal, J.D., "The structures of cement hydration compounds," Proc. 3rd International Symposium on the Chemistry of Cement, London, 1952, pp 216-236.

Biesenbach, W.J., "Cement treated bases in the Cape Province," NIRR-PCI Symposium on cement-treated crusher-run bases, Johannesburg, 1973.

Blake, L.S., "Lean mix concrete bases," The Surveyor, No. 117 (3446), London, 1958, pp 484-485.

Blight, G.E., "Fracture of pavement materials," ASCE Transportation Engineering Journal, TE 4, November 1973, pp 801-817.

Bloem, D.L., "Effect of maximum size of aggregate on strength of concrete," National Sand and Gravel Association, Circular No. 74, Washington DC, Feb. 1959.

Bloem, D.L. and Gaynor, R.D., "Effects of aggregate properties on strength of concrete," Journal, American Concrete Institute, Oct. 1963, pp 1429-1455.

Bofinger, H.E., "The measurement of the tensile properties of soil-cement," Laboratory Report 365, Road Research Laboratory, Crowthorne, 1970.

Bofinger, H.E. and Sullivan, G.A., "An investigation of cracking in soil-cement bases," Laboratory Report 379, Road Research Laboratory, Crowthorne, 1971.

Bogue, R.H. and Lerch, W., "Hydration of Portland cement compounds," Industrial and Engineering Chemistry, No. 8, Easton, 1934, pp 837-847.

Bondt, A.H. and Saathof, L.E.B., "Movements of a cracked semi-rigid pavement structure," Proc. 2nd International RILEM Conference on Reflective Cracking in Pavements, E & FN Spon, London, 1993, pp 449-457.

Bonnell, D.G.R. and Harper, F.C., "The thermal expansion of concrete," National Building Studies, Technical Paper No. 7, London, 1951.

Bonnell, D.G.R. and Harper, F.C., "Thermal expansion of concrete," Proc. Institution of Civil Engineers, 33 (4), London, 1950, pp 320-330.

Bonnot, J., "Assessing the properties of materials for the structural design of pavements," Proc. 3rd International Conference on Structural Design of Asphalt Pavements, London, 1972, Vol. 1, pp 200-213.

Bonnot, J. and Paute, J.L., "Renouveau des assises de chaussées en grave-cément," Annales de L'Institut Technique du Bâtiment et des Travaux Publics, No. 345, 1976, pp 26-44.

Brengarth, M. and Roche, J.P., "The behaviour of gravel-cement pavements constructed since 1966 in South-Western France," Bull. liaison Labo. P. et Ch., No. 99, Jan./Feb., 1979.

British Standards Institution, "Specifications for Portland cements," BS 12: 1991.

British Standards Institution, "Method for making test cubes from fresh concrete," BS 1881: Part 108: 1983.

British Standards Institution, "Method for making test cylinders from fresh concrete," BS 1881: Part 110: 1983.

British Standards Institution, "Method of normal curing of test specimens (20°C method)," BS 1881: Part 111: 1983.

British Standards Institution, "Method for determination of tensile splitting strength," BS 1881: Part 117: 1983.

British Standards Institution., "Method for determination of flexural strength," BS 1881: Part 118: 1983.

British Standards Institution, "Method for determination of the compressive strength of concrete cores," BS 1881: Part 120: 1983.

British Standards Institution, "Method for determination of static modulus of elasticity in compression," BS 1881: Part 121: 1983.

British Standards Institution., "Aggregates from natural sources for concrete," British Standard Specification, BS 882: 1983.

British Standards Institution., "Determination of particle size distribution," Section 9, BS 1377: Part 2: 1990.

British Standards Institution., "General requirements, sampling, sample preparation and tests on materials before stabilization," Stabilized Materials for Civil Engineering Purposes, BS 1924: Part 1: 1990.

British Standards Institution., "Methods of test for cement-stabilized and lime-stabilized materials," Stabilized Materials for Civil Engineering Purposes, Section 2, BS 1924: Part 2: 1990.

British Standards Institution, "Coated macadams for roads and other paved areas," Specification for constituent materials and for mixtures, BS 4987: Part 1: 1993.

British Standards Institution, "Method for the determination of the indirect tensile stiffness modulus of bituminous materials," Draft for Development 213, 1993.

Brooks, J.A., "The design of pavements for heavily trafficked high-speed roads," Quarry Manager Journal, 56 (1), 1972, pp 21-29.

Brown, A.J., Rogers, C.D.F. and Thom, N.H., "Field assessment of road foundations," Final Report submitted to TRL, July 1993.

Brown, L.S. and Carlson, R.W., "Petrographic studies of hydrated cements," Proc. ASTM, 36, Part II, 1936, pp 332-350.

Brown, S.F., "Design of pavements with lean concrete bases," Transport Research Record, No. 725, 1979, pp 51-58.

Brown, S.F., Gibb, J.M., Read, J.M., Scholz, T.V., and Cooper, K.E., "Design and testing of bituminous mixtures," Research Report, submitted to Department of Transport - EPSRC Link Programme on Transport Infrastructure and Operations, Volume 2, January 1995.

Brown, S.F., Hughes, D.A.B. and Brodrick, B.V., "Grid reinforcement for asphalt pavements," Report No. 3, Submitted to Netlon Ltd. and SERC, June 1985.

Brown, S.F., Loach, S.C. and Reilly, M.P.O., "Repeated loading of fine grained soils," Contractor Report 72, Transport and Road Research Laboratory, Crowthorne, 1987.

Brown, S.F., Tam, W.S. and Brunton, J.M., "Structural evaluation and overlay design: Analysis and implementation," Proc. 6th International Conference on the Structural Design of Asphalt Pavements, Ann Arbor, Vol. 1, 1987, pp 1013-1028.

Brown, S.F., Thom, N.H. and Brodrick, B.V., "The behaviour of pavements with lean concrete bases," Report PGR 93008 submitted to SERC, University of Nottingham, 1993.

Brunauer, S., Skalny, J., Odler, I. and Yudenfreund, M., "Hardened Portland cement pastes of low porosity, VII, Further remarks about early hydration, Composition and surface area of tobermorite gel, Summary," Cement and Concrete Research, No. 3, May 1973, pp 279-294.

Brunton, J.M., "Developments in the analytical design of asphalt pavements using computers," PhD thesis, University of Nottingham, 1983.

Bullman, J.N., "Soil stabilization in Africa," TRRL Report LR 476, Transport and Road Research Laboratory, Crowthorne, 1972.

Burt, A.R., "M4 motorway, a composite pavement: surface cracking," Highways and Transportation Journal, Institution of Highways and Transportation, December 1987, pp 16-19.

Bye, G.C., "Portland cement: Composition, Production and Properties," Pergamon Press, Oxford, 1983.

Caltabiano, M.A., "Reflection cracking in asphalt overlays," Thesis, University of Nottingham, 1990.

Catton, M.D., "Research on the physical relations of soil and soil-cement mixtures," Highway Research Board Proc., Vol. 20, 1940, pp 821-855.

Cauley, R.F. and Kennedy, T.W., "Proposal for improved tensile strength of cement treated materials," Highway Research Record, No. 442, Washington DC, 1973.

Coetzee, N.F. and Monismith, C.L., "Reflection cracking: Analysis, laboratory studies and design considerations," Association of Asphalt Paving Technologists, Volume 49, 1980.

Colombier, G. and Marchand, J.P., "The precracking of pavement underlays incorporating hydraulic binders," Proc. 2nd International RILEM Conference on Reflective Cracking in Pavements, E & FN Spon, London, 1993, pp 273-281.

Colombier, G., et al., "Fissuration de retrait des chausées à assises traitées aux liants hydrauliques," Bull. Liaison Lab., des Ponts et Chausées, No. 156, pp 37-66, et No. 157, 1988, pp 59-87.

Copeland, L.E., "Specific volume of evaporable water in hardened Portland cement pastes," Journal of American Concrete Institute, 1956, pp 863-874.

Copeland, L.E. and Bragg, R.H., "Determination of $Ca(OH)_2$ in hardened cement pastes with the X-ray spectrometer," Portland Cement Association Report, Chicago, May 1953.

Copeland, L.E., Kantro, D.L. and Verbeck, G., "Chemistry of hydration of Portland cement," Proc. 4th International Symposium on the Chemistry of Cement, Washington DC, 1960, pp 429-465.

Croney, D. and Croney, P., "The design and performance of road pavements". 2nd edition, McGraw-Hill Book Company, London, 1991.

Czernin, W., "Cement chemistry and physics for civil engineers," Crosby Lockwood, London, 1962.

Degeimbre, R. and Rigo, J.M., Forewords, Proc. First International RILEM Conference on Reflective Cracking in Pavements, Liege, 1989.

Dempsey, B.J., et al., "Development of a preliminary ALRS stabilized material pavement," Report ESL-TR-83-34, Engineering and Service Laboratory, Air Force Engineering and Service Centre, Florida, 1984.

Department of Transport HD 26/94., "Pavement design and maintenance," Design Manual for Roads and Bridges, Vol. 7, 1994, Revised February 1996.

Department of Transport HD 25/94., "Pavement design and maintenance," Design Manual for Roads and Bridges, Vol. 7, 1994.

Department of Transport, HA 35/87., "Structural design of new road pavements," Highways and Traffic Advice 35/88, 1987.

Department of Transport, HA 38/88., "Structural maintenance of road pavements with flexible composite construction," Highways and Traffic Advice 38/88, 1989.

Department of Transport., "Notes for guidance on the specification for highway works," Manual of Contract Documents for Highway Works, Volume 2, 1991.

Department of Transport., "Specification for Highway Works," Manual of Contract Documents for Highway Works, Volume 1, Series 1000, 1991, reprinted in 1993.

Department of Transport., "Specification for Highway Works, HM Stationary Office, London, 1986.

Department of Transport., "Specification for Road and Bridge Works, HM Stationary Office, London, 1976.

European Standards, "Cement - composition, specifications and conformity criteria: Common cements," ENV 197-1: 1992.

Felt, E.J., Factors influencing physical properties of soil-cement mixtures," Highway Research Board Bulletin, No. 108, 1955, pp 138-162.

Fleming, P.R. and Rogers, C.D.F., "Assessment of pavement foundations during construction," Transport, Proc. of the Institution of Civil Engineers, 111 (2), pp 105-115, May 1995.

Flint, E.P. and Wells, L.S., "Study of the system $CaO–SiO_2–H_2O$ at 30 ^{o}C and the reaction of water on the anhydrous calcium silicates," Journal of Research National Bureau, No. 687, 1934, pp 751-783.

Fossberg, P.E., Mitchell, J.K. and Monismith, C.L., "Load deformation characteristics of a pavement with cement stabilised base and asphalt surfacing," Proc. 3rd International Conference on the structural design of asphalt pavements, London 1972, Proc. Vol. 1, pp 795-811.

Foulkes, M.D. and Kennedy, C.K., "The limitation of reflective cracking in flexible pavements containing cement bound layers," Proc. International Conference on Bearing Capacity of Roads and Airfields, Plymouth, 1986, pp 105-115.

Francken, L., "Laboratory simulation and modelling of overlay systems," Proc. Second International RILEM Conference on Reflective Cracking in Pavements, Liege, 1993, pp 75-99.

French Standard, NF P 98-230-1, "Preparation of hydraulically bound or non-hydraulically bound materials," Part 1: Specimen compaction using vibrocompression April 1992.

French Standard, NF P 98-230-2., "Determination of the mechanical characteristics of materials treated with hydraulic binders," Part 2: Direct tensile test on gravels and sands, Sept. 1992.

Gaarkeuken, G., Scarpas, A. and Blaauwendraad, J., "Capa - 2D tutorial guide," Report ISSN, February 1996.

Galloway, J.W. and Raithby, K.D., "Effects of rate of loading on flexural strength and fatigue performance of concrete," Laboratory Report 547, Transport and Road Research Laboratory, Crowthorne, 1973.

Galloway, J.W., Harding, H.M. and Raithby, K.D., "Effects of age on flexural, fatigue, and compressive strength of concrete," Laboratory Report 865, Transport and Road Research Laboratory, Crowthorne, 1979.

Galloway, J.W., Harding, H.M. and Raithby, K.D., "Effects of moisture changes on flexural and fatigue strength of concrete," Laboratory Report 864, Transport and Road Research Laboratory, Crowthorne, 1977.

Gardner, N.J. and Zhao, J.W., "Creep and shrinkage revisited," ACI Materials Journal, Technical Paper 90-M26, American Concrete Institute, Michigan, May-June 1993, pp 236-246.

George, K.P. "Shrinkage cracking of soil-cement bases," Highway Research Record, No. 351, Washington D.C., 1971, pp 115-133.

George, K.P., "Cracking in cement treated bases and means to minimize it," Highway Research Record, No. 255, Washington D.C., 1968, pp 59-71.

George, K.P., "Cracking in soil-cement". The Seventh Conference of the Australian Road Research Board, Vol. 7, Adelaide, 1974, pp 38-53.

George, K.P., "Mechanism of shrinkage cracking of soil-cement bases," Highway Research Record, No. 442, Washington D.C., 1973, pp 1-10.

George, K.P. and Davidson, D.T., "Development of a freeze-thaw test for design of soil-cement," Highway Research Record, No. 36, 1963, pp 77-96.

George[1], K.P., "Final report on the study of criteria for strength and shrinkage of cement treated bases," Engineering Experiment Station, University of Mississippi, May 1968.

George[2], K.P., "Shrinkage characteristics of soil-cement mixtures," Highway Research Record, No. 255, 1968, pp 42-58.

Giannini, F. and Camomilla, G., "Procedure for the structural design of pavements on Italian motorways," Fourth International Conference on the Structural Design of

Asphalt Pavements, Proc., Vol. 1, University of Michigan, Ann Arbor, Michigan, 1977, pp 353-369.

Giertz, H.S., "The physical structure of hydrated cements," Proc. 2nd International Symposium on the Chemistry of Cement, Stockholm, 1938, pp 505-534.

Glanville, W.H., Collins, A.R. and Matthews, D.D., "The grading of aggregates and workability of concrete," Road Research Laboratory, Technical Paper No. 5, HMSO, London, 1947.

Graham, G. and Martin, F.R., "Heathrow, the construction of high-grade quality concrete paving for modern transport aircraft," Proc. Institution of Civil Engineers, Airport Paper No. 1, April 1946, pp 117-263.

Haas, R. and Ponniah, E.J., "Design orientated evaluation of alternatives for reflection cracking through pavement overlays," Proc. First International RILEM Conference on Reflective Cracking in Pavements, Liege, 1989.

Haas, R.C. and Topper, T.H., "Thermal fracture phenomena in bituminous surfaces," Highway Research Board, Report 101, 1969, pp 136-153.

Hajek, J.J. and Haas, R.C., "Predicting low-temperature cracking frequency of asphalt concrete pavements," Highway Research Record, No. 407, Washington D.C., 1972, pp 39-54.

Han, M.Y. and Lytton, R.L., "Theoretical prediction of drying shrinkage of concrete," American Society of Civil Engineers, Journal of Materials in Civil Engineering, New York, Nov. 1995, pp 204-207.

Hansen, W. and Almudaiheem, J.A., "Ultimate drying shrinkage of concrete-influence of major parameters, ACI Materials Journal, 84, No. 3, 1987, pp 217-223.

Haywood, A.T.J., "A review of the full scale road experiments with expanded metal under rolled asphalt laid on a concrete base," Research Report RN-2353-ATJH, Road Research Laboratory, Department of Scientific and Industrial Research, London, 1955.

Hensley, M.J., "Open graded asphalt concrete base for the control of reflective cracking," Association of Asphalt Paving Technologists, Vol. 49, 1980.

Hermite, R.L., "Volume changes of concrete," Proc. 4th International Symposium on the Chemistry of Cement, Washington D.C., 1960, pp 659-694.

Higginson, E.C., Wallace, G.B. and Ore, E.L., "Effect of maximum size of aggregate on compressive strength of mass concrete," Symposium on Mass Concrete, ACI SP-6, Detroit, 1963, pp 219-256.

Highways Agency, "Structural Assessment Methods," Design Manual for Roads and Bridges, Volume 7, Pavement Design and Maintenance, HD 29/94, 1994.

Holmgren, J., "Advanced tunnel support using steel fibre reinforced shotcrete," Proc. US-Sweden Joint Seminar, Swedish Cement and Concrete Research Institute, Stockholm, June 1985, pp 361-376.

Horii, H., Shin, H.C. and Pallewatta, T.M., "Mechanism of fatigue crack growth in concrete," Journal Cement and Concrete Composites, Elsevier Science Publishers Ltd., Printed in Britain, 1992, pp 83-89.

Houk, I.E., Borge, O.E. and Houghton, D.L., "Studies of autogenous volume change in concrete for Dworshak Dam," Journal, American Concrete Institute, No. 66, July 1969, pp 560-568.

Hughes, D.A.B., "Polymer grid reinforcement of asphalt pavements," Thesis, University of Nottingham, 1986.

Hveem, F.N. and Zube, E., "California mix design for cement-treated bases," Highway Research Record, No. 36, Washington, 1963, pp 11-55.

Jacob, T.R., "Design limits of common reflective crack repair techniques," Proc. Second International RILEM Conference on Reflective Cracking in Pavements, Liege, 1993, pp 169-176.

Jofre, C., Vaquero, J. and Kraemer, C., "Performance of precracked cement treated layers in Spain," Proc. 3rd International RILEM Conference on Reflective Cracking in Pavements, October 1996, pp 72-81.

Johnston, C.D. and Sidwell, E.H., "Testing concrete in tension and in compression," Magazine of Concrete Research, 1968, pp 221-228.

Judycki, J., "Structural characterization of road base materials treated with hydraulic binders," Publication of Road and Transport Laboratory, University of Oulu, Finland, 1991.

Kelly, J.W., "Cracks in concrete - the causes and cures," Concrete Construction, No. 9, April 1964, pp 89-93.

Kennedy, J., "Cement bound materials for sub-bases and roadbases: material selection and mix design, construction and control testing," Cement and Concrete Association, 1983, republished by British Cement Association, 1990.

Kennedy, J., "The economic viability of cement bound materials in pavements," Journal of the Institution of Highway Engineers, November 1980, pp 20-21.

Kesler, C.E., "Effect of speed of testing on flexural fatigue strength of plain concrete," Proc. Highway Research Board, No. 32, 1953, pp 251-258.

Kolias, S., "Evaluation of the strength and elastic properties of cement stabilised materials," PhD thesis, University of Surrey, 1975.

Kolias, S. and Williams, R.I.T., "Cement bound road materials: strength and elastic properties measured in the laboratory," Report SR 344, Transport and Road Research Laboratory, Crowthorne, 1978.

Larsen, T.J. and Nussbaum, P.J., "Fatigue of soil cement," Journal of PCA Research and Development Laboratories, May 1967, pp 37-59.

Le Service d'Études Techniques des Routes et Autoroutes (SETRA)., "Techniques pour limiter la remontée des fissures," Note d' Information du SETRA, n° 57, 1990.

Lea, F.M., "Cement research: Retrospect and prospect," Proc. 4th International Symposium on the Chemistry of Cement, Washington D.C., 1960, pp 5-8.

Leclerc, R.V., "Cement-treated bases," Paper presented at the Sun Valley WASHO Conference and reported in Western Construction and Industry Magazine, No. 41 (12), 1966, pp 38 and 43.

Lilley, A.A., "Cement stabilised materials for bases and sub-bases of road and airfield pavements, MPhil thesis, City University, London, 1970.

Lilley, A.A., "Current overseas practice," Journal of the Institution of Highway Engineers, No. 19 (3), 1972, pp 4-11.

Lofti, H., Witczak, M.W., "Dynamic characterization of cement treated base and sub-base materials," TRR, No. 1031, 1985, pp 41-47.

Majidzadeh, K., Luther, M.S. and Skylut, H., "A mechanistic design procedure for fabric reinforced pavement systems," Proc. 2nd International Conference on geotextiles, Las Vegas, Vol. 2, 1982, pp 529-534.

Manser, C.J., "The effect of aggregate type on the compressive strength of lean concrete mixes," MSc project report, University of Surrey, Guildford, UK, 1969.

Manual of Testing Procedures, Vol. 1, Texas Highway Dept., Materials and Test Division, Revised Edition, 1971.

Marais, C.P., Otte, E. and Bloy, L.A.K., "The effect of grading on lean mix concrete," Highway Research Record, No. 441, 1973, pp 86-96.

Marais, G.P., "Transvaal experience with cement-treated crushed rock bases," NIRR-PCI Symposium on cement-treated crusher-run bases, Johannesburg, 1973.

Marais, G.P., Otte, E. and Bloy, L.A.K., "The effect of grading on lean-mix concrete," HRR, No. 441, 1973, pp 86-96.

Margery, I.D., "Romans roads in Britain," John Baker, London, 1987.

Markwick, A.H.D. and Keep, H.S., "The use of low-grade aggregates and soils in the construction of bases for roads and aerodromes," Proc. Institution of Civil Engineers, Road Paper No. 9, pp 3-30, discussion, pp 31-54, 1943.

Mayhew, H.C., and Harding, H.M., "Thickness design of concrete roads," Research Report 87, Transport and Road Research Laboratory, Crowthorne, 1987.

Mayhew, H.C. and Potter, J.F., "Structural design and performance of lean concrete roads," Proc. International Conference on Bearing Capacity of Roads and Airfields, Plymouth, 1986, pp 61-70.

Metcalf, J.B., "Flexure tests on small soil-cement beams," Australian Road Research Board, Proc. 1966, Vol. 3, Part 2, pp 1562-1574.

Mitchell, J.K. and Monismith, C.L., "A thickness design procedure for pavements with cement-stabilized bases and thin surfacings," Fourth International Conference on Structural Design of Asphalt Pavements, Ann Arbor, Vol. 1, 1977, pp 409-416.

Mitchell, J.K., Dzwilewski, P. and Monismith, C.L., "Behaviour of stabilized soils under repeated loading," A summary report with a suggested structural pavement design procedure, Report 6, California University, Berkeley, October 1974.

Murdock, J.W., "The mechanism of fatigue failure in concrete," PhD thesis submitted to the University of Illinois, 1960.

Murphy, H.W., Baran, E. and Gordon, R.G., "Cement treated bases for pavements," Institution of Engineers, Australia (Queensland division), 21 (29), Brisbane, 1980, pp 9-31.

Murray, C.D., "Simulation testing of geotextile membranes for reflection cracking," Proceedings 2nd International Conference on geotextiles, Las Vegas, Vol. 1, 1982, pp 511-516.

Muskhelishivili, N.I., "Some basic problems of the mathematical theory of elasticity," P. Noordhoff Ltd., Groningen, 1953, pp 324-328.

Nair, K., Smith, W.S. and Chang, C.Y., "Characterization of asphalt concrete and cement treated granular base course," Materials Research and Development, Oakland, California, Feb. 1972.

Nakayama, H. and Handy, R.L., "Factors influencing shrinkage of soil-cement," Highway Research Record, No. 86, 1965, pp 15-27.

Nanni, A., "Splitting tension test for fibre reinforced concrete," Technical paper 85-M27, ACI Materials Journal, July/Aug. 1988, pp 229-233.

Nanni, A. and Johari, A., "RCC pavement reinforced with steel fibres," Concrete International: Design and Construction, March 1989, pp 64-69.

Nanni, A., "Fatigue behaviour of steel fibre reinforced concrete," Journal Cement and Concrete Composites, Elsevier Science Publishers Ltd., Printed in Britain, 1992, pp 239-245.

Natt, G.S. and Joshi, R.C., "Properties of cement and lime fly-ash stabilized aggregate," TRR, No. 998, 1984, pp 32-40.

Neal, J.A. and Kesler, C.E., "The fatigue of plain concrete," Proc. International Conference on the Structure of Concrete, Cement and Concrete Association, London, 1968, pp 226-237.

Nelson, E.L., Carrasquillo, R.L. and Fowler, D.W., "Behaviour and failure of high strength concrete subjected to biaxial-cyclic compression loading," ACI Materials Journal, 85, No. 4, 1988, pp 248-253.

Neville, A.M., "Properties of concrete," Fourth edition, Longman Group Limited, Essex, 1995.

Neville, A.M., "Role of cement in creep of mortar," Journal of American Concrete Institute, March 1959, pp 963-984.

Nichols, F.P., "Manufactured sand and crushed stone in Portland cement concrete," Concrete International, No. 8, 1982, pp 56-63.

Nilson, L.O., "Hygroscopic moisture in concrete-drying measurements and related material properties," Division of Building Materials, Research Report TVBM-1003, Institution of Technology of Lund, Sweden, 1980.

Norling, L.T., "Minimizing reflective cracks in soil-cement pavements," A status report of laboratory studies and field practices, HRR, No. 442, 1973, pp 22-33.

Nunn, M.E., "An investigation of reflection cracking in composite pavements in the United Kingdom," Proc. First International Conference on Reflective Cracking in Pavements, Liege, 1989, pp 146-153.

Obi, B.C.A., "Soil-cement under thin bituminous surfacing," Transportation Engineering Journal, ASCE, May 1972, TE 2, pp 167-175.

Ople, F.S. and Hulsbos, C.L., "Probable fatigue life of plain concrete with stress gradient," Journal American Concrete Institution, 63, 1966, pp 59-81.

Örbom, B., "Experience in Sweden of cement-bound road bases," Cembureau (Paris) translation of paper presented at the Congress of Nordiska Vägtekniska Förbundet, Gothenburg, 1965.

Otte, E., "Factors affecting the behaviour of cement treated layers in pavements," The 9th Australian Road Research Board Conference, University of Queensland, Brisbane, Vol. 9, 1978, pp 191-202.

Otte, E., "Thermal effects in cemented pavement layers," The Highway Engineers Magazine, Dec. 1978, pp 2-8.

Otte E., Savage, P.F. and Monismith, C.L., "Structural design of cemented pavement layers," Transportation Engineering Journal of ASCE, July 1982, TE 4, pp 428-445.

Paris, P.C., and Erdogan, F., "A critical analysis of crack propagation laws," Journal of basic engineering, Transaction of the American Society of Mechanical Engineering, Series D, Vol. 85, 1963, pp 528-553.

Patankar, V.D. and Williams, R.I.T., "Bitumen in dry lean concrete," Highways and Traffic Engineering, Vol. 38, No. 1721, Jan. 1970, pp 32-35.

Pell, P.S. and Brown, S.F., "Implementation of analytical pavement design and cement treated layers," The Course on Bituminous Pavements - Materials, Design and Evaluation, University of Oulu, April 1991.

Pell, P.S. and Brown, S.F., "The characteristics of materials for the design of flexible pavement structures," Proceedings, Third International Conference on the Structural Design of Asphalt Pavements, London, Vol. 1, 1972, pp 326-342.

Pendola, H.J., Kennedy, T.W. and Hudson, W.R., "Evaluation of factors affecting the tensile properties of cement treated materials," Research Report No. 98-3, Centre for Highway Research, University of Texas at Austin, Jan. 1970.

Petit, J., "Development of lean concrete construction technique in Belgium (Oral contribution)," International Colloquium on Concrete Roads, Besancon, Cembureau, Paris, 1978, pp 8-36.

Petit, J., "Nouvelles perspectives pour les fondations routieres en beton maigre," La Technique Routiere, No. 1, Brussels, 1979, pp 36-56.

PIARC., "Technical committee report on flexible roads," Permanent International Association of Road Congresses, 17th World Road Congress, Sydney, October 1983, pp 93-103.

Portland Cement Association., "Concrete technology instructor's guide," 1965.

Portland Cement Association., "Soil-cement construction," SC3-7, PCA, Skokie, Illinois, 1956.

Portland Cement Association., "Soil-cement mixtures," Laboratory Handbook, 1st edition, PCA, Skokie, Illinois, 1942.

Powell, W.D., Potter, J.F., Mayhew, H.C. and Nunn, M.E., "The structural design of bituminous roads," Laboratory Report LR 1132, Transport and Road Research Laboratory, 1984.

Powers, T.C., "The non-evaporable water content of hardened Portland cement paste: its significance for concrete research and its method of determination," ASTM Bulletin No. 158, May 1949, pp 68-76.

Pretorious, P.C. and Monismith, C.L., "Prediction of shrinkage stresses in pavements containing soil-cement bases," HRR, No. 362, 1971, pp 63-86.

Raad, L., Monismith, C.L. and Mitchell, J.K., Tensile strength determination of cement treated materials," TRR, No. 641, 1977, pp 48-52.

Raithby, K.D. and Galloway, J.W., "Effect of moisture condition, age and rate of loading on fatigue of plain concrete," Abeles Symposium on Fatigue of Concrete, SP-41, ACI, 1974, pp 15-34.

Read, J.M., "Fatigue cracking of bituminous paving mixtures," PhD Thesis, University of Nottingham, May 1996.

Research Focus, No. 25, "Flexible composite pavements - design developments," Institution of Civil Engineers, April 1996, pp 2.

RILEM Committee Report 36-RDL, "Long term random dynamic loading of concrete structure," Volume 17, Paris, 1984.

Robnett, D.L. and Thompson, M.R., "Soil stabilization literature reviews," Illinois Cooperative Highway Research Program, June 1969.

Ross, A.D., "Shape, size and shrinkage," Concrete and Constructional Engineering, London, Aug. 1944, pp 193-199.

Scarpas, A., Blaauwendraad, J., Bondt, A.H. and Molenaar, A.A.A., "Capa: A modern tool for the analysis and design of pavements," Proc. 2nd International RILEM Conference on Reflective Cracking in Pavements, E & FN Spon, London, 1993, pp 121-128.

Scarpas, A., Bondt, A.H., Molenaar, A.A.A. and Gaarkeuken, G., "Finite element modelling of cracking in pavements," Proc. 3rd International RILEM Conference on Reflective Cracking in Pavements, October 1996(a), pp 83-91.

Scarpas, A., Bondt, A.H. and Gaarkeuken, G., "Reflective cracking control via reinforcing systems, Finite element modelling of reinforced overlays," Proc. 3rd International RILEM Conference on Reflective Cracking in Pavements, October 1996(b), pp 83-91.

Schmidt, M., "Theoretical considerations and measures for the prevention of reflective cracking in asphalt roads with cement bound bases," First International Conference on Reflective Cracking in Pavements, Liege, 1989, pp 217-224.

Shacklock, B.W., "Concrete constituents and mix proportions," Cement and Concrete Association, London, 1974.

Shah, S.P. and Chandra, S., "Fracture of concrete subjected to cyclic and sustained loading," Journal American Concrete Institute, October 1970, pp 816-825.

Shahid, M.A., "Investigation of site trials with controlled cracking of cement bound bases," Report PGR 96021, University of Nottingham, May 1996.

Shahid, M.A., "Pavements with cement bound bases," Report PGR 94023, University of Nottingham, December 1994.

Shahid, M.A. and Thom, N.H., "Performance of cement bound bases with controlled cracking," Proc. 3rd International RILEM Conference on Reflective Cracking in Pavements, October 1996(a), pp 55-64.

Shahid, M.A. and Thom, N.H., "Controlled cracking in cement bound bases," Journal of the Institution of Highways and Transportation, Vol. 43, No. 10, October 1996(b), pp 20-23.

Shahid, M.A., Thom, N.H. and Peaston, C.H., "Steel fibre reinforcement in cement bound bases," Report PGR 96016, University of Nottingham, April 1996.

Shahid, M.A., Thom, N.H., Dawson, A.R. and York, D., "Controlled cracking of cement bound bases," Report PGR 95018, University of Nottingham, Nottingham, September 1995.

Shahid, M.A., Thom, N.H. and Fleming, P.R., "In-situ assessment of road foundations," Paper accepted and due to be published in the Journal of the Institution of Highways and Transportation, November 1997.

Shi, X.P., Fwa, T.F. and Tan, S.A., "Flexural fatigue strength of plain concrete," ACI Materials Journal, 90, No. 5, 1993, pp 435-440.

Smith, R.D., "Laboratory testing of fabric interlayers for asphalt concrete paving," Interim Report, Transportation Research Record, No. 916, 1982.

Sokolnikoff, I.S., "Mathematical theory of elasticity," McGraw Hill Book Co., New York, 1956, pp 280-284.

Steinour, H.H., "The reactions and thermochemistry of cement hydration at ordinary temperature," Proc. 3rd International Symposium on the Chemistry of Cement, London, 1952, pp 261-289.

Suresh, S., "Fatigue of materials," Cambridge University Press, 1994, pp 126-140.

Tassios, T.P. and Scarpas, A., "A model for local crack behaviour," IABSE Colloquium on Computational Mechanics of Reinforced Concrete, Delft, 1987.

Taylor, G.D. and Williams, R.I.T., "Restrained thermal contraction in lean concrete roadbases," Highways and Public Works, 49 (1856), 1981, pp 6-12.

Tepfers, R., "Tensile fatigue strength of plain concrete," Journal American Concrete Institution, 76, No. 8, 1979, pp 919-933.

Timoshenko, S., "Theory of elasticity," McGraw Hill Book Co., New York, 1934, pp 104-108.

Thom, N.H., "A simplified approach to the prediction of fatigue cracking in asphalt pavements," Paper presented to the European Flexible Pavements Study Group, Liverpool, 1997.

Transport Research Board., "State of the art: lime stabilization," Transportation Research Circular, No. 180, Committee on Lime and Lime Fly-ash Stabilization, Washington D.C., September 1978.

U.S. Bureau of Reclamation, Concrete Manual, 5th edition, Denver, Colorado, 1949.

Vanelstraete, A. and Francken, L., "Numerical modelling of crack initiation under thermal stresses and traffic loads," Proc. Second International RILEM Conference on Reflective Cracking in Pavements, Liege, 1993, pp 136-145.

Van Cauwelaert, F. and Petit, J., "Pourquoi des structures routieres semi-rigids a fondation en beton maigre," La Technique Routiere/De Wegentechniek, 25 (1), 1980, pp 1-20.

Verhée, F., "Préfissuration par film plastique," Proc. 3rd International RILEM Conference on Reflective Cracking in Pavements, October 1996, pp 47-54.

Vos, B.H., "Moisture migration in concrete," First International Conf. on Structural Mechanics in Reactor Technology, Paper H2/5, Berlin, 1971.

Wang, J.W.H., "Use of additives and expansive cements for shrinkage crack control in soil-cement: a review," Highway Research Record, No. 442, Washington D.C., 1973, pp 11-21.

Wang, M.C. and Huston, M.T., "Direct tensile stress and strain of a cement stabilised soil," Highway Research Record, No. 379, Highway Research Board, 1972, pp 19-24.

Williams, R.I.T, "Cement treated pavements: materials, design and construction," Elsevier Applied Science Publishers, UK, 1986.

Williams R.I.T., "Properties of cement stabilised materials," Journal of the Institution of Highway Engineers," Vol. 19, No. 2, Feb. 1972, pp 5-19.

Williams, R.I.T. and Patankar, V.D., "The effect of cement type, aggregate type and mix water content on the properties of lean concrete mixes," Roads and Road Construction, Feb. 1968, pp 34-41 and 65-69.

Winterbaum, H.F., "State-of -the-art survey of soil stabilization," Vol. 1, Naval Air Engineering Centre, Philadelphia, 1968.

Wright, P.J.F., "Comments on an indirect tensile test on concrete cylinders," Magazine of Concrete Research, No. 20, 1955, pp 87-96.

Yoder, E.J. and Witczak, M.W., "Principles of pavement design," 2nd edition, John Wiley and Sons, New York, 1975.

Young, J.F., "The microstructure of hardened Portland cement paste," Creep and shrinkage in concrete structures, John Wiley and Sons, Ltd, New York, 1982, pp 3-22.